Genetic Basis for the Breadth and Potency of HIV-1 V2-Specific Antibodies

David Sacks

A thesis submitted to the School of Pathology, Faculty of Health Sciences, University of the Witwatersrand, Johannesburg, in fulfilment of the requirements for the degree of Doctor of Philosophy.

Johannesburg, 2020

Declaration

I, David Sacks, declare that this thesis is my own, unaided work. It has been submitted for the Degree of Doctor of Philosophy at the University of the Witwatersrand, Johannesburg. It has not been submitted before for any degree or examination at any other any other university.

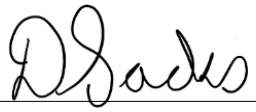

David Sacks

28 October 2020

Date

Presentations and publications from this study

Presentations

Sacks D, Bhiman JN, Gorman J, Morris L and Moore PL. Somatic hypermutation to counter a rare viral immunotype drove off-track antibodies in the CAP256-VRC26 V2-directed bNAb lineage. HIV Research for Prevention (Madrid, Spain, 2018). Oral presentation.

Sacks D, Bhiman JN, Gorman J, Morris L and Moore PL. Viral immunotypes that drove the evolution of an “off-track” member of the CAP256-VRC26 V2-directed broadly neutralizing lineage. Keystone Symposia HIV Vaccines (C9) (Colorado, USA, 2017). Poster.

Sacks D, Bhiman JN, Gorman J, Morris L and Moore PL. Mutations and Viral Variants that Restrict Antibody Neutralization Breadth and Potency. The University of the Witwatersrand Molecular Biosciences Research Thrust Research Day (Johannesburg, 2017). Oral presentation.

Sacks D, Bhiman JN, Gorman J, Morris L and Moore PL. Genetic Determinants of Breadth and Potency in the CAP256 HIV-1 Specific bNAb Lineage. HIV Research for Prevention (Chicago, USA, 2016). Poster.

Sacks D, Bhiman JN, Gorman J, Morris L and Moore PL. Genetic Determinants of Breadth and Potency in the CAP256 HIV-1 Specific bNAb Lineage. The University of the Witwatersrand Faculty of Health Sciences Research Day (Johannesburg, 2016). Oral presentation.

Publications

Sacks D, Bhiman JN, Wiehe K, Gorman J, Kwong PD, Morris L, Moore PL. Somatic hypermutation to counter a globally rare viral immunotype drove off-track antibodies in the CAP256-VRC26 HIV-1 V2-directed bNAb lineage. PLOS Pathog. 2019;15(9):e1008005.

Abstract

Some HIV infected people develop broadly neutralizing antibodies (bNAbs) that block many diverse unrelated strains of HIV from infecting target cells, and through passive immunization, protect animals from SHIV infection. Therefore, understanding the development of bNAbs and their neutralization can inform the design of an HIV vaccine. We investigated the genetic basis for the neutralization capacity of members of a bNAb family that target the variable loop 2 (V2) of the HIV-1 Envelope trimer. This lineage, CAP256-VRC26, contains bNAbs and closely related "off-track" members that lack breadth. We found that few mutations in the third complementarity-determining region of the heavy chain (CDRH3), which forms most of the paratope, restricts the breadth of two off-track antibodies. Furthermore, we established that a globally rare viral variant guided one of these antibodies away from breadth, indicating that vaccine immunogens should represent common circulating strains. Analysis of the sequence of the unmutated common ancestor (UCA) of the CAP256-VRC26 lineage showed that the off-track mutations were predicted to occur with a higher probability than the breadth-conferring mutations. Most of the improbable mutations were located in the CDRH3 and we found that transferring the CDRH3 from bNAb CAP256.25 into the CAP256.UCA introduced breadth and tolerance for emerging viral variants. In addition, we showed that the framework and light chain contributed to potency and that the second complementarity-determining region of the light chain forms part of the paratope of CAP256.25. Together, approximately half of the mutations in CAP256.25 were necessary for broad neutralization, indicating that immunogens that target affinity maturation to key sites, including the CDRHs and light chain, could rapidly elicit breadth. In addition to neutralization, antibodies mediate effector functions via the Fc domain which is important for both active and passive immunization. By determining the breadth and effector functions of newly identified IgG4 class switched members of the CAP256-VRC26 lineage, we showed that effector functions can vary dramatically across related antibodies and the Fab sequence can impact these functions. Furthermore, we demonstrated that IgG4-mediated phagocytosis was greater than IgG1 matched antibodies which may be important for passive immunization since both IgG1 and IgG4 cross into the placenta. Together, we have identified key regions and mutations that confer breadth and potency, and modulate Fc effector function for a V2-specific bNAb lineage. This informs the design of a vaccine that directs affinity maturation and the formulation of functional monoclonal antibodies for passive immunization.

Acknowledgements

Penny, thank you for the invaluable guidance, advice and support over the years. I am deeply grateful for the confidence you have had in me. I have learnt so much from you as a supervisor and scientist.

Lynn, I am indebted to you for my postgraduate studies. Thank you for the freedom to pursue my research in the best possible environment.

The Morris lab has been my second home for so many years, thank you for the support and assistance.

I would like to acknowledge the Poliomyelitis Research Foundation and the University of the Witwatersrand for their financial contribution.

To Mom and Dad, I would not have completed my studies without your constant support. My success is a result of you. Brett and Marc, are good brothers. Special thanks to Sebastian. Ben, thank you for the endless support, understanding, and dedication over all these years.

Table of contents

List of figures

List of tables

Abbreviations

A	aa	Amino acid
	Ad5	Adenovirus type 5
	ADCC	Antibody-dependent cellular cytotoxicity
	ADCD	Antibody-dependent complement deposition
	ADCP	Antibody-dependent cellular phagocytosis
	ADCT	Antibody-dependent cellular trogocytosis
	AID	Activation-induced cytidine deaminase
	AIDS	Acquired immunodeficiency syndrome
	ART	Antiretroviral therapy
B	BCR	B-cell receptor
	bNAb	Broadly neutralizing antibody
C	C1-5	Constant regions 1-5
	CA	Capsid
	CAP256	CAPRISA donor 256
	CAPRISA	Centre for the AIDS Program of Research in South Africa
	CCR5	C-C chemokine receptor type 5
	CD	Cluster of differentiation
	CD4bs	CD4 binding site
	CDRH	Complementarity-determining region of the heavy chain
	CDRL	Complementarity-determining region of the light chain
	CFSE	Carboxyfluorescein hydroxysuccinimidyl ester
	CH1-3	Constant heavy chains 1-3
	CMV	Cytomegalovirus
	CO_2	carbon dioxide
	CRF	Circulating recombinant form
	CSR	Class switch recombination
	C-terminus	Carboxyl-terminus
	CTL	Cytotoxic T-lymphocyte
	CXCL	Chemokine (C-X-C motif) ligand
	CXCR4	C-X-C chemokine receptor type 4
D	DEAE-dextran	Diethylaminoethyl-dextran
	DMEM	Dulbecco’s modified Eagle's medium
	DNA	Deoxyribonucleic acid
E	EDTA	Ethylenediaminetetraacetic acid
	ELISA	Enzyme-linked immunosorbent assay

	Env	Envelope
	eOD-GT	External outer domain - germline-targeting
F	Fab	Fragment of antigen binding
	FACS	Fluorescence-activated cell sorting
	FBS	Fetal bovine serum
	Fc	Fragment crystallisable
	FcR	Fc receptor
	FDC	Follicular dendritic cell
	FITC	Fluorescein isothiocyanate
	FR	Framework region
G	Gag	Group-specific antigen
	GALT	Gut-associated lymphoid tissue
	GC	Germinal center
	GM	Geometric mean
	gp160	Glycoprotein 160 kDa
	Group M	HIV-1 major group
	Group N	HIV-1 non-M, non-O group
	Group O	HIV-1 outlier group
	Group P	HIV-1 group pending (the identification of further cases)
H	HC	Heavy chain
	HCl	Hydrochloric acid
	HIV-1, HIV-2	Human immunodeficiency virus type-1, -2
	HVTN	HIV Vaccine Trials Network
I	IC_{50}	50% inhibitory concentration
	IFN	Interferon
	Ig	Immunoglobulin
	IGHC	Immunoglobulin heavy chain constant gene
	IGHD	Immunoglobulin heavy chain diversity gene
	IGHJ	Immunoglobulin heavy chain joining gene
	IGHV	Immunoglobulin heavy chain variable gene
	IGKC	Immunoglobulin kappa light chain constant gene
	IGKJ	Immunoglobulin kappa light chain joining gene
	IGKV	Immunoglobulin kappa light chain variable gene
	IGLC	Immunoglobulin lambda light chain constant gene
	IGLJ	Immunoglobulin lambda light chain joining gene
	IGLV	Immunoglobulin lambda light chain variable gene
	IL	Interleukin
	IMGT	ImMunoGeneTics information system

	IN	Integrase
L	LB	Lysogeny broth
	LC	Light chain
	LTR	Long terminal repeat
M	MA	Matrix
	mAb	Monoclonal antibody
	MALT	Mucosa-associated lymphoid tissue
	MPER	Membrane proximal external region
	mRNA	Messenger RNA
	MSH2/6	DNA mismatch repair protein 2/6
N	NC	Nucleocapsid
	Nef	Negative factor
	NK	Natural killer cell
	N-nucleotide	Non-templated nucleotide
	nt	Nucleotide
	N-terminus	Amino-terminus
P	p6	Protein 6
	PBMC	Peripheral blood mononuclear cell
	PBS	Phosphate-buffered saline
	PCR	Polymerase chain reaction
	PDB	Protein Data Bank
	PEI	Polyethylenimine
	PES	Polyethersulfone
	pi	Post infection
	PI virus	Primary infecting virus
	PKH26	Paul Karl Horan 26
	P-nucleotide	Palindromic nucleotide
	Pol	Polymerase
	Pr	Peptide precursor
	PR	Protease
R	RAG1/2	Recombination-activating genes 1/2
	Rev	Regulator of expression of viral proteins
	RNA	Ribonucleic acid
	RNase H	Ribonuclease H
	RPMI	Roswell Park Memorial Institute culture medium
	RSS	Recombination signal sequences
	RT	Reverse transcriptase
S	SHIV	SIV and HIV chimera

	SHM	Somatic hypermutation
	SIV	Simian immunodeficiency virus
	SU virus	Superinfecting virus
T	T/F	Transmitted/founder virus
	TAE	Tris-acetate-EDTA
	Tat	Trans-activator
	TdT	Terminal deoxynucleotidyl transferase
	T_{FH}-cell	T-follicular helper cell
	T_{FR}-cell	T-follicular regulatory cell
	TGFβ	Transforming growth factor beta
	Tris-Cl	Tris(hydroxymethyl)aminomethane-chloride
U	UCA	Unmutated common ancestor
	UNG2	Uracil-DNA glycosylase 2
V	V1-5	Variable loops 1-5
	VDJ	(V) variable (D) diversity (J) joining genes
	VH	Variable heavy chain
	Vif	Viral infectivity factor
	VL	Variable light chain
	Vpr	Viral protein R
	Vpu	Viral protein unique
W	wk	Week

Symbols and units

SI unit prefixes

k	Kilo	10^{3}
c	Centi	10^{-2}
m	Milli	10^{-3}
µ	Micro	10^{-6}
n	Nano	10^{-9}
p	Pico	10^{-12}

SI base and derived units

°C	Degree Celsius
kg	Kilogram
m	Meter
mol	Mole
s	Second (sec)
m^2	Square meter

Non-SI units

Å	Angstrom
bp	Base pair
Da	Dalton
g	Standard gravity
L	Liter
M	Molar (mol)
min	Minute
pH	Cologarithm of hydrogen
RLU	Relative light units
rpm	Revolutions per minute
U	International unit

Symbols

3', 5'	Three prime, five prime
α	Alpha
~	Approximately
β	Beta

Δ, δ	Delta
ε	Epsilon
γ	Gamma
κ	Kappa
λ	Lambda
μ	Mu

Amino acids

A	Ala	Alanine
R	Arg	Arginine
N	Asn	Asparagine
D	Asp	Aspartate
C	Cys	Cysteine
E	Glu	Glutamate
Q	Gln	Glutamine
G	Gly	Glycine
H	His	Histidine
I	Ile	Isoleucine
L	Leu	Leucine
K	Lys	Lysine
M	Met	Methionine
F	Phe	Phenylalanine
P	Pro	Proline
S	Ser	Serine
T	Thr	Threonine
W	Trp	Tryptophan
Y	Tyr	Tyrosine
V	Val	Valine

Nucleotides

A	Adenine	H	A, C or T
C	Cytosine	R	A or G
G	Guanine	S	G or C
T	Thymine	W	A or T
U	Uracil	Y	C or T

1. Introduction

1.1 Human immunodeficiency virus (HIV)

1.1.1 The HIV pandemic

During the 1980s there were increasing reports of a fatal acquired immunodeficiency syndrome (AIDS) [1–4] that was caused by the human immunodeficiency virus (HIV) [5,6]. Spread through sexual contact and contaminated blood products, the incidence of HIV infection rapidly increased [7]. Over the ensuing decades, HIV/AIDS has had devastating social and public health consequences with close to 40 million people dying of AIDS-related illnesses [8]. Today, approximately 37 million people are living with HIV, with sub-Saharan Africa experiencing the highest HIV/AIDS burden [8]. However, HIV/AIDS was transformed from a terminal disease to a chronic manageable illness [9] during the mid-1990s when combination antiretroviral therapy (ART) became available [10,11]. In addition, the development of, and access to, effective preventative measures has reduced new infections by 50% since the peak in the 1990s [8]. Condoms and pre-exposure prophylaxis reduce the risk of infection by 80-90% and intravaginal rings and microbicidal gels decrease infection by 50-70% [12–18]. Improvements in public health services have ensured that nearly 80% of people who know their status receive ART and approximately 50% of all infected individuals are virally suppressed [8]. Sustained viral suppression decreases morbidity, increases life-expectancy and profoundly reduces the risk of sexual [19] and perinatal [20] transmission of HIV. Despite continued progress, a preventative vaccine is urgently needed as more than a million people become infected with HIV each year [8].

1.1.2 The origin of HIV

HIV is related to the simian immunodeficiency virus (SIV) which is endemic to more than 40 species of Old World African primates [21]. At least five independent zoonoses of SIV have occurred, giving rise to HIV type 1 (HIV-1) groups M, N, O and P, and HIV type 2 (HIV-2) [22,23]. The pandemic form of HIV-1, group M, was likely transmitted from an SIV infected chimpanzee in the Democratic Republic of the Congo in the early 20th century [22,24]. Group M consists of nine subtypes (A-D, F-H, J and K) and nearly 100 circulating recombinant forms (CRF) [25]. Globally, subtype C is the most prevalent (47% of infections) and is predominant in sub-Saharan Africa [26]. Subtype A (10%) is common in central and eastern Africa and eastern Europe, and subtype B (12%) is widespread in the Americas and western Europe [22,24,27].

CRF02_AG (9%) and CRF01_AE (5%) are commonly found in west and central Africa, respectively [26]. Group O and P viruses are related to gorilla SIV [28,29], and group N viruses are related to chimpanzee SIV [30]. These viruses are rare and typically found in equatorial west Africa where group O viruses account for <1% of infections and only 16 group N and two group P infections have been identified thus far [22,28–30]. HIV-2 is derived from SIV infected sooty mangabeys and accounts for 5% of global infections, predominantly in north west Africa [31,32].

1.1.3 HIV genome and virus structure

Like other lentiviruses, HIV reverse transcribes its RNA into DNA before it is integrated into the host cell's genome [33]. HIV is spherical, 100–120 nm in diameter and surrounded by a lipid membrane [33]. The genome consists of two single strands of positive sense RNA (9200-9600 nucleotides) that encode nine genes which are flanked by long terminal repeats (LTR) (Figure 1.1 A) [34,35]. The *gag* gene is adjacent to the 5' LTR and is transcribed in the first reading frame and translated into a 55 kDa precursor (Pr) protein, Gag (Pr55), which is cleaved to form the matrix (MA, p17), capsid (CA, p24) and nucleocapsid (NC, p7) structural proteins (Figure 1.1 A) [34,36]. MA lines the inner side of the viral membrane and CA forms the hexameric lattice of the fullerene-shaped virion core [37]. Within the core, the viral genome associates with, and is protected by, the NC (Figure 1.1 B) [37]. *Gag* is followed by *pol* which encodes the reverse transcriptase (RT, p51), integrase (IN, p31), protease (PR, p10) and RNase H (p15) enzymes in the third reading frame (Figure 1.1) [34]. RT synthesizes DNA from the viral RNA, RNase H degrades the RNA template, IN integrates the provirus into the host genome [38] and PR cleaves the polyproteins into the constituent proteins [36,39]. *Env* (gp160) follows *pol* in the same reading frame and encodes the gp120 and gp41 surface glycoproteins (Figure 1.1) [40]. The regions encoding the viral infectivity factor (Vif, p23), viral protein r (Vpr, p15) and viral protein u (Vpu, p16) are located between *pol* and *env* [41]. Negative regulatory factor (Nef, p27) is adjacent to the 3' LTR and the regulator of the expression of virion proteins (Rev, p19) and HIV trans-activator (Tat, p14) are translated at sites flanking *env* (Figure 1.1 A) [35,41].

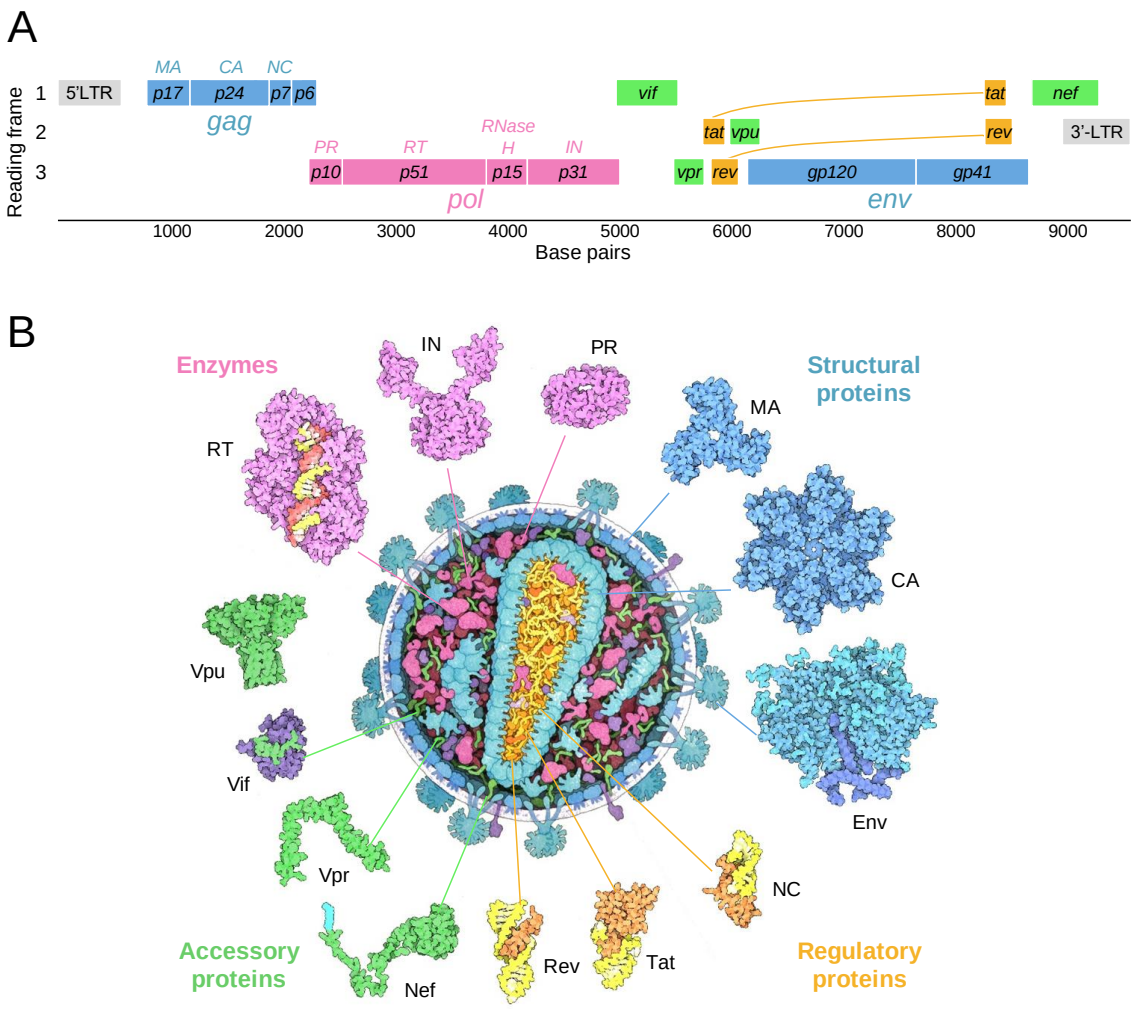

Figure 1.1. The genome and structure of HIV-1.

(A) The genome of HIV-1 is ~9.4 kb and consists of two single stranded RNA molecules that encode *gag* (blue), *pol* (pink), *env* (blue), *nef*, *vpr*, *vif*, *vpu* (green), *tat* and *rev* (orange) [33]. The molecular weights of each protein (p) are shown in kDa. (B) *Gag* is translated into three major structural proteins, including the matrix (MA), capsid (CA) and nucleocapsid (NC) [36]. *Pol* encodes the protease (PR), reverse-transcriptase (RT), integrase (IN) and RNase H enzymes. *Env* (envelope) is transcribed into the surface glycoproteins, gp41 and gp120 [36]. The regulatory proteins are necessary for translation of the provirus [33]. Figure adapted from pdb101.rcsb.org/browse/hiv-and-aids.

1.1.4 HIV diversity

The exceptional plasticity of the HIV genome allows for rapid evolution, resulting in resistance mutations to ART and immune responses [42]. Since the error-prone viral RT and host RNA pol II lack proof-reading capabilities, as many as 3.4 x 10^{-5} mutations per base per replication cycle are introduced [43,44]. Furthermore, there is extensive recombination during reverse transcription, as RT moves as many as 5-14 times between templates [45]. Together with high viral load [46] and high virus turnover [47], escape mutations quickly develop because every possible single point mutation, and most double mutations, appear daily within an infected individual [48]. Consequently, HIV exists as a heterogeneous quasi-species with the sequence

of *env* differing by up to 5% within an infection person, 10-15% within subtypes, 20-30% between subtypes and 30-50% between groups [42,49]. Therefore, a successful vaccine must elicit protective immunity against substantially different HIV types, groups and subtypes.

1.2 The life cycle of HIV-1

The primary entry receptor for HIV-1 is the cluster of differentiation 4 (CD4) and the co-receptors are the C-C chemokine receptor type 5 (CCR5) or the C-X-C chemokine receptor type 4 (CXCR4) [50]. Helper T-cells (subsequently referred to as T-cells) and memory T-cells are particularly permissive to HIV as they express high levels of CD4 and CXCR4, and CD4 and CCR5, respectively [51]. Env mediates entry by binding to CD4 and CCR5/CXCR4 which initiates a cascade of conformational changes resulting in the fusion of the viral and target cell plasma membranes [50], discussed in detail in 1.3.

Following fusion, the virion core is delivered into the cytoplasm where it disassembles, releasing the dimeric RNA genome [52]. The core rearranges to protect the genome from innate immune sensors [53] and to facilitate reverse transcription [54]. Further CA changes drive the migration of the transcribed DNA into the nucleus and its integration into an actively expressed site in the host genome [38]. Basal transcription produces transcripts that are doubly spliced and are translated into the regulatory proteins Tat, Rev and Nef [35,55]. Subsequent transcription increases dramatically as Tat improves the processivity of RNA pol II [55]. Rev exports the viral mRNA from the nucleus before splicing [56] allowing for the translation of Vif, Vpr, Vpu, Env, Gag and Gag-Pol [35]. A stop codon and a secondary structure between *gag* and *gag-pol* stalls translation which shifts the reading frame [35] such that Gag and Pol are produced in the ratio necessary virus assembly (2,500 Gag:125 Pol molecules) [57]. Gag embeds into the host membrane via the myristoylated N-terminal MA domain and the CA subunit oligomerizes and forms a continuous hexameric lattice [36,52]. The lattice surrounds the NC which binds to, and condenses, two copies of the viral genome via zinc fingers [58]. Vif, Vpr and host factors associate with the NC and are packaged within the CA [52] and Nef binds to the cytoplasmic tail of gp41. Together Vif, Vpr and Nef are indispensable for viral infectivity, immunosuppression and cellular activation [41].

Through an interaction between the gp41 cytoplasmic tail and MA, 7-21 Env [59] embed into the cell membrane at the sites of budding viruses [39]. The membrane proximal external region (MPER) consists of the C-terminus of gp41 and the extracellular portion of the transmembrane domain [60]. The *gag* encoded p6 protein recruits the host cell's endosomal transport

machinery which extrudes the viral core from the cell [39]. During or following release, autoproteolysis frees PR which then cleaves the Gag and Pol polyproteins, releasing the structural and enzymatic subunits [39,61]. This results in the maturation of the virus into infectious particles [39] through the reorganization of the core into a fullerene cone [61].

1.3 HIV-1 Envelope (Env)

Env is trimeric and consists of three gp120 molecules non-covalently bound to three gp41 molecules [62-64] (Figure 1.2). The outer domain of gp120 is formed by five heavily glycosylated variable loops (V1-5) which shield an inner domain of five constant regions (C1-5) [64,65]. Although the prefusion trimer is generally in a closed conformation, it transiently samples open states [66]. Therefore, the trimer apex, formed by V1, V2 and V3, briefly reveals sites in C2 (loop D, Figure 1.2, light pink) and C3 (CD4 binding loop, Figure 1.2, brown) to CD4 which destabilizes the trimer thereby exposing a bridging sheet of β-barrels in C1, C2 and C4 [67] and the V3 GDIR co-receptor binding site motif (mustard) to CCR5 or CXCR4 [68]. These changes reorder gp41 and promote gp120 dissociation [69], which reveals the hydrophobic N-terminus of gp41, the fusion peptide (Figure 1.2, cyan), which inserts into the membrane of the target cell [70]. Finally, the viral and target cell membranes are brought together by the bundling of six alpha helices that connect the fusion peptide to the MPER [40,70].

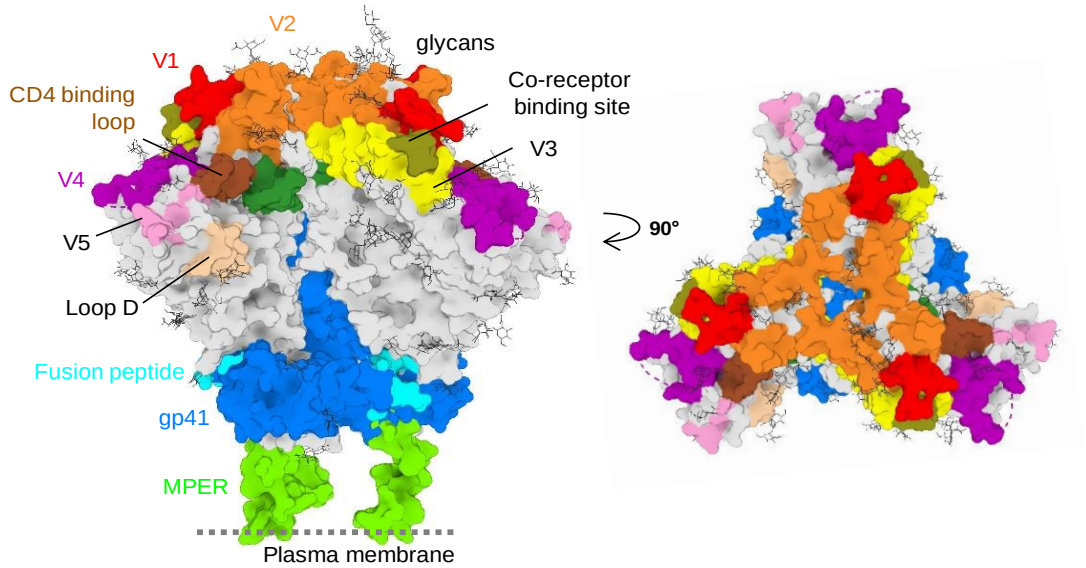

Figure 1.2. The HIV-1 Env trimer.

The surface of HIV-1 is decorated by trimers that are formed by three non-covalently linked gp120-gp41 heterodimers [62-64]. Gp120 consists of five variable regions (V1-5) interspersed with five constant regions (C1-5), with V1V2 (red and orange) forming the trimer apex [62-64]. Gp120 projects from the virus and at the proximal end of gp41 (blue) is the MPER (green) which is embedded in the viral membrane (grey dotted line). Glycans are shown as sticks (black). The figure is based on gp41 (PDB: 4G6F) and Env trimers (PDB: 5FYJ and 4TVP).

Approximately half of the mass of Env is comprised of glycans and since these structures are self-derived, the trimer is generally protected from immune recognition [71]. N-linked glycosylation begins in the endoplasmic reticulum where oligomannose glycan precursors are covalently attached to nascent proteins at N residues in the N-X-S/T (where X is any amino acid besides P) motif [72]. If accessible, the terminal moieties are partially or fully trimmed allowing for the addition of carbohydrate components (including fucose, galactose and sialic acid) to form hybrid or complex type glycans, respectively [73].

1.4 HIV-1 pathogenesis

Although the risk of HIV transmission is greatest for blood transfusions and vertically from mother-to-child, most infections occur during sexual intercourse [74]. Following the exposure of mucosae to infected fluids, HIV encounters Langerhans cells which bind to virions via C-type lectin receptors, leading to the internalization and degradation of the virus [75]. While Langerhans cells and local dendritic cells are relatively resistant to infection due to low expression of the entry receptors and the activity of intracellular restriction factors [76–81], these cells transport infectious virus to T-cell rich sites in secondary lymphoid organs [82]. Here, naïve T-cells probe the surface of dendritic cells as they search for cognate antigen [83]. Microdomains on the dendritic cell plasma membrane rich in HIV-1 efficiently transfer one to five virions (the transmitted/founder virus/es, T/F) to T-cells across a virological synapse [83–85]. An infection is rapidly established due to the short life cycle of ~2 days [86] and the production of up to $5x10^4$ viruses by an infected T-cell each day [87]. The acute infection lasts for ~1 month and is characterized by an exponential increase in viremia, massive T-cell depletion and the establishment of a latent viral reservoir [88]. T-cell depletion in the gut-associated lymphoid tissues (GALT) results in chronic immune hyperactivation since the ability of these tissues to prevent systemic translocation of microbial products is compromised [89]. Viremia peaks at ~$5x10^6$ RNA copies/mL and decreases to a stable set point of ~$2x10^4$ RNA copies/mL as an effective cytotoxic T-lymphocyte (CTL) response develops [90,91]. Although most individuals remain asymptomatic for 8-10 years [92], the length of the chronic infection varies substantially, partly due to differing CTL specificities [93] and human leukocyte antigen class I (HLA-1) allele diversity [94,95]. Ultimately, chronic immune hyperactivation, diminishing T-cell turnover and increasing senescence and apoptosis profoundly impairs the adaptive immune response [96,97]. Consequently, most individuals become increasingly susceptible to opportunistic infections, which if left untreated, culminates in AIDS and death after 1-2 years [97].

1.5 Humoral immunity

While CTL kill infected cells, the extracellular spaces are protected from pathogens by antimicrobial peptides, complement and antibodies [98].

1.5.1 Antibody structure

Antibodies, or immunoglobulins (Ig), neutralize microbes by obstructing their entry into target cells [99], activate the complement cascade and drive cell-mediated effector functions [98]. Antibodies are large (~150 kDa) "Y" shaped glycoproteins consisting of two symmetrical halves joined by a disulfide bond (Figure 1.3) [100]. The Fab (fragment of antigen binding) domain, at the N-terminus, is formed by two variable heavy chains and two variable light chains connected by a disulfide bond (Figure 1.3) [100]. The variable heavy and light chains consist of three relatively invariant framework (FR) regions that support three variable complementarity-determining regions (CDR) (Figure 1.3, inset) [100]. Regions of the Fab forms the antigen-binding surface (paratope) which interacts with its target (epitope) via hydrogen bonds, hydrophobic interactions and van der Waals forces [101]. Therefore, the sequence and conformation of the Fab determines the specificity of the antibody [100,101]. The Fab is linked by a hinge to the C-terminus Fc (fragment crystallizable) domain and the identity of the Fc (isotype) governs the effector functions by differentially binding to Fc-receptors (FcR) on effector cells (Figure 1.3) [100].

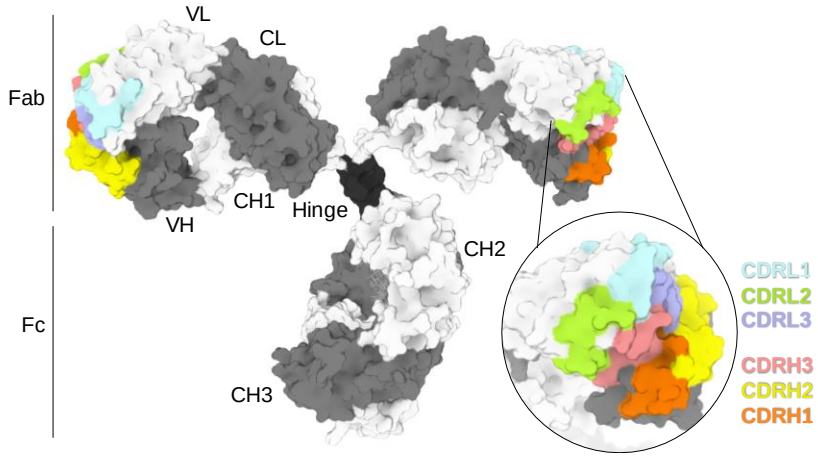

Figure 1.3. Antibodies consist of variable heavy and light chains, and constant domains.
Monomeric antibodies are composed of two sets of variable heavy chains (VH) and variable light chains (VK or VL), linked to a constant domain, forming the Fab [100]. The inset shows the antigen binding surface (paratope) which is formed by the CDRL1 (blue), CDRL2 (green), CDRL3 (lavender), CDRH1 (orange), CDRH2 (mustard) and CDRH3 (salmon). The Fab is connected by a hinge (black) to the Fc region which is composed of constant domains (C_H) [100]. This schematic is based on the structure of a murine IgG2 antibody (PDB: 1IGT).

1.5.2 Antibody genetics and VDJ recombination

Each individual has 38-46 IGHV, 23 IGHD, six IGHJ genes and nine constant genes (IGHD, IGHM, IGHG1-4, IGHA1-2 and IGHE) located on chromosome 14 [98,102]. The Ig heavy chain is the product of a recombined IGHV, IGHD and IGHJ gene (Figure 1.4, upper panel). IGHV encodes the CDRH1 and CDRH2, and the CDRH3 is at the junction of the recombined VDJ genes (Figure 1.4, lower panel, Figure 1.3, inset). The FR1, FR2 and FR3 regions are encoded by IGHV and the FR4 is a product of the IGHJ gene. There are 34-38 IGKV, five IGKJ and one IGKC gene on chromosome two, and 29-33 IGLV, 4-5 IGLJ and 4-5 IGLC genes on chromosome 22. Both the IGKC and IGLC constant chains have only one domain. The light chain is encoded by an IGKV or IGLV gene recombined with an IGKJ or IGLJ gene, respectively (Figure 1.4, upper panel). The light chain, including the FR1, CDRL1, FR2, CDRL2 and FR3 are translated from an IGKV or IGLV gene (Figure 1.3, inset). The CDRL3 is at the junction between IGKV/IGKJ or IGLV/IGLJ genes, and the FR4 is encoded by the IGKJ/IGLJ gene (Figure 1.4, lower panel, Figure 1.3, inset).

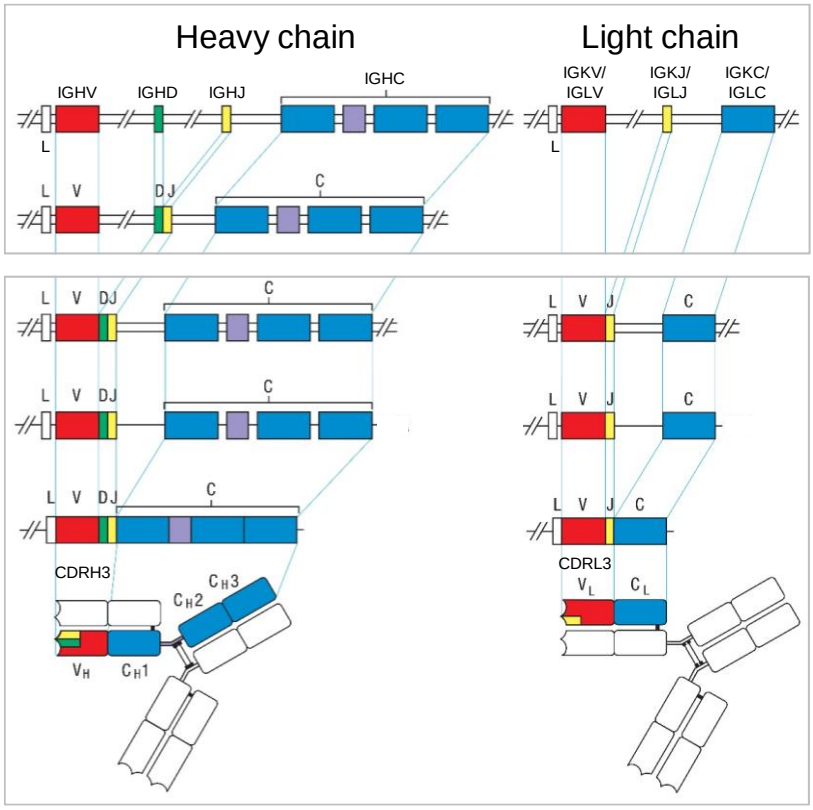

Figure 1.4. Antibodies are formed by variable and constant domains.

(Upper panel) Recombination between IGHV (red), IGHD (green) and IGHJ (yellow) forms the heavy chain. (Lower panel) The CDRH3 is encoded by the sequence at the junction of these three genes [98]. (Upper panel) The light chain consists of a recombined IGKV (red) or IGLV (yellow) gene with an IGKJ or IGLJ gene, respectively [100,103]. (Lower panel) The CDRL3 sequence is formed at the junction of these two genes [98]. (Lower panel) The heavy constant (blue) domains are formed by one of nine different isotypes while each light chain constant domain is encoded by one gene each. Figure adapted from [98].

Recombination is carried out by the VDJ recombinase set of enzymes which include RAG1/2, Artemis and terminal deoxynucleotidyl transferase (TdT) (Figure 1.5) [104,105]. RAG1/2 brings together genes for rearrangement by binding to recombination signal sequences (RSS) that flank the Ig genes (Figure 1.5) [104,105]. The DNA between the RSS and V, D and J genes is nicked resulting in the excision of the intervening DNA and the formation of hairpins [104,105]. Artemis opens the hairpins forming palindromic sequences (P-nucleotides, Figure 1.5, salmon) and TdT randomly adds or removes nucleotides (N-nucleotides, Figure 1.5, blue) at the VDJ junction before the backbone is ligated [104]. The random recombination of the heavy and light chains gives rise to $>10^6$ unique antibody configurations, and following editing by TdT, the number of unique antigen receptors in the naïve repertoire increases to $>10^{12}$ [106].

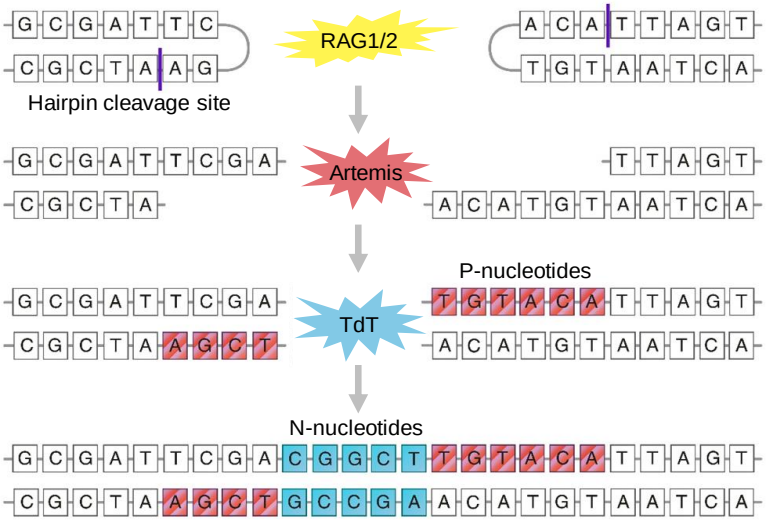

Figure 1.5. Non-templated nucleotides introduced during recombination increase receptor diversity.
During recombination, RAG1/2 (yellow) brings the antibody genes together, excises the intervening material and forms hairpins at ends of the processed genes [104,105]. Artemis (salmon) then opens the hairpins at different sites, creating short palindromic sequences (P-nucleotides, salmon) [107]. TdT (blue) inserts non-templated nucleotides (N-nucleotides, blue) between the junctions of the recombined genes [107]. Figure adapted from [108].

1.5.2.1 Antibody isotype

Humans have five classes of constant domains, including IGHD (IgD), IGHM (IgM), IGHG (IgG), IGHA (IgA) and IGHE (IgE) (Table 1.1) [102,109]. IgG is the most abundant isotype (~70%), followed by IgA (~20%), IgM (~10%), and IgE and IgD (<0.2%). IgA is monomeric (IgA1) or dimeric (IgA2) and has an affinity for FcαR (found on granulocytes and lymphocytes), FcδR (lymphocytes) and the polymeric immunoglobulin receptor (pIgR), with the latter transporting IgA and IgM into mucosae [110]. IgM is pentameric and forms immune complexes which bind

to FcμR (expressed on T-cells and macrophages) [111] and IgE has a strong affinity for FcεRI/II (on mast cells and basophils) and induces allergic responses [112]. Aside from their role during B-cell development, the function of IgD is unclear, but may contribute to allergy [113].

IgG is divided into four subclasses (IgG1-4) which recognize members of the FcγR family, including FcγRI (found on monocytes), FcγRIIa (granulocytes), FcγRIIb (lymphocytes) and FcγRIIIa/b (granulocytes and lymphocytes) [114]. Both IgG1 and IgG4 are transported into the placenta via the neonatal FcR [109,114]. IgG1 and IgG3 are typically induced by soluble and membrane bound proteins and have high strong affinity for FcγRs [109]. IgG2 is elicited by bacterial polysaccharides and binds relatively weakly to granulocytes expressing FcγRIIa and FcγRIIIa [109]. IgG4 typically appears after repeated or chronic antigen exposure and only has moderate/weak affinity for FcγRI, FcγRIIa/b and FcγRIIIa [109,115]. As such, class switching to IgG4 may be an adaptive response to attenuate immune exhaustion [115-117]. Due to weak interchain bonds, IgG4 dissociates and combine with other IgG4 antibodies, resulting in the formation of natural bispecific antibodies [109,115]. The half-lives of IgG1, IgG2 and IgG4 antibodies are ~20 days, IgG3, IgM and IgA are cleared after 5-8 days and IgD and IgE circulate for 2-3 days (Table 1.1) [98].

Table 1.1. Antibody isotypes and Fc receptors.

Fc receptor	Antibody isotype								
	IgG1	IgG2	IgG3	IgG4	IgA1	IgA2	IgM	IgE	IgD
FcγRI		-			-	-	-	-	-
FcγRIIa					-	-	-	-	-
FcγRIIb		-			-	-	-	-	-
FcγRIIIa					-	-	-	-	-
FcγRIIIb		-		-	-	-	-	-	-
FcαR	-	-	-	-			-	-	-
FcμR	-	-	-	-	-	-		-	-
Fcα/μR	-	-	-	-				-	-
FcδR	-	-	-	-	-	-		-	
FcεRI	-	-	-	-	-	-	-		-
FcεRII	-	-	-	-	-	-	-		-
pIgR	-	-	-	-				-	-
Serum (mg/mL)	9	3	1	0.5	3	0.5	1.5	0.03	<0.01
Half-life (days)	23	23	8	23	6	6	5	2.5	3
Mucosae	-	-	-	-				-	-
Placenta					-	-	-	-	-

Activity	Strong	Moderate	Weak	None

Red, yellow and green indicate strong, moderate and weak FcR binding (upper panel) or tissue transport (lower panel), respectively. Figure adapted from [98].

1.5.3 B-cell activation and the germinal center (GC) reaction

Following successful VDJ recombination and light chain pairing, immature B-cells display the Ig as a B-cell receptor (BCR) on the cell surface [118]. Since the bone marrow is devoid of foreign antigen, B-cells stimulated by self-antigen are eliminated, inactivated or their specificity edited [119]. Surviving B-cells migrate to the spleen and are again tested for autoreactivity before further differentiation into mature naïve B-cells [119]. These cells home to secondary lymphoid organs, including lymph nodes and mucosa/gut-associated lymphoid tissues (MALT/GALT) where they encounter foreign antigen [98,119]. Within lymph nodes, B-cells migrate into the outer cortex and aggregate into follicles that are supported by a network of antigen-bearing follicular dendritic cells (FDCs) (Figure 1.6) [120]. The paracortex is occupied by T-follicular helper (T_{FH}) and regulatory (T_{FR}) cells [121] and the inner medulla houses macrophages and plasma cells (Figure 1.6) [122]. Antigen rich lymph and antigen bearing dendritic cells and Langerhans cells enter draining lymph nodes via afferent vessels [122]. The lymph passes through the cortex and paracortex where antigen is trapped on the surface of cortical FDC and phagocytosed by paracortical dendritic cells (Figure 1.6) [120]. Naïve follicular B-cells that are stimulated by cognate antigen migrate to the cortex-paracortex border and are activated by T_{FH}-cells specific for the same antigen (Figure 1.6) [123,124]. Some activated B-cells differentiate into short-lived antibody producing plasma cells but most return to the outer cortex and form secondary follicles of rapidly proliferating cells (Figure 1.6) [123,124]. This follicle polarizes into a germinal center that consists of a dark zone of B-cells (centroblasts) undergoing mutative cell division and a light zone in which high affinity clones (centrocytes) are selected (Figure 1.6) [123,124]. This secondary diversification of the Ig repertoire is mediated by activation-induced cytidine deaminase (AID) which facilitates somatic hypermutation (SHM), class switch recombination (CSR) and Ig gene conversion [125].

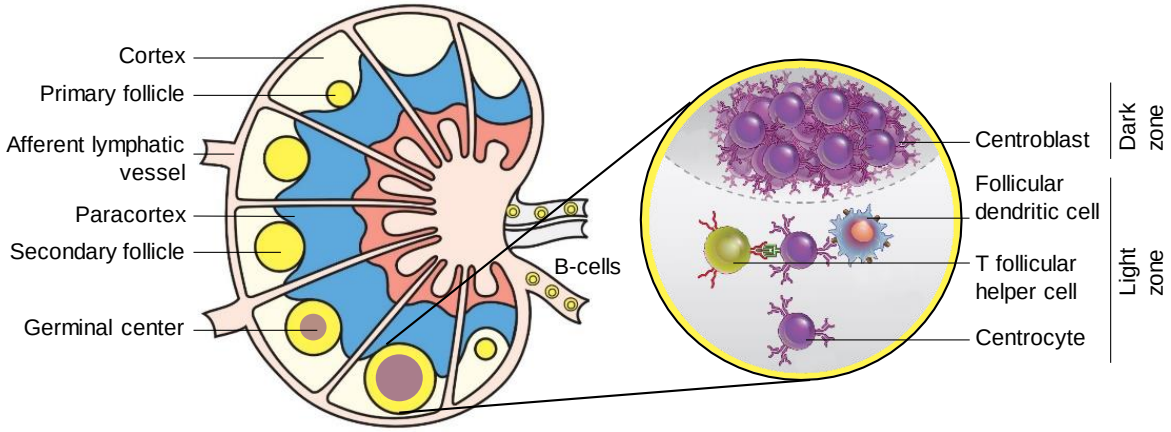

Figure 1.6. B-cells undergo affinity maturation in lymph nodes.

Lymph enters via afferent vessels and passes through the outer cortex, paracortex and medulla [98,122]. Naïve B-cells aggregate into primary follicles and engage cognate antigen on FDC [120]. Stimulated B-cells migrate to the

T_{FH}-cell rich paracortex where they are activated by cognate T_{FH}-cells [118]. These B-cells proliferate in the cortex and form secondary follicles and differentiate into plasma or memory cells [126]. Some cells continue to proliferate and form germinal centers that polarize into a dark zone of centroblasts and a light zone of centrocytes [124]. Centroblasts rapidly proliferate, undergo SHM and migrate to the light zone as centrocytes to compete for antigen and T_{FH}-cell help [125]. Figure adapted from [98].

1.5.3.1 Secondary diversification

The activity of AID is semi-random due to the presence of hot-spot (WRCH/Y and WA, where W=A/T, R=A/G, H=A/C/T and Y=C/T) and cold-spot (SYC) motifs distributed unevenly throughout the Ig variable genes [125,127,128]. The probability that a particular amino acid substitution may occur is dependent upon the local nucleotide sequence and the number of mutations required for the specific non-synonymous change [125,127,128]. Accordingly, improbable mutations occur in AID cold-spots and require multiple base changes, while probable mutations arise in AID hot-spots where only one base change is necessary [125,127,128].

AID is active in centroblasts where it initiates SHM by removing an amine group from cytidine, thereby converting the base into uracil, resulting in a U:G mismatch [125,129]. Depending on how this lesion is handled, single or multiple transition and transversion mutations can be introduced which lead to one mutation per 1000 bases per cell division [125,129]. Since uracil is treated as thymine, transition substitutions occur during DNA replication (Figure 1.7, left branch) [125,129]. Alternatively, transitions and transversions arise when uracil is excised from the deoxyribose backbone by uracil-DNA glycosylase 2 (UNG2) as any nucleotide can be inserted opposite the abasic site during DNA synthesis (Figure 1.7, middle branch) [130]. In addition, if the MSH2/6 mismatch repair protein complex recognizes the lesion, it drives the excision of both uracil and the adjacent bases which are subsequently filled by error prone polymerases (Figure 1.7, right branch) [129].

If the activity of UNG is followed by apurinic/apyrimidinic endonuclease 1, the abasic site is excised leaving a single-stranded nick. This discontinuity can be resolved through homologous recombination resulting in gene conversion, with neighboring IGHV genes replacing the original antibody genes [125]. CSR or isotype switching, which can happen multiple times, occurs as AID activity in GC rich regions often leads to double stranded breaks that can result in non-homologous recombination with adjacent constant genes [131]. Stretches of GC repeats are found in the intronic switch regions between IGHJ and IGHM, and the remaining constant region isotypes [131]. The double-stranded break repair complex brings together the

discontinuous switch regions and the intervening DNA is excised, and the deoxyribose backbone ligated [131]. Cytokines secreted by T_{FH}-cells, dendritic cells and macrophages determine the nature of the class switch isotype [129,131]. For example, IL-4 drives switching to IgG1, IgG4 and IgE, IL-5 and TGFβ to IgA, IFNγ and IL10 to IgG3 [114,129,131]. Conversely, switching to IgG3 is inhibited by IL-4 and TGFβ, and IFNγ blocks IgG1 and IgE switching [114,129,131].

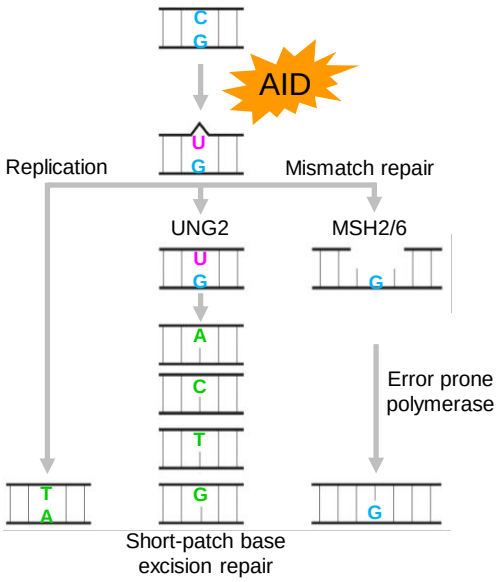

Figure 1.7. AID creates lesions that are repaired by error prone pathways.
AID typically deaminates cytosine in WRCY, WRCH and WA motifs, resulting in U:G mismatches [129]. (Left branch) During replication, U is treated as T and is therefore paired with A in the nascent strand [129]. (Middle branch) Alternatively, during short-patch base excision repair, UNG2 excises U, which is replace with any nucleotide during replication [130]. (Right branch) If MSH2/6 recognizes the mismatch, U and surrounding bases are excised and filled in by error prone polymerases [129]. Figure adapted from [129].

1.5.3.2 Affinity maturation

Most of the mutations that arise during SHM impair the ability of the centroblast to bind antigen and these cells are eliminated as they fail to compete for antigen and survival signals [118,123,124]. In contrast, B-cells with improved antigen affinity survive and transition into centrocytes and move into the light zone [118,123,124] (Figure 1.6). Here the centrocytes compete for antigen and T_{FH}-cell help which ensures that only high affinity clones survive. Some cells differentiate into plasmablasts or memory cells while other centrocytes re-enter the dark zone and the cycle of SHM and selection is repeated, further improving antigen specificity and affinity [118,123,124] (Figure 1.6). This cyclic re-entry can occur many times as the sequence of some antibodies diverges by as much as >40% from the unmutated rearranged germline sequence [132,133]. Most mutations accumulate in the CDRs as they form the

antigen-binding surface, and because the FR are critical to the antibody structure, they are more sensitive to substitutions [101].

1.6 Antibody-mediated effector functions

Antibodies activate antimicrobial effector functions via interactions between the Fc and FcRs on lymphocytes and innate immune cells [109]. FcRs vary in their ability to activate or inhibit cellular effector functions and are distributed unevenly across immune cells [134]. Furthermore, FcRs have variable affinities for each isotype and so antibodies with the same specificity but different isotype can mediate diverse effector functions (Table 1.1) [134].

These functions include phagocytosis [135], cytotoxicity [136], trogocytosis [137] and complement deposition [138]. Antibody-dependent cellular phagocytosis (ADCP) occurs when IgG and IgA coated antigen binds to the FcγR and FcαR, respectively, on monocytes, macrophages, neutrophils and eosinophils [135]. This stimulates antigen internalization and destruction by proteolysis and reactive oxygen and nitrogen species [135]. In addition, antigen bound by IgG1 and IgG3 activates FcγRIII expressing cytotoxic cells, including NK cells and neutrophils leading to antibody-dependent cellular cytotoxicity (ADCC) [136,139]. Fc binding enhances the contact between the target and effector cells, and the latter releases perforin and granzyme B into the cellular junction [136]. Perforin pierces the plasma membrane of the target cell allowing granzyme B to enter and activate caspases, resulting in apoptosis of the infected cell [136]. Furthermore, IgG binding to the FcγR on effector lymphocytes can initiate antibody-dependent cellular trogocytosis (ADCT), whereby fragments of the plasma membrane from the target cell are transferred to the surface of the effector cell, resulting in the death of the donor cell [137]. In addition to the recruitment of effector cells, antibodies can trigger antibody-dependent complement deposition (ADCD) via the classical complement cascade upon engagement with antigen, resulting in lysis [138,140]. IgG1 and in particular IgG3 have a strong affinity for the activating FcγRs (FcγRI, FcγRIIa and FcγRIIIa), which potently mediate ADCP, ADCC and ADCT and ADCD [141,142]. In contrast, IgG2 and IgG4 have a poorer affinity for the activating FcγRs and IgG4 can block effector cell activation due to its binding of the inhibitory receptor FcγRIIb [134].

Antibody dependent cell-mediated responses and FcRs are associated with altered disease progression and HIV-1 transmission. For example, homozygosity for a low affinity allele of FcγRIIa is associated with accelerated disease progression [143] and there is a decreased risk of vertical transmission in mothers expressing a high affinity allele of FcγRIIIa [144].

Furthermore, broad ADCC responses are associated with slower T-cell decline and delayed disease progression [145,146]. In contrast, IgG4 class switching may be more common in chronically infected individuals, particularly in rapid progressors [107,147–149].

1.7 The humoral response to HIV infection

The first HIV-specific antibodies appear ~8 days after viremia is detected and consist of polyspecific IgM [150]. Approximately 5 days later, non-neutralizing gp41-specific IgG antibodies arise and ~15 days thereafter V3-specific IgG responses are detected [150,151]. While IgM titers are moderate and wane after a few months, IgG remains elevated throughout infection [148,150]. Although a vigorous humoral response develops, neutralizing antibodies have little impact on the outcome of the infection [152–156].

By six months post infection most individuals develop antibodies that neutralize viruses from that same person (autologous viruses) [157]. Although the potency of autologous responses may increase over time, these antibodies often remain strain-specific, failing to neutralize viruses isolated from other individuals (heterologous viruses) [153,157]. However, over two to five years of infection, 20-30% of infected individuals gradually develop antibodies that potently neutralize >80% of heterologous viruses [152,153,158–161]. The broadly neutralizing phenotype is associated with high viral loads, high viral diversity and low CD4+ T-cell counts [160,162]. Although ADCT and ADCD responses are higher in bNAb producing individuals [163], broad and potent neutralizing antibodies do not impact the course of the infection nor the progression to AIDS [152–156].

1.7.1 Broadly neutralizing antibodies (bNAbs)

Monoclonal broadly neutralizing antibodies (bNAbs) that potently neutralize heterologous viruses have been recovered from individuals with broad plasma [164]. The first bNAbs, isolated using hybridomas and phage display libraries, neutralized 41-98% of heterologous viruses, with an average potency of ~2 μg/mL [165,166]. With the subsequent development of high-throughput neutralization assays and antigen-specific B-cell flow cytometry >100 bNAbs have been isolated (hiv.lanl.gov/catnap). By mapping bNAb epitopes, relatively conserved sites spanning almost the entirety of Env have been identified [160,167,168]. These regions of vulnerability, which represent potential vaccine targets, include the membrane proximal external region (MPER), gp120-gp41 interface, fusion peptide, N332 supersite, silent face, CD4 binding site (CD4bs) and the V1V2 apex [160,167,168].

1.7.1.1 The membrane proximal external region (MPER)

The bNAbs that target the MPER are highly somatically mutated (18-27%) and exhibit modest potency (0.25-3.41 μg/mL) [169,170]. In addition, these bNAbs are amongst the broadest (>98%) due to the conserved sequence of the MPER [169,170]. The MPER-targeting bNAbs DH511.2 [171], 10E8 [172] and 4E10 [165] (Figure 1.8 A) recognize discontinuous residues in the C-terminus of the MPER and 2F5 [165] and z13e1 [173] target linear epitopes at the N-terminus [169,174]. Long (20-24 aa) hydrophobic CDRH3s, common in this class of bNAb [175,176], enables these antibodies to access membrane associated epitopes. Consequently, these antibodies are frequently autoreactive due to their affinity for self-derived lipids [170] and B-cells with such specificities are often deleted/edited during tolerance checkpoints [169,170].

1.7.1.2 The gp120-gp41 interface and fusion peptide

Many bNAbs that target the interface between gp120 and gp41 are variably dependent on glycans, including N276 (PGT151 [177] and 8ANC195 [178]), N234 (35O22 [179] and 8ANC195) and N88 (35O22) (Figure 1.8 B). Long CDRH3s (PGT151) or FR3s (8ANC195 and 35O22 [178–180]) contact and penetrate the glycan shield and bind to epitopes in both gp120 and gp41, including in C1, loop D, C3, C5, V4, V5 and gp41 [178–180]. In addition, the gp41-gp41 interface is targeted by bNAbs 3BC176 and 3BC315 (Figure 1.8 B) which induce gp120 shedding by accelerating trimer destabilization [181].

Binding in the vicinity of each other, the footprint of the bNAbs that target the fusion peptide overlap with those of the interface antibodies [182–184]. The fusion peptide bNAbs VRC34.01 and ACS202 (Figure 1.8 B) [182–184] contact the fusion peptide with their CDRH3s [182,183,185].

1.7.1.3 The N332 supersite

Many antibodies target the N332 glycan and the nearby mannose glycans which shield the CCR5 binding loop at the base of the V3 (Figure 1.8 C) [186]. N332-specific bNAbs are typically modestly mutated, broad, potent and have long CDRH3s (20-26 aa) [68,161,165,187,188]. The PGT121, PGT128, PCDN and DH270 class of bNAbs primarily contact the N332 and N301 glycans and bind to the conserved V3 GDIR motif [68,161,165,187,189] (Figure 1.8 C). PGT128 and DH270.1 bind perpendicular to the trimer, PGT135 approaches parallel to V3 and

PGT124 binds between PGT128 and PGT135 [187] (Figure 1.8 C). PGT135 and 2G12 do not contact the GDIR motif, and 2G12, a product of an IGHV domain swop, does not breach the glycan shield and contacts N295, N332, N339 and N392 [161,165] (Figure 1.8 C). Due to the divergent modes of recognition, multiple angles of approach and variable glycan dependencies, this region is considered a “supersite” [167] and is an attractive vaccine target [71].

1.7.1.4 The silent face

Recently, bNAbs have been identified that target the densely glycosylated silent face adjacent to the CD4bs between the N332 supersite and the gp120-gp41 interface [64,65]. The paratope of the silent face bNAb VRC-PG05 [190] primarily consists of the long CDRH3 and CDRL1 (both 17 aa) which wedge between the N262, N295 and N448 glycans and contact residues in C2 and C4 (Figure 1.8 C) [190]. In contrast, the CDRH3 (23 aa) and CDRL1 (8 aa) of the silent face bNAb SF12 [191] form a pocket to accommodate the N448 glycan and contact sites in C1, C2 and C4 (Figure 1.8 C) [191]. It is estimated that VRC-PG05-like specificities are present in 10% of infected individuals [190].

1.7.1.5 CD4 binding site (CD4bs)

Since the CD4bs is highly conserved the bNAbs that target this site are very broad (80-98%). Many are encoded by the VH1-2 (“VRC01-class”) or VH1-46 (“8ANC131-class”) genes [192] (Figure 1.8 D). These bNAbs contact the CD4 binding loop and CD4bs via the CDRH2 and FR3, respectively [193] (Figure 1.8 D). To avoid clashes with the loop D and N276 glycan, the CDRL3s of VRC01-class antibodies are short and pivot, and the CDRL1 acquires deletions or substitutions [194]. In contrast HJ16 [195] and the PCIN63 lineage [196] are dependent upon the N276 glycan. In addition to the VH-restricted bNAbs, those derived from unrelated genes, such as CH103 [197] and VRC13 [192] bind to the CD4bs via long CDRH3s (13 and 21 aa, respectively) from an angle that is similar to CD4 (Figure 1.8 D). Although CD4bs bNAbs generally lack substantial autoreactivity and are extremely potent they are extensively somatically mutated (>40%) [132].

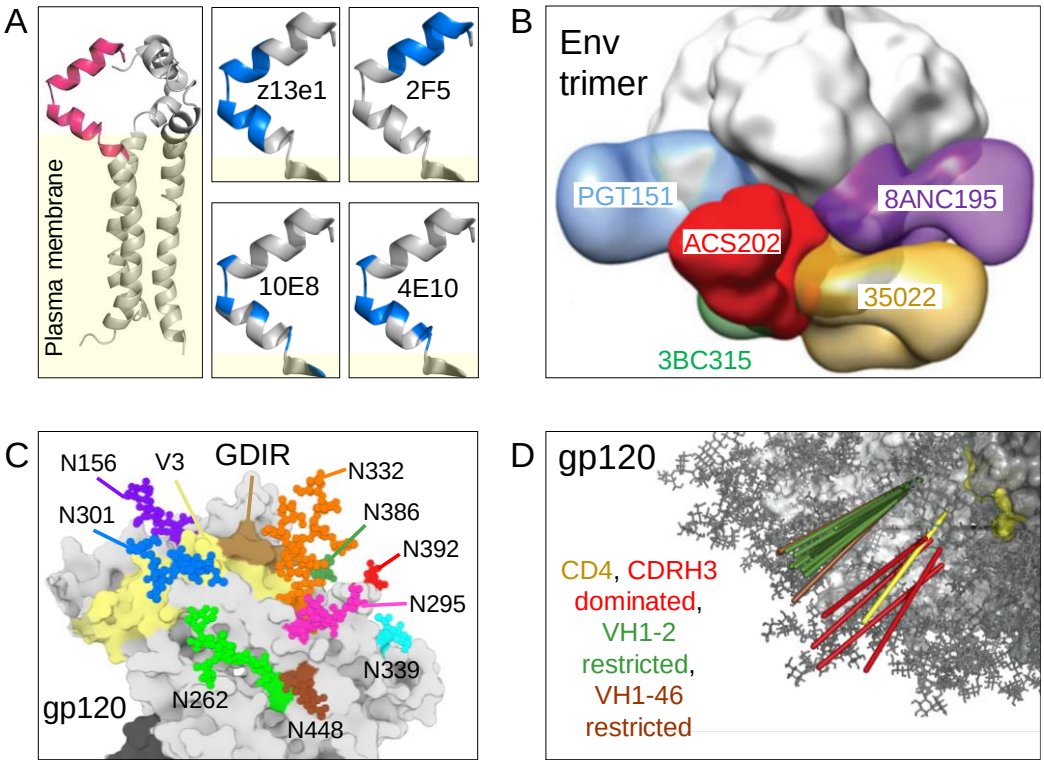

Figure 1.8. Targets of broadly neutralizing antibodies

(A) BNAbs that target the MPER (pink) often interact with the self-derived lipid membrane (yellow) [198]. The MPER-specific bNAbs 2F5 and z13e1 recognize continuous epitopes (blue), while 10E8 and 4E10 bind to discontinuous sites (blue) [174]. Figure adapted from [174]. (B) The bNAbs that target the interface and fusion peptides have overlapping epitopes and shared angle of approach [183]. (C) Most N332 supersite-specific bNAbs recognize the GDIR motif (tan, which interacts with entry co-receptors) and are dependent on glycans in and around the V3 loop (yellow), including N332 (orange), N295 (pink), N301 (blue), N339 (cyan), N386 (green), and N392 (red) [186]. (D) The CD4bs (mustard) of gp120 is targeted by bNAbs that share genetic (VH-restricted) and/or structural (CDRH3 dominated) similarities, figure adapted from [192].

1.7.1.6 Variable loops 1 and 2 (V1V2)

The trimer apex is formed by the convergence of the distal V1V2 loops which creates a quaternary epitope that is absent on gp120 (Figure 1.9 A and B) [167]. Therefore, V1V2 bNAbs, including PG9 [199], PG16 [199], CH01-04 [200], PGT141-145 [161], PGDM1400 [201], N90 [202], PC64 [203] and the CAP256-VRC26 lineage [204,205] generally only recognize native closed trimers. These antibodies are typically not autoreactive, are moderately somatically hypermutated (12-17%) and extremely potent [132,160,168]. In addition, V1V2-targetting bNAbs are variably dependent on glycans at N156, N160 and N173 (Figure 1.9 B) and have unusually long anionic CDRH3s (24-37 aa, Figure 1.9 C-E) [206,207]. This allows the tip of the CDRH3 to lie alongside cationic residues in strands B and C, including R166, D167, R/K168, K169 and K171 (Figure 1.9 C-E) [206,207]. Furthermore, PG9 [199], PG16 [199] and the CAP256-VRC26 lineage [204,205] share the 3-3*01 IGHD gene which encodes a Tyr sulfated YYD motif at the tip of the CDRH3 [205,208,209].

The orientation and conformation of the CDRH3s of V1V2 bNAbs vary considerably [207]. For example, the CDRH3 of PG9 and PG16 [208,209] forms a flat bifurcated hammerhead (Figure 1.9 C), the CDRH3 of PGT145 [210] is upright and perpendicular to the antibody and the CDRH3 of CAP256-VRC26.25, CAP256-VRC26.09 and CH04 is elongated and has a right-angle bend [206,207] (Figure 1.9 D and E). In contrast to the prototypical V1V2 bNAbs described above, N90 [202] has an average length CDRH3 and makes side-chain contacts, thereby reducing the distance the CDRH3 must traverse.

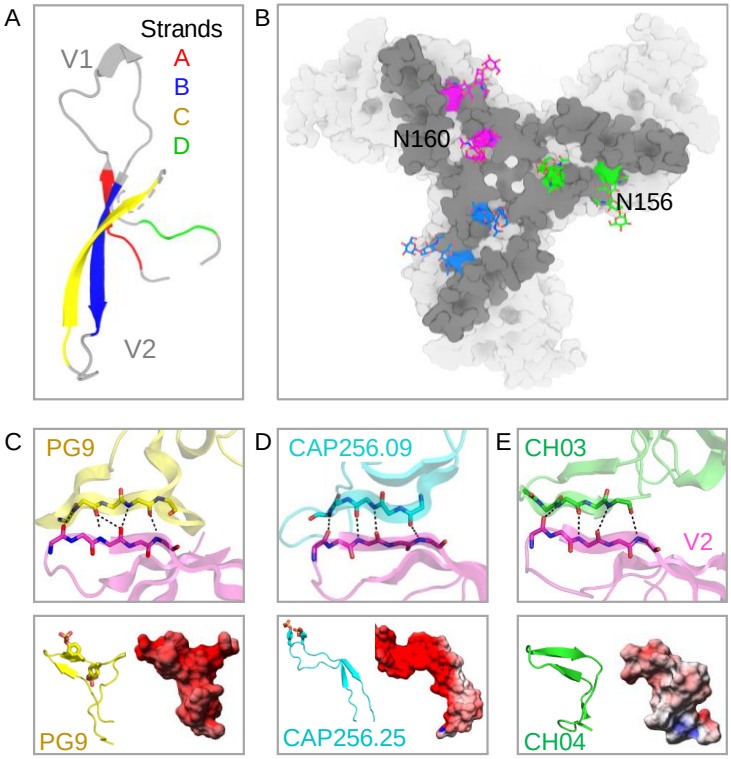

Figure 1.9. The V1V2 loops form a quaternary epitope at the trimer apex.

(A) The V1V2 at the distal end of each protomer form a quaternary epitope in (B) trimerized Env (dark grey) [167]. (A) Strands A-D (colored) intersperse hypervariable loops (grey) [64,65]. (B) The N156 and N160 glycans on BG505 SOSIP.664 (PDB: 5ACO) [211] are shown as sticks and colored differently on each protomer, this trimer lacks the N173 glycan. (C-E) The interaction between V2 (pink) and (C) PG9, (D) 256.09 and (E) CH03 are shown above the conformation of the PG9, 256.25 and CH04 CDRH3s, figure adapted from [207].

1.8 The ontogeny of bNAbs

Since bNAbs exhibit exceptional *in vitro* neutralization breadth and potency, and *in vivo* protection (see 1.9.3), it is believed that a vaccine capable of inducing these antibodies would prevent HIV-1 infection [164,212-215]. Central to this strategy is defining the steps from the activation of a bNAb ancestor to the co-evolution with autologous viruses and the development

of breadth [158,160,215–219]. As the first generation bNAbs [165,166] were isolated from cross-sectional samples, the paucity of sequence data precluded the reliable inference of germline precursors due to the extensive edits at the IGHD junctions [132]. Consequently, "germline-revertants" were designed which retained their mature CDRH3 and CDRL3 [160]. However, native CDRs can be inferred from longitudinal sequences, allowing for the reconstruction of an unmutated common ancestor (UCA) of a bNAb lineage [197]. In addition, the identification of contemporaneous viruses sensitive to the UCA ("bNAb initiating Env") and intermediates allows for the establishment of bNAb ontogeny. To date, the developmental pathways of eight bNAb lineages have been elucidated and include those for the CH103 [197], CH235 [220], DH270 [187], PCDN [189], BF520.1 [221,222], PCT64 [203], PCIN63 [196] and CAP256-VRC26 [204,205,223] lineages. Together with other studies [171,178,193,194,197,200,224–247] several common features of bNAb maturation have been identified which has informed vaccine design [158,160,215–219].

1.8.1 Common factors in the development of breadth

1.8.1.1 Helper lineages

The co-operation between antibody lineages has been shown to have directed the development of breadth in two individuals [187,197,220]. An antibody "helper lineage" is one that drives viral escape mutations which sensitize the virus to an unrelated antibody lineage. The CH103 and CH235 lineages, isolated from donor CH505 [197,220] bound to overlapping epitopes in the CD4bs, but mutations rapidly evolved in loop D which lead to escape from the CH235 antibodies. However, these mutations increased the sensitivity of the viruses to the CH103 antibodies which drove the maturation of this lineage [197,220]. Similarly, the DH270 bNAb lineage, recovered from CH848, developed with the co-operation of two unrelated B-cell families (DH272 and DH475) that targeted overlapping epitopes [187]. Although DH270 could not bind to the T/F, the DH272 and DH475 antibodies were reactive with this virus, and drove escape by decreasing the length of V1 which resulted in sensitivity to the DH270 lineage [187].

1.8.1.2 Viral diversification

Another common feature in bNAb maturation, which has been observed in the CH103 [197], CH235 [220], PCT64 [203] and CAP256-VRC26 [204,205,223] lineages, is extensive viral diversification in and around bNAb epitopes immediately prior to the development of breadth [248]. This exposes maturing lineages to novel epitope variants ("immunotypes") and breadth emerges as the paratope evolves a decreased dependence on mutable sites and is instead focused on conserved epitopes [193,197,225,227,228,230,232,234,249]. Since breadth

typically develops after two years, this protracted co-evolution accounts for the extensive affinity maturation that is characteristic of most bNAbs.

1.8.1.3 Antibody structure

No differences have been identified between the germline IGHV repertoires of individuals that develop bNAbs compared to those that do not [250]. In addition, besides CD4bs bNAbs [192] and some N332-targetting antibodies [251], gene usage amongst bNAbs is not restricted. However, bNAbs do share structural and functional similarities, particularly within classes. These include unusually long [199,203–205] or short [194] CDRs with increased hydrophobicity [175,176] or electronegativity [199,203–205] and rigid FR regions [252].

Despite a strong positive association between SHM and neutralization, modestly somatically mutated bNAbs [221,253] and highly mutated strain-specific antibodies [223] have been identified. For example, bNAbs BF520.1 [221,222] and AIIMS-P01 [253] are <7% mutated, which is within the range induced by vaccination [219,254–256], but are >50% broad. In contrast, strain-specific "off-track" antibodies, which are extensively mutated and closely related to broad lineage members have been recovered from several individuals [197,201,223,242,244]. For example, while PGDM1400 (83% breadth), is closely related to PGDM1406, the latter exhibits only limited breadth (6%) [201]. Similarly, within the PGT121 lineage, two heavy chains (6H and 22H) were recovered that when paired with a light chain display no neutralization despite a high degree of sequence identity to broad members [242]. In addition, 1AZCETI5, a member of the CH103 lineage, shares the same CDRH3 length and degree of SHM with CH103, but 1AZCETI5 lacks breadth [197]. Since antibody isolation techniques are optimized to recover bNAbs, the proportion of off-track members in these bNAb lineages is unknown, but may be as high as 40% [244].

1.8.1.4 The germinal center reaction

The frequency of HIV-specific T_{FH}- and T_{FR}-cells [257–259], AID activity [163] and the cytokine milieu [257] in the germinal center reaction are associated with anti-HIV humoral responses. This relationship is informed by the observation that children, which develop broader and more potent antibodies, and more rapidly, compared to adults, have a greater magnitude of T_{FH}- and T_{FR}-cells [221,253,260,261]. In addition, the T_{FH}-cells in children secrete more IL-21 compared to adults, which increases the magnitude and quality of the T_{FH}- and T_{FR}-cells [257].

1.9 Vaccines

Vaccination has profoundly decreased the morbidity and mortality associated with many infectious diseases, including diphtheria, mumps, measles, pertussis, tetanus, hepatitis A/B, *Haemophilus influenza*, varicella, polio, rubella, and in the case of smallpox, complete eradication [262–264]. Protection against these diseases is primarily mediated by neutralizing antibodies [265,266] which are induced, alongside cellular responses, by vaccination with attenuated pathogens, inactivated pathogens or acellular components [267]. To strongly activate the innate immune system which drives a robust adaptive response, antigens can be conjugated to highly immunogenic polysaccharides [268] and co-administered with adjuvants [269], such as alum. Furthermore, the induction of durable, high titer neutralizing antibodies can be achieved by boosting the response to the primary vaccination with subsequent boosts [270]. In addition, the elimination of intracellular pathogens, such as *Mycobacterium tuberculosis* and *Plasmodium falciparum* require robust CD8 T-cell responses [271]. These can be elicited by vaccination with infectious vectors or nucleic acids that encode pathogen-associated peptides [271]. Furthermore, the passive administration of antigen-specific antibodies can prevent infection or treat diseases [272]. For example, palivizumab, targets the human respiratory syncytial virus and protects susceptible infants from infection [273], and enterovirus, parvovirus and ebola infections are successfully treated with immunoglobulins [272,274,275].

1.9.1 HIV-1 vaccine trials

The initial optimism that an HIV vaccine would be rapidly developed has waned during the decades since the virus was discovered and the completion of more than 200 vaccine trials [276]. Early HIV vaccines designed to induce humoral responses consisted of virus-like particles, structural and enzymatic proteins, trimers, monomers and peptides [276]. While these immunogens were well-tolerated, only laboratory adapted strains (tier 1A viruses) were sensitive to neutralization, while difficult to neutralize primary viruses (tier 2 and 3) were resistant [276,277]. Nevertheless, two phase III trials (VAX003 [278], and VAX004 [279]) were set up to test the efficacy of a subtype matched bivalent gp120 vaccine. While vaccinees developed HIV-1 specific responses [278–280], the vaccines failed to protect against infection or delay disease progression [278,279]. Furthermore, likely due to repeated vaccinations, the VAX003 participants developed high IgG4 titers which may have contributed to the failure of the trial since IgG4 poorly mediates neutralization and effector functions [281].

An alternative strategy was tested in phase IIb trials (STEP [282] and Phambili [283]) where participants were vaccinated with a replication-defective recombinant adenovirus expressing subtype B Gag, Pol and Nef. Most vaccinees developed HIV-specific T-cell responses, which in some individuals exerted pressure on founder viruses [284] and may have reduced viremia [285]. However, the vaccine failed to protect against infection, and in a subset of vaccinees, increased the incidence of infection [282,283]. A similar lack of efficacy was observed in the HVTN 505 phase IIb trial [286] where a DNA prime and adenovirus boost was tested. In contrast, a recombinant canarypox vector [287] and protein boost was found to elicit both CTL and binding and neutralizing antibodies in phase II trials [288,289]. The success of this combination lead to the phase III RV144 trial [290], where a subtype matched canarypox vaccine (Gag and gp120-gp41) boosted with the VAX003 immunogen (AIDSVAX B/E) was found to be modestly protective [290]. The vaccine exhibited 60% efficacy after one year and 31% after 42 months, but did not affect viremia or CD4 T-cell count in infected individuals [290]. The risk of infection for RV144 vaccinees was inversely correlated with the titer of ADCC-mediating V1V2-specific IgG1 and IgG3 binding antibodies [281], and positively correlated with Env-specific IgA titers [291]. Subsequently, the phase IIb/III HVTN 702 trial [292] was initiated in South Africa with a subtype C matched RV144 regimen. Discouragingly, during a recent interim review, the HVTN 702 vaccine was found to be safe but non-efficacious [293].

1.9.2 Novel Env-based immunogens

The failure of the first generation of proteinaceous vaccines was largely because the humoral responses were transient, strain-specific, weakly neutralizing and non-functional [294–297]. This was partly due to modifications made to improve Env stability, such as cleavage site deletion [298], the inclusion of peptide bonds [299], or the use of gp120 or gp160, which introduced non-native epitopes, thereby limiting or abrogating responses to relevant sites.

1.9.2.1 Native-like trimeric Env

More recently, modifications have been identified that allow for the expression of stable, soluble, glycosylated trimers which closely resemble the closed conformation of pre-fusion native Env [300–304]. For example, the introduction of a disulfide bond (SOS gp140) between gp120 and gp41 [305], an I559P mutation (SOSIP gp140) in gp41 [306] and truncation of MPER at residue 664 (SOSIP.664) [62] improves stability, trimerization and solubility, respectively. In addition, flexible links [303], increased number of hydrophobic, aromatic and charged residues, as well as cysteine, glycine and proline substitutions [307–309], further

improves stability. These adjustments have been applied to other trimers, including BG505, KNH1144, 16055, Du422, ZM197M, B41 and JRFL [62,303,310–312].

Crucially, bNAbs bind to these trimers while non-neutralizing antibodies, that target non-native epitopes, are substantially less reactive [303,304,310]. Mice [313,314], guinea pigs [315–318] and rabbits [313,314,318–326] immunized with near-native trimers typically develop autologous tier 2 neutralizing antibodies but potent heterologous responses rarely evolve [319,323,327–330]. Although rhesus macaques typically develop similar, albeit weaker responses compared to small animals [320,324,330], bilateral immunizations and extended vaccination schedules can elicit high titer autologous tier 2 antibodies [331].

1.9.2.2 Germline-targeting immunogens

The inability to reliably induce broad responses is exemplified by the failure of antigens to engage bNAb precursors constituted as BCRs [224–226]. However, glycan and variable loop deletions reduce steric hindrance thereby improving epitope accessibility which enhances *in vitro* BCR-antigen affinity [227]. Such studies have informed the design of germline-targeting immunogens such as eOD-GT8 [332,333] and BG505 SOSIP-GT1 [334], which activate naive VRC01 precursors in transgenic mice. Furthermore, neutralizing responses against native glycosylated BG505 SOSIP-GT3 evolved following an eOD-GT8 prime and BG505 SOSIP-GT3 boost [335]. In addition, N332 supersite germline-targeting immunogens, such as BG505 SOSIP 11MUT$_B$ (which has an N332 deletion), activate PGT121 precursors in transgenic mice, and boosts with increasingly native trimers elicit heterologous tier 2 neutralizing antibodies [233,336]. Further modifications to 11MUT$_B$ (RC1) allowed for the induction of antibodies in rhesus macaques with CDRH3s and light chains similar to germline PGT121 and 10-1074 [337]. Moreover, creating “glycan holes” through the deletion of V1V2 glycans has led to the development of V1V2-specific neutralizing responses in wild-type rabbits [325].

Importantly, the frequency of VRC01-class precursors in humans may be as high as 23 cells per lymph node [338], N332-specific BG18-like naïve B-cells have been identified in unimmunized people [339] and ~0.4% of naïve B-cells in humans may have very long CDRH3s that are common in V1V2-targetting bNAbs [216]. In addition, germline-targeting immunogens can drive the selection of improbable neutralization-conferring mutations in knock in mice and wild-type rhesus macaques [340].

1.9.3 Passive immunization

The value of bNAbs is highlighted by the success of passive infusions that protect animals against SHIV/HIV (HIV Env pseudotyped SIV) infection, reduce viremia, minimize latent infection and clear infected cells [341–350]. Passive immunization for prevention and treatment [351] become feasible following the discovery of potent bNAbs, including PGT121, VRC01 and 10E8 [342,352]. In particular, compared to the first generation bNAbs, ~300-fold less of the exceptionally potent CAP256-VRC26.25 is sufficient to protect rhesus macaques from infection [344]. If used for prophylaxis, complementary combinations of bNAbs [343], and/or bispecific/trispecific molecules [353] may be necessary to offer maximum protection and inhibit the evolution of resistance. In addition, the half-lives and protective efficacy of bNAbs can be improved through modifications to the Fc domain [354,355]. For example the M428L and N434S (LS) mutations increase the affinity of the Fc to the Fc neonatal receptor which modulates IgG homeostasis and mucosa localization [354,355]. Compared to VRC01, the VRC01-LS variant has a longer duration of efficacy and is superior in protecting against intrarectal challenges [345]. Numerous human trials have been initiated to test the safety and efficacy of bNAbs, including the phase IIb HVTN 703 and 704 trials testing the ability of VRC01 to prevent infection [356]. In humans, bNAb monotherapy (VRC01 or 3BNC117) [357] or dual-therapy (3BNC117 and 10-1074) [358] delay viral rebound following treatment interruption.

1.10 The HIV infected donor, CAP256

Between 2004 and 2005, a cohort of HIV negative high-risk women was established in KwaZulu-Natal, South Africa, by the Centre for the AIDS Programme of Research in South Africa (CAPRISA) [359]. An African woman, CAP256 was enrolled in the CAPRISA 002 acute infection cohort in 2005. Six weeks later CAP256 was found to be HIV positive and she was superinfected 13-15 weeks thereafter [360]. Both the primary infecting virus (PI) and the superinfecting virus (SU) were subtype C [360].

1.10.1 The neutralization breadth, potency and specificity of CAP256 plasma

Autologous neutralizing responses were detected in the plasma of CAP256 6-10 months post infection (pi) and heterologous breadth (17%) developed by 1 year pi [157]. Breadth increased during the second (52%) and third (76%) years pi and plateaued thereafter [360] (Figure 1.10). At 3 years pi, 88% and 83% of subtype C and subtype A viruses, respectively, were neutralized while 50% of subtype B viruses were sensitive [360]. The median titers for subtype C (1:968) and subtype A viruses (1:658) were particularly potent, with titers against CAP210, ZM53 and

CAP45 above 1:10,000 [360]. While plasma neutralization was not impacted by gp120 or gp145 absorptions [153], mutations in V2, particularly at R166 and K169, knocked out neutralization. In addition, the epitope included F159, N160, L165, D167 and K171, and the fine specificity changed over time, as greater tolerance for variation at these sites developed [153,360]. Generally, sensitive viruses share a motif in V2 ($F_{159}N_{160}L_{165}R_{166}D_{167}K_{169}K_{171}$) that is common to subtype C and A viruses, but less represented in subtype B viruses [360].

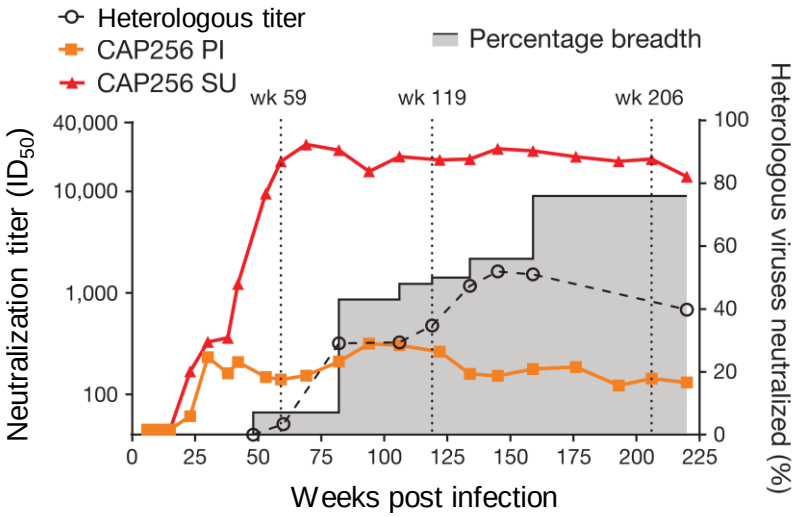

Figure 1.10. CAP256 gradually developed neutralization breadth over three years.

Donor CAP256 was superinfected (SU, red) with a subtype C virus 13-15 weeks after primary infection (PI, orange) [360]. Within weeks of infection autologous neutralization was detected, with titers against the SU remaining high throughout infection [360]. Heterologous neutralization developed by 1 year pi, and breadth and potency increased each year until the fourth year, where breadth was maintained but potency waned [360]. Figure adapted from [205].

1.10.2 The CAP256-VRC26 bNAb lineage

A 33 member clonal lineage of V2-specific antibodies, the CAP256-VRC26 lineage (hereafter referred to as CAP256.01-33) was recovered from CAP256 by B-cell culture and antigen-specific (BG505 SOSIP.664) B-cell sorting [204,205]. The antibodies were isolated from PBMC from 59 (CAP256.01), 119 (CAP256.02-09 and CAP256.14-18), 159 (CAP256.26-33), 193 (CAP256.22-25) and 206 (CAP256.10-13 and CAP256.19-21) weeks pi [204,205] (Figure 1.11, left). The sequence of the CAP256.UCA was inferred and closely related sequences were identified 34 weeks pi [205]. The heavy chains are 4-17% divergent from the CAP256.UCA and are encoded by the IGHV3-30*18, IGHD3-3*01 and IGHJ3*02 genes [204]. The light chains utilize IGLV1-51*02 and IGLJ1*01 and are 4-15% somatically mutated compared to the germline sequence [204]. The breadth of the lineage members ranges from 63% (CAP256.25) to 2% (CAP256.20) and the potencies from 0.003 µg/mL (CAP256.25) to 5.00 µg/mL (CAP256.07) (Figure 1.11, right) [204]. In addition to bNAbs, the lineage contains “off-track”

antibodies, which failed to acquire substantial heterologous breadth, despite a high degree of sequence identity with the bNAbs [204,205,223].

In concordance with the emergence of plasma neutralization at 6-10 months pi [157], the CAP256-VRC26 antibodies exhibited increasing autologous breadth and potency from ~7 months pi [204,205]. While the CAP256.UCA binds to the 15-wk SU, viruses circulating at 34 weeks pi were neutralized (<10 μg/mL) by this antibody, suggesting such a virus initiated the lineage [223]. Autologous viruses from 15-59 weeks pi were generally sensitive to most members of the lineage, while the 6-wk PI was only sensitive to CAP256.25 and CAP256.06 [204,205].

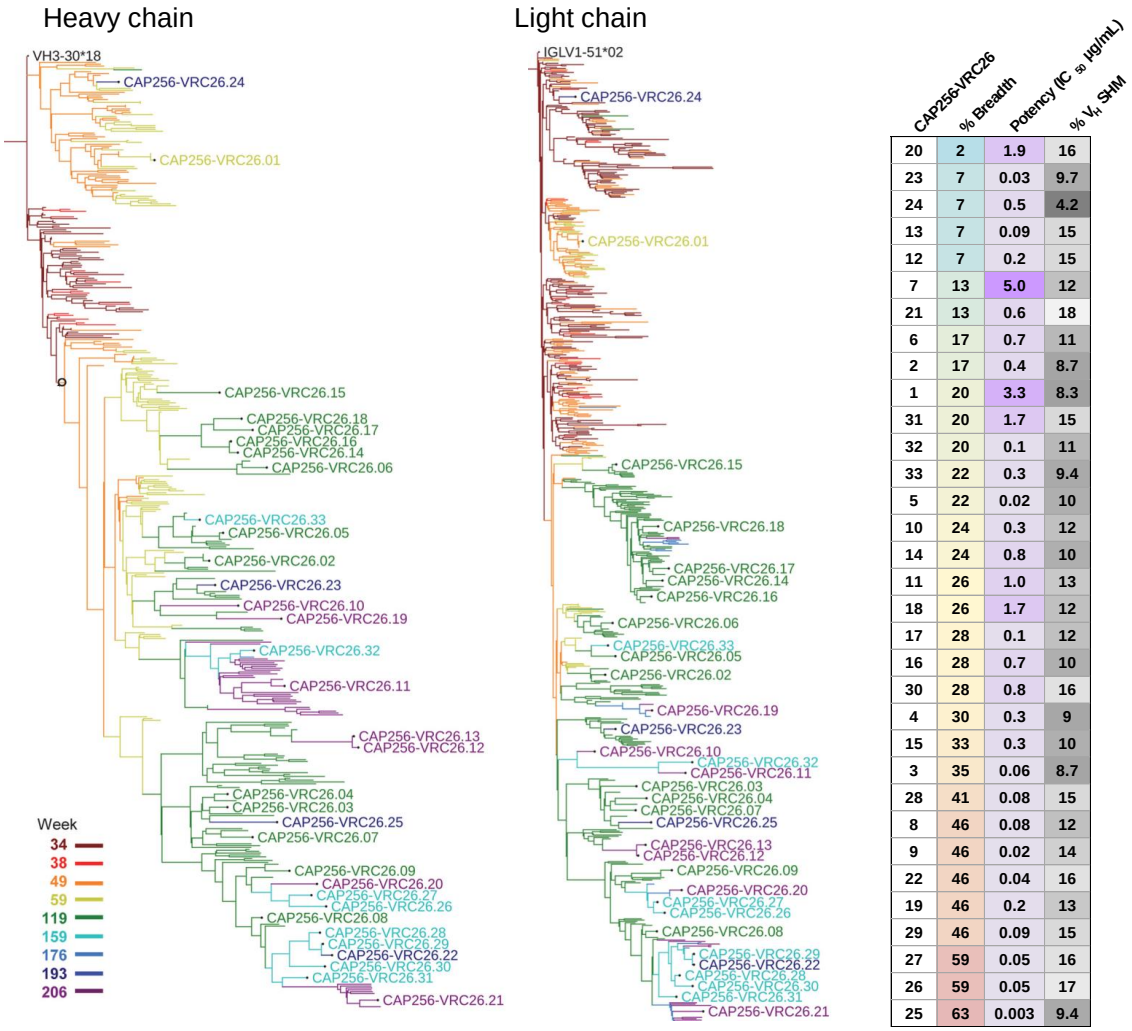

CAP256-VRC26	% Breadth	Potency (IC_{50} μg/mL)	% V_H SHM
20	2	1.9	16
23	7	0.03	9.7
24	7	0.5	4.2
13	7	0.09	15
12	7	0.2	15
7	13	5.0	12
21	13	0.6	18
6	17	0.7	11
2	17	0.4	8.7
1	20	3.3	8.3
31	20	1.7	15
32	20	0.1	11
33	22	0.3	9.4
5	22	0.02	10
10	24	0.3	12
14	24	0.8	10
11	26	1.0	13
18	26	1.7	12
17	28	0.1	12
16	28	0.7	10
30	28	0.8	16
4	30	0.3	9
15	33	0.3	10
3	35	0.06	8.7
28	41	0.08	15
8	46	0.08	12
9	46	0.02	14
22	46	0.04	16
19	46	0.2	13
29	46	0.09	15
27	59	0.05	16
26	59	0.05	17
25	63	0.003	9.4

Figure 1.11. The CAP256-VRC26 lineage consists of 33 clonally related antibodies.

(Left) A maximum likelihood phylogenetic tree of the CAP256-VRC26 lineage [204]. The heavy chains and light chains are in the first and second panel, respectively. The colors indicate from which week pi each antibody was recovered. (Right) Tabulated are the breadth, potency and SHM of each lineage member [204]. Figure adapted from [204].

1.10.2.1 The CAP256-VRC26 paratope and epitope

The lineage members have extremely long CDRH3s (35-37 aa) which form the majority of the paratope [204–207]. The CDRH3 forms a two-stranded β-sheet that is stabilized by a disulfide bond and projects ~20 Å from the surface of the antibody, and due to flexibility at the base, the tip can rotate ~17 Å [206]. Similar to other V1V2 bNAbs, the CDRH3s of the lineage members are anionic [204] and like PG9 and PG16, the tip of the CDRH3 contains a tyrosine sulfated YYD motif [199,208,209].

Like the plasma, subtype C and A viruses were particularly sensitive to these antibodies, neutralization could not be absorbed by gp120, and the antibodies were dependent on R166 and K169 [204,205,223]. The structures of CAP256.UCA (PDB: 4ODH), CAP256.01 (PDB: 4OCR), CAP256.03 (PDB: 4OD1), CAP256.04 (PDB: 4ORG), CAP256.06 (PDB: 4OCW), CAP256.07 (PDB: 4OD3), CAP256.10 (PDB: 4OCS) and CAP256.25 (PDB: 5DT1) have been resolved [204–206]. In addition, a stable prefusion 34-wk Env trimer was visualized by cryogenic electron microscopy in complex with CAP256.25 [206]. This structure indicates that the CDRH3 penetrates the trimer apex by 9.6 Å, where, unlike other V1V2 bNAbs, it interacts with both the apex hole and C-strand [206]. This combined mode of epitope recognition together with the binding of one antibody per trimer, likely accounts for the exceptional potency of CAP256.25 [206]. Once inserted, the CDRH3 lies anti-parallel with the C-strand and the sulfated tyrosines (Y100h and Y100i) form salt bridges with R166 on each protomer and K169 on two protomers [206]. In addition, salt-bridges form between E100b and K170, E100c and K168, D100g with D167 and K169, and D100j with K169 [206,207]. Furthermore, E100b hydrogens bonds with K171, E100c with K169, W100d with K169, W100e and K168 and K169, and S100f with D167 [206,207]. The more potent members of the CAP256 lineage can generally tolerate glycovariation at N156 and N160 [204,205,239,361,362] and the CDRH1 sits adjacent to, and is predicted to make contacts with, glycans at N130 and N160 [206], although the latter has not been experimentally verified.

Recently, the isotype of CAP256.25 was identified as IgG3, and compared to the IgG1 variant, this antibody was more potent and drives greater ADCP and ADCT [363]. Consequently, if utilized as a biotherapeutic, CAP256.25 IgG3 may be particularly effective in preventing infection and clearing infected cells [351,364].

1.11 Research questions

The CAP256-VRC26 HIV-1 V2-specific bNAb lineage was recovered from a subtype C infected participant in the CAPRISA 002 acute infection study [153,204,205,360]. The broadest member, CAP256.25, neutralizes 63% of heterologous viruses and is amongst the most potent of all known bNAbs [204]. CAP256.25 and other broad lineage members are modestly somatically mutated and closely related to lineage members that lack substantial neutralization [223]. The CAP256.UCA weakly neutralizes contemporaneous viruses and breadth and potency increase as the lineage matures [223]. With subsequent antigen-specific sorts, the CAP256-VRC26 lineage has continued to expand to include new members. While the ontogeny of the lineage has been reported [204,205,223], much of the genetic basis for the breadth and potency remains unknown. Together these data can inform the design of an HIV vaccine that guides the development of broad and potent antibodies.

1.11.1 Which somatic hypermutations and viral immunotypes drove the development of off-track antibodies in the CAP256-VRC26 HIV-1 V2-directed bNAb lineage?

In addition to bNAbs, the CAP256-VRC26 lineage consists of “off-track” antibodies that are genetically similar to the broad members, but are strain-specific. It is not clear which antibody regions and mutations confer breadth and potency to the bNAbs and strain-specificity to the off-track members, nor which viral variants drive this development. Elucidation of the pathways toward and away from breadth can contribute to the development of immunogens that induce breadth and minimize strain-specificity.

1.11.2 What is the role of heavy and light chain somatic hypermutation in conferring breadth and potency to the CAP256-VRC26 bNAb lineage?

Concomitant with the maturation of the CAP256-VRC26 lineage was the development of breadth and potency. The role of the heavy chain, light chain, framework and complementarity-determining regions to breadth and potency remain unknown. We sought to ascertain which mutations were sufficient to introduce neutralization into the CAP256.UCA. These data inform the design of immunogens that activate bNAb precursors and drive targeted maturation to efficiently elicit broad humoral responses.

1.11.3 Does the breadth, potency and effector functions of the IgG4 class switched members of the CAP256-VRC26 lineage differ from the matched IgG1 variants?

Recently, new members of the CAP256-VRC26 lineage were recovered by an antigen-specific sort. Notably, these antibodies were isolated as IgG4, whereas the isotype of most of the previously described lineage has not been identified. The impact that the isotype has on the breadth, potency and cell-mediated effector functions of these new members of the CAP256-VRC26 lineage is unknown. We expressed these antibodies as both IgG1, the most common isotype, and IgG4, and assessed neutralization and effector functions. Since effector functions contribute to protection against infection, understanding the role of the isotype in modulating these properties is key to an effective active and passive vaccine.

2. General materials and methods

2.1 Study participant

CAP256 was a participant enrolled in the CAPRISA 002 Acute Infection study, established in 2004 in KwaZulu-Natal, South Africa. The CAPRISA 002 study was reviewed and approved by the research ethics committees of the University of KwaZulu-Natal (E013/04), the University of Cape Town (025/2004) and the University of the Witwatersrand (MM040202). The human research ethics committee for the University of the Witwatersrand approved (M160934) the study reported herein (see 7.2, Appendix B: Ethics certificate). The specificity of her plasma has been described, monoclonal antibodies isolated and autologous Env evolution characterized [204,205,223,360,365].

2.2 Antibody subcloning

2.2.1 CMVR expression vector

The CMVR vector (Figure 2.1) (NIH AIDS Reagent Program) [366], which consists of the human cytomegalovirus (CMV) promoter, a kanamycin resistance gene, antibody leader and constant domain sequences, was used to express recombinant monoclonal antibodies [366]. Heavy chains (HC) were cloned into $CMVR_{HC}$ which encodes the IgG1 constant domain and light chains (LC) were cloned into $CMVR_{LC}$, with includes the IGKC constant region [367].

2.2.2 Restriction digest

The variable gene locus in CMVR is flanked by the AgeI and SalI (BsiW1 in $CMVR_{LC}$) restriction sites with BamHI downstream of the constant domain (Figure 2.1). CMVR (1.6 µg) was linearized for subcloning according to the manufacturer's instructions with 1.6 µL of both the AgeI and SalI FastDigest restriction enzymes in 1x FastDigest Buffer (Thermo Fisher Scientific) in a final volume of 50 µL. Following 90 min incubation at 37°C, the products were diluted in loading dye (0.25% bromophenol blue, 30% glycerol) and were separated on 1% agarose gels (1X TAE) alongside the DNA Molecular Weight Marker VII (Roche). The $CMVR_{HC}$ (5464 bp) and $CMVR_{LC}$ (4758 bp) vectors were cut out of the gel and purified with the QIAquick Gel Extraction Kit (Qiagen) as per the suggested protocol and eluted in 30 µL of Tris-Cl (10 mM, pH 8.5) and stored at -20°C.

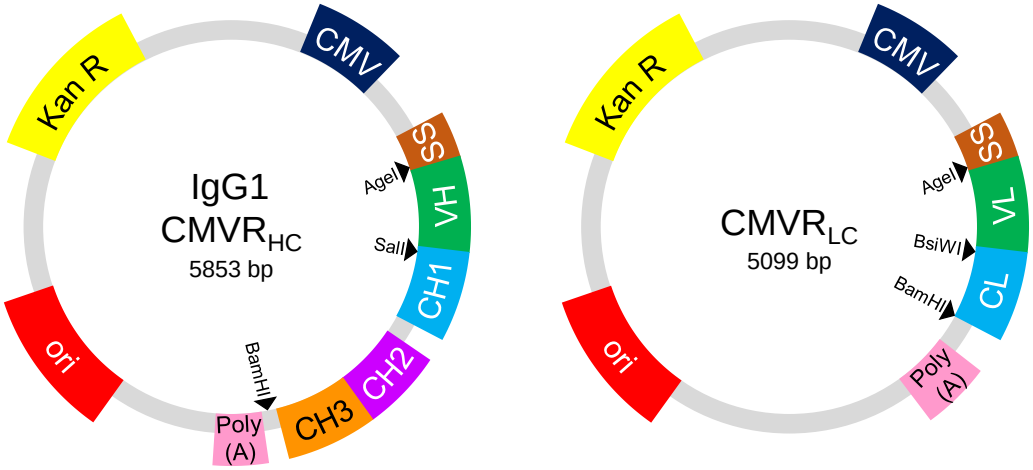

Figure 2.1. Plasmid maps of the CMVR$_{HC}$ and CMVR$_{LC}$ antibody expression vectors.
The expression of the antibody heavy (CMVR$_{HC}$) and light (CMVR$_{LC}$) chains are under the control of the CMV promoter [366]. The SV40 polyadenylation sequence flanks the 3' end of constant domain and the plasmids are selected by kanamycin. The AgeI and SalI/BsiWI restriction sites are 5' and 3' of the variable and constant genes, respectively, with BamHI following the constant region. The lengths of the plasmids include the antibody sequence.

2.2.3 Gene synthesis

Antibody chimeras with multiple CDR exchanges were synthesized by GenScript Biotech and cloned into the pUC57 vector (2579 bp). The variable genes were designed with the AgeI and SalI restriction sites flanking the 5' and 3' ends of the genes, respectively. In addition, the final three codons of the leader sequence were included between AgeI and the start of the variable domain, and the first two bases of the constant region were included before SalI. The fragments (~440 bp) were recovered from pUC57 following the same protocol as in 2.2.2.

2.2.4 DNA ligation

The heavy and light chain genes were ligated into the CMVR$_{HC}$ and CMVR$_{LC}$ vectors, respectively, with the Rapid DNA Ligation Kit (Roche). The suggested protocol was followed and the reaction included the T4 DNA ligase (5 U), 1x T4 DNA Ligation Buffer and 1x DNA Dilution Buffer in a final volume of 20 µL. The mixture was incubated for 30 min at 25°C, and the product was stored at -20°C.

2.3 Site-directed mutagenesis

The QuikChange Multi Site-Directed Mutagenesis Kit (Agilent Technologies) was used to introduce mutations into antibody and *env* genes, and to exchange CDRH1 and CDRH2

regions between antibodies. The PCR reactions were set up according to the manufacturer's recommendations and included 100 ng of both the template DNA and mutagenesis primers (Inqaba Biotec), 1x QuikChange Lightning Multi reaction buffer, 0.75 µL/reaction of QuikSolution and 1 µL of the QuikChange Lightning Multi enzyme blend in a final volume of 25 µL. The cycling parameters for the mutagenesis PCR were 1x 95°C for 2 min, 30x 95°C for 20 sec, 55°C for 30 sec and 65°C for 3 min and 10 sec (for antibody variable genes) or 4 min (for *env*), and 1x 5 min at 65°C. The template DNA was digested with 20 U of DpnI (Agilent Technologies) at 37°C for 2 hours and stored at -20°C. Mutagenized plasmids were transformed into JM109 cells (Promega) as detailed in 2.5.

2.4 Overlapping PCR

Exchanging the CDRH3s between antibodies was achieved with a two-step overlapping PCR that allowed for restriction-free cloning (Figure 2.2). Primers were designed to be complementary to the recipient antibody and used to amplify the CDRH3 from a donor plasmid. This was possible due to the high degree of sequence similarity between the members of the CAP256-VRC26 lineage. The product of this PCR, the "megaprimer", was used in a subsequent PCR to amplify the recipient antibody. The megaprimers anneal to the recipient plasmid while the mismatched CDRH3 sequence is displaced and, because it is not replicated, the native CDRH3 is replaced by the exogenous sequence from the donor antibody.

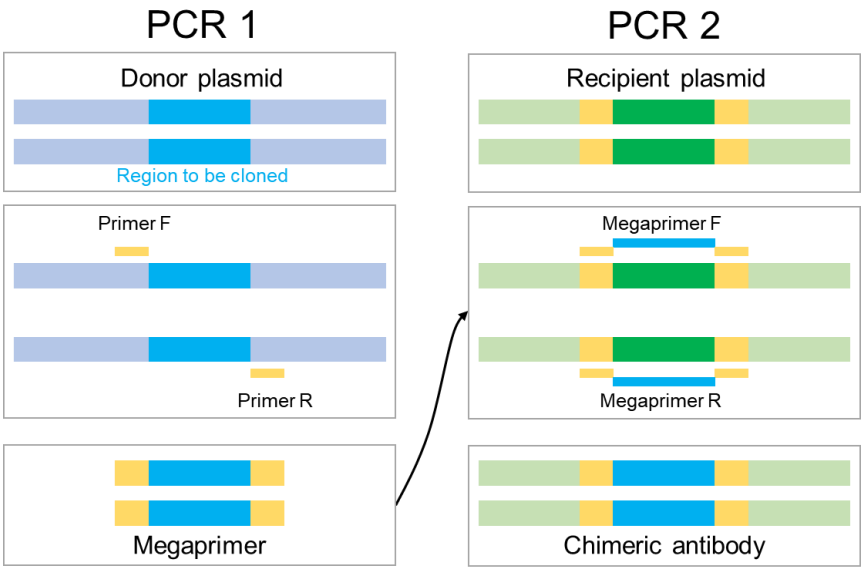

Figure 2.2. Schema of the restriction-free cloning technique.

(PCR 1) Primers (yellow) are designed to amplify the region of interest (blue), to match the sequence of the recipient plasmid adjacent to the site that will be replaced (green). (PCR 2) The product of PCR 1, the megaprimer, amplifies the recipient plasmid in PCR 2. The megaprimer anneals to the complementary sequences flanking the region targeted for replacement and the exogenous sequence (blue) is incorporated during extension.

To generate the megaprimers the AccuPrime *Pfx* DNA Polymerase (1.75 U), 1x AccuPrime *Pfx* Reaction Mix (Thermo Fisher Scientific) and 0.3 µM each of the forward and reverse primers (Inqaba Biotec) were used to amplify 50 ng of the recipient antibody in a 50 µL volume. The thermocyling conditions were 1x 95°C for 2 min, 25x 95°C for 15 sec, 56°C for 30 sec and 68°C for 12 sec. As detailed in 2.2.2, the products were separated by agarose gel electrophoresis (1.5%, 1x TAE) and the megaprimers (~180 bp) were cut out and purified. Next, the QuikChange Lightning Multi Site-Directed Mutagenesis Kit (Stratagene) was used according the manufacturer's guidelines (as detailed in 2.3) to amplify 100 ng of the recipient antibody with 100 ng of the megaprimers. Thereafter the digested and cleaned chimeric plasmids (see 2.2.2) were transformed into XL10-Gold Ultracompetent Cells (Stratagene).

2.5 Bacterial transformation

Ligation mixtures (2 µL) were transformed into XL10-Gold Ultracompetent Cells (Stratagene) with β-mercaptoethanol on ice for 30 min as per the manufacturer's instructions. The cells were then heat shocked for 30 sec at 42°C, placed on ice for 2 min and incubated in antibiotic-free super optimal broth at 37°C for 1 hour on an orbital shaker at 150 rpm. Thereafter, an aliquot of the culture was spread onto agar (Sigma-Aldrich) plates with 50 µg/mL kanamycin (for CMVR, Sigma-Aldrich) or 50 µg/mL ampicillin (for pcDNA 3.1, see 2.10, Sigma-Aldrich) and incubated overnight at 37°C, and later stored at 4°C. Purified plasmids (1 µL) (see 2.6) were transformed into JM109 Competent Cells (Promega) on ice for 5 min. Thereafter, the same protocol was followed as described for the XL-Gold Ultracompetent cells.

2.6 Plasmid preparation

For small-scale plasmid preparations (<15 µg), 2 mL of antibiotic supplemented lysogeny broth (LB, Sigma-Aldrich) was inoculated with an individual colony and incubated overnight at 37°C at 150 rpm. Plasmids were purified with the QIAprep Spin Miniprep kit (Qiagen) according to their guidelines and eluted in 50 µL of Tris-HCl (10 mM, pH 8.5). For larger plasmid preparations (<500 µg), a single colony was expanded in 2 mL of LB for 8 hours at 37°C at 150 rpm and then diluted 1:1000 in 150 mL of fresh LB. The culture was incubated overnight at 37°C at 150 rpm and the plasmids were purified with the QIAprep Spin Maxiprep kit (Qiagen) according the recommended protocol and eluted in 400 µL of Tris-HCl (10 mM, pH 8.5). The purity and concentration of the plasmid DNA was determined with a NanoDrop 1000 Spectrophotometer (Thermo Fisher Scientific) and the preparations were stored at 4°C.

2.7 Sanger sequencing

Antibodies and *env* subcloned into CMVR and pcDNA 3.1 (see 2.10), respectively, were sequenced with the ABI Genetic Analyzer 3500 (Applied Biosystems) and the BigDye Terminator v3.1 Cycle Sequencing Kit. The suggested protocol for the PCR reaction was followed but the final volume was reduced to 10 µL and included 3 pmol of the PCR primer (Appendix table 1), 0.25x BigDye Terminator v3.1 Ready Reaction Mix and 1x BigDye Terminator v3.1 sequencing buffer. The thermocyling conditions were 1x 96°C for 5 min, 25x 96°C for 10 sec, 50°C for 5 sec and 1x 60°C for 4 min. Following PCR, the products were precipitated for 30 min at 2000 g in sodium acetate (3M, pH 4.6, Sigma-Aldrich) diluted in ethanol (VWR International) and washed in 70% ice-cold ethanol for 5 min at 2000 *g*. After drying at 65°C for 4 min, the sequencing reactions were resuspended in 10 µL of the Hi-Di Formamide solution (Applied Biosystems) and loaded onto the ABI Genetic Analyzer 3500 for capillary electrophoresis.

2.8 Maintenance of mammalian cell lines

The TZM-bl (NIH AIDS Reagent Program) and 293T (obtained from Dr. George Shaw, University of Pennsylvania, Philadelphia) cell lines were used for the antibody neutralization assays and for pseudovirus growth, respectively. The cells were cultured at 37°C (5% CO_2) in Dulbecco's modified Eagle medium (DMEM, Gibco) supplemented with 10% heat-inactivated HyClone fetal bovine serum (FBS, GE Healthcare), 50 µg/mL gentamicin (Sigma-Aldrich) and 25 mM HEPES (Gibco). At confluency monolayers were disrupted with 0.25% trypsin and 1 mM EDTA (Gibco) and diluted at 1:10. The 293F suspension cell line (Life Technologies) was used for monoclonal antibody expression and was maintained in serum and antibiotic free FreeStyle 293 Expression media (Life Technologies) at 37°C (10% CO_2) on an orbital shaker (130 rpm) and diluted 1:10 when cell densities reached 3 x 10^6 cells/mL.

2.9 Recombinant monoclonal antibody production

Antibodies were expressed by 293F cells that were seeded at 1x10^6 cells/mL the day before the transfection. The 40 kDa linear polyethylenimine (PEI) MAX (Polysciences) transfection reagent was used to co-transfect 0.5 µg/mL of $CMVR_{HC}$ and 0.5 µg/mL of $CMVR_{LC}$ in 293F cells. The plasmid DNA and PEI MAX (3 µg per microgram of plasmid DNA) were diluted in Opti-MEM (Gibco) and co-incubated for 30 min at room temperature. Next, the transfection mixture was added to 293F cells (~2x10^6 cells/mL) and incubated at 37°C (10% CO_2) in an

orbital shaker (130 rpm) for seven days. Thereafter, the cultures were centrifuged at 2000 *g* for 1 hour, the supernatants were passed through a 0.22 µm polyethersulfone (PES) Stericup filter (Merck Millipore) and loaded onto Protein A (Pierce) filled Econo-Pac columns (Bio-Rad). After passing through the column twice, the Protein A resin was washed twice with 1x PBS pH 7.2 (Gibco) and the antibody was eluted with a glycine-HCl buffer (0.1 M, pH 2.5, Sigma-Aldrich) and neutralized with Trizma-HCl (1 M, pH 8, Sigma-Aldrich). The eluent was passed through 0.22 µm PES filter (Sartorius) and loaded onto Vivaspin 50 kDa cut-off PES centrifugation spin columns (Sartorius) for buffer exchange (1x PBS pH 7.2, Gibco) and concentration. Before storage at -80°C, the purified antibody was quantified with the NanoDrop 1000 Spectrophotometer (Thermo Fisher Scientific) and mass was determined by SDS-PAGE.

2.9.1 Sodium dodecyl sulfate-polyacrylamide gel electrophoresis (SDS-PAGE)

Precast 4-12% NuPAGE polyacrylamide Bis-Tris gels (Thermo Fisher Scientific) were used to separate antibodies by size under denaturing conditions. The suggested protocol was followed, and samples were prepared by mixing 0.5 µg of antibody with 1x NuPAGE LDS Sample Buffer and 1x NuPAGE Reducing Agent to a final volume of 10 µL. Following heating at 70°C for 10 min, the samples together with the Rainbow Molecular Weight Marker (Merck) were loaded onto the gel in 1x SDS Running Buffer supplemented with NuPAGE Antioxidant. After electrophoresis, gels were stained with 0.1% Coomassie Brilliant Blue R-250 (Sigma-Aldrich), destained in diluted in methanol and acetic acid.

2.10 HIV-1 pseudovirus production

Pseudoviruses were produced in the 293T cell line by co-transfection with *env* subcloned into the pcDNA 3.1 vector (Thermo Fisher Scientific) and the $pSG3_{\Delta env}$ plasmid (NIH AIDS Reagent Program). The $pSG3_{\Delta env}$ plasmid was derived from the HIV-1 subtype B SG3.1 provirus, and includes non-functional *env* and *vpu*, subcloned into the ampicillin resistant pTZ19U vector [368].

2.10.1 Pseudovirus transfection

The day before transfection, $8x10^6$ 293T cells in 20 mL of supplemented growth media were aliquoted into 75 cm^2 cell culture flask (Corning). The following day, the cells were co-transfected with 0.3 µg/mL of both the pcDNA 3.1-*env* and $pSG3_{\Delta env}$ plasmids and 3 µg of the

PEI MAX transfection reagent (Polysciences) per microgram of plasmid DNA. The plasmids and PEI MAX were diluted in unsupplemented DMEM (Gibco) and co-incubated at room temperature for 30 min. Next, the transfection solution was added to the 293T cells and incubated at 37°C (5% CO_2) for 8 hours. Thereafter, the media was replaced and following a further 48-72 hour incubation, the supernatant was harvested, passed through a 0.45 µm PES filter (Sartorius), the FBS (Hyclone, GE Healthcare) was adjusted to 20% and the pseudoviruses were stored at -80°C.

2.10.2 Pseudovirus titration

The titer of pseudovirus that results in 40 000-80 000 relative light units (RLUs) following infection of TZM-bl cells was determined for the neutralization assay (see 2.11) [369]. Pseudovirus was serially diluted four-fold in supplemented growth media in 96-well flat-bottomed plates (Corning), to a final volume of 50 µL/well. Next, 10^4 TZM-bl cells in 20 µL of supplemented growth media and 10 mg/mL of dextran was added to each well. Thereafter, the same protocol detailed in 2.11, was followed.

2.11 Neutralization assay

Antibody-mediated neutralization was assessed by measuring the reduction of the infection of TZM-bl cells by HIV-1 pseudoviruses. TZM-bl cells are modified HeLa cells which stably express CD4, CCR5, CXCR4 and a Tat-inducible firefly luciferase gene [370]. The assay was set up in 96-well flat-bottomed plates (Corning). Antibodies were serially diluted ten-fold from a starting concentration of 20-100 mg/mL in supplemented growth media and 25 µL was added per well. The pseudovirus was diluted in supplemented growth media as per the titer determined in 2.10.2. Pseudovirus (25 µL) was added to the diluted antibody and incubated for 1 hour at 37°C (5% CO_2) and then 10^4 TZM-bl cells in 20 µL of supplemented growth media and 10 mg/mL of DEAE-dextran hydrochloride (Sigma-Aldrich) was added to each well. The plates were incubated at 37°C (5% CO_2) and after 24 hours, 130 µL of fresh supplemented growth media was added to each well. Following another 24-48 hour incubation, 100 µL per well of supernatant was removed, 100 µL of Bright-Glo Luciferase Reagent (Promega) was added and after 2 min at room temperature, 150 µL per well of the mixture was transferred to a black 96-well flat-bottomed plate (Corning) and fluorescence was measured on a VICTOR3 1420 Multilabel Counter (PerkinElmer). The percentage of neutralization was calculated by dividing the difference between the average RLU of each antibody dilution and the average RLU of the cell control by the difference between the average RLU of the virus control and the

average RLU of the cell control [369]. Antibody titers (IC_{50}) were calculated as the reciprocal of the dilution required to inhibit 50% of the RLU signal [371].

2.12 Antibody and HIV-1 Env models

The crystal or cryo-electron microscopy structures for antibodies, Env trimers and gp120 monomers were downloaded from the Protein Data Bank (PDB, rcsb.org). In the absence of an antibody structure, the amino acid sequence of the antibody was fitted to the structure of a related antibody in Swiss-PdbViewer (v4.1.0) (Swiss Institute of Bioinformatics) [372]. Structures and models were aligned and visualized in the PyMOL Molecular Graphics System (v2.0.2) (Schrödinger).

2.13 Data analysis

Graphs were created with GraphPad Prism 8 (GraphPad Software), chromatograms were analyzed in Sequencher (v5.4.1) (Gene Codes) and nucleotide sequences were aligned in BioEdit (v7.2.5) (Ibis Therapeutics). Maximum likelihood phylogenetic trees were constructed in MEGA X (v10.0.4) with the Tamura-Nei model [373]. Statistical testing was conducted with GraphPad Prism 8 and comparisons between groups were done with two-sided non-parametric tests at the 0.05 alpha level. Paired groups were compared with the Wilcoxon matched-pairs signed rank test and the Mann-Whitney test was utilized for unpaired groups. Significant differences at the 0.05 alpha level for parametric paired data was done with two-sided paired t-tests.

3. Somatic hypermutation to counter a globally rare viral immunotype drove off-track antibodies in the CAP256-VRC26 HIV-1 V2-directed bNAb lineage

David Sacks[1,2], Jinal N. Bhiman[1,2#], Kevin Wiehe[3], Jason Gorman[4], Peter D. Kwong[4], Lynn Morris[1,2,5] and Penny L. Moore[1,2,5]

[1] Centre for HIV and STIs, National Institute for Communicable Diseases (NICD) of the National Health Laboratory Service (NHLS), Johannesburg, South Africa

[2] Faculty of Health Sciences, University of the Witwatersrand, Johannesburg, South Africa

[3] Duke Human Vaccine Institute, Duke University School of Medicine, Durham, North Carolina, USA

[4] Vaccine Research Center, National Institute of Allergy and Infectious Diseases, National Institutes of Health, Bethesda, Maryland, USA

[5] Centre for the AIDS Programme of Research in South Africa (CAPRISA), University of KwaZulu-Natal, Durban, South Africa

[#] Current address: Department of Immunology and Microbiology, The Scripps Research Institute, La Jolla, CA 92037, USA

The supplementary figures in the published version of this chapter (7.5, Appendix E: David Sacks et al, PLOS Pathogens, 2019) are incorporated into the main body of this chapter. In addition, the materials and methods (3.4) have been integrated into the general materials and methods (2).

3.1 Abstract

Previously we have described the V2-directed CAP256-VRC26 lineage that includes broadly neutralizing antibodies (bNAbs) that neutralize globally diverse strains of HIV. We also identified highly mutated “off-track” lineage members that share high sequence identity to broad members but lack breadth. Here, we defined the mutations that limit the breadth of these antibodies and the probability of their emergence. Mutants and chimeras between two pairs of closely related antibodies were generated: CAP256.04 and CAP256.25 (30% and 63% breadth, respectively) and CAP256.20 and CAP256.27 (2% and 59% breadth). Antibodies were tested against 14 heterologous HIV-1 viruses and select mutants to assess breadth and epitope specificity. A single R100rA mutation in the third complementarity-determining region of the heavy chain (CDRH3) introduced breadth into CAP256.04, but all three CAP256.25 heavy chain CDRs were required for potency. In contrast, in the CAP256.20/27 chimeras, replacing only the CDRH3 of CAP256.20 with that of CAP256.27 completely recapitulated breadth and potency, likely through the introduction of three charge-reducing mutations. In this individual, the mutations that limited the breadth of the off-track antibodies were predicted to occur with higher a probability than those in the naturally paired bNAbs, suggesting a low barrier to the evolution of the off-track phenotype. Mapping studies to determine the viral immunotypes (or epitope variants) that selected off-track antibodies indicated that unlike broader lineage members, CAP256.20 preferentially neutralized viruses containing 169Q. This suggests that this globally rare immunotype, which was common in donor CAP256, drove the off-track phenotype. These data show that affinity maturation to counter globally rare viral immunotypes can drive antibodies within a broad lineage along multiple pathways towards strain-specificity. Defining developmental pathways towards and away from breadth may facilitate the selection of immunogens that elicit bNAbs and minimize off-track antibodies.

3.2 Author summary

Broadly neutralizing antibodies (bNAbs) develop in some HIV infected individuals, partly due to their complex evolutionary pathways that are characterized by extensive somatic hypermutation (SHM). Furthermore, bNAbs within a lineage may form a minor subset, amidst many strain-specific “siblings”, indicating that minor sequence differences between lineage members can significantly effect neutralization. Here, we define mutations that limit breadth in two “off-track” members of the CAP256-VRC26 bNAb lineage, and show that these occur with relatively high probability. A dominant autologous virus with a globally rare V2 sequence appears to have selected for an off-track antibody, providing a mechanism for the development of this antibody during infection. These data highlight the complex interdependencies between high levels of SHM and breadth, as mutations that neutralize autologous viruses may limit heterologous breadth. Consequently, strategies to increase SHM by repeated vaccinations will require careful antigen selection to focus the humoral response to globally common epitopes, limiting off-track responses.

3.3 Introduction

Antiretroviral therapy has transformed HIV from a progressive fatal infection to a manageable chronic disease [8]. However, a preventative vaccine is urgently needed as drug resistance, access to medication and adverse side effects hamper the utility of antiretroviral drugs. Despite intensive research, strategies to induce protective immune responses by vaccination have achieved little success [290]. While neutralizing antibodies are elicited during HIV infection, the response is typically strain-specific. However, ~20% of individuals develop broadly neutralizing antibodies (bNAbs) which potently neutralize diverse global viruses *in vitro* and protect non-human primates from infection [152,153,159,374–376]. Therefore, understanding the mechanisms behind the elicitation and evolution of bNAbs is central to the development of an HIV vaccine.

During infection, the humoral response targets the HIV envelope (Env) glycoprotein which consists of three heavily glycosylated non-covalently linked gp41-gp120 protomers. While strain-specific antibodies recognize exposed and variable sites, bNAbs target relatively conserved and occluded sites, including the membrane proximal external region (MPER), gp120-gp41 interface, CD4-binding site (CD4bs), silent face, N332 supersite and a quaternary V1V2 epitope at the trimer apex [167]. Many V1V2 directed bNAbs have atypically long (>24 amino acids) third complementarity-determining regions of the heavy chain (CDRH3) which provides access to glycan shielded and buried epitopes [161,172,204,205,232]. Additionally, bNAbs frequently exhibit unusually extensive somatic hypermutation (SHM), which suggests multiple rounds of affinity maturation. Understanding how these unusual features arise is critical to recapitulating this process by vaccination.

The degree to which SHM and affinity maturation occurs is influenced by HIV diversity and antigen load [123]. A number of longitudinal studies describing the “arms race” between viral quasispecies and bNAb lineages have provided insights into the evolution of breadth [377]. These studies have identified “bNAb-initiating Envs” that engage antibody precursors as well as emerging viral variants, which select bNAb intermediates [187,189,197,203,205,220,223,229]. We have extensively studied virus/antibody co-evolution in the superinfected CAP256 donor from whom 33 members of the CAP256-VRC26 V2-targetting bNAb lineage were isolated [204,205,223]. The evolution of this lineage was elucidated through the analysis of longitudinal viral and antibody deep sequences from 59-206 weeks post infection [204,205,223]. Viruses from six weeks post infection were sensitive to neutralization by CAP256 lineage members but by 59 weeks post infection most viruses were resistant. Similar to other V2-directed bNAbs, the CAP256-VRC26 lineage members have very

long (35-37 amino acid, aa) anionic and tyrosine sulfated CDRH3s that recognize the electropositive V2 apex [207]. Modeling and mapping studies show that several residues within the CDRH3 are critical for epitope recognition, including the tyrosine sulfated YYD motif at the apex of the CDRH3 [207]. This motif is present in the unmutated common ancestor (UCA) of the CAP256-VRC26 lineage, 27 of the 33 lineage members as well as other V2-directed bNAbs such as PG9 and PG16 [204,232]. In addition, the CDRH1 has been shown to stabilize the CDRH3, and residues in CDRH2 have been implicated in glycan recognition [206,361]. Within strands B and C of the viral Env protein, the CAP256-VRC26 lineage's footprint includes residues N160, R166, D167, K168 and K169 and is similar to other V2 glycan bNAbs (PG9 and PG16). The breadth, potency and extent of SHM of CAP256-VRC26 lineage members ranges from 2-63%, 0.003-5.00 μg/mL and 4.2-18%, respectively [204].

SHM, which is mediated by activation-induced cytidine deaminase (AID), is essential for breadth as bNAb germline-revertants generally lack substantial binding and neutralization [193,225,227,232,234]. Mutations that are selected during affinity maturation may increase antibody-antigen affinity directly at the paratope or indirectly by improving stability [378,379]. SHM is a semi-random process as AID hot-spots (WRCH/Y, W=A/T, R=A/G and H=A/C/T) and cold-spots (SYC, S=C/G and Y=C/T) are distributed throughout the antibody variable regions. Consequently, mutations associated with breadth are unlikely to occur if they are in cold-spots and/or require more than one nucleotide change [128,380]. Additionally neutral mutations can accumulate via co-selection and constitutive background mutational noise [379]. Although increased SHM is generally associated with neutralization breadth, exceptions exist within the CAP256-VRC26 and other bNAb lineages. We have previously described these non-broad but highly mutated CAP256 antibodies as "off-track" [223]. Such off-track antibodies have been recovered from bNAb lineages in several individuals. 1AZCETI5 is a clonal member of the CD4bs CH103 bNAb lineage, and shares VDJ genes, CDRH3 length and extent of SHM with bNAb CH103, but the former only neutralizes autologous viruses [197]. The PGDM1400 bNAb, a member of the V2 glycan targeting PGDM lineage with 83% breadth has similar genetic properties to PGDM1406, but the latter exhibits limited breadth (6%) [201]. Similarly, within the PGT121 N332 targeting bNAb lineage are two heavy chains (22H and 6H) that are related to broad members but exhibit no neutralization [242]. As monoclonal antibody isolation methodologies are designed to recover bNAbs, the proportion of off-track antibodies in bNAb lineages is unknown. However, the finding that 40% of related antibodies recovered by flow cytometry from the donor of the CD4bs bNAb, VRC-PG04, were off-track it indicates that such antibodies may be common [244].

Collectively, studies into co-evolution and bNAb targets have identified candidate antigens to initiate antibody lineages and guide the development of breadth. Indeed, native-like Env trimers administered in combination or sequentially elicits tier 2 neutralizing antibodies in mice and rabbits, providing a strong rationale to test similar immunogens in people [233,294,318,336,381]. Importantly, the mutations crucial for breadth and potency as well as those that confer an off-track phenotype in bNAb lineages are largely unknown. Identification of these mutations will inform the design of vaccine antigens that elicit breadth but dampen the evolution of off-track responses. The high degree of sequence identity between CAP256-VRC26 bNAbs and their off-track relatives, the richly populated lineage and the availability of contemporaneous viral sequences is an ideal opportunity to compare off-track antibodies with bNAbs to determine why these antibodies lack breadth.

Here we define key residues that restrict neutralization breadth and potency in two off-track antibodies within the CAP256-VRC26 lineage. We found that in one off-track/bNAb pair, residues in each of the three CDRHs were necessary for potency and that a key breadth-conferring mutation in the CDRH3 was highly improbable. In the second pair, we show that the CDRH3 was completely responsible for modulating neutralization and that the mutations leading to the off-track phenotype were relatively probable. Lastly, through epitope mapping we identified viruses that guided the evolution of an off-track antibody toward a globally rare immunotype. This study highlights the stochastic nature of SHM and shows that breadth-restricting mutations typically arise with a greater probability than breadth-conferring mutations. This work provides insights into the evolution of breadth and mature strain-specificity, informing the design of immunogens that minimize the elicitation of off-track mutations while guiding evolution to globally conserved sites.

3.4 Materials and Methods

3.4.1 Ethics statement

The human research ethics committee for the University of the Witwatersrand approved (M160934) the study reported herein (see 7.2, page 111, Appendix B: Ethics certificate). Refer to 2.1 (page 31) for additional information.

3.4.2 Overlapping PCR and site-directed mutagenesis

Exchanging the CDRH3s between monoclonal antibodies was achieved with a two-step overlapping PCR (2.4, page 33) and site-directed mutagenesis (2.3, page 32). The primers used for the reactions are in Appendix table 2. Genes with CDRH1, CDRH2 and CDRH3 exchanges were synthesized (GenScript, 2.2.3, page 32) and cloned in $CMVR_{HC}$ as per 2.2.2 and 2.2.4 (pages 31 and 32, respectively). Mutations in both antibody and *env* genes were introduced by site-directed mutagenesis (2.3) with primers listed in Appendix table 2 and Appendix table 3, respectively. Plasmids were sequenced (see 2.7, page 35) with primers in Appendix table 1.

3.4.3 Cell lines

Briefly, the TZM-bl, 293T and 293F cell lines were utilized for the antibody neutralization assays, pseudovirus growth and monoclonal antibody production, respectively. For additional details, see 2.8 (page 35).

3.4.4 Pseudovirus production

Refer to 2.10 (page 36) for the protocol. Briefly, 293T cells were co-transfected with PEI MAX (Polysciences) with *env* and $pSG3_{\Delta env}$ plasmids, and the supernatants were titered with the TZM-bl cell line.

3.4.5 Antibody expression

The method in 2.9 (page 35) was followed. Briefly, the 293F cell line was co-transfected with PEI MAX (Polysciences) with the $CMVR_{HC}$ and $CMVR_{LC}$ plasmids and the monoclonal antibodies were isolated from the supernatant with Protein A resin (Pierce) columns.

3.4.6 Neutralization assays

Antibody-mediated neutralization was measured with the TZM-bl neutralization assay as a function of the reduction of Tat-inducible luciferase fluorescence. See 2.11, (page 37) for additional information.

3.4.7 Models

The crystal structures of CAP256.04 (PDB: 4ORG) was aligned to the crystal structure of CAP256.25 and CAP256 34-week trimer in PyMOL (v2.0.2). No structures were available for CAP256.20 and CAP256.27, therefore the amino acid sequences of these antibodies were fitted to the crystal structure of CAP256.25 in Swiss-PdbViewer (v4.1.0) and aligned in PyMOL as detailed in 2.12 (page 38). Protein model representations were created with Swiss-PdbViewer and PyMOL. Graphs were created in GraphPad Prism 6, sequence alignments were made in BioEdit (v7.2.5) and phylogenetic trees were constructed in MEGA (v6.06).

3.4.8 Probability of antibody mutations

The Antigen Receptor Mutation Analyzer for Detection of Low Likelihood Occurrences (ARMADiLLO) program estimates the probability of amino acid substitutions prior to antigenic selection [380]. Briefly, 10^4 simulated mature sequences per site of interest are generated with the S5F mutability and substitution models through comparison of the nucleotides sequences of the CAP256.UCA and a given mature lineage member [128]. The probability of particular amino acid substitutions is then estimated by the frequency of the observed site in the set of simulated sequences. Here, a mutation of <2% probability is classified as “improbable” as this reflects a frequency ≤2 B-cells per germinal center harboring that particular mutation [380]. Probabilities of combinations of mutations are derived from the products of individual probabilities.

3.4.9 Data analysis

Graphs were created with GraphPad Prism 8 (GraphPad Software), chromatograms were analyzed in Sequencher (v5.4.1) (Gene Codes) and nucleotide sequences were aligned in BioEdit (v7.2.5) (Ibis Therapeutics). Maximum likelihood phylogenetic trees were constructed in MEGA X (v10.0.4) and statistical testing was conducted with GraphPad Prism 8. See 2.13 (page 38) for more information.

3.5 Results

3.5.1 Neutralization breadth is mediated by the CAP256-VRC26 antibody heavy chain

To determine the genetic determinants that controlled the off-track phenotype, we selected two bNAbs with high sequence identity to two off-track antibodies. Off-track antibodies were defined as having low neutralization breadth despite their capacity to neutralize early autologous viruses [223], extensive sequence maturation and identity to related bNAb lineage members. The CAP256.25 bNAb was paired with the off-track antibody CAP256.04 and bNAb CAP256.27 was paired with the off-track antibody, CAP256.20. The two pairs of antibodies cluster together on a maximum likelihood tree (Figure 3.1 A), consistent with our previous observations that antibodies with considerably different breadth may differ by relatively few amino acids [223]. The heavy and light chain of CAP256.04 (30% breadth, 0.27 µg/mL potency, 9% SHM) both share 92% sequence identity with the heavy and light chain of bNAb CAP256.25 (63% breadth, 0.003 µg/mL potency, 12% SHM) (Figure 3.1 A). Within the second pair, the heavy and light chain of CAP256.20 (2% breadth, 1.87 µg/mL potency, 16% SHM) shares 93% and 96% sequence identity with the CAP256.27 heavy and light chain (59% breadth, 0.047 µg/mL potency, 16% SHM), respectively (Figure 3.1 A). A total of eighteen amino acids differ between the heavy chain and 11 amino acids between the light chain of CAP256.04 (orange) and CAP256.25 (brown) which are displayed as yellow spheres in an alignment of the two antibodies (Figure 3.1 B). Seventeen amino acids (yellow spheres) differentiate the heavy chains and four the light chains of CAP256.27 (purple) and CAP256.20 (light purple) (Figure 3.1 B).

As neutralization by members of the CAP256 bNAb lineage has been largely attributed to the heavy chain (HC) [205], we first confirmed that the light chain (LC) was not responsible for the off-track phenotype of CAP256.04 and CAP256.20. We generated chimeras between the heavy chains (HC) and light chains (LC) of each off-track/bNAb pair (25 HC + 04 LC, 04 HC + 25 LC and 27 HC + 20 LC, 20 HC + 27 LC) and tested their neutralization against both CAP256 infecting viruses (the primary and superinfecting viruses) and 14 heterologous viruses. The titers did not differ significantly (Wilcoxon matched-pairs) between the chimeric antibodies and the natural antibody from which the heavy chain was donated (Figure 3.1 C). These data indicate that the light chain has no impact on the neutralization breadth within these pairs, consistent with structural analyzes showing no light chain contacts with the viral epitope [206], and we therefore focused on the heavy chain in subsequent studies.

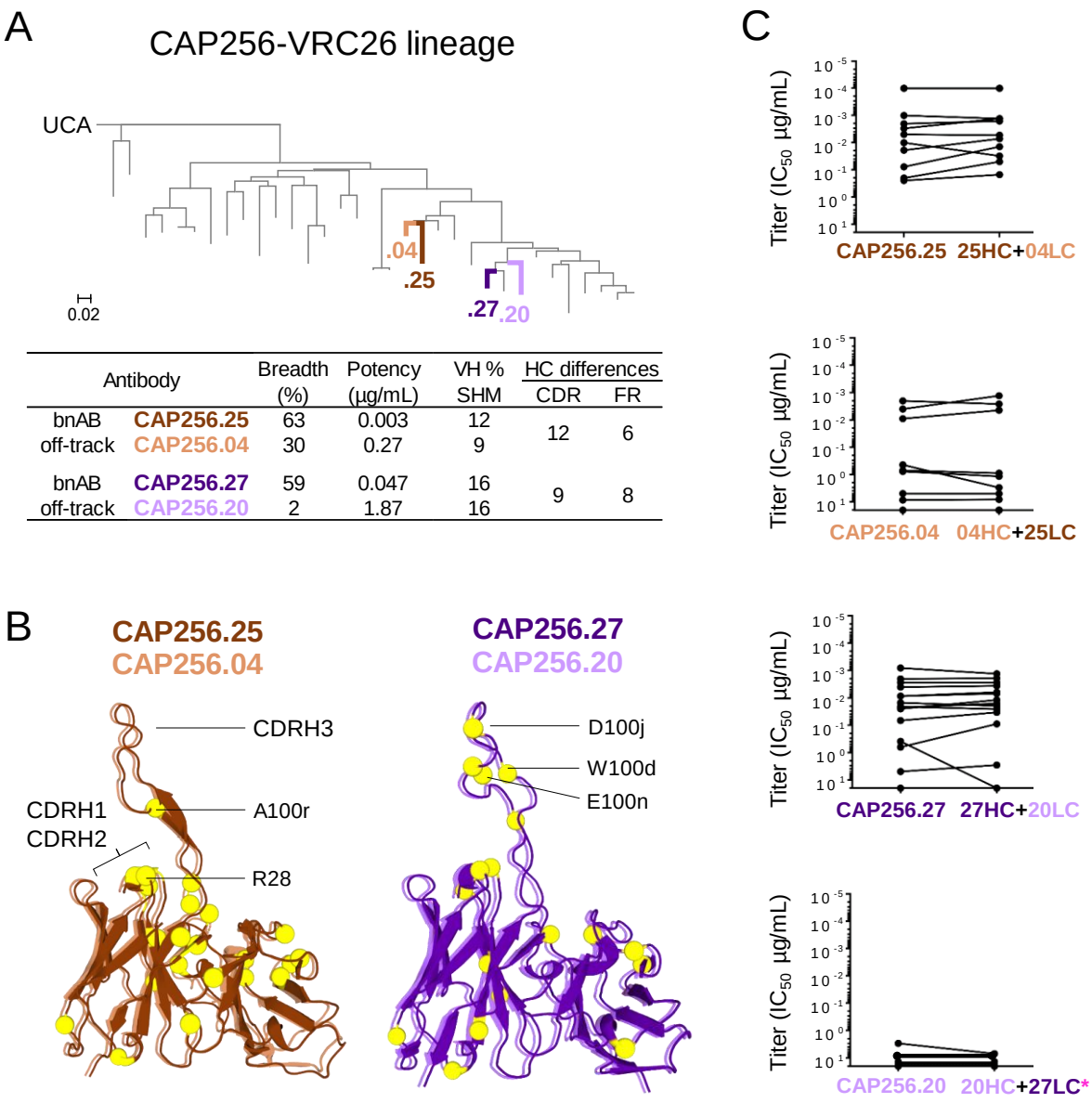

Antibody		Breadth (%)	Potency (µg/mL)	VH % SHM	HC differences CDR	HC differences FR
bnAB	CAP256.25	63	0.003	12	12	6
off-track	CAP256.04	30	0.27	9		
bnAB	CAP256.27	59	0.047	16	9	8
off-track	CAP256.20	2	1.87	16		

Figure 3.1. The heavy chain mediates the off-track phenotype.

(A) Maximum likelihood phylogenetic tree, rooted on the CAP256.UCA, with 33 clonally related VH sequences of monoclonal antibodies isolated from donor CAP256. Highlighted are CAP256.04 (orange), CAP256.25 (brown), CAP256.20 (light purple) and CAP256.27 (purple). Neutralization breadth, potency, VH SHM (related to CAP256.UCA) and the number of amino acids that differ between the CDR and FR of each pair are tabulated below. Breadth and potency (mean IC_{50}) was calculated from a panel of 46 heterologous viruses [204]. (B, left) The amino acid sequence of CAP256.04 (orange) was fitted to a structure of CAP256.25 and CAP256 34-week trimer in Swiss-PdbViewer (v4.1.0), aligned in PyMOL (v2.0.2) and displayed as cartoons. (B, right) The amino acid sequences of CAP256.27 (purple) and CAP256.20 (light purple) were fitted to CAP256.25 in Swiss-PdbViewer (v4.1.0) and aligned in PyMOL (v2.0.2). The amino acids that differ between each bNAb and matched off-track antibody are represented as yellow spheres. (C) The light chains were exchanged between each bNAb/off-track pair and *neutralization (IC_{50}, µg/mL) was tested against (n=16) pseudoviruses.

3.5.2 Introduction of potency into CAP256.04 requires a combination of the CAP256.25 CDRHs

To determine which regions of the heavy chain restrict the breadth of CAP256.04, we constructed several chimeras and point mutants between CAP256.25 and CAP256.04, focusing initially on the CDRHs. The sequence variation between the CDRHs is shown in Figure 3.2 A and includes charge and hydrophobicity differences between the two antibodies (R28S, D30N, G31R, H53Y, K57T, A100rR and N100ddF) and an insertion (G100w) in CAP256.25 that is absent from CAP256.04 (Figure 3.1 A). We first transplanted all the CAP256.25 CDRHs (12 amino acid changes in total) into CAP256.04, creating CAP256.04^{25H123} (Figure 3.2 B). Antibodies were tested against a panel of 16 viruses that were sensitive to CAP256.25 (geometric mean, GM, potency of 0.002 μg/mL against this panel), of which 8 were neutralized by CAP256.04 (with a 230-fold lower GM potency of 0.17 μg/mL) (Figure 3.2 B). The neutralization breadth and potency of the CAP256.04^{25H123} chimera (which neutralized all 16 viruses with a GM potency of 0.008 μg/mL) matched that of CAP256.25 (0.003 μg/mL) (Figure 3.2 B). In the reverse experiment, introducing the framework (FR) regions from CAP256.25 into CAP256.04 (CAP256.04^{25FR123}) had no effect on breadth (Figure 3.2 B). These data suggest that the mutations in the CDRs, rather than the FR regions restrict the breadth of CAP256.04.

Next, to dissect the role of individual CDRHs, each was individually swapped between the two parental antibodies. CAP256.04^{25H1} neutralized two additional viruses (ZM214 and ZM249) that were resistant to CAP256.04 (Figure 3.2 B). In addition, we observed virus-specific increases in potency for some sensitive viruses (with a 6-18-fold improvement for Du156, Q259, and Du422 and a 250-fold increase in potency for CAP45). In contrast, CAP256.04^{25H2} neutralized the same number of viruses as CAP256.04 (Figure 3.2 B), though again slight virus-specific differences in potency were observed, with CAP45 becoming resistant to CAP256.04^{25H2} while PVO gained sensitivity (Figure 3.2 B). The largest effect of a single CDRH swap was observed for the CDRH3 which differed by six amino acids. CAP256.04^{25H3} neutralized six additional viruses (ZM109, PVO, ZM214, ZM249, Q461 and Q842) (Figure 3.2 B) although with similar potency to CAP256.04 (0.39 μg/mL and 0.17 μg/mL, respectively). This was confirmed in the reverse experiment, where the CAP256.04 CDRH3 was introduced into CAP256.25 (CAP256.25^{04H3}) resulting in reduced breadth (Figure 3.2 B). Overall, these data suggest that the breadth of the CAP256.04 off-track phenotype is modulated by the CDRH3, but potency is attenuated by a combination of all three CDRHs.

A

Antibody		CDRH1 (26)	CDRH2 (51)	CDRH3 (95 100d 100m 100r 100w)	Length	Charge
bNAb	CAP256.25	QFRFDGYG	ISHDGIKK	DLREDECEEWWSDYYDFGKQLPCAKSRGGLVGIADN	36	-5
off-track	CAP256.04	..S.NR..	..Y..TD.	.....R....-VA..F.K	35	-3

B

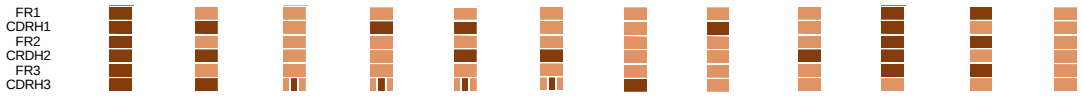

Pseudovirus	256.25	256.04^{25H123}	256.04 R100rA	256.04^{25H1} R100rA	256.04^{25H12} R100rA	256.04^{25H2} R100rA	256.04^{25H3}	256.04^{25H1}	256.04^{25H2}	256.25^{04H3}	256.04^{25FR123}	256.04
CAP256.15-wk.SU	0.00001	0.0001	0.001	0.002	0.0002	0.001	0.003	0.001	0.0001	0.001	0.003	0.002
CAP256.6-wk.PI	0.09	1.62	>100	>100	>100	>100	>100	>100	>100	>100	>100	>100
CAP210.E8	0.00001	0.00003	0.01	0.005	0.003	0.004	0.01	0.01	0.004	0.005	0.005	0.01
ZM53 M.PB12.2	0.0001	0.0003	0.004	0.004	0.001	0.002	0.01	0.001	0.001	0.004	0.01	0.004
ZM197.7	0.002	0.002	0.04	0.04	0.04	0.08	0.07	0.19	0.39	8.17	3.80	0.44
Du156.12	0.001	0.002	0.78	0.28	1.74	9.46	1.88	0.77	24.79	50.97	6.38	4.92
Q259.d2.17	0.002	0.005	0.03	0.01	0.04	0.38	0.04	0.04	5.66	14.95	1.13	0.70
CAP45.G3	0.00002	0.0003	0.004	0.002	0.01	0.04	0.002	0.003	>100	>100	0.86	0.77
Du422.01	0.0007	0.03	2.32	0.14	0.38	15.33	5.28	0.52	9.72	8.02	5.40	8.50
ZM109.4	0.003	0.01	16.66	2.04	31.34	>100	29.45	>100	>100	>100	>100	>100
PVO.04	0.08	0.30	35.35	15.48	37.88	50.12	46.51	>100	50.16	>100	>100	>100
ZM214.15	0.003	0.002	3.95	0.31	0.41	4.51	1.88	45.65	>100	>100	>100	>100
ZM249.1	0.01	0.004	0.52	0.10	0.01	0.10	0.24	13.73	>100	>100	>100	>100
AC10.29	0.25	11.47	84.63	38.21	>100	>100	>100	>100	>100	>100	>100	>100
Q461.e2	0.01	0.02	35.28	18.94	>100	>100	94.64	>100	>100	>100	>100	>100
Q842.d12	0.01	0.50	13.09	6.65	1.31	2.34	20.93	>100	>100	>100	>100	>100
MLV	>100	>100	>100	>100	>100	>100	>100	>100	>100	>100	>100	>100
Geo mean IC_{50}	0.002	0.008	0.46	0.18	0.09	0.25	0.44	0.09	0.23	0.37	0.25	0.17
% neutralization	100	100	94	94	81	75	88	63	50	44	50	50

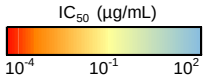

Figure 3.2. One mutation is required to introduce breadth into CAP256.04 while mutations in CDRH1, CDRH2 and CDRH3 are required for potency.

(A) Comparison of the CDR sequences, including the length and charge of the CDRH3 of CAP256.04 (orange) and CAP256.25 (brown). The blue boxes highlights key off-track mutations. (B) Neutralization data using mutants and chimeras (indicated schematically above the table) between CAP256.25 and CAP256.04, with neutralization potency indicated by color, as shown in the key. Neutralization data represents the arithmetic mean titers (IC_{50}, µg/mL) from at least two experiments.

3.5.3 Introduction of breadth into CAP256.04 requires a single improbable CDRH3 mutation

As the CAP256.25 CDRH3 conferred additional breadth into CAP256.04, we assessed which residue(s) were responsible for this effect (Figure 3.2). Mutating CDRH3 residues that altered the charge (K102N) or aromaticity (F100ddA) of the CDRH3 failed to improve the neutralization of CAP256.04 (Figure 3.3). In contrast, the R100rA mutation, which removed a positive charge from the CDRH3, improved the breadth of CAP256.04 from 50% to 94% of this panel, with seven viruses resistant to CAP256.04 becoming sensitive to CAP256.04 R100rA (Figure 3.2 B). Interestingly, this single mutation recapitulated the breadth introduced into CAP256.04 by the entire CAP256.25 CDHR3. The reverse mutant, CAP256.25 A100rR similarly resulted in a

substantial loss of breadth (Figure 3.3). The combination of R100rA with the CAP256.25 CDRH1 did not confer additional breadth beyond that introduced by R100rA (Figure 3.2 B) and, surprisingly, the addition of the CDRH2 to either CAP256.04 R100rA or CAP256.04^{25H1} R100rA reduced the breadth of these antibodies (Figure 3.2 B).

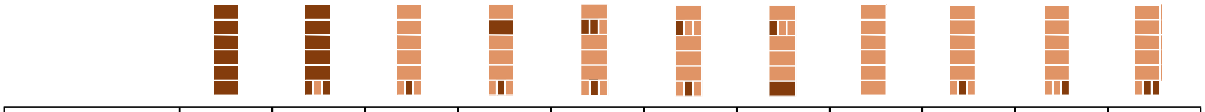

Pseudovirus	256.25	256.25 A100rR	256.04 R100rA	256.04^{25H1} R100rA	256.04 S28R N30D R100rA	256.04 S28R R100rA	256.04^{25H3} S28R	256.04	256.04 F100ddA	256.04 K102N	256.04 F100ddA K102N
CAP256.15-wk.SU	0.0001	0.0001	0.001	0.002	0.001	0.031	0.008	0.002	<0.02	<0.02	0.002
CAP256.6-wk.PI	4.120	>100	>100	>100	>100	>100	>100	>100	>100	>100	>100
CAP210.E8	0.0001	0.0001	0.01	0.005	0.006	0.143	0.088	0.009	<0.02	<0.02	0.006
ZM53 M.PB12.2	0.0001	0.0001	0.004	0.004	0.004	0.128	0.066	0.004	<0.02	<0.02	0.005
ZM197.7	0.002	0.006	0.04	0.04	0.14	2.36	1.32	0.44	1.73	3.06	1.77
DU156.12	0.001	0.02	0.78	0.28	0.41	0.08	0.06	4.92	7.08	10.68	6.91
Q259.d2.17	0.002	0.01	0.03	0.01	0.03	0.66	2.30	0.70	0.40	1.16	0.44
CAP45.G3	0.0002	0.0005	0.004	0.002	0.006	0.07	0.25	0.77	0.79	7.97	0.65
DU422.01	0.05	0.02	2.32	0.14	1.27	29.44	40.33	8.50	15.26	24.81	10.90
ZM109.4	0.003	>100	16.66	2.04	15.10	>100	>100	>100	>100	>100	>100
PVO.04	0.08	1.15	35.35	15.48	>100	>100	>100	>100	>100	>100	>100
ZM214.15	0.003	>100	3.95	0.31	1.01	2.126	5.762	>100	>100	>100	>100
ZM249.1	0.005	>100	0.52	0.10	0.30	0.821	2.622	>100	>100	>100	>100
AC10.29	0.25	>100	84.63	38.21	>100	>100	>100	>100	>100	>100	>100
Q461.e2	0.03	0.72	35.28	18.94	47.64	>100	>100	>100	>100	>100	>100
Q842.d12	0.010	2.86	13.09	6.65	47.57	>100	>100	>100	>100	>100	>100
MLV	>100	>100	>100	>100	>100	>100	>100	>100	>100	>100	>100
Mean IC_{50}	0.005	0.009	0.46	0.18	0.21	0.44	0.51	0.17	nd	nd	0.20
% breadth	100	69	94	94	81	63	63	50	50	50	50

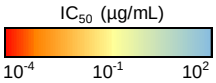

Figure 3.3. Neutral and deleterious mutations in the CAP256.25/04 pair.

Neutralization data using mutants (indicated schematically above the table) between CAP256.25 and CAP256.04, potency indicated as per the key. Arithmetic mean titers (IC_{50}, µg/mL) from at least two experiments are reported.

To model the interactions between V2 and CAP256.04 or CAP256.25, we fitted the sequence of CAP256.04 to the crystal structure of CAP256.25 in complex with the CAP256-34 week trimer which shares key contact residues for the CAP256-VRC26 lineage, including N160, R166, D167, K168 and K169 with CAP256.15-wk SU (Figure 3.4 A), and which likely triggered the lineage [223]. The model showed that the N130 glycan projects from the trimer and is situated proximal to the CDRH1. The CAP256.25 R28 residue was predicted to hydrogen bond with the N130 glycan while CAP256.04 S28 was not predicted to interact with this glycan. Surprisingly, the introduction of S28R to CAP256.04 R100rA and CAP256.04^{25H3} (Figure 3.3) decreased the breadth of these antibodies by five and four viruses, respectively, although the potency remained unchanged. Together with R100rA, the combination of S28R and N30D increased the breadth compared to S28R alone, but two viruses (PVO.04 and AC10.29)

remained resistant to neutralization (Figure 3.3). The conformation of the CDRH3 is partly supported by the intermolecular interactions between this loop and the CDRH1 and CDRH2 [206,361]. Consequently, the interaction between R28 and the CDRH3 may shift the CDRH1 toward the N130 glycan, which may be countered by the N30 residue (Figure 3.4 A, top panel). Furthermore, the model showed that 100r was positioned in close proximity to the viral residue K168, and that K168 was hydrogen bonded to the CDRH3 residue E100c (Figure 3.4 A, bottom panel). Therefore, due to electrostatic repulsion, R100r likely displaces K168, disrupting the interaction between K168 and E100c. In contrast, CAP256.25 has a small, uncharged Ala at position 100r which would not obstruct the adjacent bond. This suggests that an R100rA mutation may reduce electrostatic repulsion and therefore increase antigen affinity, providing a mechanism for the enhanced breadth associated with this mutation.

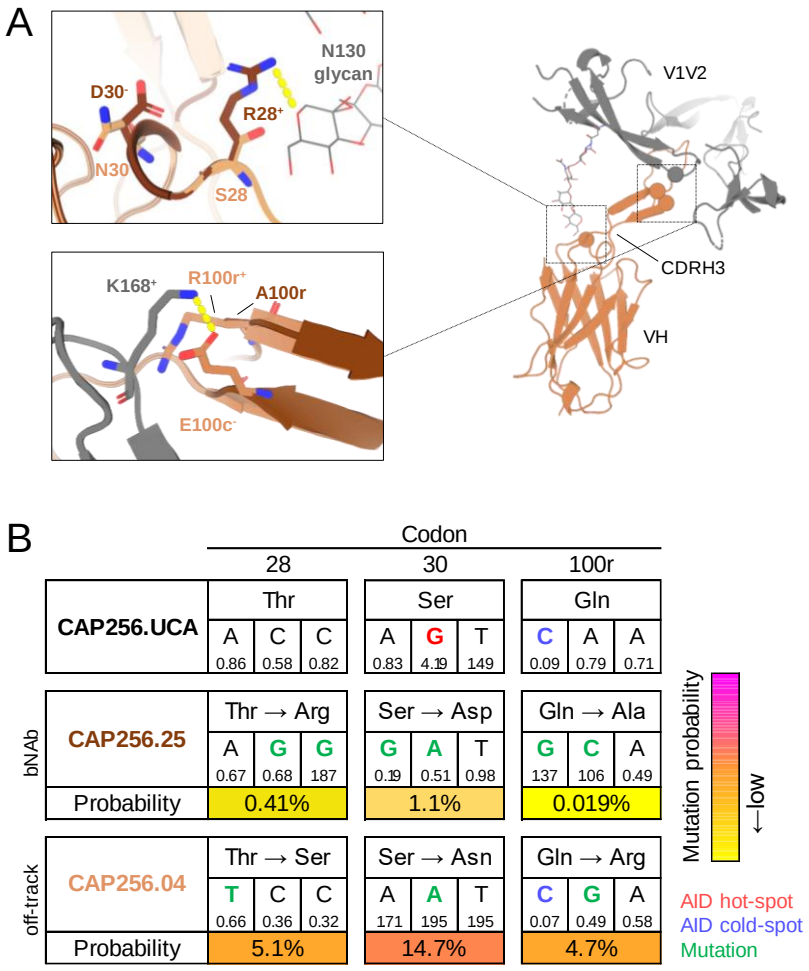

Figure 3.4. The structural effect and probabilities of the CAP256.04 off-track mutations S28, N30 and R100r.
(A) The amino acid sequence of CAP256.04 (orange) was fitted to a model of CAP256.25 (brown) and the V1V2 of trimeric CAP256 34-week Env (grey, [206]) in Swiss-PdbViewer (v4.1.0) and visualized in PyMOL (v2.0.2). The top inset shows the CAP256.25 CDRH1 D30 (brown) residue and a hydrogen bond between CAP256.25 CDRH1 residue R28 (brown), and the glycan at N130. The bottom inset displays CAP256.04 R100r (orange) in proximity to V2 K168. Symbols $^{+}$ and $^{-}$ denote positive and negative charge, respectively. (B) The germline (T28, S30 and Q100r)

and mature amino acid sequences (CAP256.25 T28R, S30D and Q100rA, and CAP256.04 T28S, S30N and Q100rR) at codons 28, 30 and 100r are displayed with the nucleotide sequence of each codon. Blue and red text indicates AID cold-and hotspots, respectively. Green text refers to mutations and yellow to pink shading indicates low and high probability mutations, respectively. The mutability scores are shown below each nucleotide.

Next, to estimate the probability of the occurrence of mutations prior to selection that are associated with the off-track phenotype, we utilized the ARMADiLLO software [380]. We first assessed the probability of the CDRH1 T28 residue (found in the CAP256.UCA) mutating to either 28R (as in CAP256.25) or 28S (in CAP256.04, Figure 3.2 A). We found that the CAP256.25 T28R mutation was improbable (0.41%), requiring two base changes (ACC to AGG), whereas T28S (in CAP256.04) was ten times more probable (5.1%), requiring only one change (ACC to TCC, Figure 3.4 B). Similarly, two base changes were necessary for the improbable (1.1%) mutation S30D (in CAP256.25), whereas S30N (in CAP256.04) was a probable (14.7%) event as it occurred in an AID hot-spot (Figure 3.4 B). The combination of T28R and S30D (in CAP256.25), which was necessary for neutralization when transplanted into CAP256.04, was a highly improbable event (0.004%, Figure 3.4 B). Furthermore, the CDRH3 Q100rA mutation, that confers breadth to CAP256.25, was predicted to occur very rarely with a ~0.019% probability, requiring two base changes (CAA to GCA), one of which was in an AID cold-spot (Figure 3.4 B). In contrast, we found that Q100rR that results in the off-track phenotype was predicted to occur with a much higher probability of 4.7%, requiring only a single nucleotide change that was not located within an AID cold-spot (Figure 3.4 B). Furthermore, the improbability of the evolution of T28R, N30D and Q100rA was reflected in next-generation sequences of the CAP256 lineage [223,382], where T28R, S30D and Q100rA together accounted for <2% of the sequences. Altogether, this suggests that a single relatively probable mutation in the CDRH3 primarily limits the neutralization breadth of CAP256.04.

3.5.4 The CDRH3 alone modulates neutralization breadth and potency of the off-track antibody CAP256.20

Subsequently, we sought to determine which sites were responsible for the off-track phenotype of CAP256.20 compared to the related bNAb, CAP256.27 (Figure 3.5 A). Of the 6 amino acids that distinguish these CDRH3s, several were charge changes, with overall CDRH3 charge of -7 and -3 in CAP256.27 and CAP256.20, respectively. First, we transplanted the CDRH3 from CAP256.27 into CAP256.20 (CAP256.20^{27H3}) and tested this chimera for neutralization breadth. In contrast to the CAP256.04/.25 pair, transfer of only the CAP256.27 CDRH3 into CAP256.20 introduced both bNAb-like breadth and potency into the off-track antibody, increasing breadth from 1/16 to 14/16 viruses and potency from 2.92 to 0.05 µg/mL (Figure 3.5 B). In the reverse

experiment, replacing the CDRH3 of CAP256.27 with that of CAP256.20 (CAP256.27^{20H3}) almost completely abrogated neutralization (Figure 3.5 B).

A

Antibody		CDRH1 (26)	CDRH2 (51)	CDRH3 (95 100d 100j 100n 100w)	Length	Charge
bNAb	CAP256.27	QFPFSHYG	ITNDGTKK	DQREDECEEWWSDYYDFGKELPCRKFRGLGLAGIFDI	37	-7
off-track	CAP256.20	..A..N..	.....N..	.........R.....H..RV.....Y.......V...	37	-3

B

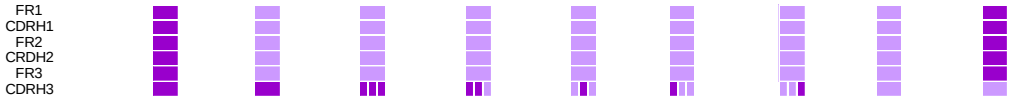

Pseudovirus	256.27	256.20^{27H3}	256.20 R100dW H100jD V100nE	256.20 R100dW H100jD	256.20 H100jD	256.20 R100dW	256.20 V100nE	256.20	256.27^{20H3}
CAP256.15-wk.SU	0.002	0.002	0.001	0.002	0.007	0.06	5.30	>100	>100
CAP256.6-wk.PI	>100	>100	>100	>100	>100	>100	>100	>100	>100
CAP210.E8	0.004	0.006	0.003	0.009	0.20	2.73	>100	>100	>100
CAP45.G3	0.004	0.004	0.006	4.31	>100	>100	>100	>100	>100
ZM53 M.PB12.2	0.001	0.002	0.001	0.001	0.004	0.01	1.01	2.92	2.27
ZM109.4	0.05	0.04	0.05	13.44	>100	>100	>100	>100	>100
ZM197.7	0.007	0.01	0.006	0.02	0.47	5.61	>100	>100	>100
ZM249.1	0.58	0.69	1.65	>100	>100	>100	>100	>100	>100
ZM214.15	0.39	3.07	0.46	3.91	>100	>100	>100	>100	>100
Du156.12	0.005	0.008	0.006	0.63	>100	>100	>100	>100	>100
Du422.01	0.07	0.03	0.05	2.61	>100	>100	>100	>100	>100
Q259.d2.17	0.02	0.05	0.05	4.20	>100	>100	>100	>100	>100
Q461.e2	0.03	0.04	0.004	0.23	>100	>100	>100	>100	>100
Q842.d12	6.60	39.72	10.57	>100	>100	>100	>100	>100	>100
PVO.04	0.54	0.66	0.56	0.89	>100	>100	>100	>100	>100
AC10.29	>100	>100	>100	>100	>100	>100	>100	>100	>100
MLV	>100	>100	>100	>100	>100	>100	>100	>100	>100
Geo mean IC_{50}	0.03	0.05	0.03	0.27	0.04	0.33	2.31	2.92	2.27
% neutralization	88	88	88	75	25	25	13	7	7
CDRH3 charge	-7	-7	-7	-6	-5	-4	-4	-3	-3

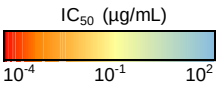

Figure 3.5. The CDRH3 alone restricts the neutralization breadth and potency of CAP256.20.

(A) Comparison of the CDR sequences of CAP256.20 (light purple) and CAP256.27 (purple). The blue box highlights key off-track mutations. (B) Neutralization data using mutants and chimeras (indicated schematically above the table) between CAP256.27 and CAP256.20, with neutralization potency by color, as shown in the key. Neutralization data represents the arithmetic mean titers (IC_{50}, µg/mL) from at least two experiments.

To determine which of the six residues within the CDRH3 of 256.20 limited breadth, we focused on three residues which altered the electronegativity of the loop, R100d, H100j and V100n (Figure 3.5 A), and mutated these sites alone and in combination. The V100nE mutation, which slightly decreased the charge of the CDRH3 only marginally improved neutralization breadth by one additional virus (the autologous superinfecting virus, CAP256.15-wk SU) (Figure 3.5 B). R100dW also decreased the charge and increased breadth by an additional three viruses (CAP256.15-wk SU, CAP210 and ZM197). Similarly, introduction of an H100jD mutation

conferred neutralization of the same three additional viruses but with greater potency than R100dW (GM potency of 0.04 compared to 0.33 µg/mL, respectively). The combination of R100dW and H100jD increased potency and breadth to a total of 12/16 viruses, while V100nE, R100dW and H100jD together introduced the same bNAb-like broad neutralization and potency as the entire CDRH3 transplant (Figure 3.5 B). In the reverse experiment, mutating positions 100d, 100j and 100n in the CDRH3 of CAP256.27 to match the sequence of CAP256.20 knocked out neutralization against previously sensitive viruses (Figure 3.6). Therefore, of the 17 residues that differentiate the heavy chain of CAP256.27 and CAP256.20 only three amino acids, all within the CDRH3, were responsible for limiting the breadth of CAP256.20.

Pseudovirus	256.27	256.20	256.27 W100dR	256.27 D100jH	256.27 E100nV	256.27 W100dR D100jH E100nV
CAP256.15-wk.SU	0.002	>100	0.002	0.001	0.0002	>100
CAP256.6-wk.PI	>100	>100	>100	>100	>100	>100
CAP210.E8	0.004	>100	0.005	0.05	0.004	>100
CAP45.G3	0.004	>100	>100	>100	0.09	>100
ZM53 M.PB12.2	0.001	2.92	0.002	0.001	0.001	18.80
ZM109.4	0.05	>100	>100	>100	0.83	>100
ZM197.7	0.007	>100	0.08	0.67	0.02	>100
ZM249.1	0.58	>100	>100	>100	0.25	>100
ZM214.15	0.39	>100	>100	>100	23.26	>100
Du156.12	0.005	>100	>100	>100	0.003	>100
Du422.01	0.07	>100	>100	>100	0.50	>100
Q259.d2.17	0.02	>100	>100	>100	0.45	>100
Q461.e2	0.03	>100	>100	>100	0.06	>100
Q842.d12	6.60	>100	>100	>100	15.68	>100
PVO.04	0.54	>100	63.83	94.54	0.70	>100
AC10.29	>100	>100	>100	>100	>100	>100
MLV	>100	>100	>100	>100	>100	>100
Mean IC_{50}	0.03	2.92	0.04	0.08	0.09	18.80
% neutralization	88	7	31	31	88	7
CDRH3 charge	-7	-3	-6	-5	-6	-3

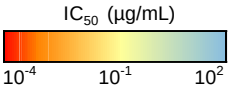

Figure 3.6. Off-track conferring mutations knock out CAP256.27 neutralization.

Neutralization data using mutants (indicated schematically above the table) between CAP256.27 and CAP256.20, potency indicated as per the key. Arithmetic mean titers (IC_{50}, µg/mL) from at least two experiments are reported.

Comparison of the probabilities of the breadth-conferring and restricting mutations between CAP256.27 and the CAP256.UCA showed that the G100nE bNAb mutation was improbable (0.89%), since two base changes were required (Figure 3.7 A). In contrast, the W100dR, D100jH and G100nV mutations that took CAP256.20 off-track are highly probable (10%, 14% and 3%, respectively), as only single base changes were necessary, with the H100j mutation

in an AID hot-spot (Figure 3.7 A). The probability of retaining all three mutations that confer breadth (W100d, D100j and G100n) in the absence of selection is 0.33%. Overall, the relatively higher probability of these mutations which restrict breadth highlights the potential ease with which members of this bNAb lineage may mature along undesirable pathways.

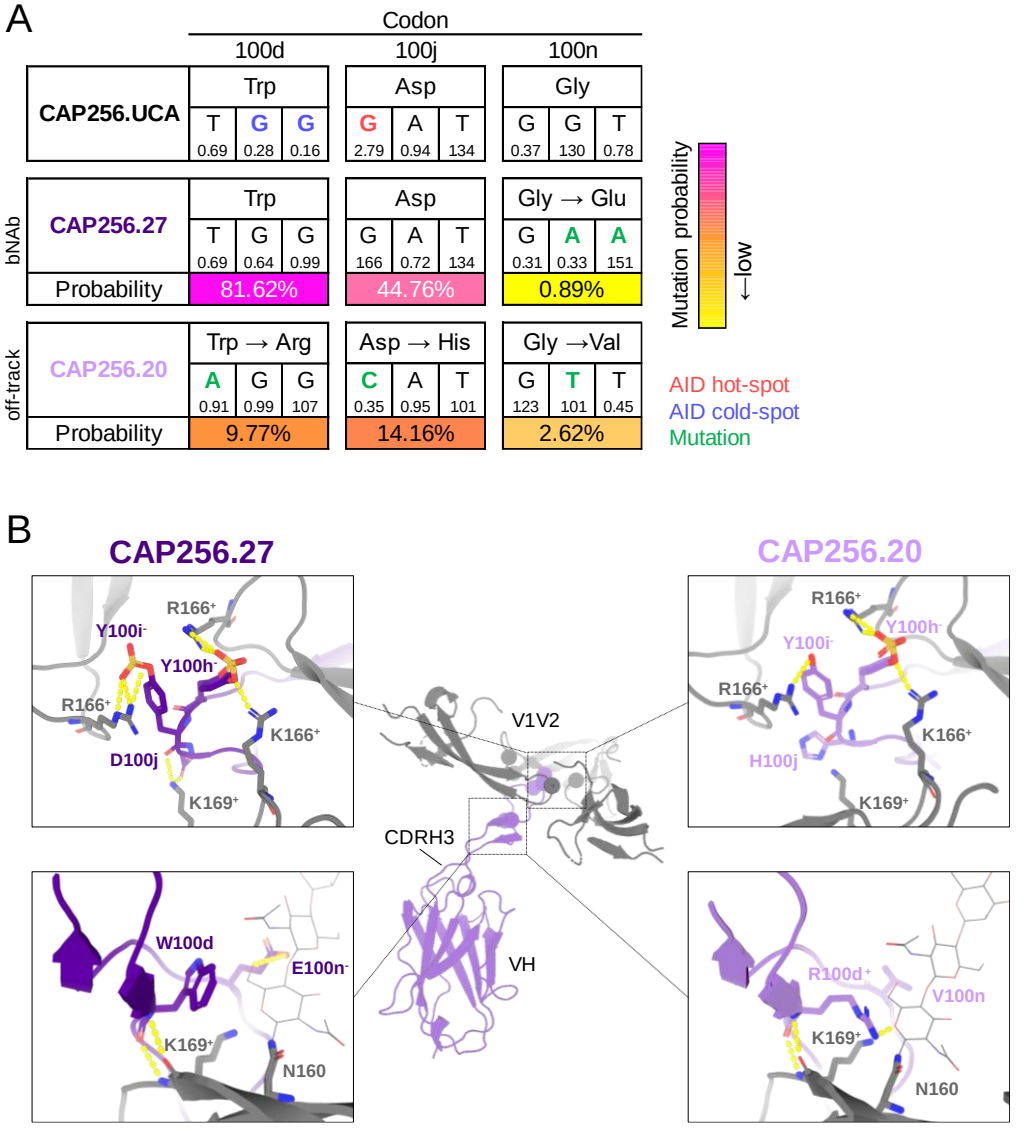

Figure 3.7. The probability and structural effect of the CAP256.20 off-track mutations W100dR, D100jH and G100nV. (A) The germline (W100d, D100j and G100n) and mature nucleotide and amino acid sequences (CAP256.27 W100d, D100j and G100nE and CAP256.20 W100dR, D100jH and G100nV) at codons 100d, 100j and 100n are displayed. Blue and red text indicate AID cold- and hot-spots, respectively. Green text refers to mutations, and yellow to pink shading indicates low and high probability mutations, respectively. The mutability scores are below each nucleotide. (B) The sequence of CAP256.20 (light purple) and CAP256.27 (purple) were fitted to a structure of CAP256.25 and trimeric CAP256 34-week Env [206] in Swiss-PdbViewer (v4.1.0) and aligned and visualized in PyMOL (v2.0.2). The top panels shows the interaction between the CDRH3 YYD motif (purple/light purple) and the V2 epitope (grey). The bottom panel displays the CAP256.27 residues W100d and E100n (purple) and CAP256.20 R100d and V100n (light purple) in proximity to K169, $^{+}$ and $^{-}$ denotes positive and negative charge, respectively.

To explore the basis of these results, we fitted the amino acid sequences of the CAP256.20 and CAP256.27 heavy chains to the crystal structure of the CAP256.25 heavy chain in Swiss-PdbViewer (v4.1.0), and then aligned this to a CAP256-34 week trimer structure (Figure 3.7 B, [206]). The YYD motif of CAP256.27 was predicted to hydrogen bond with two K166 residues on two protomers and R166 and K169 on the remaining protomer (Figure 3.7 B, top left). The mutations in CAP256.20 likely disrupt these interactions by placing a positive charge (H100j) proximal to K169 and possibly preventing sulfation of the preceding Tyr [383], which would knock out contacts with K166 (Figure 3.7 B, top right).

Furthermore, the hydrogen bond between E100n, present in CAP256.27, and the N160 glycan was disrupted by the CAP256.20 V100n substitution (Figure 3.7 B, bottom left). In addition, the CAP256.20 R100d mutation, places a positive charge next to K169 resulting in electrostatic repulsion (Figure 3.7 B, bottom right) and possibly preventing the backbone interactions between these residues. Therefore, key interactions between the highly electronegative CDRH3 of CAP256.27 (-7) and the electropositive V2 epitope are abrogated by the more electropositive CDRH3 of CAP256.20 (-3), resulting in the off-track phenotype.

3.5.5 CAP256.20 was dependent on a globally rare Q169 immunotype

We were interested in determining which viral immunotypes (or epitope amino acid variants) drove CAP256.20 away from breadth. The K169 immunotype, which forms part of the CAP256 epitope, is fairly conserved within subtype C viruses (65.9%) (hiv.lanl.gov) (Figure 3.8 A) [205]. In contrast, the 169Q immunotype is present in only 6.5% of subtype C viruses (Figure 3.8 A) but dominated the viral population in donor CAP256 across 21 of 28 time points from six to 206 weeks post infection (Figure 3.8 B and Figure 3.9 A). We hypothesized that this globally rare immunotype, which predominated in CAP256, contributed to the evolution of CAP256.20. Introduction of 169Q mutations into eleven heterologous viruses slightly improved the neutralization of four viruses by CAP256.20 (Figure 3.9 B), suggesting a preference of CAP256.20 for 169Q, though other viral determinants clearly contribute to neutralization sensitivity/resistance.

As autologous viruses, rather than heterologous viruses, select mutations during SHM, we determined the sensitivity of autologous viruses containing either a 169Q or 169K immunotype to neutralization by CAP256.20 and CAP256.27. We identified two viruses that naturally

contained a 169Q (42-wk 5 and 48-wk 10), and were sensitive to CAP256.20 and CAP256.27^{20H3}. Introduction of Q169K mutations into these viruses knocked out neutralization by these antibodies, and their matched CDRH3 chimeras (Figure 3.8 C). In the reverse experiment, introduction of a 169Q into three autologous viruses (34-wk 80, 59-wk 10b and 15-wk SU, containing 169K/I and resistant to CAP256.20 and CAP256.27^{20H3}) resulted in increased sensitivity to these antibodies (Figure 3.8 C). In all five viruses, the 169K immunotype was associated with increased neutralization potency by CAP256.27, CAP256.20^{27H3} and the additional broad CAP256.20 mutants and chimeras (Figure 3.9 C), consistent with previous studies [204,205]. These data indicate a CDRH3-mediated preference of CAP256.20 for the 169Q immunotype, which limited the evolution of breadth in this antibody.

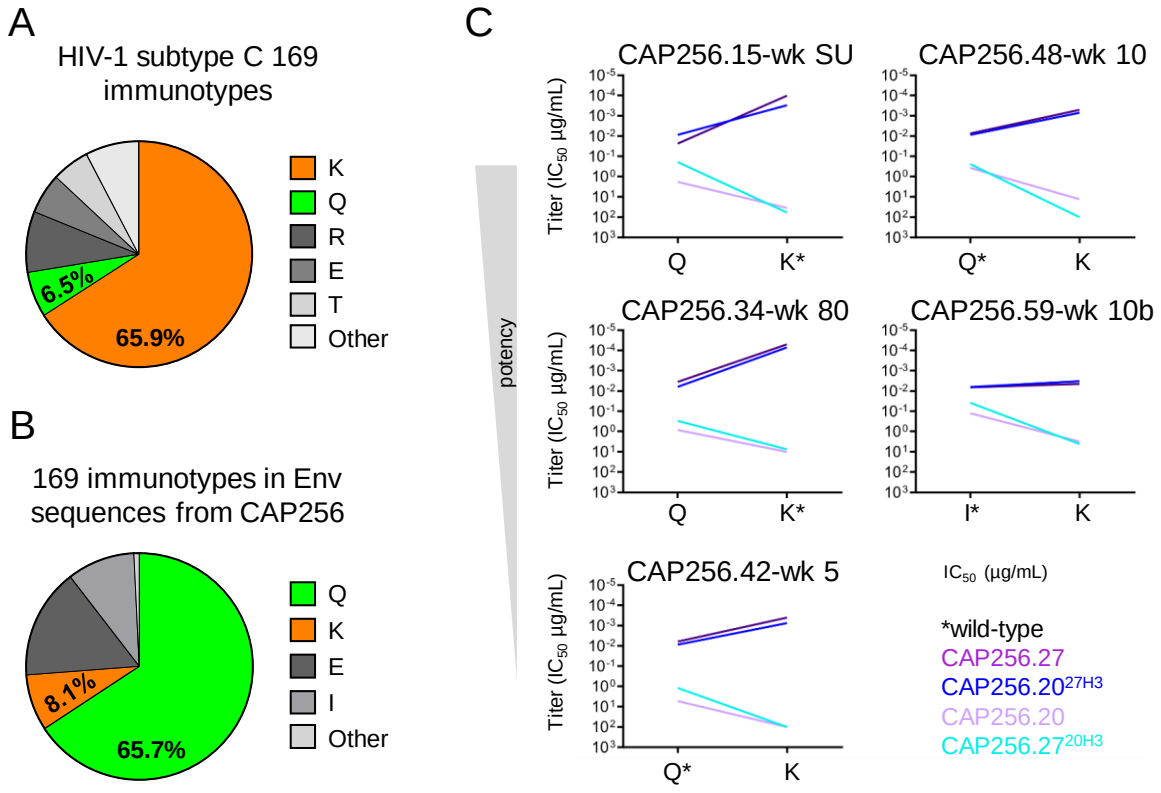

Figure 3.8. The off-track antibody CAP256.20 neutralizes a globally rare 169Q immunotype that was common in donor CAP256.

(A) The K169 (orange) immunotype is common in globally circulating viruses, (B) while 169Q (green) predominates in CAP256 across most time points. (C) Slope graphs displaying the change in neutralization titer (IC_{50}) of CAP256.20 (light purple), CAP256.27 (purple), CAP256.20^{27H3} (blue) and CAP256.27^{20H3} (cyan) against K169 and 169Q autologous viruses.

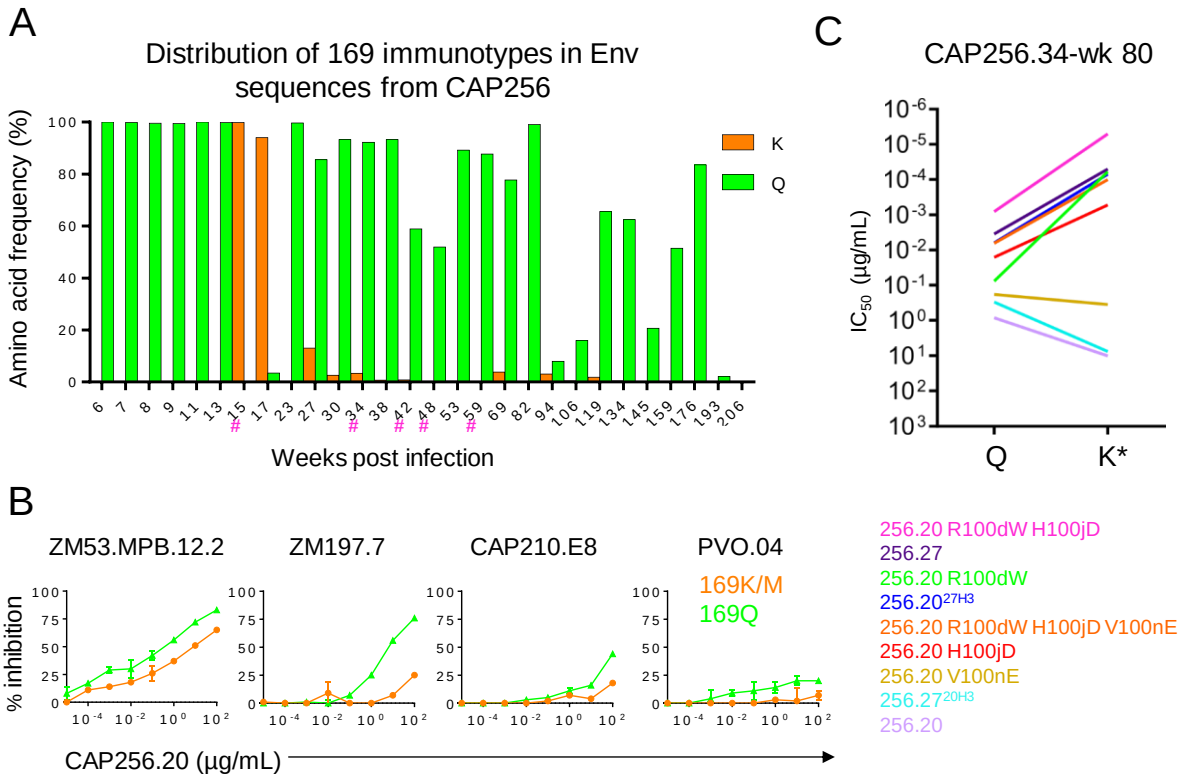

Figure 3.9. 169Q immunotype predominates in CAP256 and CAP256.20 exhibits weak neutralization of heterologous 169Q viruses.

(A) The frequency of the 169Q (green) and 169K (orange) Env immunotypes across 28 time points from six to 206 weeks post infection. #The viruses tested in Figure 3.8 C were isolated at the indicated time points. (B) CAP256.20 neutralization curves of wild-type (orange, 169K/M as indicated) and 169Q mutant (green) heterologous viruses. (C) An extension of Figure 3.8 C, the neutralization titers of the CAP256.27/20 wild-type and chimeric antibodies (from Figure 3.5 B) were tested against the 34-wk 80 virus.

3.6 Discussion

A major focus of HIV vaccine design is based on a deep understanding of the development of bNAbs during HIV infection. Studies of HIV/antibody co-evolution have provided a template for the maturation of breadth that is now the basis of B-cell lineage vaccine strategies [187,189,197,203,205,220,223,229]. However, much less is known about the maturation of antibodies within bNAb-containing lineages that fail to acquire breadth. We have previously shown that these include both “dead-end” antibodies (that fail to acquire breadth and exhibit low SHM), and “off-track” antibodies that acquire substantial SHM, but little breadth, and are the focus of this study [223]. Here we used previously identified strain-specific “off-track” antibodies that are closely related to broad members of the CAP256-VRC26 bNAb lineage to probe the genetic and viral contributors to their maturation [223]. In two pairs, we identified key breadth-restricting mutations, and defined the probabilities of their occurrence. Furthermore, we show the preferential neutralization of a globally rare immunotype by CAP256.20 impeded the evolution of breadth, providing a mechanism for the development of off-track responses in infection. Together these data provide insights into the challenges associated with driving maturation of antibodies towards breadth, a central question in HIV vaccine design.

Studies of bNAb lineages have highlighted the substantial plasticity in their maturation, enabling the development of breadth through multiple pathways [189,204,205,382]. This suggests that immunization strategies promoting high levels of SHM along diverse pathways may enhance bNAb development. Our data suggests that similarly, the development of off-track antibodies can occur by multiple pathways, and through the acquisition of very few mutations. Indeed, within the CAP256.20/27 pair, only three mutations were sufficient to divert CAP256.20 away from both breadth and potency. Furthermore, the enhanced breadth of CAP256.04 R100rA, which contains a single CDRH3 mutation, in contrast to the six mutations in CAP256.04^{25H3}, suggests substantial mutational “noise”. Additionally, we found a reduction of breadth when the CAP256.25 CDRH2 or single CDRH1 mutations were introduced into CAP256.04. These data confirm that extensive SHM does not necessarily result in breadth and suggests that many mutations do not impact or negatively affect breadth.

The maturation of bNAbs towards breadth includes a requirement for functionally relevant but improbable mutations [380]. Consistent with previous studies, we find that the key breadth-conferring mutations in the CAP256-VRC26 lineage, such as Q100rA and G100nE, are highly improbable [380] and that mutations that restricted breadth were in many cases relatively probable. Interestingly, the two pairs of CAP256 antibodies provide distinct examples of how the probability of mutations could shape on- versus off-track maturation. In CAP256.20/27, the

potential for high probability breadth-limiting mutations (e.g. W100dR, D100jH and G100nV) is evident in pulling the B-cell off-track. In contrast, in the CAP256.04/25 pair, an important improbable mutation associated with breadth, Q100rA, represents a potential bottleneck that CAP256.25 has overcome to achieve breadth, but CAP256.04 has not. The more probable R100r mutation is also present in broader lineage members, suggesting compensatory mechanisms and that multiple pathways to breadth exist. Together these data indicate that, in some instances, the pathway to the off-track phenotype offers less “resistance” compared to the requirement for highly improbable mutations associated with breadth, and will require careful selection of immunogens to avoid this phenotype [380].

Several studies, including our previous work in the CAP256-VRC26 lineage, have shown how exposure to diverse viral variants contributes to the development of breadth [204,205,223]. This study extends this work to define the mechanisms that select the off-track phenotype within a single lineage. The enrichment of the globally rare 169Q immunotype in CAP256 and the preferential neutralization of this immunotype by CAP256.20, implicates 169Q autologous viral variants in the evolution of this off-track antibody. Early CAP256-VRC26 lineage members (CAP256.01 and CAP256.24) and other off-track antibodies (CAP256.12 and CAP256.13) are unable to neutralize 169Q viruses. However, most lineage members, especially those with breadth, are able to neutralize this immunotype, though to a lesser extent than K169 viruses. This indicates that whereas most lineage members tolerate 169Q, CAP256.20 is uniquely reliant on the globally rare Q169 immunotype, explaining the strain-specificity of this antibody. Structurally, this may be a consequence of the reduced dependence of bNAbs on specific side chain residues within the epitope, compared to an increased dependence of off-track antibodies such as CAP256.20 on such side chains. These data highlight the fact that evolution towards breadth, a desirable outcome from a vaccinology perspective, is distinct from antibody maturation to counter circulating autologous viral variants.

This study provides evidence that affinity maturation to counter globally rare viral immunotypes can drive antibodies within a broad lineage away from breadth. As with the maturation of breadth, off-track antibodies can develop through multiple evolutionary pathways. Furthermore, limited breadth despite high levels of SHM can occur by the introduction of few, but relatively probable, mutations. The inherently stochastic nature of affinity maturation may make avoiding off-track antibodies challenging. Furthermore, additional research is needed to determine if the expansion of off-track B-cell lineages prevents or limits the maturation of bNAbs. However, defining pathways towards and away from breadth will facilitate the selection of immunogens that elicit bNAbs and minimize off-track antibodies. Our data suggests that by selecting sequential immunogens that present globally conserved epitopes, the elicitation of off-track

antibodies can be minimized. As immunization strategies improve to allow targeting of specific antibody residues, these data inform the design of immunogens to elicit V2-directed bNAbs.

4. Complementary roles of heavy and light chain somatic hypermutation in conferring breadth and potency to the CAP256-VRC26 bNAb lineage

David Sacks[1,2], Kevin Wiehe[3], Lynn Morris[1,2,4] and Penny L. Moore[1,2,4]

[1] Centre for HIV and STIs, National Institute for Communicable Diseases (NICD) of the National Health Laboratory Service (NHLS), Johannesburg, South Africa

[2] Faculty of Health Sciences, University of the Witwatersrand, Johannesburg, South Africa

[3] Duke Human Vaccine Institute, Duke University School of Medicine, Durham, North Carolina, USA

[4]Centre for the AIDS Programme of Research in South Africa (CAPRISA), University of KwaZulu-Natal, Durban, South Africa

Manuscript in preparation for the Journal of Virology.

4.1 Introduction

First practiced millennia ago, inoculations have profoundly reduced the morbidity and mortality of more than 20 infectious diseases [264,267]. Yet, no effective vaccines exist for many major pathogens, including HIV, which infects approximately 37 million people and has resulted in nearly 40 million deaths [8]. Most vaccines confer protection via the induction of neutralizing antibodies [265,266]. But due to the substantial diversity of the exposed HIV Env glycoprotein, which is targeted by antibodies, the elicitation of broad neutralizing responses remains an ongoing challenge. However, about 20% of HIV infected individuals develop broadly neutralizing antibodies (bNAbs) that potently neutralize >50% of circulating strains [152,153,159,374]. Importantly, passive immunization of non-human primates with bNAbs protects against repeated high titer SHIV challenges [341–345]. Therefore, the induction of bNAbs via immunization is a central focus in the development of an HIV vaccine [164,212–215,218].

Despite the mutability of Env, which consists of a trimer of gp120-gp41 heterodimers, conserved sites exist due to functional constraints [160,167,168]. These regions include the membrane proximal external region (MPER), the gp120-gp41 interface, fusion peptide, CD4 binding site (CD4bs), N332 glycan supersite, gp120 silent face and variable loops 1 and 2 (V1V2) [160,167,168]. However, these vulnerable sites are typically buried in the viral membrane, hidden within the trimer core and/or occluded by glycans [160,167,168]. Consequently, many bNAbs have unusual characteristics that evolve over 2-3 years and/or are encoded by rare naïve B-cells. These features include very long or short complementarity-determining regions (CDR) of the heavy and/or light chain. In particular, the third CDR of the heavy chain (CDRH3) of N332 and V1V2 targeting bNAbs are unusually long (>20 amino acids), which grants them access to buried epitopes [167]. In contrast, the third CDR of the light chains (CDRL3) of some CD4bs bNAbs are unusually short to avoid clashes with glycans [167]. Moreover, many bNAbs, particularly those targeting the MPER, are markedly autoreactive likely because these antibodies make contacts with the host-derived viral membrane [170]. Furthermore, germline-reverted bNAbs, which are an approximation of their precursor, are generally non-neutralizing and most bNAbs accumulate extensive somatic hypermutations (SHM, >40% [193]) in the CDRs and framework (FR) to accommodate viral mutations and to focus contacts on conserved sites [193,197,225,227,228,230,232,234,249]. In addition, many of the mutations critical for breadth are predicted to occur with a low probability as they are situated in sites where activation-induced cytidine deaminase (AID), the enzyme that mediates SHM, has reduced activity and/or the mutation requires two or more base changes [128,380,384]. Together, the restricted CDR lengths, autoreactivity and high degree of SHM contribute to the rare presence of bNAbs in infected individuals.

However, exceptions exist, particularly within HIV infected children, who develop breadth within the first year of infection following modest somatic hypermutation [221,253,260,261]. For example, the N332 supersite-targeting bNAbs BF520.1 [221,222] and AIIMS-P01 [253], both isolated from pediatric donors, achieve 58% and 67% breadth, respectively, but the variable heavy and light chains are <10% mutated. In addition, among adult-derived bNAbs, the broadest members of the PCIN63 lineage of VRC01-class CD4bs bNAbs developed within two years and are substantially less mutated (~13%) than other members of this class, such as VRC01 (>40% SHM) [196]. Furthermore, approximately half of the somatic mutations in VRC01 do not appreciably contribute to neutralization [256]. This indicates that breadth can be achieved through moderate levels of SHM, within the range induced by vaccination [219,254,255].

With longitudinal sampling of antibody and viral sequences throughout infection, the unmutated common ancestor (UCA) of a bNAb lineage [187,189,196,197,203,205,220,222], and in some instances a "bNAb-initiating Env" [189,197,203,220,222,223] can be identified. These and other ontogenetic studies [171,194,244-247] provide a template for the design of stabilized native-like germline-targeting immunogens engineered to selectively trigger bNAb precursors. For example, the VRC01-class precursor targeting immunogens, eOD-GT8 [332,333] and BG505 SOSIP-GT1 [334] activated VRC01 progenitors in transgenic mice [332,334], which developed autologous neutralization following boosts [335]. Similarly, the V3 precursor-specific immunogen 11MUTB activated germline-PG121 in knock in mice, which evolved breadth after boosting [233,336]. Furthermore, rhesus macaques vaccinated with the N332-precursor targeting RC1 immunogen developed anti-V3 antibodies with long CDRH3s and PGT121/10-1074-like CDRL1s [337]. Similarly, targeted glycan deletions exposing the epitope of V1V2 bNAb germline precursors, lead to the development of autologous neutralization in rabbits [325]. Together, the identification of moderately mutated bNAbs from infection and germline-targeting immunogens has re-energized the search for an HIV vaccine. However, to selectively drive efficient SHM, the precise mutations that are necessary for the development of breadth need to be defined, and in many cases are unknown.

To address this, we focused on the V2-targetting CAP256-VRC26 bNAb lineage because the broadest (63%) and most potent (0.003 μg/mL) member, CAP256.25, is moderately somatically mutated [204,205]. The 33 member CAP256-VRC26 lineage was recovered from a subtype C superinfected African woman whose plasma neutralized 75% of heterologous viruses [157,204,205,360]. The CAP256.UCA was first detected 34 weeks post infection (pi)

by the primary infecting virus (6-wk PI) and weakly neutralized contemporaneous viruses related to the superinfecting (15-wk SU) virus [223]. Specifically, the 34-wk 80 virus, which evolved from the 15-wk SU, was particularly sensitive to the CAP256.UCA and is thought to be a good approximation of the bNAb-initiating virus [223]. The paratope of CAP256.25 includes the CDRH1 and CDRL2 but is dominated by the germline encoded, extremely long (38 amino acids, aa), flexible and anionic CDRH3. This loop is capped by the tyrosine sulfated YYD motif which is found in other V2-specific bNAbs [204–206,208,209]. An intra-loop disulfide bond stabilizes the CDRH3 but this bond is absent in the CAP256.UCA and early non-broad lineage members [205,207]. A rigid CDRH3 is crucial as this structure penetrates the trimer apex to contact residues $F_{159}N_{160}L_{165}R_{166}D_{167}K_{169}K_{171}$ on strands B and C of the V2 [153,205,223,360]. By 59 weeks pi, escape mutations at these sites, particularly at R166 and K169 emerged, with only the broader lineage members tolerating variability at these positions [153,223,360]. Although the broader CAP256 bNAbs are generally not dependent on glycans, the structure of CAP256.25 indicates that the CDRH1 and CDRL2 of the CAP256.UCA makes contact with glycans at N156, and N130 and N160, respectively [206].

To determine which mutations are critical for neutralization, we investigated the sequence differences between bNAb CAP256.25 and the CAP256.UCA and assessed the impact of these changes on neutralization. We found that the CDRHs, in particular the CDRH3, had accumulated many somatic mutations that were predicted to occur with a low probability. Furthermore, these CDRH3 mutations were primarily responsible for heterologous breadth, the neutralization of emerging autologous viral variants and the tolerance of viral diversity. In contrast, mutations in the light chain modulated both autologous and heterologous neutralization potency, but only improved heterologous breadth. This suggests that a minimally mutated CAP256.25-like bNAb requires mutations in the CDRHs and light chain for breadth and potency, respectively. Together these data indicate that the mutations in the heavy and light chains have complementary and differential impacts on neutralization. These data inform the design of vaccine strategies that bypass the protracted evolution of bNAbs by directing affinity maturation to sites pivotal for breadth and potency [215,218].

4.2 Materials and methods

4.2.1 Ethics statement

The University of the Witwatersrand human research ethics committee approved (M160934) the study reported herein (see 7.2, page 111, Appendix B: Ethics certificate). See 2.1 (page 31) for additional information.

4.2.2 Cell lines

Refer to 2.8 (page 35) for information on cell line maintenance. Briefly, the TZM-bl, 293T and 293F cell lines were utilized for the antibody neutralization assays, pseudovirus growth and monoclonal antibody production, respectively.

4.2.3 Probability of antibody mutations

The Antigen Receptor Mutation Analyzer for Detection of Low Likelihood Occurrences (ARMADiLLO) program was utilized to estimate the probability of amino acid substitutions prior to antigenic selection [380]. For more information, see 3.4.8 (page 46).

4.2.4 Site-directed mutagenesis and overlapping PCR

The protocols for mutagenesis and the overlapping PCR are at 2.3 (page 32) and 2.4 (page 33), respectively. The primers are listed in Appendix table 4.

4.2.5 Antibody expression

Antibodies were expressed and purified as per the methods in 2.9 (page 35). Briefly, the $CMVR_{HC}$ and $CMVR_{LC}$ plasmids were co-transfected with PEI MAX (Polysciences) into the 293F cell line. Following seven days, the monoclonal antibodies were isolated from the supernatant with Protein A resin (Pierce) columns.

4.2.6 Pseudovirus production

The protocol in 2.10 (page 36) was followed for pseudovirus production. In brief, PEI MAX (Polysciences) was used to co-transfect 293T cells with *env* and pSG3$_{\Delta env}$ plasmids, and the supernatants were titered with the TZM-bl cell line.

4.2.7 Neutralization assay

Antibody-mediated neutralization, measured with the TZM-bl neutralization assay (detailed in 2.11, page 37) was assessed by the reduction of Tat-inducible luciferase fluorescence

4.2.8 Data analysis

Refer to 2.13 (page 38).

4.3 Results

4.3.1 Highly improbable mutations (<0.01%) in CAP256.25 are restricted to the heavy chain FR3 and CDRH3

Since somatic hypermutation is associated with the acquisition of neutralization breadth and potency [187,189,196,197,203,205,220-222,380], we sought to determine which mutations were critical to the development of neutralization in the CAP256-VRC26 lineage. Therefore, we compared the most broad and potent member, CAP256.25, to the CAP256.UCA which exhibits weak, strain-specific neutralization [223]. The VDJ genes of the CAP256.25 heavy chain are 23% (33 aa) mutated from the germline sequence and the VJ genes of the light chain are 16% (18 aa) divergent (Figure 4.1 A). Since many breadth-conferring mutations in bNAb lineages are improbable events [380,384-386], we calculated the probabilities of the changes between the CAP256.UCA and CAP256.25 with the ARMADiLLO program [380] to identify putative key mutations. Most of the mutations in the heavy (16/33, Figure 4.1 B) and light (10/18, Figure 4.1 C) chains were found to occur with a relatively high probability of >1-10% (1-2% = yellow, 2-10% = green and >10% = dark green) and were distributed throughout the FR and CDRs. However, both the heavy (n=9, Figure 4.1 B) and light (n=4, Figure 4.1 C) chains also harbored improbable mutations (0.1-1% = orange), especially in the CDRs. Furthermore, three rare mutations (0.01-0.01% = red) were found in the heavy chain FR3 (n=1), CDRH3 (n=2) and CDRL3 (n=1, Fig. 1C) (Figure 4.1 B and C), with four exceedingly rare mutations (<0.01% = maroon) found only in the heavy chain FR3 (n=1) and CDRH3 (n=3) (Figure 4.1 B). In total, we identified eight highly improbable mutations (≤0.1%), three of which were in the CDRH3, which forms most of the paratope of the CAP256-VRC26 antibodies.

A

	Heavy chain								Light chain							
Antibody	FR1	CDR H1	FR2	CDR H2	FR3	CDR H3	FR4	% SHM (VDJ)	FR1	CDR L1	FR2	CDR L2	FR3	CDR L3	FR4	% SHM (VJ)
256.UCA	25	8	17	8	38	37	11	0	25	8	17	3	36	12	10	0
256.25	25	8	17	8	38	38	11	23	25	8	17	3	36	12	10	16
Mutations	1	4	1	3	6	18	0		1	2	3	2	3	6	1	

B

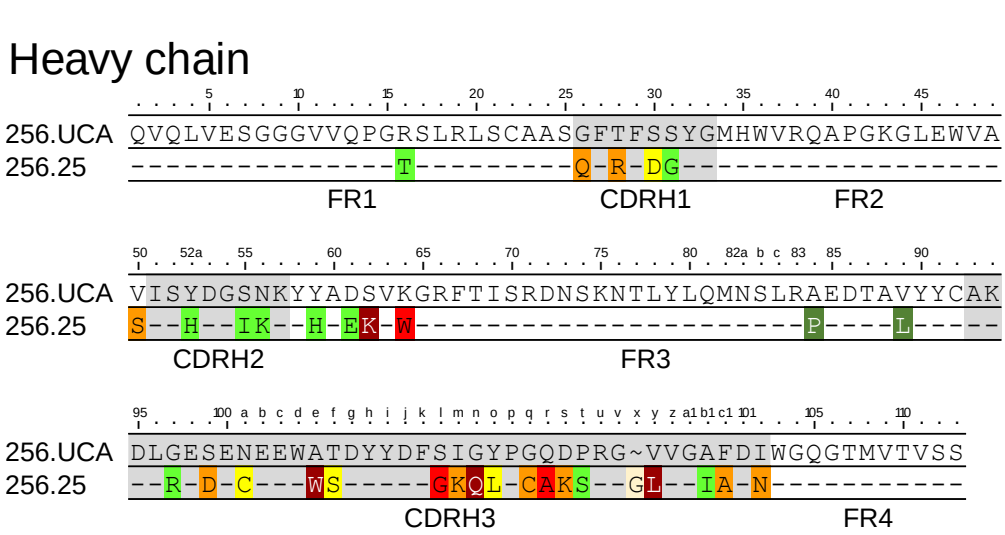

C

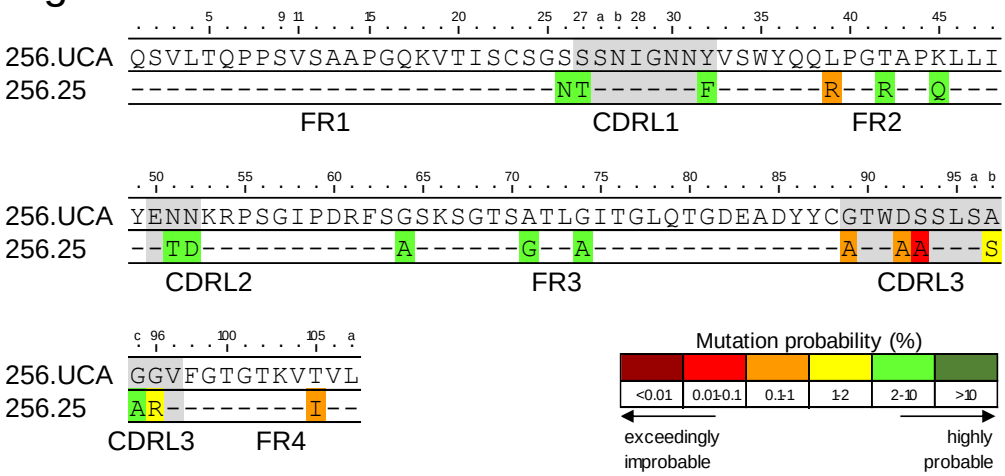

Figure 4.1. The amino acid sequence of the CAP256.UCA and CAP256.25 antibodies.

(A) The length (amino acids) of the framework (FR) and complementarity-determining regions (CDRs) of the heavy (CDRH) and light (CDRL) chains of CAP256.UCA and CAP256.25. The number of amino acids that differentiate these antibodies are reported. The amino acid sequences of the CAP256.UCA and CAP256.25 heavy (B) and light (C) chains are tabulated with the FR and CDRs (grey) indicated. Changes between the sequences are shaded according to the probability of the mutations (indicated in the key).

4.3.2 Two mutations improve autologous neutralization by the CAP256.UCA

As the CAP256.25 heavy chain harbored most of the improbable mutations (<1%), we first investigated the contribution of these sites to neutralization. Since beneficial antibody

mutations are selected by emerging, contemporaneous viral variants we initially tested autologous viruses. The CAP256.UCA, and other early antibodies with limited SHM and breadth, do not have cysteines at positions 100a and 100q, precluding the formation of a disulfide bond that is known to stabilize the CDRH3 [204,205,223]. Together, these mutations (N100aC and G100qC), which were predicted to occur with a probability of <1% (Figure 4.1) were introduced into the CAP256.UCA. We tested this antibody, UCA CC, for neutralization against 20 autologous viruses isolated from 6 to 69 weeks pi with V2 sequences ($HXB2_{160\text{-}173}$) related to either the 6-wk PI or 34-wk SU viruses (Figure 4.2). While the CAP256.UCA only weakly neutralized (<50% inhibition) the 15-wk SU at a high concentration (>50 µg/mL), as previously reported [223], the UCA CC potently neutralized this virus (0.050 µg/mL, Figure 4.2). Furthermore, although the CAP256.UCA neutralized three SU-like viruses from 34 weeks pi (34-wk 80, 34-wk 81 and 34-wk 77) with a geometric mean (GM) potency of 3.92 µg/mL, the disulfide mutant, UCA CC, neutralized these viruses with 206-fold greater potency (GM 0.019 µg/mL). Thus, the introduction of the disulfide bond into the CAP256.UCA, requiring only two amino acid changes, substantially improved potency and autologous neutralization of early SU-like viruses.

Heavy chain FR1 CDRH1 FR2 CDRH2 FR3 CDRH3	UCA	UCA CC	UCA^{25FR}	UCA^{25H2}	UCA^{25H3}	UCA^{25H23}	UCA^{25H123}	25	Titer (IC_{50} µg/mL) 10^{-5} – 10^{2} V2 160-173		
Light chain	UCA	UCA	UCA	UCA	UCA	UCA	UCA	25	-like	N160 glyc	169
6-wk PI	>50	>50	>50	>50	>50	>50	>50	0.22	PI	x	K
15-wk SU	>50	0.050	0.74	7.41	0.023	0.0097	0.006	0.00005	SU	✓	K
34-wk 80	0.79	0.0073	0.018	0.013	0.0055	0.0032	0.0026	0.00001	SU	✓	K
34-wk 81	7.82	0.053	0.29	0.096	0.015	0.008	0.004	0.00004	SU	✓	K
34-wk 77	9.74	0.018	0.050	0.17	0.004	0.002	0.0022	0.00001	SU	✓	K
34-wk 31	>50	>50	>50	>50	0.47	0.32	0.17	0.0011	SU	✓	I
34-wk 55	>50	>50	>50	>50	1.24	0.21	0.25	0.0022	SU	✓	I
34-wk 68	>50	>50	>50	>50	>50	>50	>50	>25	SU	✓	E
38-wk 16	>50	>50	>50	>50	>50	>50	>50	0.0069	PI	x	Q
38-wk 19	>50	>50	>50	>50	>50	>50	>50	>25	PI	x	Q
42-wk 1	>50	>50	>50	>50	1.02	0.45	0.35	0.00042	SU	✓	I
42-wk 5	>50	>50	>50	>50	1.39	0.63	0.61	0.00017	SU	✓	Q
42-wk 16	>50	>50	>50	>50	0.0049	0.0017	0.0023	<0.00001	PI	x	Q
42-wk 24	>50	>50	>50	>50	3.16	1.81	1.67	0.0025	SU	✓	R
42-wk 18	>50	>50	>50	>50	>50	>50	>50	0.015	SU	✓	T
59-wk 4	>50	>50	>50	>50	>50	4.76	2.81	0.091	PI	✓	Q
59-wk 2	>50	>50	>50	>50	>50	>50	>50	>25	SU	✓	E
69-wk 172	>50	>50	>50	>50	>50	>50	18.92	0.080	PI	✓	Q
69-wk 173	>50	>50	>50	>50	>50	>50	28.52	0.043	PI	✓	I
69-wk 177	>50	>50	>50	>50	>50	>50	>50	>25	PI	x	Q
Geo mean IC_{50}	3.92	0.024	0.12	0.20	0.10	0.067	0.14	0.0015			

Figure 4.2. Autologous neutralization by the CAP256.UCA heavy chain chimeras.

The sequences of the heavy (first row) and light (second row) chains for each antibody are visualized in a schematic. (First row) The variable heavy chain of CAP256.UCA (green) and CAP256.25 (purple) are shown in six segments, representing the three FR and three CDRs. (Second row) The light chains are colored according to the antibody, and the heavy chains are grey. The autologous viruses are tabulated in the first column and the neutralization titers

(IC_{50}, µg/mL) for each antibody populate the table and are colored by potency (indicated in the key). The last three columns on the right indicate the similarity of the $V2_{160-173}$ sequence to the SU or PI, whether N160 is glycosylated (✓) or not (x) and the 169 immunotype.

4.3.3 The CAP256.25 CDRH3 introduces autologous neutralization breadth

As the CDRH3 has a central role in Env recognition and harbored most of the improbable mutations, we transferred the entire CAP256.25 CDRH3 into the CAP256.UCA (UCA^{25H3}) and tested the neutralization of longitudinal autologous viruses. Compared to the CAP256.UCA, the UCA^{25H3} chimera exhibited >500-fold (GM 0.007 µg/mL) greater potency against the three 34-week viruses sensitive to the CAP256.UCA, and neutralized seven additional viruses, isolated at 15, 34 and 42 weeks pi (Figure 4.2). In contrast to the CAP256.UCA and UCA CC, which only neutralized viruses with a K169 immunotype, the UCA^{25H3} chimera neutralized SU-like viruses containing the 169I/Q/R immunotypes (Figure 4.2). Therefore, the UCA^{25H3} chimera was only half as mutated as CAP256.25 but exhibited substantial autologous neutralization (50% and 80%, respectively).

Since the CAP256.25 CDRH2 is situated >20Å from the viral V2 [206], we did not expect that the introduction of the CAP256.25 CDRH2 into the CAP256.UCA heavy chain (UCA^{25H2}) would substantially impact neutralization. Accordingly, this chimera neutralized only one additional virus (15-wk SU) compared to the CAP256.UCA and was 66-fold more potent against the SU-like 34-week viruses (Figure 4.2). Furthermore, while the combination of the CAP256.25 CDRH2 and CDRH3 (UCA^{25H23}) in the CAP256.UCA resulted in the neutralization of an additional virus (59-wk 4, Figure 4.2), the GM potency of this antibody was not substantially different (<2-fold) compared to the UCA^{25H3} chimera. Similarly, the potency remained unchanged when we introduced all three of the CAP256.25 CDRHs into the CAP256.UCA (UCA^{25H123}), although this antibody weakly neutralized two more viruses (69-wk 172 and 69-wk 173) compared to UCA^{25H23} (Figure 4.2). Together, UCA^{25H123} neutralized ten additional autologous viruses compared to CAP256.UCA, with 1,400-fold greater potency against the three viruses sensitive to CAP256.UCA. The viruses sensitive to UCA^{25H123} included three with a PI-like V2 sequence and several with 169I/Q/R immunotypes, but not 169E-containing viruses which were also resistant to CAP256.25 (Figure 4.2). These data indicate that mutations in the CDRHs, and the CDRH3 in particular, are the major determinants of neutralization of emerging autologous viral variants.

Despite the contribution of the CAP256.25 CDRHs to autologous neutralization, CAP256.25 was an order of magnitude more potent and neutralized three additional viruses (total of 17/20, Figure 4.2) compared to the closest chimera, UCA^{25H123}. This suggested that the heavy chain FR and/or the light chain, impact neutralization. We first tested a chimera consisting of the CAP256.25 FR in the CAP256.UCA (UCA^{25FR}). This antibody potently neutralized the 15-wk SU virus (0.74 μg/mL) and was 27-195-fold more potent against the three SU-like 34-wk viruses that were sensitive to the CAP256.UCA (Figure 4.2). However, the UCA^{25FR} chimera was substantially less potent compared to most of the CDRH mutants, confirming the importance of the CDRHs in mediating neutralization.

4.3.4 The CAP256.25 light chain enhances autologous neutralization potency

To test the role of the light chain in modulating neutralization we switched the light chains between the two antibodies and assessed their autologous neutralization. The CAP256.UCA heavy chain and CAP256.25 light chain chimera (UCA HC + 25 LC) neutralized the 34-week (34-wk 80, 34-wk 81 and 34-wk 77) viruses that were sensitive to the CAP256.UCA, but with 33-fold greater potency, and one additional virus (15-wk SU, Figure 4.3) was weakly neutralized. In the reverse experiment, the 25 HC + UCA LC chimera exhibited broad autologous neutralization (13/20 viruses) but was significantly ($p=0.0002$ Wilcoxon matched-pairs) less potent compared to CAP256.25 (Figure 4.3), confirming a role for the light chain in neutralization.

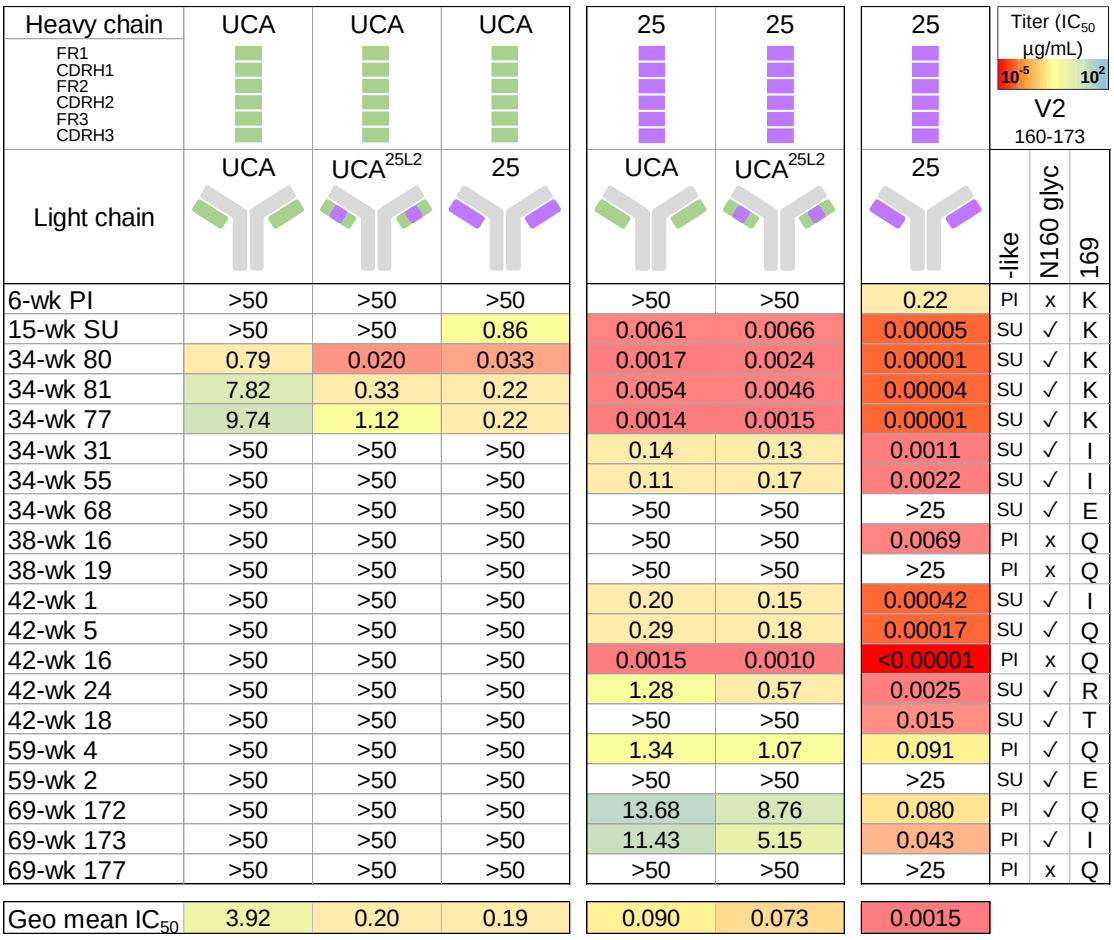

Figure 4.3. Autologous neutralization by the CAP256.UCA heavy and light chain chimeras.

The sequences of the heavy (first row) and light (second row) chains for each antibody are visualized in a schematic. (First row) The variable heavy chain of CAP256.UCA (green) and CAP256.25 (purple) are shown in six segments, representing the three FR and three CDRs. (Second row) The light chains are colored according to the antibody, and the heavy chains are grey. The autologous viruses are tabulated in the first column and the neutralization titers (IC_{50}, µg/mL) for each antibody populate the table and are colored by potency (indicated in the key). The last three columns on the right indicate the similarity of the $V2_{160\text{-}173}$ sequence to the SU or PI, whether N160 is glycosylated (✓) or not (x) and the 169 immunotype.

Since the structure of CAP256.25 and the 34-wk 80 trimer [206] indicated that the CDRL2 was in close proximity to the N156 glycan, we introduced the CAP256.25 CDRL2 into the CAP256.UCA light chain (UCA^{25L2}). This chimera (UCA HC + UCA^{25L2}) neutralized two 34-week viruses (34-wk 80 and 34-wk 81) with a potency similar to the UCA HC + 25 LC chimera (Figure 4.3), demonstrating that the CAP256.25 CDRL2 formed part of the paratope of the antibody. However, when UCA^{25L2} was paired with the CAP256.25 heavy chain (25 HC + UCA^{25L2}), we found that this chimera had the same breadth and potency as 25 HC + UCA LC (Figure 4.3), suggesting that the dominant role of the CAP256.25 heavy chain masked any contribution from the CDRL2.

To confirm the role of the light chain in modulating potency, we tested an expanded panel of chimeras between the mutated heavy chains (UCA CC, UCA^{25H2}, UCA^{25H3}, UCA^{25H23} and UCA^{25H123}) and either the CAP256.UCA or the CAP256.25 light chain (Figure 4.4). Compared to the CAP256.UCA light chain chimeras, the CAP256.25 light chain significantly improved the autologous neutralization potency of UCA^{25H3}, UCA^{25H23} and UCA^{25H123} (Figure 4.4). The potency of UCA CC and UCA^{25H2} similarly increased, but this did not reach statistical significance, likely due to the limited number of sensitive viruses (n=4, Figure 4.4). Together, these experiments indicate that the CAP256.25 light chain improves autologous neutralization potency of early SU-like viruses and that the CDRL2 was the major driver of the effect. This data supports the structural observation that the paratope of CAP256.25 includes the CDRL2 [206].

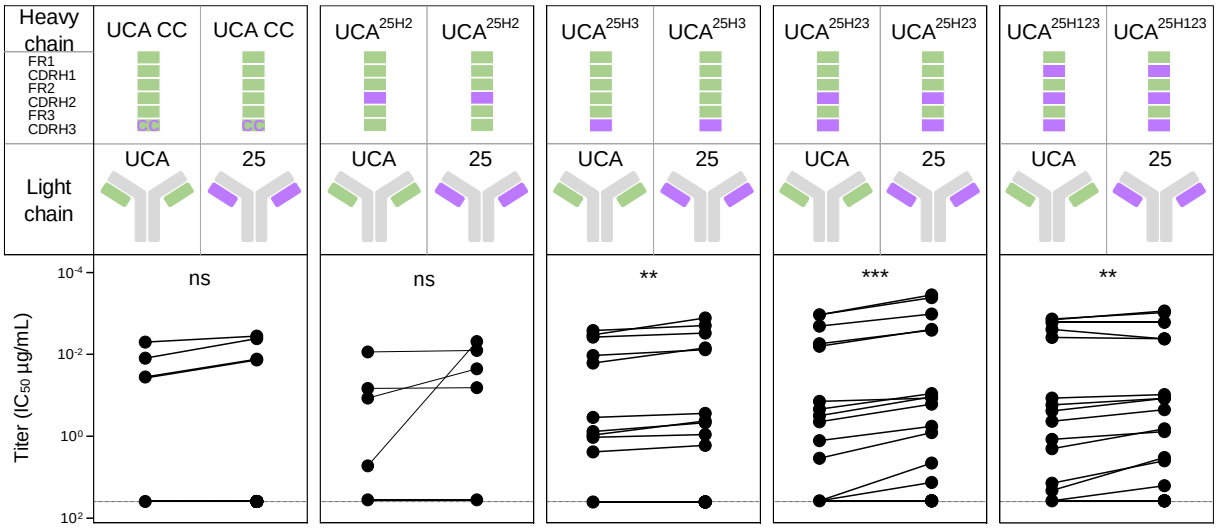

Figure 4.4. Autologous neutralization by the CAP256.UCA heavy chain chimeras paired with the CAP256.UCA and CAP256.25 light chains.

The schematics in the first and second rows detail the sequences of the heavy and light chains, respectively, for each antibody. (First row) The three FR and three CDRs of the CAP256.UCA (green) and CAP256.25 (purple) heavy chains are shown in six segments. (Second row) The light chains are colored according to the antibody, and the heavy chains are grey. The neutralization titers (IC_{50}, µg/mL) for each antibody are plotted on a logarithmic scale. The significance of the differences between each pair was determined with the Wilcoxon matched-pairs signed rank test (ns = not significant, *p=<0.05, **p=<0.01 and ***p=<0.001).

4.3.5 The CAP256.25 CDRH3 contributes to the tolerance of epitope variation

We next assessed the ability of heavy and light chain chimeric antibodies to neutralize an autologous virus mutated to contain the R166K, K169T and K169Q escape mutations [204,205,223]. These changes, which were associated with the development of breadth *in vivo*, were introduced into the bNAb-initiating Env (34-wk 80). While these viruses were resistant to

the UCA^{25FR}, UCA CC and UCA^{25H2} chimeras, regardless of which light chain was used, UCA^{25H3} was able to neutralize these viruses with varying potencies (Figure 4.5). This is consistent with the ability of the UCA^{25H3} chimera to neutralize SU-like viruses containing the 169I/Q/R immunotype (Figure 4.2). Notably, pairing UCA^{25H3} with the CAP256.25 light chain did not appreciably impact GM neutralization potency (<2-fold change, Figure 4.5). The addition of the CAP256.25 CDRH1 and/or CDRH2 to UCA^{25H3} (UCA^{25H123} and UCA^{25H23}) with the CAP256.UCA light chain improved potency by 5-fold compared to UCA^{25H3}. Pairing of these antibodies (UCA^{25H123} and UCA^{25H23}) with the CAP256.25 light chain increased their potency by only 2-3-fold (Figure 4.5). This suggests that mutations in the heavy chain, primarily in the CDRH3, rather than the FR and light chain, confers tolerance to epitope variation in emerging viral variants.

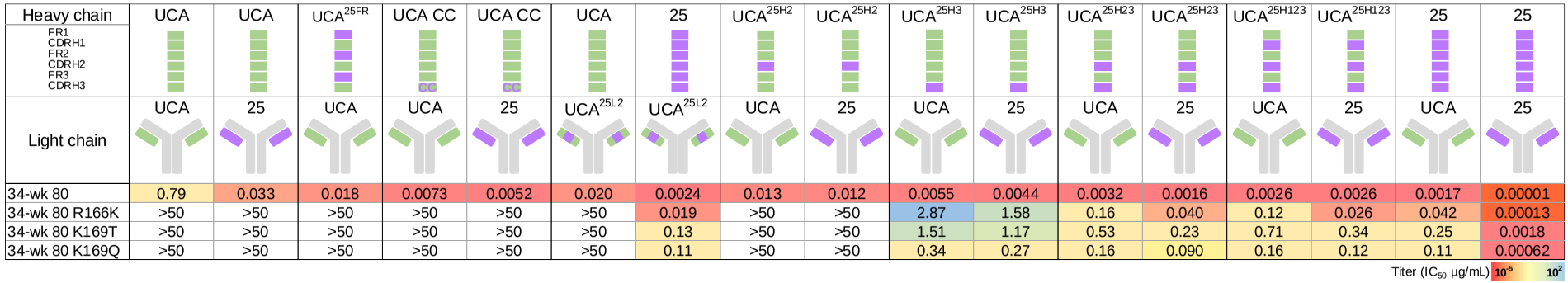

Figure 4.5. Tolerance of epitope variation in emerging autologous viral variants.

The sequences of the heavy (top row) and light (second row) chains for each antibody are visualized in a schematic. (First row) The variable heavy chain of CAP256.UCA (green) and CAP256.25 (purple) are shown in six segments, representing the three FR and three CDRs. (Second row) The light chains are colored according to the antibody, and the heavy chains are grey. The autologous viruses are tabulated in the first column and the neutralization titers (IC_{50}, µg/mL) for each antibody populate the table and are colored by potency (indicated in the key).

4.3.6 The heavy chain determines the completeness of quasi-species neutralization

A neutralization plateau of <100% suggests that there are mixed populations of viruses that are variably sensitive to neutralization, due to sequence or glycan heterogeneity [361,362,387]. We found that the neutralization curves of the viruses sensitive to the CAP256.UCA and the chimeras with the fewest somatic mutations (UCA CC, UCA^{25H2} and UCA^{25L2}), paired with either the CAP256.UCA or CAP256.25 light chain did not reach 100% neutralization (Figure 4.6). These viruses included 15-wk SU (Figure 4.6 A), 34-wk 77 (Figure 4.6 B), 34-wk 81 (Figure 4.6 C) and 34-wk 80 (Figure 4.6 D).

The UCA CC heavy chain matched with either the CAP256.UCA (dotted blue line) or CAP256.25 light chain (solid blue line), incompletely neutralized the 15-wk SU virus (80%, Figure 4.6 A). The neutralization curves of the UCA^{25H2} chimera, matched with the CAP256.UCA (dotted red curve) or CAP256.25 light chain (solid red curve), neutralized only 60-70% of the 15-wk SU (Fig. 6A) and 34-wk 77 (Figure 4.6 B) viruses at the highest concentration of antibody tested. Similarly, the CAP256.UCA heavy chain paired with the CAP256.25 light chain (solid green line) displayed incomplete neutralization against 15-wk SU (50%, Figure 4.6 A), 34-wk 77 (70%, Figure 4.6 B) and 34-wk 81 (75%, Figure 4.6 C), while neutralization of 34-wk 80 was close to 100% (Figure 4.6 D). The UCA^{25L2} chimeric paired with the CAP256.UCA heavy chain (solid orange line), exhibited the most limited neutralization against 15-wk SU (50%, Figure 4.6 A), 34-wk 77 (50%, Figure 4.6 B) and 34-wk 81 (70%, Figure 4.6 C). These data suggest that the more germline-like the sequence of the heavy chain, the lower the capacity to neutralize all viruses at high antibody concentrations. However, the minor changes introduced into UCA CC were sufficient to allow for the neutralization of 100% of 3/4 viruses suggesting that the rigidity of the CDRH3, conferred by these mutations, is important for the tolerance of emerging viral variants and glycans.

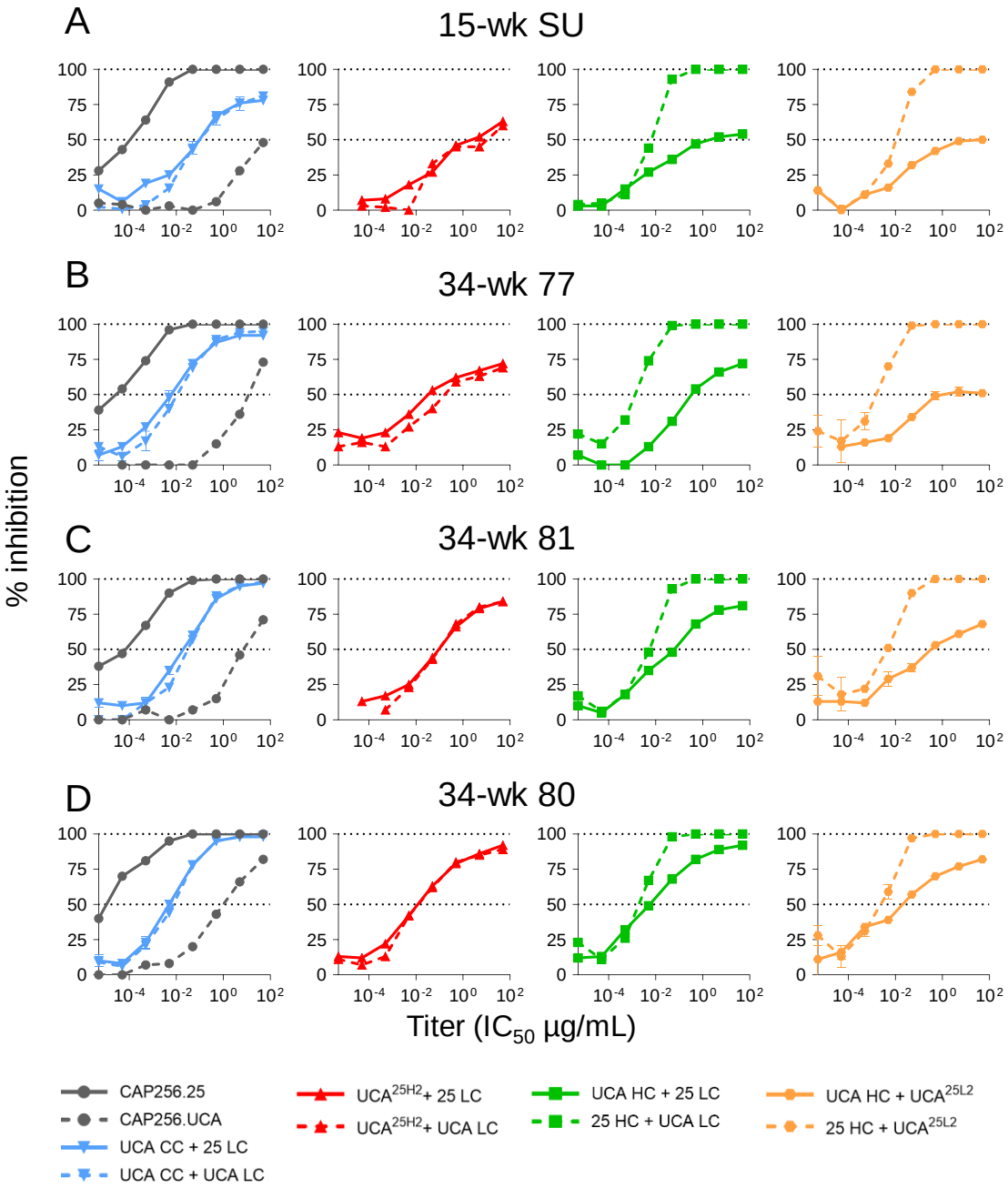

Figure 4.6. Incomplete neutralization of heterogeneous viral species.

The neutralization curves of the (A) 15-wk SU, (B) 34-wk 77, (C) 34-wk 81 and (D) 34-wk 80 autologous viruses by CAP256.UCA, CAP256.25 and the heavy and light chain chimeras. Antibody-mediated inhibition (%) of pseudovirus infection, colored by antibody (as per the key) is plotted against the antibody concentration (µg/mL). The dotted lines on the y axis indicate the 50% and 100% inhibition level.

4.3.7 Both the CAP256.25 heavy chain, especially the CDRH3, and the light chain modulate broad heterologous neutralization

Next, we assessed the ability of the CAP256.UCA and CAP256.25 chimeras to neutralize 14 heterologous viruses that are variably sensitive to the members of the CAP256-VRC26 lineage. The virus panel includes two tier 1B, 11 tier 2 and one tier 3 virus from subtypes A, B and C

[277]. First, we tested the heavy chain chimeras (UCA CC, UCA^{25FR}, UCA^{25H2}, UCA^{25H3}, UCA^{25H23} and UCA^{25H123}) matched with the CAP256.UCA light chain (Figure 4.7). The UCA CC chimera neutralized one virus, ZM53, with modest potency (0.84 µg/mL, Figure 4.7). Interestingly, despite the dominant role of the CDRs in forming the antibody paratope, the CAP256.UCA chimera with the CAP256.25 heavy chain FR1, FR2 and FR3 (UCA^{25FR}) neutralized three viruses (CAP210, ZM53, and ZM197), albeit with low potency (GM 9.63 µg/mL, Figure 4.7). While the CAP256.25 CDRH2 chimera (UCA^{25H2}) exhibited no heterologous neutralization (Figure 4.7), the CAP256.25 CDRH3 (UCA^{25H3}) chimera neutralized five viruses (GM 0.69 µg/mL). Compared to UCA CC and UCA^{25FR}, the UCA^{25H3} chimera neutralized ZM53 with 34- and 148-fold greater potency, respectively (Figure 4.7). Breadth was further improved (9/14) in UCA^{25H23}, and with all three CDRHs together (UCA^{25H23}), breadth increased by an additional two viruses (11/14) (Figure 4.7). However, this chimera did not neutralize all the viruses sensitive to CAP256.25, nor as potently. In addition, there was no significant difference in the GM potencies between UCA^{25H3}, UCA^{25H23} and UCA^{25H123}. Together, these data indicate that the heavy chain, and the CDRH3 in particular, substantially, but not entirely, confers heterologous breadth.

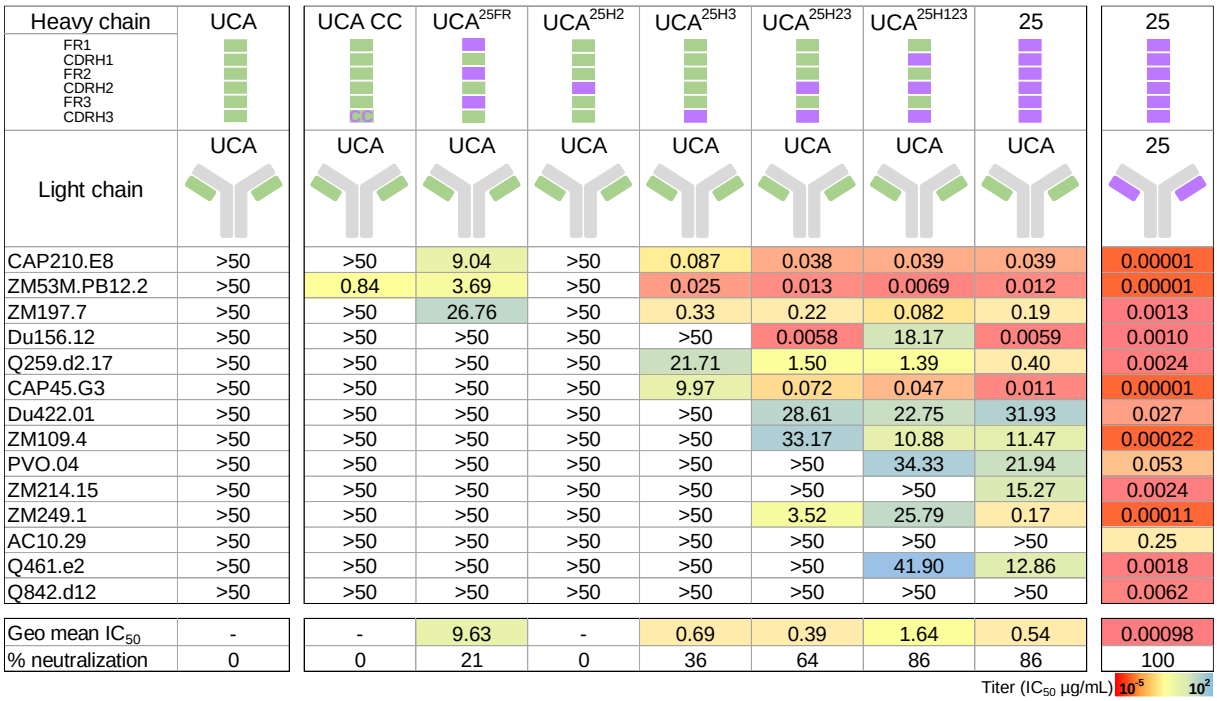

Figure 4.7. Heterologous neutralization by the CAP256.UCA heavy chain chimeras.

The sequences of the heavy (first row) and light (second row) chains for each antibody are visualized in a schematic. (First row) The variable heavy chain of CAP256.UCA (green) and CAP256.25 (purple) are shown in six segments, representing the three FR and three CDRs. (Second row) The light chains are colored according to the antibody, and the heavy chains are grey. The autologous viruses are tabulated in the first column and the neutralization titers (IC_{50}, µg/mL) for each antibody populate the table and are colored by potency (indicated in the key).

We also assessed the role of the light chain in neutralization of heterologous viruses and found that the UCA HC + 25 LC chimera, like the CAP256.UCA, failed to neutralize any heterologous viruses (Figure 4.8). However, the 25 HC + UCA LC chimera exhibited considerable breadth (12/14 viruses), though it showed a significant decrease in potency (p=0.0005, Wilcoxon matched-pairs) compared to CAP256.25 (Figure 4.8). Unlike autologous neutralization, this effect could not be attributed to the CDRL2, as the introduction of the CAP256.25 CDRL2 (25 HC + UCA^{25L2}) did not improve neutralization potency (Figure 4.8) compared to 25 HC + UCA LC (Figure 4.7 and Figure 4.8).

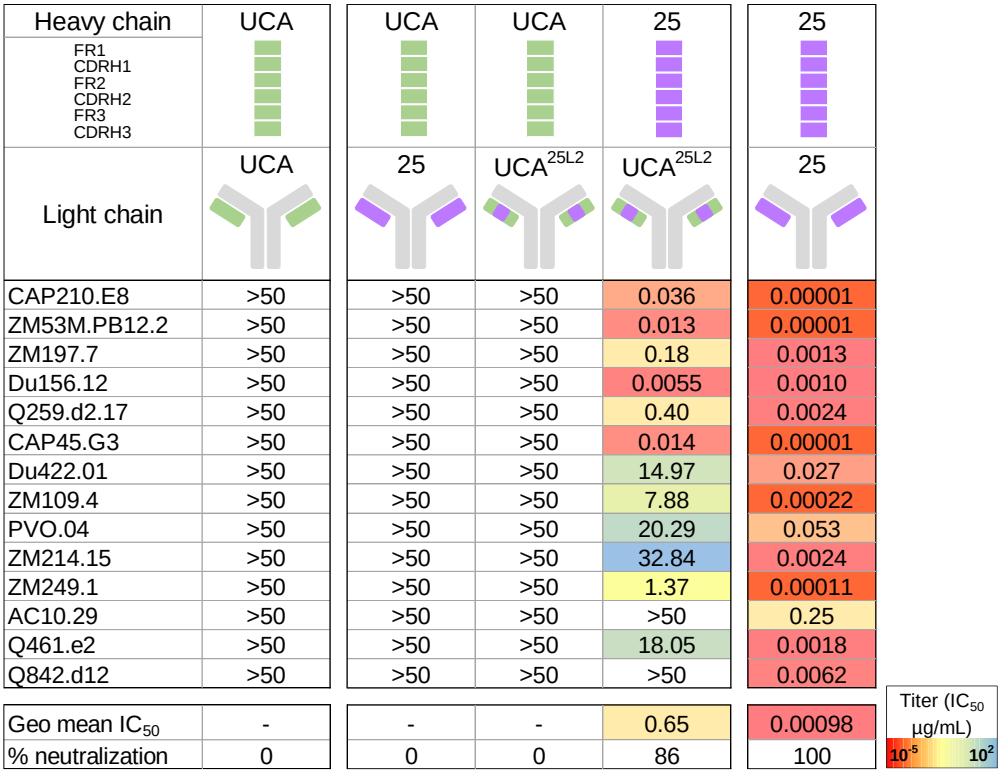

Figure 4.8. Heterologous neutralization by the CAP256.UCA heavy and light chain chimeras.
The sequences of the heavy (first row) and light (second row) chains for each antibody are visualized in a schematic. (First row) The variable heavy chain of CAP256.UCA (green) and CAP256.25 (purple) are shown in six segments, representing the three FR and three CDRs. (Second row) The light chains are colored according to the antibody, and the heavy chains are grey. The autologous viruses are tabulated in the first column and the neutralization titers (IC_{50}, µg/mL) for each antibody populate the table and are colored by potency (indicated in the key).

To further assess the impact of the entire CAP256.25 light chain on potency, we tested the heterologous neutralization of four heavy chain chimeras matched with either the CAP256.UCA or CAP256.25 light chain (Figure 4.9). We found that pairing the UCA^{25H23} and UCA^{25H123} heavy chains with the CAP256.25 light chain, significantly improved potency (p=0.004 and p=0.003, respectively, Wilcoxon matched-pairs) (Figure 4.9) with a similar trend for the UCA^{25H3} light chain chimeras (Figure 4.9). In addition to potency, the CAP256.25 light

chain improved the breadth of the CAP256.UCA heavy chain chimeras as the UCA^{25H3} heavy chain paired with the CAP256.25 light chain neutralized two additional viruses (Figure 4.9) compared to the CAP256.UCA light chain variant. Similarly, both the UCA^{25H23} and UCA^{25H123} chimeras matched with the CAP256.25 light chain neutralized an additional four and two viruses, respectively (Figure 4.9). Therefore, compared to autologous neutralization, the light chain has a greater impact on heterologous breadth. Together these data indicate that the light chain has a substantial yet variable impact on both heterologous and autologous neutralization potency.

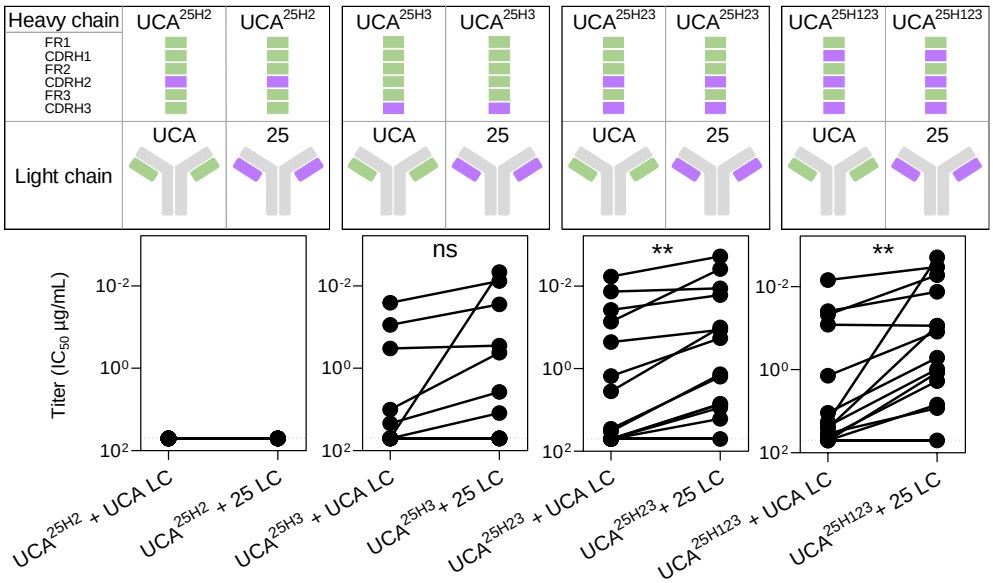

Figure 4.9. Heterologous neutralization by the CAP256.UCA heavy chain chimeras paired with the CAP256.UCA and CAP256.25 light chains.

The schematic in the first and second rows detail the sequences of the heavy and light chains, respectively for each antibody. The three FR and three CDRs of the CAP256.UCA (green) and CAP256.25 (purple) heavy chains are shown in six segments. The light chains are colored according to the antibody, and the heavy chains are grey. The neutralization titers (IC_{50}, µg/mL) for each antibody are plotted on a logarithmic scale. The significance of the differences between each pair was determined with the Wilcoxon matched-pairs signed rank test (ns = not significant, *p=<0.05 and **p=<0.01).

4.3.8 Minimally mutated CAP256.25 antibodies are generally more potent than most bNAbs

We utilized the CATNAP (Compile, Analyze and Tally NAb Panels, hiv.lanl.gov/catnap) database of bNAb titers to compare the neutralization of the antibodies we developed to those that have been previously characterized (Figure 4.10). Plotted are the titers from CATNAP (grey) for each antibody (average of 99 per virus), CAP256.25 (red), UCA^{25H123} (blue), UCA^{25H23} (green) and UCA^{25H3} (orange), and the GM potency is indicated (black bar). Both the UCA^{25H123}

and UCA^{25H23} chimeras were an order of magnitude more potent than the GM of the unrelated bNAbs against three viruses (CAP210, CAP45 and ZM53). Furthermore, UCA^{25H3}, with half of the heavy chain mutations compared to CAP256.25, exhibited greater potency than the GM against three viruses. This demonstrates that a minimally mutated CAP256.25 antibody would be substantially more potent compared to many other bNAbs against particular viruses.

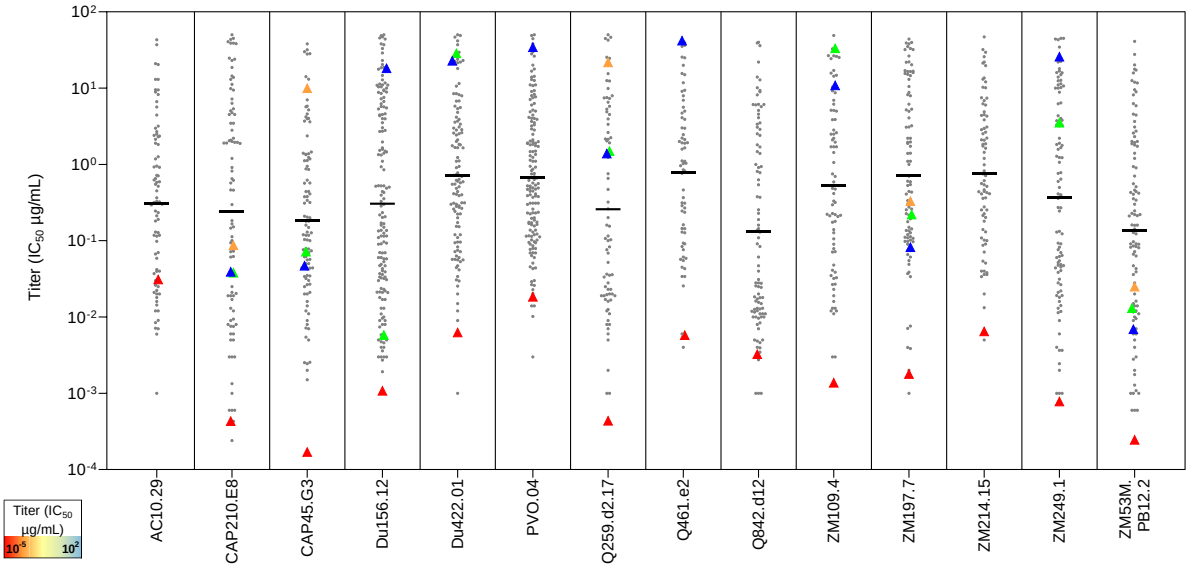

	AC10.29	CAP210.E8	CAP45.G3	Du156.12	Du422.01	PVO.04	Q259.d2.17	Q461.e2	Q842.d12	ZM109.4	ZM197.7	ZM214.15	ZM249.1	ZM53M.PB12.2
# of antibodies	81	89	102	153	118	151	77	67	95	78	96	79	99	103
Geo mean IC$_{50}$	0.31	0.24	0.18	0.31	0.71	0.67	0.26	0.77	0.13	0.54	0.71	0.77	0.37	0.14
CAP256.25 ▲	0.25	0.00001	0.00001	0.0010	0.027	0.053	0.0024	0.0018	0.0062	0.00022	0.0013	0.0024	0.00011	0.00001
UCA^{25H123} ▲	>50	0.039	0.047	18.17	22.75	34.33	1.39	41.90	>50	10.88	0.082	>50	25.79	0.0069
UCA^{25H23} ▲	>50	0.038	0.072	0.0058	28.61	>50	1.50	>50	>50	33.17	0.22	>50	3.52	0.013
UCA^{25H3} ▲	>50	0.087	9.97	>50	>50	>50	21.71	>50	>50	>50	0.33	>50	>50	0.025

Figure 4.10. Minimally mutated CAP256.25 antibodies are very potent compared to other bNAbs.
Reported are the titers from the CATNAP (Compile, Analyze and Tally NAb Panels, hiv.lanl.gov/catnap) database for an average of 99 bNAbs per virus (grey). Plotted are CAP256.25 (red), UCA^{25H123} (blue), UCA^{25H23} (green), UCA^{25H3} (orange), and the GM potencies (black bar). The first row of the table shows the number of antibodies included for each virus, below that is the GM potency, and the titers for CAP256.25 and chimeras populate the last four rows.

4.4 Discussion

Innovative antigen formulations and vaccine strategies are probably necessary to elicit protective responses against HIV infection since traditional approaches have not succeeded thus far [164,212–215,218]. Valuable insights for vaccine design have been gained from bNAb lineage ontogeny studies [187,189,196,197,203,205,220–222], leading to the development of germline-targeting immunogens that have shown potential for triggering bNAbs precursors in several studies [216,325,332–335,337–339]. However, because these precursors typically lack neutralization [178,187,229–238,193,239–243,197,200,224–228], such antibodies will need to acquire breadth through somatic hypermutation. Consequently, understanding which mutations introduce breadth and potency, and which mutations have minimal or no impact, are crucial to the design of vaccines [215,218]. Here, we investigated the genetic basis for neutralization by CAP256.25, a member of the CAP256-VRC26 V2-specific lineage that is moderately mutated compared to many other bNAbs [204,205]. We found that the heavy chain CDRs, particularly the CDRH3 which is known to be a major part of the paratope, predominantly modulated both autologous and heterologous neutralization. However, the light chain contributed to autologous neutralization potency and had an impact on both the breadth and potency of heterologous neutralization. Together, we demonstrate that about half of the CAP256.25 mutations are necessary for breadth. This suggests that focusing SHM to the CDRHs and the light chain of V2-bNAb precursors may hasten the development of breadth and potency.

Here, we have shown that the mutations in the CAP256.25 CDRH3 (14 improbable mutations, 3 probable mutations and one insertion) are the primary determinants of neutralization since transferring this loop into the CAP256.UCA introduced substantial autologous and some heterologous neutralization. Furthermore, as few as two of these improbable mutations, which introduced a stabilizing disulfide bond in the CDRH3 [206,207], enhanced autologous neutralization. In addition, the CDRH3 was largely responsible for conferring tolerance of emerging autologous viral variants. Moreover, the addition of three probable mutations from the CAP256.25 CDRH2, further improved breadth and potency of the CAP256.25 CDRH3 chimera. Together, our data indicate that about half of the mutations present in the CAP256.25 heavy chain are required for ~60% breadth and 0.39 μg/mL potency. These findings are concordant with other studies on minimally mutated bNAbs, including BF520.1 [221,222] and VRC01 [256], where approximately half of the mutations were necessary to confer breadth. Therefore, only selected improbable mutations, particularly in the CDRH3, and not the FR, may be essential for V2-specific antibodies.

We found that the heavy and light chains had different but complementary roles in contributing to breadth and potency, respectively. We demonstrated that the heavy chain, and in particular the presence of a disulfide bond in the CDRH3, was responsible for ensuring that neutralization reached 100% at high antibody concentrations. The disulfide bond rigidifies the CDRH3 [206] which may allow the antibody to tolerate glycovariants since, as others have shown, the CAP256.UCA and germline-revertants are dependent upon particular glycoforms for neutralization [239,361,362]. Although the structure of CAP256.25 indicates that the CDRL2 is in close proximity to the V1V2 N130 and N160 glycans [206], the role of the light chain has not previously been confirmed. We established that the CAP256.25 CDRL2 was responsible for modulating autologous neutralization potency, but that other mutations were necessary to recapitulate the exceptional breadth of CAP256.25. Our data support the conclusion that the CDRL2 contributes to the paratope of CAP256.25 and suggests that V2 vaccine strategies may need to include immunogens that select for light chain mutations.

Although the FR typically does not contact the epitope and it evolves at a slower rate than the CDRs, it plays a role in neutralization potency [228,230,249,252]. Our data also show that the CAP256.25 heavy chain FR germline-revertant retained most of the broad neutralization of the wild-type antibody but that potency was impaired. This is concordant with the 10E8 FR germline-revertant, which has been shown to be similarly broad as 10E8, but substantially less potent [230]. Furthermore, matching the CAP256.25 FR germline-revertant with the mature CAP256.25 light chain improved potency, as has been previously observed with the VRC01 FR germline-revertant paired with the mature VRC01 light chain [230]. Together, our data provide further evidence that the FR [228,230,249,252] regions and light chain modulate bNAb potency.

While V1V2-targetting bNAbs generally have unusually long CDRH3s, the frequency of naïve B-cells with CDRH3s of >30 amino acids may be as high as ~0.4% [216]. In addition, it may be possible to activate these rare precursors with antigens displaying exposed V1V2 neutralizing epitopes [325,388] and drive targeted affinity maturation through boosts with increasingly native and varied antigens. Our data suggest that maturation targeted to the CDRH2 and CDRH3 can introduce substantial breadth and potency into CAP256.25-like precursors. In addition to informing vaccine design, identification of the mutations necessary for neutralization may be important to minimize the immunogenicity of passively infused bNAbs [230,389], thereby improving antibody half-life by slowing their clearance.

In this study, we show that the CAP256.25 heavy chain is central to mediating breadth and that approximately half of the heavy chain mutations are essential for neutralization. Moreover, the CDRH3 is the principal determinant of heterologous neutralization and it confers tolerance of emerging autologous viral variants. Furthermore, we demonstrate that the light chain and FR contribute to potency but have a smaller impact on breadth. Together these data suggest that a modestly mutated V2-targetting bNAb is a tractable vaccine goal since affinity maturation targeted to the CDRHs and light chain can efficiently introduce neutralization breadth and potency.

5. New IgG4 class switched members of the CAP256-VRC26 lineage mediate greater phagocytosis than matched IgG1 variants

David Sacks[1,2], Simone I. Richardson[1,2], Bronwen E. Lambson[1,2], Nonhlanhla N. Mkhize[1,2], Lynn Morris[1,2,3] and Penny L. Moore[1,2,3]

[1] Centre for HIV and STIs, National Institute for Communicable Diseases (NICD) of the National Health Laboratory Service (NHLS), Johannesburg, South Africa

[2] Faculty of Health Sciences, University of the Witwatersrand, Johannesburg, South Africa

[3] Centre for the AIDS Programme of Research in South Africa (CAPRISA), University of KwaZulu-Natal, Durban, South Africa

5.1 Introduction

The exceptional diversity and high mutation rate of HIV contributes to the challenge of eliciting an immune response that protects against transmission, controls viremia or eradicates infection [40,160,214,377,390,391]. Although the development of an HIV vaccine has progressed slowly, studies of HIV infection have identified antibodies that neutralize diverse unrelated strains of HIV [152,153,158–161]. Crucially, passive administration of these broadly neutralizing antibodies (bNAbs) protects mice [348] and primates [349] from infection, improves viral suppression and drives the clearance of infected cells. However, the antiviral activity of passively infused bNAbs is not entirely dependent on neutralization as ablation of Fc receptor (FcR) binding, which prevents antibody engagement of effector cells, can dramatically reduce the efficacy of passive immunization [346,348,349]. Together, neutralization and effector functions are the key determinants of antibody-mediated protection.

The Fc domain, determined by antibody isotype, mediates effector functions by binding to complement, lectins and Fc receptors (FcR) on innate immune cells and lymphocytes [98]. There are five classes of Fc in humans (IgM, IgD, IgG, IgA and IgE) and each class targets particular FcRs (FcμR, FcδR, FcγR, FcαR and FcεR, respectively) [102,109]. In addition, there are six Fc subclasses (IgA1, IgA2, IgG1, IgG2, IgG3 and IgG4) and FcεR and FcγRs consist of several members (FcεRI/II, FcγRI, FcγRIIa/b/c and FcγRIIIa/b) and alleles [98]. The receptors have variable affinities for their target Fcs, with the high affinity FcRs (FcεRI and FcγRI) strongly activating effector cells and an inhibitory receptor (FcγRIIb), blocking stimulation [114]. In addition, since the FcRs are not uniformly expressed by all immune cells, antibodies with the same specificities can activate a variety of different effector functions [134].

Antibody-mediated effector functions include the initiation of the complement cascade [138], phagocytosis [135], cytotoxicity [136] and trogocytosis [137]. Antibody-dependent complement deposition (ADCD) stimulates phagocytosis and the formation of the cell-killing membrane attack complex and is strongly driven by IgM [140], IgG1 and IgG3 [135]. Antibody-dependent cellular phagocytosis (ADCP) results in the degradation of engulfed microbes and is mediated by natural killer (NK) cells, macrophages, monocytes, mast cells, dendritic cells and neutrophils [135]. Antibody-dependent cellular cytotoxicity (ADCC) leads to the apoptosis of target cells via the release of perforin and granzyme B by activated cytotoxic T-cells and NK cells [136,139]. Antibody-dependent cellular trogocytosis (ADCT) is the fatal extraction of a target cell's membrane and is mediated by lymphocytes, granulocytes, macrophages, monocytes, dendritic cells and NK cells [137]. Since IgG1 and in particular IgG3 strongly bind to the activating FcγRs, antibodies with these isotypes potently mediate ADCP, ADCC and ADCT, and initiate ADCD

[141,142]. In contrast, IgG2 and IgG4 have a poor/no capacity to fix complement and have substantially lower affinity for the activating FcγRs [114]. Both IgG2 and IgG4 have a shorter hinge region than either IgG1 or IgG3, which may impact Fc flexibility and accessibility [114]. Furthermore, IgG4 engages the inhibitory receptor (FcγRIIb) which blocks effector cell activation and this isotype is more common in HIV infected individuals, particularly in rapid progressors [107,147–149]. Since IgG4 is induced after repeated or chronic antigenic stimulation, class switching to IgG4 is likely an adaptive response to attenuate immune exhaustion [115–117]. Consequently, isotype and effector cell functionality should be considered together with neutralization when assessing the ability of an HIV specific antibody to block infection, suppress viremia and clear infected cells.

To explore the impact of isotype on neutralization and effector function, we utilized the CAP256-VRC26 V2-specific bNAb lineage [204,205]. These antibodies were isolated by antigen-specific sorting and B-cell culture of peripheral blood mononuclear cell (PBMC) from an HIV infected individual, CAP256, who had broadly neutralizing plasma [153,360]. This lineage targets a quaternary epitope at the distal tip of Env which is formed by the convergence of the V1V2 of each protomer [206]. Like other V2 bNAbs [161,199,201,203,206,210] the CAP256 antibodies have a very long CDRH3 (35-38 amino acids, aa) which bypass glycans and projects into the trimer apex to contact underlying conserved sites in V2 strands B and C, including K169 [204–206]. The heavy (IGHV3-30*18) and light chain (IGLV1-51*02) genes of the lineage members are modestly divergent (4-17% and 4-15%, respectively) from the unmutated common ancestor (UCA) and breadth and potency ranges from 2%-63% and 5.00-0.003 μg/mL, respectively [204]. Since the isotype of these antibodies was unknown, they were expressed as IgG1, which is the most common isotype overall [204,205]. CAP256.25 is the broadest and most potent member of the lineage and protects passively infused primates from infection at very low concentrations and modifications to the Fc substantially improves the half-life [344]. Furthermore, the CAP256 plasma breadth is mediated in part by IgG3 antibodies, and CAP256.25 expressed as IgG3 has enhanced potency and greater effector functions compared to IgG1 [363].

In antigen-specific sorts performed in 2016, additional antibodies were recovered from CAP256 and the constant domains have been sequenced to identify the isotypes. Here we report new members of the CAP256-VRC26 lineage and describe their genetic and functional characteristics. Seven new CAP256-VRC26 lineage members were recovered as IgG4 and we assessed neutralization and effector functions (ADCC, ADCD, ADC and ADCT) of four antibodies as both IgG4 and IgG1. The IgG1 (33-80% breadth and 0.11-0.78 μg/mL potency) variants were broader and more potent compared to the matched IgG4 antibodies (27-60%

breadth and 0.06-5.66 μg/mL). However, regardless of isotype, the antibodies mediated ADCC and ADCT in response to a heterologous antigen. Surprisingly, the IgG4 variants were significantly better than IgG1 at mediating ADCP. Two antibodies differed by one amino acid in the CDRH3 which had a significant impact on the effector functions of the antibodies suggesting that the Fab domain may impact Fc-mediated effector function. Together, these data provide further insights into the maturation of the CAP256-VRC26 lineage and indicate that while V2-specific IgG4 antibodies are less broad and potent compared to IgG1, they can mediate similar or improved effector functions. This may inform the design of passive immunization strategies since IgG4, in addition to IgG1, is readily transferred across the placenta.

5.2 Materials and methods

5.2.1 Ethics statement

The human research ethics committee for the University of the Witwatersrand approved (M160934) this study (see 7.2, page 111, Appendix B: Ethics certificate). For further details see 2.1 (page 31).

5.2.2 Memory B-cell sorting

Memory B-cells were isolated from PBMCs collected from donor CAP256 at 193 weeks pi by antigen-specific fluorescence-activated cell sorting (FACS) by Dr. Nono Mkhize. To identify V2-specific antibodies the sort strategy included a wild-type BG505 SOSIP.664 trimer and BG505 SOSIP.664 K169E mutant. Reverse transcription, Ig amplification by nested PCR and Sanger sequencing was performed by Dr. Bronwen Lambson, as previously described [204,205]

5.2.3 Heavy and light chain gene identification

To identify the heavy chain (IGHV, IGHD and IGHJ), kappa light chain (IGKV and IGKJ) and lambda light chain (IGLV and IGLJ) genes and alleles, sequences were submitted to the ImMunoGeneTics V-QUEry and Standardization (IMGT/V-QUEST) tool at imgt.org/IMGT_vquest/input [392]. The IGHC isotype was assigned according to the IMGT *Homo sapiens* constant domain reference directory.

5.2.4 Cloning

Antibodies identified with natural IgG4 isotypes were cloned into a $CMVR_{HC}$ IgG4 expression vector [393] provided by Dr. Andrew Crowley, Dartmouth College, Hanover, NH. To follow the same cloning protocol detailed in 2.2 (page 31), restriction sites in the IgG4 $CMVR_{HC}$ vector were modified by site-directed mutagenesis and subcloning.

5.2.4.1 PCR and site-directed mutagenesis to introduce restriction enzyme sites

Restriction sites were incorporated into the variable genes of the newly identified CAP256-VRC26 IgG4 lineage members to subclone into the genes into the $CMVR_{HC}$ IgG4 vector. This was achieved by amplification with gene-specific primers for the heavy chain (5' AgeI VH3 and 3' SalI JH3) and light chain (5' AgeI VL1 and 3' XhoI CL) (Appendix table 5). One microliter of the first round PCR product was amplified with the AccuPrime *Pfx* DNA Polymerase (1.25 U) in 1x AccuPrime *Pfx* Reaction Mix and 25 µM each of the forward and reverse primers in 50 µL. The thermocyling conditions were 95°C for 2 min, 30x 95°C for 15 sec, 55°C for 30 sec and 68°C for 45 sec and 1x 68°C for 5 min. The products were cleaned with the QIAquick PCR Purification Kit (Qiagen) according to the manufacturer's protocol. Next, the purified PCR products were digested with the AgeI and SalI FastDigest (Thermo Scientific) restriction enzymes as described in 2.2.2 (page 31). Thereafter, the digested fragments were cleaned with the QIAquick PCR Purification Kit (Qiagen) and stored at -20°C.

The IgG4 $CMVR_{HC}$ plasmid had an additional AgeI sequence in the CH1 and lacked a SalI site at the beginning of the CH1. Consequently, primers were designed to remove the AgeI sequence and introduce the SalI sequence by site-directed mutagenesis. Mutagenesis was carried out with the QuikChange Multi Site-Directed Mutagenesis Kit (Agilent) as described in 2.3 (page 32) with primers listed in Appendix table 5. As per the methods in 2.2.2 (page 31), the PCR products were digested with DpnI, transformed into JM109 cells and the purified plasmids were sequenced.

5.2.4.2 CMVR modification and IgG4 subcloning

To remove a second unwanted SalI site located 5' to the antibody signal sequence, the antibody variable and constant IgG4 domains were subcloned into a $CMVR_{HC}$ plasmid without this additional SalI sequence. AgeI and BamHI were used according to the protocol in 2.2.2 (page 31) to cut the 5' end of the variable gene and 3' to the IgG4 CH3 domain, respectively. Similarly, the IgG1 $CMVR_{HC}$ plasmid was cut with the same enzymes (the "recipient plasmid"). Thereafter, the variable and constant domain fragment was ligated into the recipient plasmid with the Rapid DNA Ligation Kit (Roche) according to the protocol in 2.2.4 (page 32). The light chain genes were subcloned into the $CMVR_{LC}$ vector following the same procedures in 2.2 (page 31). Thereafter, the products were transformed into the XL10-Gold Ultracompetent Cells (Stratagene), and the plasmids purified and sequenced as explained in 2.5 (page 34), 2.6 (page 34) and 2.7 (page 35), respectively.

5.2.5 Antibody expression and purification

Antibody expression and purification is detailed in 2.9 (page 35). Briefly, the 293F cell line was co-transfected with PEI MAX (Polysciences) with the $CMVR_{HC}$ and $CMVR_{LC}$ plasmids and the monoclonal antibodies were isolated from the supernatant with Protein A resin (Pierce) columns.

5.2.6 Neutralization assays

The TZM-bl neutralization assay was performed as described in 2.11 (page 37) and measured antibody-mediated neutralization through the reduction of Tat-inducible luciferase fluorescence.

5.2.7 Cell lines

The TZM-bl and 293F cell lines, utilized for the antibody neutralization assay and monoclonal antibody production, respectively, were maintained as in 2.8 (page 35). The CEM.NKR.CCR5 CD4+ T cell line and THP-1 monocyte cell line (NIH AIDS Reagent Program) were utilized as target and effector cells, respectively, for the Fc assays. These suspension cells were cultured in R10 which consisted of Roswell Park Memorial Institute 1640 (RPMI) media (Thermo Scientific) supplemented with 10% heat-inactivated FBS and 1% penicillin-streptomycin (Gibco). In addition, the THP-1 cell line growth media included 0.05 mM 2-mercaptoethanol (Gibco). The cell lines were cultured at 37°C (5% CO_2) and passaged 1:10 when the density of the CEM and THP-1 cells reached $2x10^6$ cells/mL and $4x10^5$ cells/mL, respectively.

5.2.8 Fc functional assays

The antibody-dependent cellular cytotoxicity (ADCC), antibody-dependent complement deposition (ADCD), antibody-dependent cellular trogocytosis (ADCT) and antibody-dependent cellular phagocytosis (ADCP) Fc assays were performed on the FACSAria II (BD Biosciences) flow cytometer in collaboration with Dr. Simone Richardson. The BG505 SOSIP.664 trimer was used as the antigen for the functional assays and was produced by Dr. Thandeka Moyo. Unless otherwise specified, cells were harvested at 400 *g* for 5 min, washes were done with R10 at

400 *g* for 5 min and incubation during staining with fluorochromes was done in the dark. Assays were conducted in a 96-well format.

5.2.8.1 Antibody-dependent cellular cytotoxicity (ADCC)

Cellular cytotoxicity was measured by granzyme B activity in the target CEM cells with the GranToxiLux (OncoImmunin) assay [394]. One million CEM cells were incubated with 10 µg/mL of BG505 SOSIP.644 trimer in R10 for 75 min at 37°C with agitation every 30 min. For identification and to exclude dead cells, the CEM cells were stained with the TFL4 and NFLI fluorescent markers (1:1000 dilution), respectively, for 15 min at 37°C, and then washed twice and diluted to $0.4x10^6$ cells/mL in R10. PBMC from an HIV negative donor were used as effector cells and resuspended to $1.2x10^7$ cells/mL in R10. Granzyme B substrate was mixed with $1x10^4$ coated CEM and $3x10^5$ PBMC (1:30 ratio), incubated at room temperature for 5 min and then serially diluted antibody (5-fold dilutions, starting at 50 µg/mL) was added. The suspension was incubated at room temperature for 15 min and after centrifugation for 1 min at 300 *g*, the cells were incubated for 1 hour at 37°C (5% CO_2) and finally washed twice with 1% FBS-PBS. The percentage of singlet granzyme B positive live (NFL1-) CEM cells (TFLR4+) out of the total viable CEM population was determined by flow cytometry. Subtracted from this was the percent of FITC+ events from a control containing only effector/target cells and no antibody. Palivizumab and A32, which is a potent mediator of ADCC, were included as a negative and positive control, respectively.

5.2.8.2 Antibody-dependent complement deposition (ADCD)

Complement deposition was assessed by measuring the C3b complement component on CEM cells [395]. CEM cells were washed twice with RPMI, resuspended to $1x10^6$ cells/mL and then incubated with 10 µg/mL of BG505 SOSIP.644 trimer for 1 hour at room temperature. Next, the cells were washed with RPMI and $1x10^5$ cells were incubated for 15 min with 0.5 mg/mL of CAP256-VRC26 antibody in RPMI. HIV negative plasma was used a source of complement and was diluted 10-fold in 0.1% gelatin/veronal buffer (Sigma-Aldrich), added to the CEMs and antibody, and incubated for 20 min at 37°C. Thereafter, the cells were washed with 15 mM EDTA-PBS and then stained for 15 min at room temperature with FITC conjugated mouse anti-human C3/C3b/iC3b antibody (Cedarlane) diluted 1:50 in 1x PBS. Following a wash in 1x PBS the cells were fixed in 4% paraformaldehyde. Heat-inactivated HIV negative plasma and CEM were used as negative controls. An ADCD score was calculated by multiplying the geometric mean (GM) fluorescence intensity by the percent of cells positive for C3b deposition.

5.2.8.3 Antibody-dependent cellular trogocytosis (ADCT)

Trogocytosis is the fatal extraction of a target cell's plasma membrane by an effector cell and was measured through the detection of CEM membrane on THP-1 cells [137]. One million washed CEM cells were incubated with 10 µg/mL of BG505 SOSIP.644 trimer for 75 min at 37°C, with agitation every 30 min. The cells were washed twice in 1x PBS and $2x10^6$ cells were stained with the PKH26 fluorescent membrane dye (Sigma-Aldrich) (diluted 1:332) according to the manufacturer's protocol for 5 min at room temperature in a final volume of 332 µL. Staining was stopped by the addition of 800 µL of FBS and the cells were washed twice in ice cold 1x PBS (Gibco) and resuspended to $2x10^6$ cells/mL. Thereafter, 50 µL of the CEM cells were co-incubated with 50 µL of antibody (5 µg/mL) in V bottom 96-well plates (Corning) for 30 min at 37°C and then washed twice. During the incubation, $1x10^6$ washed THP-1 effector cells were stained with carboxyfluorescein succinimidyl ester (CFSE) live/dead intracellular dye (1:2000 dilution) for 3 min at room temperature in 332 µL of 1x PBS. Staining was stopped by the addition of 400 µL of FBS and after 1 min the cells were washed twice in ice cold 1x PBS and diluted to $6.7x10^5$ cells/mL in 1x PBS. Next, 150 µL of the THP-1 cells were added to the CEM and antibody mixture and incubated for 1 hour at 37°C (5% CO_2) and then the cells were washed with 15 µM EDTA-PBS and then washed again with 1x PBS before fixing in 4% paraformaldehyde. Palivizumab and polyclonal HIV+ IgG (NIH AIDS Reagent Program) were included as negative and positive controls, respectively. Flow cytometry was used to detect THP-1 cells (CFSE) that had extracted labeled membrane (PKH26+) from the CEM cells (CFSE-) and was represented as a proportion of the total population of THP-1 cells.

5.2.8.4 Antibody-dependent cellular phagocytosis (ADCP)

The uptake of antigen coated beads by THP-1 cells was measured to determine an ADCP score [396]. AviTag (Avidity) conjugated BG505 SOSIP.664 trimer (1 mg/mL) was incubated with 1 µM of NeutrAvidin agarose beads (FITC) (Thermo Scientific) in a 4:1 ratio at 4°C overnight. Next, the beads were washed twice with 0.1% bovine serum albumin-PBS and diluted 1:100 in the same wash buffer. Antibody (50 µg/mL), including palivizumab (negative control) and pooled IgG from HIV+ donors (positive control), were diluted 3-fold in R10 and incubated for 2 hours at 37°C with 10 µL of coated NeutrAvidin beads in 96-well round bottom plates. Thereafter, the beads were washed with R10 and incubated with $1x10^5$ THP-1 cells in 200 µL of R10 at 37°C (5% CO_2) overnight. Thereafter, the cells were pelleted and fixed in 4% paraformaldehyde. An ADCP score was calculated by multiplying the GM fluorescence intensity by the phagocytosed beads by the percent of bead uptake.

5.2.9 Data and statistical analysis

Flow cytometric data was analyzed with FlowJo v10 (BD Biosciences) and GraphPad Prism 8 (GraphPad Software) was used to construct graphs and for statistical comparisons as detailed in 2.13 (page 38).

5.2.10 Models

Heavy and light chain antibody sequences were fitted to the structure of CAP256.25 in the Swiss-PdbViewer (v4.1.0) (Swiss Institute of Bioinformatics) [372]. The antibody models and the structures of X1193.c1 SOSIP.664 (PDB: 5FYJ) and BG505 SOSIP.664 (PDB: 5V8L and 4NCO) were aligned to the structure of antibody CAP256.25 complexed with the 34-wk 80 virus Env trimer [206] in PyMOL Molecular Graphics System (v2.0.2) (Schrödinger).

5.3 Results

5.3.1 New members of the CAP256-VRC26 lineage are IgG4 class switched

Previously, 92 memory B-cells that bound differentially to BG505 SOSIP.664 and a K169E mutant of this protein were sorted from PBMC isolated from donor CAP256 at 193 weeks pi. The heavy chain variable genes for 25 antibodies were amplified with gene specific primers and the sequences of the heavy chains were submitted to IMGT/V-QUEST for identification (Figure 5.1 A and B) [392]. The heavy chains belonged to diverse IGHV families, including VH1 (n=9), VH3 (n=14) and VH4 (n=2) (Figure 5.1 A), and aside from IGHD7 and IGHJ1, all of the IGHD and IGHJ genes were represented (Figure 5.1 A). Two groups of clonal relatives were identified, one set of two clonally related VH1-69*01 antibodies (highlighted in green), and seven antibodies that shared the IGHV3-30*18, IGHD3-3*01 and IGHJ3*02 genes and CDRH3 sequence with members of the CAP256-VRC26 lineage (Figure 5.1 A, yellow shading) [204,205]. These seven new CAP256-VRC26 lineage heavy chains were 11.5-16.0% divergent from the CAP256.UCA sequence. Notably, aside from 10B which was IgA, the novel CAP256-VRC26 antibodies were all IgG4 class switched. Thus far, the IgG4 isotype has not been observed in the CAP256-VRC26 lineage, and these antibodies are described in more detail below.

Of the singletons, the IGHV somatic hypermutation from the germline nucleotide sequence ranged from 3.1-32% (median 11.8%), the median lengths of the CDRH1, CDRH2 and CDRH3 were 8, 8 and 15 aa respectively, and the median lengths of the FR1, FR2, FR3 and FR4 were 25, 17, 38 and 11 aa, respectively (Figure 5.1 B). IgG was the most common isotype (n=12) and there was sufficient sequence data to identify six antibodies as IgG1 and two as IgG3 (Figure 5.1 B). The five remaining antibodies were IgA (Figure 5.1 B).

Of the seven novel members of the CAP256-VRC26 lineage, the light chains of five (2G, 4G, 8F, 9E and 12B) were successfully amplified and found to share the same IGLV1-51*02 and IGLJ1*01 alleles as CAP256-VRC26 antibodies (Figure 5.1 C). The light chains had diverged from the germline nucleotide sequence by 13-14.7% (Figure 5.1 C). The median lengths of the CDRL1, CDRL2 and CDRL3 were 8, 3 and 8 aa (the latter having the same four residue deletion as previously described antibodies CAP256.11, 12, 13 and 32). The median lengths of the FR1, FR2, FR3 and FR4 were 25, 17, 36 and 10 aa (Figure 5.1 C).

Maximum likelihood phylogenetic trees of the heavy and light chains of the 33 previously described members CAP256-VRC26 lineage and the newly identified antibodies were constructed [204]. Antibodies 9E, 12B, 4G, 4C, 2G and 8F were most closely related to the CAP256.11 and CAP256.32, while 10B was more closely related to CAP256.18 (Figure 5.2). Antibodies 2G and 8F shared the same light chain sequence and their heavy chains differed by only one amino acid in the CDRH3 (Q98 and E98, respectively). In total, we identified five new matched heavy and light chain genes of IgG4 class switched members of the CAP256-VRC26 lineage.

A

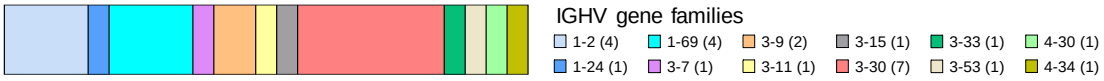

B

Heavy chain

	Antibody	IGHV	IGHD	IGHJ	V SHM (nt) %	CDRH (aa) H1	H2	H3	FR (aa) FR1	FR2	FR3	FR4	CDRH3	Isotype
	2F	1-2*02	2-21*01	4*02	11.8	8	8	10	25	17	38	11	ATGIPSDLDY	G
	3B	1-2*02	3-10*01	5*02	12.5	8	8	15	25	17	38	11	TRDSSRRDTNWWLDP	G1
	7G	1-2*02	D6-19*01	2*01	10.1	8	8	17	25	17	38	11	ARLIEHSSAWARGHFDL	A
	8C	1-2*02/03	3-3*02	5*02	12.5	8	8	15	25	17	38	11	TTHLSSRDFSWSWDP	G1
	7D	1-24*01	3-10*01	6*03	11.8	8	8	28	25	17	38	11	ATGAKGTAYTRSWSFLSRLKYYFYYMDV	G
	8B	1-69*09	6-13*01	6*03/4*03	3.1	8	8	21	25	17	38	11	ARNCLRSSSWFRQDLCGYMDV	G1
	11F	1-69*15	3-10*02	3*02	16.7	8	8	12	25	17	38	11	VREYYNLDAFDI	G
	4E	3-7*02/03/04	1-26*01	4*02/5*02	4.2	8	8	19	25	17	38	11	ARAGESQLSHRFSGNYFSS	G1
	6F	3-9*01	2-2*01	3*01/02	6.9	8	8	15	25	17	38	11	AKDRGSTWRYDPFDL	A
	10D	3-9*01	3-3*01	4*02	11.8	8	8	20	25	17	38	11	ARDLHTYHDYWNGYFGSFDY	G1
	8H	3-11*04	6-19*01	6*03	15.6	8	8	25	25	17	38	11	ARDGSRWSPVPDSYQSYHHYYYMDV	G3
	11C	3-15*01/05	3-22*01	4*02	8.8	8	10	19	25	17	38	11	TTTPGLKWYRFLLYKTPDY	G1
	4H	3-33*01/06	3-10*01	2*01	12.2	8	8	8	25	17	40	11	ARHHKGDL	A
	10F	3-53*01	3-10*01	4*02	8.2	8	7	13	15	17	40	11	ASAGSFFRYYLDY	A
	1D	4-30-4*01/03	3-10*01	4*02	32.0	10	7	11	25	17	44	11	ARVWGRRAFDQ	G
	5F	4-34*01	3-22*01	5*02	7.7	8	7	15	25	17	40	11	ARGNY(Y/C)DGSGLPLSPW	G3
	3H	1-69*01	5-12*01	6*03	7.6	8	8	28	25	17	38	11	ARDAVDVVAKMDEEVDKMDENYYYYMDV	G1
	8G	1-69*01	5-12*01	6*03	10.0	8	8	28	25	17	38	11	ARDAVDVVAKMDEEVDKMDENYYYYMDV	G1
CAP256-VRC26	**UCA**	**3-30*18**	**3-3*01**	**3*02**	**0.0**	**8**	**8**	**37**	**25**	**17**	**38**	**11**	**AKDLGESENEEWATDYYDFSIGYPGQDPRGVVGAFDI**	-
CAP256-VRC26	4C	3-30*18	3-3*01	3*02	14.6	8	8	37	25	17	38	11	VKDLRELECEEWASDYYDFGKPQPCLDSRGVSGISAM	G4
CAP256-VRC26	10B	3-30*18	3-16*01	3*01	14.6	8	8	37	25	17	38	11	ARDLREMECEEWQSDYYDFGKGGPCRDNRGVVGVFDV	A
CAP256-VRC26	12B	3-30*18	3-3*01	3*02	11.5	8	8	37	25	17	38	11	VKDMRELECEEWASDYYDFGKPNQPCLDRRGVSGISAF	G4
CAP256-VRC26	2G	3-30*18	3-3*01	3*02	13.4	8	8	37	25	17	38	11	VKDLRQLECEEWASDYYDFGKPQPCLDSRGVSGISAM	G4
CAP256-VRC26	4G	3-30*18	3-3*01	3*02	16.0	8	8	37	25	17	38	11	VKDLRELECEEWASDYYDFGKPQPCLDSRGVSGISAM	G4
CAP256-VRC26	8F	3-30*18	3-3*01	3*02	13.4	8	8	37	25	17	38	11	VKDLRELECEEWASDYYDFGKPQPCLDSRGVSGISAM	G4
CAP256-VRC26	9E	3-30*18	3-3*01	3*02	15.3	8	8	37	25	17	38	11	AKDLRELECELWTSDYYDFGRPQPCIDRRGVSGICDM	G4

C

Light chain

	Antibody	IGLV	IGLJ	V SHM (nt) %	CDRL (aa) L1	L2	L3	FR (aa) FR1	FR2	FR3	FR4	CDRL3
CAP256-VRC26	**UCA**	**1-51*02**	**1*01**	**0.0**	**8**	**3**	**12**	**25**	**17**	**36**	**10**	**GTWDSSLSAGGV**
CAP256-VRC26	12B	1-51*02	1*01	14.4	8	3	8	25	17	36	10	GTWNGRMN
CAP256-VRC26	2G	1-51*02	1*01	14.4	8	3	8	25	17	36	10	GTWNGRLN
CAP256-VRC26	4G	1-51*02	1*01	13.7	8	3	8	25	17	36	10	GTWTGRLN
CAP256-VRC26	8F	1-51*02	1*01	14.7	8	3	8	25	17	36	10	GTWNGRLN
CAP256-VRC26	9E	1-51*02	1*01	13.0	8	3	8	25	17	36	10	ATWDGRLN

Figure 5.1. Gene usage and characteristics of the novel antibodies isolated from CAP256.

(A) The horizontal slices represent the proportion of the IGHV gene families identified in the heavy chain sequences from the newly sorted CAP256 antibodies. (B) Tabulated are the IGHV, IGHD and IGHJ genes, the divergence from the germline sequence (%), CDRH (amino acids, aa) and FR length (aa), CDRH3 sequence and isotype. (C) Similar to (B), here the light chain gene usage and other characteristics are listed for the light chains matched with CAP256-VRC26 lineage heavy chains.

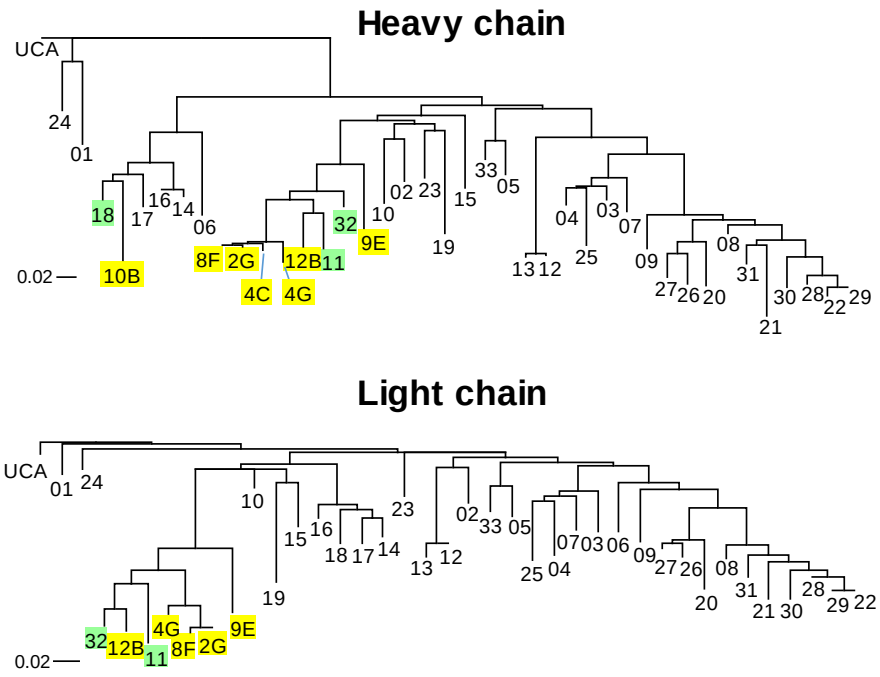

Figure 5.2. Phylogenetic trees of the 33 member CAP256-VRC26 lineage and the new members.
Maximum phylogenetic trees of the heavy (top) and light (bottom) variable chains of the CAP256-VRC26 antibody lineage and the new lineage members (yellow). CAP256.11, CAP256.18 and CAP256.32 (green) are most closely related to the novel antibodies. The scale represents the rate of nucleotide change per site between nodes.

5.3.2 Autologous neutralization breadth is similar between the isotypes but the IgG1 variants are slightly more potent

To explore the impact that the natural IgG4 isotype of the new CAP256-VRC26 antibodies had on neutralization, we cloned the variable heavy and light chain genes into an IgG4 $CMVR_{HC}$ and $CMVR_{LC}$ expression vector, respectively. In addition, we produced IgG1 variants of each antibody since IgG1 is the most common isotype in serum antibodies and the previously described CAP256-VRC26 antibodies were expressed as IgG1 [204,205]. We were unsuccessful in cloning antibody 12B and so in the subsequent experiments, we focused on 2G, 4G, 8F and 9E. Neutralization was tested in the TZM-bl neutralization assay against 20 autologous viruses isolated from 6 to 69 weeks pi. Antibodies 2G, 4G, 8F and 9E expressed as IgG1 neutralized 12, 13, 13 and 16 viruses, respectively, with geometric mean (GM) potencies of between 0.057 and 0.19 µg/mL (Figure 5.3). The IgG4 variants of 4G and 8F neutralized the same viruses as the IgG1 versions but the GM potencies were ~3-fold less (Figure 5.3). In contrast, the IgG4 variants of 2G and 9E neutralized 1 and 2 fewer viruses, respectively, than the IgG1 versions. While the GM potencies of 2G IgG1 and IgG4 were similar, 9E IgG4 was ~8-fold less potent than the matched IgG1 antibody (Figure 5.3). Both 9E isotype variants neutralized the greatest number of autologous viruses, including the 6-wk PI which is resistant to most of the CAP256-VRC26 lineage members, aside from broadest antibodies

such as CAP256.25 (Figure 5.3) [204]. Together, these data suggest that autologous viruses are sensitive to both isotype variants but that the natural IgG4 versions are variably less potent compared to IgG1.

	2G			4G			8F			9E			
Virus	IgG1	IgG4	Fold	IgG1	IgG4	Fold	IgG1	IgG4	Fold	IgG1	IgG4	Fold	CAP256.25
6-wk PI	>50	>50	-	>50	>50	-	>50	>50	-	11.26	28.48	2.5	0.22
15-wk SU	0.0066	0.0095	1.4	0.0043	0.013	2.9	0.0047	0.012	2.6	0.016	0.27	16.4	0.00005
34-wk 80	0.0018	0.0027	1.5	0.0018	0.0057	3.1	0.0017	0.0091	5.4	0.010	0.12	11.6	0.00001
34-wk 81	0.0045	0.011	2.5	0.0057	0.014	2.4	0.0077	0.020	2.6	0.011	0.25	22.6	0.00004
34-wk 77	0.0022	0.0055	2.5	0.0016	0.0045	2.7	0.0013	0.0047	3.7	0.0073	0.11	15.5	0.00001
34-wk 31	0.16	0.39	2.4	0.11	0.41	3.7	0.13	0.37	3.0	0.17	3.57	21.4	0.0011
34-wk 55	0.17	0.35	2.0	0.19	0.67	3.5	0.17	0.44	2.5	0.23	4.59	19.7	0.0022
34-wk 68	>50	>50	-	>50	>50	-	>50	>50	-	>50	>50	-	>25
38-wk 16	>50	>50	-	>50	>50	-	>50	>50	-	12.10	>50	KO	0.0069
38-wk 19	>50	>50	-	>50	>50	-	>50	>50	-	26.76	>50	KO	>25
42-wk 1	0.070	0.15	2.1	0.064	0.19	2.9	0.048	0.11	2.3	0.078	1.56	20.1	0.00042
42-wk 5	0.14	0.24	1.7	0.13	0.36	2.9	0.12	0.32	2.8	0.14	3.17	22.6	0.00017
42-wk 16	0.0021	0.0030	1.4	0.0011	0.0046	4.1	0.0011	0.0022	2.1	0.0021	0.091	43.8	<0.00001
42-wk 24	0.94	1.65	1.8	0.58	1.90	3.3	0.99	1.56	1.6	1.24	22.26	17.9	0.00249
42-wk 18	>50	>50	-	>50	>50	-	>50	>50	-	>50	>50	-	0.015
59-wk 4	0.38	0.75	2.0	0.13	0.45	3.4	0.16	0.45	2.8	0.16	2.10	13.3	0.091
59-wk 2	>50	>50	-	>50	>50	-	>50	>50	-	>50	>50	-	>25
69-wk 172	46.88	>50	KO	3.99	12.38	3.1	9.60	23.61	2.5	0.36	7.26	20.3	0.080
69-wk 173	>50	>50	-	23.70	31.77	1.3	22.01	31.70	1.4	0.78	10.59	13.5	0.043
69-wk 177	>50	>50	-	>50	>50	-	>50	>50	-	>50	>50	-	>25
Breadth	60	55		65	65		65	65		80	70		80
Geomean	0.057	0.059	1.0	0.059	0.17	2.9	0.064	0.17	2.6	0.19	1.59	8.5	0.0015

Titre (IC_{50} µg/mL) 10^{-5} 10^{2}

Figure 5.3. The IgG4 antibodies have similar autologous neutralization compared to the IgG1 isotype but are less potent.

Neutralization of autologous viruses from the first 69 weeks of infection by antibodies 2G, 4G, 8F and 9E tested as IgG1 and their natural isotype, IgG4. The fold change in the potency between the isotypes is indicated alongside each pair and potency is indicated by color (as in the key). Neutralization data represents the arithmetic mean titers (IC_{50}, µg/mL) from at least two experiments and CAP256.25 IgG1 is included as a reference.

5.3.3 Heterologous neutralization is reduced for antibodies expressed as IgG4

Heterologous neutralization was assessed with a panel of 15 viruses that included two tier 1B, 12 tier 2 and one tier 3 virus from subtypes A, B and C [277]. Antibodies 2G, 4G and 8F, regardless of isotype, exhibited limited breadth of between 27% and 47% (Figure 5.4), which is similar to CAP256.11 and 32, with which these antibodies cluster on the phylogenetic tree (Figure 5.2) In contrast, 9E, which is less closely related to CAP256.11 and 32 (Figure 5.2), was considerably broader, as either isotype, compared to the other antibodies, and as IgG1 it neutralized five additional viruses, resulting in 80% breadth (Figure 5.4). Du156, ZM197, CAP210 and ZM53 were sensitive to both the IgG1 and IgG4 variants of all four antibodies (Figure 5.4). In addition, 4G (as IgG1 and IgG4) neutralized Du422, and 2G, 4G and 8F IgG1

neutralized PVO and BG505 was neutralized by 4G and 8F IgG1 (Figure 5.4). Antibody 9E as IgG1 neutralized 12/15 viruses with a GM potency of 0.78 µg/mL whereas the IgG4 version neutralized 9/15 viruses with a significantly lower (p=0.0039, Wilcoxon matched-pairs) GM potency of 5.66 µg/mL. Overall, although heterologous neutralization was similar between each isotype, the IgG4 versions were less potent and less broad compared to the IgG1 variants, with these differences reaching significance for 9E (Figure 5.2).

	2G			4G			8F			9E			256.11	256.18	256.32	256.25
Virus	IgG1	IgG4	Fold	IgG1	IgG4	Fold	IgG1	IgG4	Fold	IgG1	IgG4	Fold				
DU156.12	0.010	0.034	3.5	0.0043	0.031	7.2	0.0043	0.014	3.3	0.022	0.49	22.2	>50	>50	>50	0.0010
ZM214.15	>50	>50	-	>50	>50	-	>50	>50	-	>50	>50	-	>50	>50	>50	0.0024
ZM197.7	0.18	0.57	3.2	0.17	0.74	4.4	0.17	0.54	3.2	0.23	4.84	21.4	0.055	1.89	0.10	0.0013
CAP45.G3	>50	>50	-	>50	>50		>50	>50	-	>50	>50	KO	>50	>50	>50	0.00001
DU422.01	>50	>50	-	31.29	48.87	1.6	>50	>50	-	0.68	9.29	13.6	11.50	5.40	>50	0.027
ZM249.1	>50	>50	-	>50	>50	-	>50	>50	-	0.45	12.11	27.0	34.5	>50	16.8	0.00011
PVO.04	37.91	>50	KO	18.11	>50	-	21.05	40.80	1.9	1.67	18.44	11.0	10.8	>50	17.8	0.053
Q842.d12	>50	>50	-	>50	>50	-	>50	>50	-	4.50	>50	KO	>50	>50	>50	0.0062
ZM109.4	>50	>50	-	>50	>50	-	>50	>50	-	9.12	>50	KO	>50	>50	>50	0.00022
Q259.d2.17	>50	>50	-	>50	>50	-	>50	>50	-	20.07	>50	KO	>50	5.31	>50	0.0024
Q461.e2	>50	>50	-	>50	>50	-	>50	>50	-	>50	>50	-	>50	>50	>50	0.0018
CAP210.E8	0.013	0.024	1.8	0.015	0.045	2.9	0.014	0.037	2.7	0.045	0.97	21.4	0.073	0.019	0.008	0.00001
ZM53M.PB12.2	0.015	0.028	1.8	0.013	0.047	3.8	0.011	0.028	2.6	0.051	1.07	21.0	0.081	0.010	0.011	0.00001
BG505.W6M.C2	>50	>50	-	9.68	>50	KO	40.72	>50	KO	2.16	38.51	17.9	4.20	1.90	>50	0.0010
AC10.29	>50	>50	-	>50	>50	-	>50	>50	-	4.94	30.65	6.2	>50	>50	>50	0.25
% Breadth	33	27		47	33		40	33		80	60		47	40	33	100
Potency (µg/mL)	0.11	0.06	0.6	0.36	0.30	0.8	0.21	0.20	0.9	0.78	5.66	7.3	1.29	0.52	0.30	0.00098

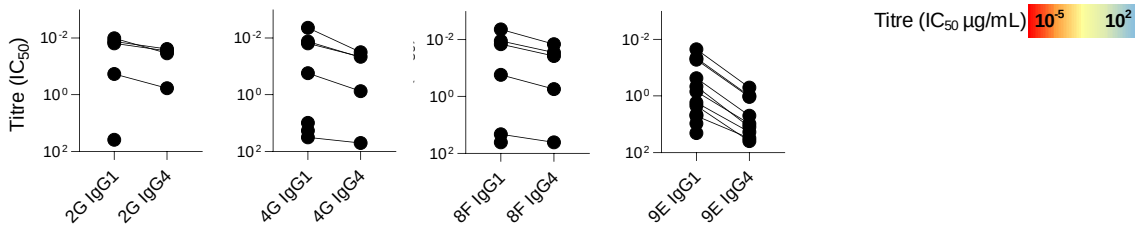

Figure 5.4. The IgG1 variants were slightly more broad and potent than the natural IgG4 versions.
Heterologous neutralization by IgG1 and IgG4 isotype variants and two closely related clonal relatives (CAP256.11 and CAP256.32, titers from [204]). Fold changes are indicated alongside each isotype pair. Neutralization potency is indicated by color (as in the key) and the data represents the arithmetic mean titers (IC_{50}, µg/mL) from at least two experiments. Below each antibody column, the titers for the IgG1 and IgG4 pairs are plotted on the axes.

5.3.4 IgG1 and IgG4 differentially activate diverse Fc functions

Since IgG4 is known to have an impact on antibody-mediated effector functions [114], we tested the effect of isotype on Fc function (ADCC, ADCT, ADCP and ADCD) using the sorting probe BG505 SOSIP.664 trimer as the viral antigen. We found that all of the antibodies, both as IgG1 and IgG4, mediated ADCC, with 2G and 9E mediating the highest levels of ADCC, followed by 8F and then 4G (Figure 5.5 A). For 2G, 4G and 9E, we observed no difference in the ability of either isotype to drive ADCC (p>0.057, paired t-test) (Figure 5.5 A). In contrast, for antibody 8F, the IgG4 version was significantly better (p=0.017, paired t-test) at mediating ADCC compared to the matched IgG1 antibody (Figure 5.5 A).

Similarly, all of the antibodies, regardless of isotype, mediated ADCT (Figure 5.5 B). Antibody 9E IgG1 most potently activated ADCT, followed by 8F, 4G and 2G (Figure 5.5 B). However, 4G IgG1 and 9E IgG1 were significantly better ($p<0.029$, paired t-test) at driving ADCT compared to the matched IgG4 variants (Figure 5.5 B). In contrast, 8F IgG4 exhibited slightly greater ($p=0.010$, paired t-test) ADCT than the 8F IgG1 variant (Figure 5.5 B). Furthermore, we observed that each of the antibodies as IgG4-mediated ADCP (Figure 5.5 C). No difference was observed in the ability of 9E to mediate ADCP either as IgG1 or IgG4 ($p>0.65$, Figure 5.5 C). Antibodies 2G and 4G expressed as IgG4 variably mediated ADCP, however the same antibodies expressed as IgG1 showed no activity in this assay (Figure 5.5 C). The greatest ADCP was mediated by 8F IgG4. Finally, aside from 2G IgG1, none of the antibodies of either isotype mediated ADCD (Figure 5.5 D). Together these data suggest that Fc functions are impacted differently by class switching, even within members of the same antibody lineage.

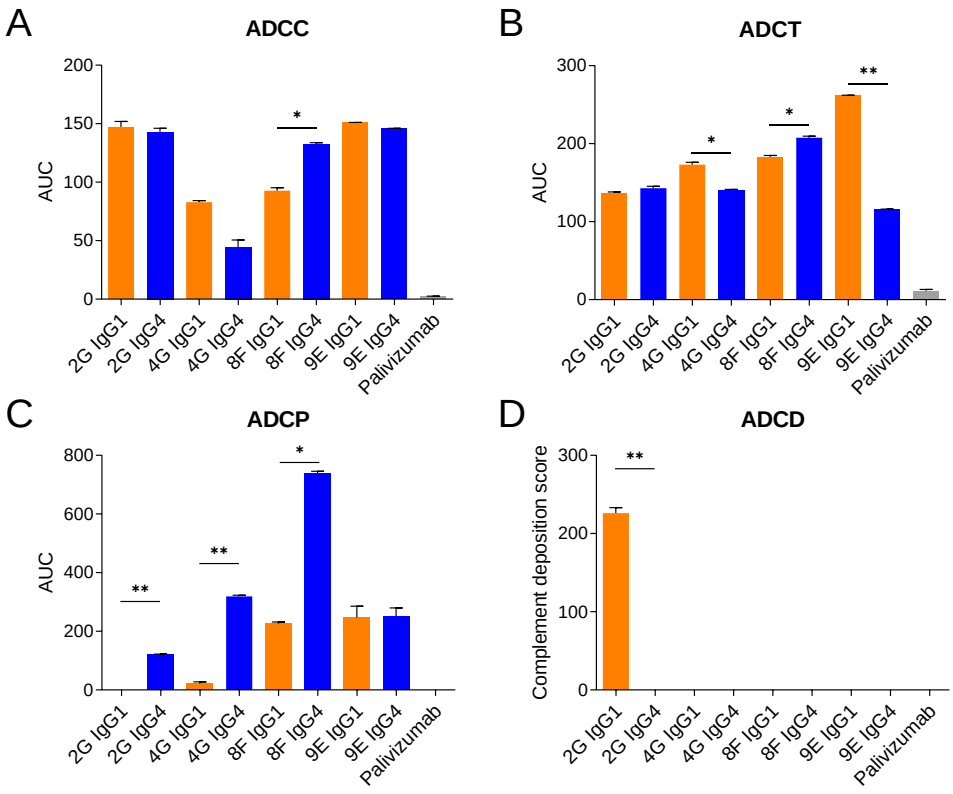

Figure 5.5. Fc effector functions mediated by new CAP256-VRC26 antibodies expressed as IgG1 and IgG4.
The Fc-mediated effector functions were tested with BG505 SOSP.664 in (A) ADCC, (B) ADCT, (C) ADCP and (D) ADCD assays by flow cytometry. The IgG1 variants are shown in orange and IgG4 in blue. Plotted are the means and the standard deviation of the area under the curve (AUC) or complement deposition score. Significant differences, determined by paired t-tests, are indicated by asterisks (*$p<0.05$ and **$p<0.01$). Palivizumab was used as a negative control for each assay.

5.3.5 2G and 8F diverge by one amino acid but mediate significantly different Fc effector functions

The light chains of 2G and 8F have the same sequence but the heavy chains differ by one amino acid (Q98 and E98, respectively) in the CDRH3 (Figure 5.1 and Figure 5.2). Although these two antibodies, expressed as either isotype, had similar autologous (Figure 5.3) and heterologous (Figure 5.4) neutralization, the effector functions differed significantly suggesting that the accessibility of the Fc to the FcR varied between these antibodies (Figure 5.5). Consequently, we modeled these changes on the structure of CAP256.25 complexed with the 34-wk 80 virus [206] and found that neither the Q98 (2G) or E98 (8F) residues interacted with the antibody or the autologous trimer (Figure 5.6). In contrast, alignment of the structures of the BG505 SOSIP.664 (PDB: 5V8L and 4NCO) and X1193.c1 SOSIP.664 (PDB: 5FYJ) trimers to the 34-wk 80 V1V2 domains revealed that both 2G Q98 (Figure 5.6 top row) and 8F E98 (Figure 5.6 bottom row) are in close proximity to these heterologous viral glycans. However, while the model suggested that the N156 and N160 glycans, on different protomers, may form up to three bonds with 2G Q98 (Figure 5.6 A, B and C), this was not true of 8F E98, due to a larger distance (~5 Å) between the residues (Figure 5.6 D and E). Furthermore, 8F E98 was situated <2 Å from a N156 terminal mannose (Figure 5.6 F), which can result in steric hindrance between the CDRH3 and the glycan. Therefore, the single change between 2G and 8F may result in a different angle of approach so that 8F can accommodate the glycan clash. This may account for the differences observed in Fc effector function, which is dependent upon the accessibility of the Fc, but not impact neutralization.

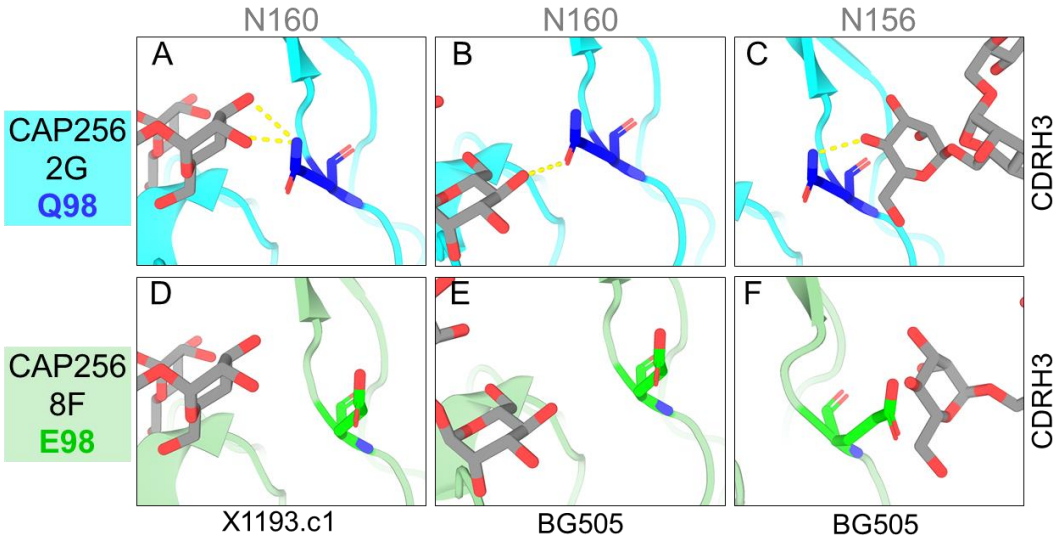

Figure 5.6. The CDRH3 residue E98 clashes with the N156 glycan and does not interact with N160.
The structures of the (A, D) X1193.c1 SOSIP.664 (PDB: 5FYJ) and (B, C, E and F) BG505 SOSIP.664 trimers (PDB: 5V8L and 4NCO) were aligned with the structure of CAP256.25 in complex with the 34-wk 80 trimer [206]. The top panels show the CDRH3 Q98 (blue) residue of 2G, the bottom panels show E98 (green) of 8F, and the glycans are shown in grey. The yellow lines in A, B and C represent interactions predicted by PyMOL (v2.0.2) between the indicated residues.

5.4 Discussion

Broadly neutralizing antibodies (bNAbs) have an increasingly important role in HIV vaccinology, prophylaxis and treatment [233,325,332–337]. bNAb ontogeny studies inform vaccine design by providing valuable insights into the evolution of breadth [187,189,196,197,203,220–222] and when used for passive immunization, bNAbs prevent infection, reduce viremia and clear infected cells [341–350]. The efficacy of bNAbs as biotherapeutics and prophylaxes is dependent on both neutralization and antibody-mediated effector functions [346,348,349]. Therefore, understanding the relationship between the Fab and Fc, and their combined impact on neutralization and effector functions, will allow for the design of optimal passive immunization regimens. Here, we assessed the impact of sequence variation and isotype on four newly identified IgG4 class switched members of the CAP256-VRC26 HIV-1 V2-targetting bNAb lineage [204,205,223]. We found that although the IgG4 antibodies were less broad and potent compared to their matched IgG1 variants, they exhibited similar ADCC and ADCT. Notably, however, as IgG4 these antibodies generally mediated greater ADCP. In addition, we found that a single residue that differentiated two of the antibodies had a dramatic impact on effector function but not neutralization. Together, although IgG4-mediated neutralization is reduced compared to IgG1, these data suggest that V2-specific IgG4 antibodies maintain overall functionality and that ADCP may be improved.

A total of twenty-five heavy chain sequences were amplified from the memory B-cells sorted from CAP256, but many of these were either not members of the CAP256-VRC26 family, or a matched light chain could not be recovered, limiting further analysis. Interestingly, in addition to the seven CAP256-VRC26 antibodies which have very long CDRH3s typical of this lineage, six of the unrelated heavy chains also had CDRH3s of ≥20 amino acids, which is a substantially higher frequency than others have reported [216,339,397]. Long CDRH3s arise during recombination through the incorporation of multiple IGHD genes [398], or as has been suggested for the CAP256-VRC26 lineage, by extensive N-nucleotide additions [205,399]. This may suggest that in individuals such as CAP256, who produce bNAbs with long CDRH3s [400], such antibodies may be generally enriched for, an area that will be explored in future studies.

We found that the antibodies of either isotype generally mediated ADCC, ADCT and ADCP. However, only 2G expressed as IgG1 mediated ADCD. Although IgG4 has a weaker affinity for the FcγRs compared to IgG1, the IgG1 variants were only significantly better at mediating ADCT. Unexpectedly, three of the IgG4 antibodies mediated greater ADCP compared to the IgG1 versions, which has not been shown before for a V2-directed antibody.

Since passive immunization is being considered for the prevention of mother-to-child transmission [351], this study may inform passive infusion formulations since IgG4, in addition to IgG1, readily crosses into the placenta [114]. Furthermore, a number of clinical trials are in development that will evaluate the safety and pharmacokinetics of passively infused bNAbs in exposed infants and HIV positive children [356]. While IgG4 improves phagocytosis, which may be advantageous for antibody-mediated protection, neutralization is diminished. However, expressing broader and more potent antibodies, such as CAP256.25 as IgG4, may offset the reduction in neutralization.

In addition, despite the high degree of sequence identity between 2G and 8F, the effector function profile of these antibodies differed significantly. The single change between 2G (Q98) and 8F (E98) was at a CDRH3 residue that was predicted to have substantially different interactions with glycans at N156 and/or N160. This difference in binding may result in a minor change in the angle of approach between these antibodies. Such a change may not impact neutralization but rather the accessibility of the Fc may be compromised. In combination with the study of off-track antibodies in chapter 3, we therefore show that slight changes in amino acid sequence can have a dramatic impact on both antibody neutralization and effector function.

Together, we show that the IgG4 isotype has a similar impact on heterologous and autologous neutralization, and that IgG4 antibodies mediate greater ADCP than matched IgG1 variants. Since little is known about V2-specific IgG4 class switched antibodies, our observations may be unique to CAP256-VRC26-like antibodies. Nevertheless, these data can inform the design of antibodies engineered for passive immunization since effector functions are critical to the efficacy of such interventions.

6. General discussion and conclusion

While ART significantly reduces the morbidity and mortality associated with HIV/AIDS, there are more than a million new infections each year [8]. Both in response to vaccination and during infection, the humoral response to HIV is strain-specific and does not protect against infection or impact disease progression, respectively [152–156]. However, 20-30% of infected individuals develop broadly neutralizing antibodies (bNAbs) that neutralize unrelated strains of HIV [152,153,158–161] and protect animals from HIV/SHIV infection [341–350]. Consequently, understanding bNAb ontogeny is critically important [164,215,218]. Here we extend several previous studies on the 33 member CAP256-VRC26 bNAb lineage [204,205,223] to address the genetic determinants of breadth. We found that very few mutations differentiate bNAbs from closely related strain-specific "off-track" relatives, and that these are selected by viral variants with features distinct from circulating viruses. These data suggest that immunogens that represent commonly circulating variants can elicit breadth and minimize strain-specificity. In addition, we demonstrated that only approximately half of the mutations in the broadest lineage member, CAP256.25, were necessary for breadth, suggesting that immunogens targeting key sites can efficiently drive the development of breadth. Furthermore, we show that antigen binding and isotype impacts neutralization and effector function, highlighting the importance of isotype for bNAbs utilized in passive immunization. Together, our data show that few mutations within antibodies can have dramatic effects on neutralization breadth, potency and effector functions.

Ontogeny studies have illuminated the diverse pathways of antibody/virus co-evolution that result in breadth [164,214,216,217]. We show that multiple pathways can lead to the development of off-track antibodies and confirm that extensive somatic hypermutation is not sufficient for breadth. By producing chimeras between two closely related bNAb/off-track pairs in the CAP256-VRC26 lineage, we demonstrated that the CDRH3 is the major determinant of neutralization breadth. In one pair, we found that mutating three residues in the CDRH3 of the off-track antibody, CAP256.20, to match the sequence of a close bNAb relative, CAP256.27, introduced bNAb-like breadth and potency. In another pair, the neutralization of the off-track antibody CAP256.04 was dramatically improved by mutating one CDRH3 residue (R100rA) to match that of the CAP256.25 bNAb relative. Notably, the transfer of the entire CAP256.25 CDRH3 introduced less neutralization than R100rA alone. In addition, introducing the CAP256.25 CDRH1 or CDRH2 into CAP256.04 R100rA reduced breadth. Together, this indicates that there is substantial mutational "noise" that has a deleterious impact on neutralization and that few mutations differentiate a bNAb from an off-track antibody.

We also investigated which viral variants contributed to the evolution of the off-track antibody CAP256.20. The K169 viral immunotype variant is the most common in global viruses but was a minority variant during most time points in CAP256. In contrast, Q169 was the predominant immunotype in CAP256 and viruses with this sequence were generally sensitive to CAP256.20. While broader lineage members tolerated variation at position 169, we show with mutagenesis experiments that CAP256.20 was generally reliant on 169Q. Therefore, the off-track phenotype was a consequence of evolution toward a globally rare immunotype, suggesting that vaccine immunogens should include highly conserved epitopes.

The probability that a non-synonymous mutation may occur is influenced by both the position of the codon (in an AID hot- or cold-spot) and the number of changes necessary for the change [125,127,128]. Furthermore, bNAbs typically have more improbable mutations than would be expected by chance [380,384–386]. We found that the CDRH3 of bNAbs CAP256.25 and CAP256.27 harbored most of the improbable mutations. This is in concordance with the observation from our experiments with the off-track antibodies and the CAP256.UCA, that the CDRH3 has a primary role in modulating the neutralization of these antibodies. Furthermore, we found that the mutations that confer the off-track phenotype to CAP256.04 and CAP256.20 were relatively more probable occurrences. This result highlights the challenge of eliciting bNAbs, since the evolution of off-track mutations are more common events, and in the case of CAP256.04, substantially more likely to occur than the breadth-conferring mutations of CAP256.25. While many of the mutations in the CAP256.25 CDRH2 and CDRH3 were improbable events, we established that approximately half of these mutations were sufficient for breadth, and greater potency compared to nearly 100 unrelated bNAbs. This is consistent with studies with minimally mutated versions of the bNAbs BF520.1 [221,222], VRC01 [230] and 10E8 [230], but has not been demonstrated for a V2-specific bNAb.

Neutralization by CAP256.UCA plateaued at <100% and this observation is typically the consequence of glycovariation in the viral population [362]. However, as few as two mutations in the CAP256.UCA CDRH3, which introduced a disulfide bond, improved the autologous neutralization potency of the CAP256.UCA and led to the neutralization of 100% of susceptible viruses at excess concentrations of antibody. Structural studies and models suggest that a disulfide bond would stabilize the extremely long CDRH3 [205,206] which may increase the capacity of the antibody to tolerate glycovariation.

In addition to the importance of the CDRH3s, we established for the first time that the light chain had an impact on autologous neutralization potency and on both the breadth and potency of heterologous neutralization for CAP256.25. Furthermore, we provide evidence that the CDRL2 forms part of the paratope of CAP256.25, confirming a previous structural study of this antibody [206]. Overall, although the FR had the smallest impact on neutralization, we also showed that these regions contribute to autologous neutralization potency but not breadth. A similar observation was made with 10E8 and VRC01 FR-revertants [230], where potency was reduced but breadth remained unchanged. Together, this implies that an immunogen/s that drives affinity maturation in the CDRHs, particularly in the CDRH3 and the light chain of CAP256.UCA-like-precursors may be able to efficiently elicit breadth.

Lastly, we assessed the impact of sequence variation and isotype on the neutralization and effector functions of four newly identified members of the CAP256-VRC26 lineage that were naturally IgG4 class switched. Overall, the breadth of the IgG4 variants was reduced compared to the matched IgG1 versions. This may be due to the slightly shorter hinge region of IgG4 compared to that of IgG1, which has been shown to impact neutralization [114]. However, as either isotype, these antibodies activated both ADCC and ADCT. In addition, although IgG4 has a weaker affinity for the FcγR compared to IgG1 and has an inhibitory effect on effector function [114], we found that three of the four antibodies as IgG4 mediated greater ADCP than their IgG1 counterparts. These data may have implications for passive immunization since IgG4 is transferred across the placenta [114] and effector functions are critical to the success of passive immunization. Furthermore, we found that a single residue change had a dramatic impact on effector function suggesting that Fab-Fc pairing may be optimized for maximum effector polyfunctionality.

Together, our data show that minor sequence variation differentiates a bNAb from a strain-specific off-track relative, few mutations are sufficient to introduce breadth into a V2-targetting UCA and that the Fab changes impacts Fc functionality. These data demonstrate that extensive somatic hypermutation is not necessary for breadth and suggest that targeting affinity maturation to key sites can rapidly introduce breadth.

7. Appendices

7.1 Appendix A: Change of thesis title

UNIVERSITY OF THE WITWATERSRAND, JOHANNESBURG

Private Bag 3 Wits, 2050
Fax: 027117172119
Tel: 02711 7172076

Reference: Mrs Sandra Benn
E-mail: sandra.benn@wits.ac.za

16 September 2019
Person No: 0502955K
TAA

Mr D Sacks
Po Box 469
Wendywood
2144
South Africa

Dear Mr David Sacks

Doctor of Philosophy: Change of title of research

I am pleased to inform you that the following change in the title of your Thesis for the degree of **Doctor of Philosophy** has been approved:

From:	**Genetics basis for the breadth and potency of HIV-1 V2 and MPER specific antibodies**
To:	**Genetics basis for the breadth and potency of HIV-1 V2 specific antibodies**

Yours sincerely

Mrs Sandra Benn
Faculty Registrar
Faculty of Health Sciences

7.2 Appendix B: Ethics certificate

R14/49 Mr David Sacks et al

HUMAN RESEARCH ETHICS COMMITTEE (MEDICAL)

CLEARANCE CERTIFICATE NO. M160934

NAME: (Principal Investigator)	Mr David Sacks et al
DEPARTMENT:	Virology National Institute for Communicable Diseases
PROJECT TITLE:	Genetic Basis for the Breadth and Potency of HIV-1 V2 and MPER Specific Antibodies
DATE CONSIDERED:	30/09/2016
DECISION:	Approved unconditionally
CONDITIONS:	
SUPERVISOR:	Prof Penelope Moore
APPROVED BY:	Professor P Cleaton-Jones,Chairperson, HREC (Medical)
DATE OF APPROVAL:	21/10/2016

This clearance certificate is valid for 5 years from date of approval. Extension may be applied for.

DECLARATION OF INVESTIGATORS

To be completed in duplicate and **ONE COPY** returned to the Research Office Secretary in Room 10004, 10th floor, Senate House/3rd Floor, Phillip Tobias Building, Parktown, University of the Witwatersrand. I/we fully understand the conditions under which I am/we are authorized to carry out the above-mentioned research and I/we undertake to ensure compliance with these conditions. Should any departure be contemplated, from the research protocol as approved, I/we undertake to resubmit the application to the Committee. **I agree to submit a yearly progress report**. The date for annual re-certification will be one year after the date of convened meeting where the study was initially reviewed. In this case, the study was initially reviewed in September and will therefore be due in the month of September each year.

Principal Investigator Signature Date

PLEASE QUOTE THE PROTOCOL NUMBER IN ALL ENQUIRIES

7.3 Appendix C: Certificate of submission (student)

UNIVERSITY OF THE WITWATERSRAND, JOHANNESBURG | FACULTY OF HEALTH SCIENCES

Certificate Of Submission For Examination Of Masters Research Report / Dissertation Or Phd Thesis Signed By Higher Degrees Candidates

Full name	David Sacks		
Student number	0502955k		
Title of submitted Research Project: Genetic basis for the breadth and potency of HIV-1 V2-specific antibodies *NB: If this title is different to your previously approved title, no further action can be taken by the Faculty Office until a change of title has been approved.*			
Contact no	072 389 8551	E-mail	davids@nicd.ac.za or sacksdavid@gmail.com

1. If you are likely to move in the next 6-12 months, please give the anticipated date of move: NA
2. I hereby submit my **PhD thesis for examination**
3. I have checked all copies of my thesis and declare that no pages are missing or poorly reproduced.
4. I have submitted three bound copies and one copies on CD

5. **I confirm that I have:**
   a) A signed declaration indicating my understanding of the concept of plagiarism and a denial of plagiarism in my research document.
   b) A report from "Turnitin" (or other approved plagiarism detection) software indicating the level of plagiarism in my research document included as an appendix.

6. **I confirm that I have:**
   a) Not used either human or animal tissue or records **No**
   b) If yes: I have included the ethics waiver letter pertinent to my research as an appendix **NA**
   c) Done research using animals **No**
      If yes: I have included a copy of the animal ethics committee clearance certificate as an appendix in this document **NA**
   d) Done research using human subjects, human tissue or patient records **Yes**
      If yes: I have included a copy of the human ethics clearance certificate as an appendix to the research document **Yes**
7. I understand that I may not graduate unless my University fees have been paid in full.
8. My Supervisor(s) names, departments, telephone numbers and email addresses are as follows:

Name	Prof Penny L. Moore		
Department	Virology		
Telephone	011 386 6331	E-mail	pennym@nicd.ac.za
Name	Prof Lynn Morris		
Department	Virology		
Telephone	011 386 6362	E-mail	lynnm@nicd.ac.za

List all publications, which you have published in peer-reviewed journals from your postgraduate research thesis during the course of your studies in the Faculty of Health Sciences (Include authors, year, title of paper, name of journal, volume number and page numbers). This information is mandatory. Sacks D, Bhiman JN, Wiehe K, Gorman J, Kwong PD, Morris L, Moore PL. Somatic hypermutation to counter a globally rare viral immunotype drove off-track antibodies in the CAP256-VRC26 HIV-1 V2-directed bNAb lineage. PLoS Pathog. 2019;15(9):e1008005.

Signature of candidate: _____ Date: 26 February 2020

7.4 Appendix D: Certificate of submission (supervisors)

Certificate Of Submission For Examination Signed By Supervisors Of Higher Degrees Candidates

Full name	David Sacks
Student number	0502955k

Candidate for the degree of: Doctor of philosophy

has submitted his thesis

Entitled: Genetic basis for the breadth and potency of HIV-1 V2-specific antibodies

Contact no	072 389 8551	E-mail	davids@nicd.ac.za or sacksdavid@gmail.com

Mark with an X on appropriate box	Yes	No
Has this thesis/dissertation/research report been submitted with the acquiescence of the supervisor?	X	
To the best of your knowledge are you able to verify that this is the candidate's work, except as otherwise stated by the candidate?	X	
The substance (nor any part of it) has not been submitted in the past nor is being submitted for a degree in any other university?	X	
The candidate has acknowledged wherever any information used in the thesis, dissertation or other work has been obtained by him/her while employed by, or working under the aegis of, any person or organization other than the University or its associated institutions?	X	
Have examiners been nominated and approved?	X	

I certify that this thesis report has the approval of the Animal Ethics Committee / Committee for Research on Human Subjects and the Number of the Certificate of Approval is: M160934

List all publications, which your student has published in peer-reviewed journals from his/her postgraduate research report/dissertation/thesis during the course of his/her studies in the Faculty of Health Sciences (Include authors, year, title of paper, name of journal, volume number and page numbers). This information is mandatory.

Sacks D, Bhiman JN, Wiehe K, Gorman J, Kwong PD, Morris L, Moore PL. Somatic hypermutation to counter a globally rare viral immunotype drove off-track antibodies in the CAP256-VRC26 HIV-1 V2-directed bNAb lineage. PLoS Pathog. 2019;15(9):e1008005.

Name of Supervisor 1: Prof Penny L Moore
Telephone: 011 386 6331 Email: pennym@nicd.ac.za

Signature: _____ Date: 26 February 2020

Name of Supervisor 2: Prof Lynn Morris
Telephone: 011 386 6362 Email: lynnm@nicd.ac.za

Signature: _____ Date: 26 February 2020

7.5 Appendix E: David Sacks et al, PLOS Pathogens, 2019

PLOS PATHOGENS

RESEARCH ARTICLE

Somatic hypermutation to counter a globally rare viral immunotype drove off-track antibodies in the CAP256-VRC26 HIV-1 V2-directed bNAb lineage

David Sacks[1,2], **Jinal N. Bhiman**[1,2¤], **Kevin Wiehe**[3], **Jason Gorman**[4], **Peter D. Kwong**[4], **Lynn Morris**[1,2,5], **Penny L. Moore**[1,2,5*]

1 Centre for HIV and STIs, National Institute for Communicable Diseases (NICD) of the National Health Laboratory Service (NHLS), Johannesburg, South Africa, **2** Faculty of Health Sciences, University of the Witwatersrand, Johannesburg, South Africa, **3** Duke Human Vaccine Institute, Duke University School of Medicine, Durham, North Carolina, United States of America, **4** Vaccine Research Center, National Institute of Allergy and Infectious Diseases, National Institutes of Health, Bethesda, Maryland, United States of America, **5** Centre for the AIDS Programme of Research in South Africa (CAPRISA), University of KwaZulu Natal, Durban, South Africa

¤ Current address: Department of Immunology and Microbiology, The Scripps Research Institute, La Jolla, California, United States of America,
*pennym@nicd.ac.za

Citation: Sacks D, Bhiman JN, Wiehe K, Gorman J, Kwong PD, Morris L, et al. (2019) Somatic hypermutation to counter a globally rare viral immunotype drove off-track antibodies in the CAP256-VRC26 HIV-1 V2-directed bNAb lineage. PLoS Pathog 15(9): e1008005. https://doi.org/10.1371/journal.ppat.1008005

Editor: Ronald C. Desrosiers, Miller School of Medicine, UNITED STATES

Received: April 6, 2019

Accepted: July 29, 2019

Published: September 3, 2019

Data Availability Statement: All relevant data are within the manuscript and its Supporting Information files.

Funding: We acknowledge research funding from the South African Medical Research Council (MRC) SHIP program, the National Institutes of Health (NIH) through a U01 grant (AI116086), the Centre for the AIDS Programme of Research (CAPRISA) and the Intramural Research Programs of the Vaccine Research Center, NIAID, NIH (J.G. and P.

Abstract

Previously we have described the V2-directed CAP256-VRC26 lineage that includes broadly neutralizing antibodies (bNAbs) that neutralize globally diverse strains of HIV. We also identified highly mutated "off-track" lineage members that share high sequence identity to broad members but lack breadth. Here, we defined the mutations that limit the breadth of these antibodies and the probability of their emergence. Mutants and chimeras between two pairs of closely related antibodies were generated: CAP256.04 and CAP256.25 (30% and 63% breadth, respectively) and CAP256.20 and CAP256.27 (2% and 59% breadth). Anti- bodies were tested against 14 heterologous HIV-1 viruses and select mutants to assess breadth and epitope specificity. A single R100rA mutation in the third heavy chain comple- mentarity-determining region (CDRH3) introduced breadth into CAP256.04, but all three CAP256.25 heavy chain CDRs were required for potency. In contrast, in the CAP256.20/27 chimeras, replacing only the CDRH3 of CAP256.20 with that of CAP256.27 completely reca- pitulated breadth and potency, likely through the introduction of three charge-reducing muta- tions. In this individual, the mutations that limited the breadth of the off-track antibodies were predicted to occur with a higher probability than those in the naturally paired bNAbs, sug- gesting a low barrier to the evolution of the off-track phenotype. Mapping studies to deter- mine the viral immunotypes (or epitope variants) that selected off-track antibodies indicated that unlike broader lineage members, CAP256.20 preferentially neutralized viruses contain- ing 169Q. This suggests that this globally rare immunotype, which was common in donor CAP256, drove the off-track phenotype. These data show that affinity maturation to counter globally rare viral immunotypes can drive antibodies within a broad lineage along multiple pathways towards strain-specificity. Defining developmental pathways towards and away

D.K.). CAPRISA is funded by the South African HIV/AIDS Research and Innovation Platform of the South African Department of Science and Technology, and was initially supported by the US National Institute of Allergy and Infectious Diseases, US National Institutes of Health, US Department of Health and Human Services grant U19 AI51794. P.L.M. is supported by the South African Research Chairs Initiative of the Department of Science and Technology and the NRF (Grant No 98341). D.S. is supported by the Poliomyelitis Foundation and through a NRF SARChI Chair-linked PhD bursary. The funders had no role in study design, data collection and analysis, decision to publish, or preparation of the manuscript.

Competing interests: The authors have declared that no competing interests exist.

from breadth may facilitate the selection of immunogens that elicit bNAbs and minimize off-track antibodies.

Author summary

Broadly neutralizing antibodies (bNAbs) develop in some HIV infected individuals, partly due to their complex evolutionary pathways that are characterized by extensive somatic hypermutation (SHM). Furthermore, bNAbs within a lineage may form a minor subset, amidst many strain-specific "siblings", indicating that minor sequence differences between lineage members can significantly affect neutralization. Here, we define mutations that limit breadth in two "off-track" members of the CAP256-VRC26 bNAb lineage, and show that these occur with relatively high probability. A dominant autologous virus with a globally rare V2 sequence appears to have selected for an off-track antibody, providing a mechanism for the development of this antibody during infection. These data highlight the complex interdependencies between high levels of SHM and breadth, as mutations that neutralize autologous viruses may limit heterologous breadth. Consequently, strategies to increase SHM by repeated vaccinations will require careful antigen selection to focus the humoral response to globally common epitopes, limiting off-track responses.

Introduction

Antiretroviral therapy has transformed HIV from a progressive fatal infection to a manageable chronic disease [1]. However, a preventative vaccine is urgently needed as drug resistance, access to medication and adverse side effects hamper the utility of antiretroviral drugs. Despite intensive research, strategies to induce protective immune responses by vaccination have achieved little success [2]. While neutralizing antibodies are elicited during HIV infection, the response is typically strain-specific. However, ~20% of individuals develop broadly neutralizing antibodies (bNAbs) which potently neutralize diverse global viruses *in vitro* and protect non-human primates from infection [3–8]. Therefore, understanding the mechanisms behind the elicitation and evolution of bNAbs is central to the development of an HIV vaccine.

During infection, the humoral response targets the HIV envelope (Env) glycoprotein which consists of three heavily glycosylated non-covalently linked gp41-gp120 protomers. While strain-specific antibodies recognize exposed and variable sites, bNAbs target relatively conserved and occluded sites, including the membrane proximal external region (MPER), gp120-gp41 interface, CD4-binding site (CD4bs), N332 supersite and a quaternary V1V2 epitope at the trimer apex [9]. Many V1V2 directed bNAbs have atypically long (>24 amino acids) third complementarity determining regions of the heavy chain (CDRH3) which provides access to glycan shielded and buried epitopes [10–14]. Additionally, bNAbs frequently exhibit unusually extensive somatic hypermutation (SHM), which suggests multiple rounds of affinity maturation. Understanding how these unusual features arise is critical to recapitulating this process by vaccination.

The degree to which SHM and affinity maturation occurs is influenced by HIV diversity and antigen load [15]. A number of longitudinal studies describing the "arms race" between viral quasispecies and bNAb lineages have provided insights into the evolution of breadth [16]. These studies have identified bNAb-initiating Envs that engage antibody precursors as well as

emerging viral variants, which select bNAb intermediates [12,17–23]. We have extensively studied virus/antibody co-evolution in the superinfected CAP256 donor from whom 33 members of the CAP256-VRC26 V2-targetting bNAb lineage were isolated [11,12,22]. The evolution of this lineage was elucidated through analysis of longitudinal viral and antibody deep sequences from 59–206 weeks post infection [11,12,22]. Viruses from six weeks post infection are sensitive to neutralization by CAP256 lineage members but by 59 weeks post infection most viruses are resistant. Similar to other V2-directed bNAbs, the CAP256-VRC26 lineage members have very long (35–37 amino acid, aa) anionic and tyrosine-sulfated CDRH3s that recognize the electropositive V2 apex [24]. Modelling and mapping studies show that several residues within the CDRH3 are critical for epitope recognition, including the tyrosine sulfated YYD motif at the apex of the CDRH3 [24]. This motif is present in the unmutated common ancestor (UCA) of the CAP256-VRC26 lineage, 27 of the 33 lineage members as well as other V2-directed bNAbs such as PG9/PG16 [10,11]. In addition, the CDRH1 has been shown to stabilize the CDRH3, and residues in CDRH2 have been implicated in glycan recognition [25,26]. Within strands B and C of the viral Env protein, the CAP256-VRC26 lineage's footprint includes residues N160, R166, D167, K168 and K169 and is similar to other V2 glycan bNAbs (PG9/PG16). The breadth, potency and extent of SHM of CAP256-VRC26 lineage members ranges from 2–63%, 0.003–5 μg/mL and 4.2–18%, respectively [11].

SHM, which is mediated by activation-induced cytidine deaminase (AID), is essential for breadth as bNAb germline revertants generally lack substantial binding and neutralization [10,27–30]. Mutations that are selected during affinity maturation may increase antibody-antigen affinity directly at the paratope or indirectly by improving stability [31,32]. SHM is a semi-random process as AID hot-spots (WRCH/Y, W = A/T, R = A/G and H = A/C/T) and cold-spots (SYC, S = C/G and Y = C/T) are distributed throughout the antibody variable regions. Consequently, mutations associated with breadth are unlikely to occur if they are in cold-spots and/or require more than one nucleotide change [33,34]. Additionally, neutral mutations can accumulate via co-selection and constitutive background mutational noise [32]. Although increased SHM is generally associated with neutralization breadth, exceptions exist within the CAP256-VRC26 and other bNAb lineages. We have previously described these non-broad but highly mutated CAP256 antibodies as "off-track" [22]. Such off-track antibodies have been recovered from bNAb lineages in several individuals. 1AZCETI5 is a clonal member of the CD4bs CH103 bNAb lineage, and shares VDJ genes, CDRH3 length and extent of SHM with bNAb CH103, but the former only neutralizes autologous viruses [18]. The PGDM1400 bNAb, a member of the V2 glycan targeting PGDM lineage with 83% breadth has similar genetic properties to PGDM1406, but the latter exhibits limited breadth (6%) [35]. Similarly, within the PGT121 N332 targeting bNAb lineage are two heavy chains (HC) (22H and 6H) that are related to broad members but exhibit no neutralization [36]. As monoclonal antibody isolation methodologies are designed to recover bNAbs, the proportion of off-track antibodies in bNAb lineages is unknown. However, the finding that 40% of related antibodies recovered by flow cytometry from the donor of the CD4bs bNAb, VRC-PG04, were off-track, indicates that such antibodies may be common [37].

Collectively, studies into co-evolution and bNAb targets have identified candidate antigens to initiate antibody lineages and guide the development of breadth. Indeed, native-like Env trimers administered in combination or sequentially elicits tier 2 neutralizing antibodies in mice and rabbits, providing a strong rationale to test similar immunogens in people [38–42]. Importantly, the mutations crucial for breadth and potency as well as those that confer an off-track phenotype in bNAb lineages are largely unknown. Identification of these mutations will inform the design of vaccine antigens that elicit breadth but dampen the evolution of off-track responses. The high degree of sequence identity between CAP256-VRC26 bNAbs and their

off-track relatives, the richly populated lineage and the availability of contemporaneous viral sequences is an ideal opportunity to compare off-track antibodies with bNAbs to determine why these antibodies lack breadth.

Here we define key residues that restrict neutralization breadth and potency in two off-track antibodies within the CAP256-VRC26 lineage. We found that in one off-track/bNAb pair, residues in each of the three CDRHs were necessary for potency and that a key breadth-conferring mutation in the CDRH3 was highly improbable. In the second pair, we show that the CDRH3 was completely responsible for modulating neutralization and that the mutations leading to the off-track phenotype were relatively probable. Lastly, through epitope mapping we identified viruses that guided the evolution of an off-track antibody toward a globally rare immunotype. This study highlights the stochastic nature of SHM and shows that breadth-restricting mutations typically arise with a greater probability than breadth-conferring mutations. This work provides insights into the evolution of breadth and mature strain-specificity, informing the design of immunogens that minimize the elicitation of off-track mutations while guiding evolution to globally conserved sites.

Results

Neutralization breadth is mediated by the CAP256-VRC26 antibody heavy chain

To determine the genetic determinants that controlled the off-track phenotype, we selected two bNAbs with high sequence identity to two off-track antibodies. Off-track antibodies were defined as having low neutralization breadth despite their capacity to neutralize early autologous viruses [12], extensive sequence maturation and identity to related bNAb lineage members. The CAP256.25 bNAb was paired with the off-track antibody CAP256.04 and bNAb CAP256.27 was paired with the off-track antibody, CAP256.20. The two pairs of antibodies cluster together on a maximum likelihood tree (Fig 1A), consistent with our previous observations that antibodies with considerably different breadth may differ by relatively few amino acids [22]. The HC and light chain (LC) of CAP256.04 (30% breadth, 0.27 μg/mL potency, 9% SHM) both share 92% sequence identity with the HC and LC of bNAb CAP256.25 (63% breadth, 0.003 μg/mL potency, 12% SHM) (Fig 1A). Within the second pair, the HC and LC of CAP256.20 (2% breadth, 1.87 μg/mL potency, 16% SHM) shares 93% and 96% sequence identity with the CAP256.27 HC and LC (59% breadth, 0.047 μg/mL potency, 16% SHM), respectively (Fig 1A). A total of eighteen amino acids differ between the HC and 11 amino acids between the LC of CAP256.04 (orange) and CAP256.25 (brown) which are displayed as yellow spheres in an alignment of the two antibodies (Fig 1B). Seventeen amino acids (yellow spheres) differentiate the HCs and four the LCs of CAP256.27 (purple) and CAP256.20 (light purple) (Fig 1B).

As neutralization by members of the CAP256 bNAb lineage has been largely attributed to the HC [12], we first confirmed that the LC was not responsible for the off-track phenotype of CAP256.04 and CAP256.20. We generated chimeras between the HC and LC of each off-track/bNAb pair (25HC+04LC, 04HC+25LC and 27HC+20LC, 20HC+27LC) and tested their neutralization against both CAP256 infecting viruses (the primary and superinfecting viruses) and 14 heterologous viruses. The titers did not differ significantly (Wilcoxon signed rank test) between the chimeric antibodies and the natural antibody from which the HC was donated (Fig 1C). These data indicate that the LC has no impact on the neutralization breadth within these pairs, consistent with structural analyses showing no light chain contacts with the viral epitope [26], and we therefore focused on the HC in subsequent studies.

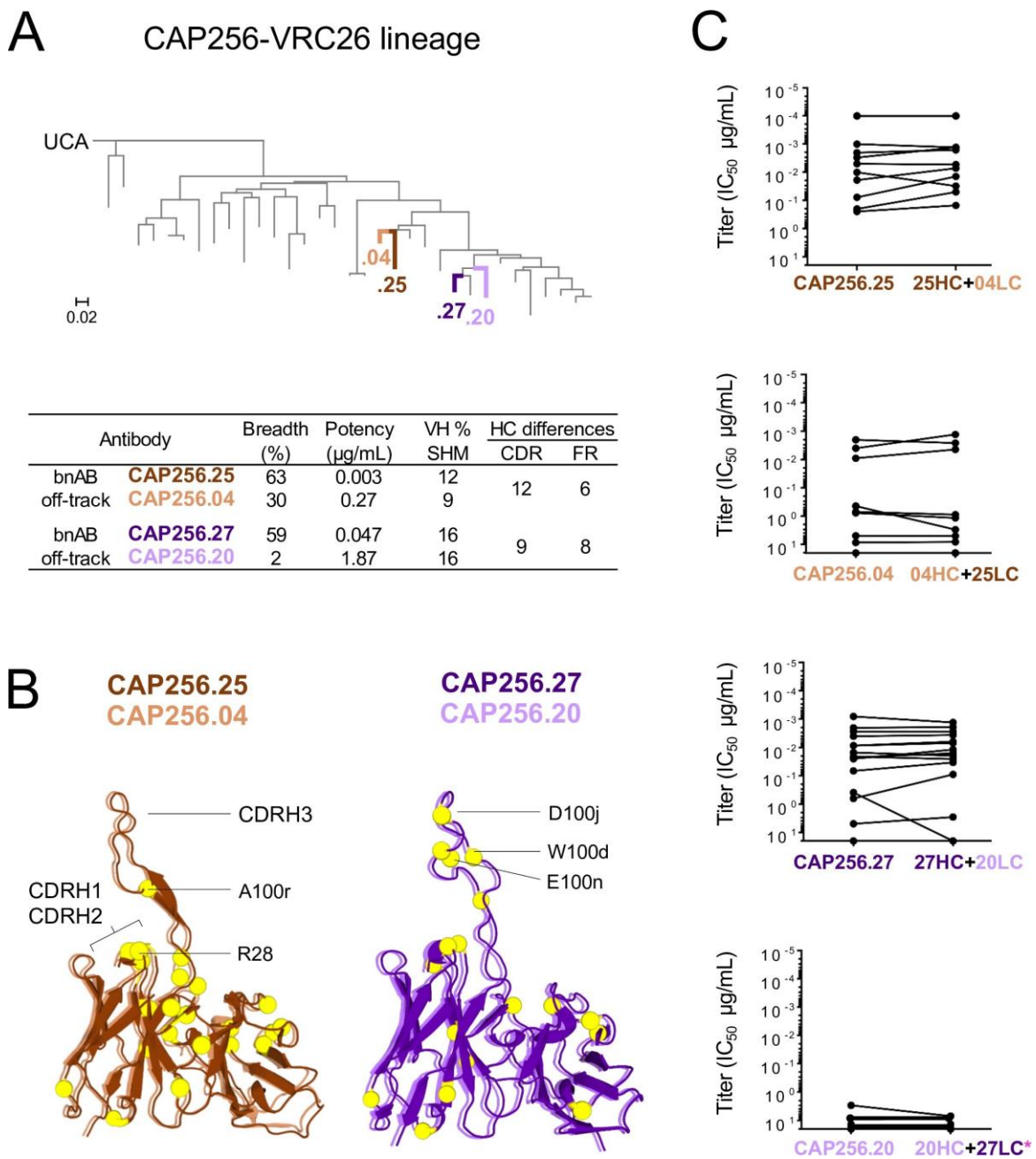

Antibody		Breadth (%)	Potency (µg/mL)	VH % SHM	HC differences CDR	HC differences FR
bnAB	CAP256.25	63	0.003	12	12	6
off-track	CAP256.04	30	0.27	9		
bnAB	CAP256.27	59	0.047	16	9	8
off-track	CAP256.20	2	1.87	16		

Fig 1. The HC mediates the off-track phenotype. (A) Maximum likelihood phylogenetic tree, rooted on the CAP256.UCA, with 33 clonally related VH sequences of monoclonal antibodies isolated from donor CAP256. Highlighted are CAP256.04 (orange), CAP256.25 (brown), CAP256.20 (light purple) and CAP256.27 (purple). Neutralization breadth, potency, VH SHM (related to CAP256.UCA) and the number of amino acids that differ between the CDR and FR of each pair are tabulated below. Breadth and potency (mean IC_{50}) was calculated from a panel of 46 heterologous viruses [11]. (B, left) The amino acid sequence of CAP256.04

(orange) was fitted to a structure of CAP256.25 and CAP256 34-week trimer in Swiss-PdbViewer (v4.1.0), aligned in PyMOL (v2.0.2) and displayed as cartoons. (B, right) The amino acid sequences of CAP256.27 (purple) and CAP256.20 (light purple) were fitted to CAP256.25 in Swiss-PdbViewer (v4.1.0) and aligned in PyMOL (v2.0.2). The amino acids that differ between each bNAb and matched off-track antibody are represented as yellow spheres. (C) The LCs were exchanged between each bNAb/off-track pair and neutralization (IC_{50}, μg/mL) was tested against (n = 16[7]) pseudoviruses.

https://doi.org/10.1371/journal.ppat.1008005.g001

Introduction of potency into CAP256.04 requires a combination of the CAP256.25 CDRHs

To determine which regions of the HC restrict the breadth of CAP256.04, we constructed several chimeras and point mutants between CAP256.25 and CAP256.04, focusing initially on the CDRHs. The sequence variation between the CDRHs is shown in Fig 2A and includes charge and hydrophobicity differences between the two antibodies (R28S, D30N, G31R, H53Y, K57D, A100rR and N100ddF) and an insertion (G100w) in CAP256.25 that is absent from CAP256.04 (Fig 1B). We first transplanted all the CAP256.25 CDRHs (12 amino acid changes in total) into CAP256.04, creating CAP256.04^{25H123} (Fig 2B). Antibodies were tested against a panel of 16 viruses that were sensitive to CAP256.25 (geometric mean potency of 0.002 μg/mL against this panel), of which 8 were neutralized by CAP256.04 (with a 230-fold lower geometric mean potency of 0.17 μg/mL) (Fig 2B). The neutralization breadth and potency of the CAP256.04^{25H123} chimera (which neutralized all 16 viruses with a geometric mean potency of 0.008 μg/mL) matched that of CAP256.25 (0.002 μg/mL) (Fig 2B). In the reverse experiment, introducing the framework (FR) regions from CAP256.25 into CAP256.04 (CAP256.04^{25FR123}) had no effect on breadth (Fig 2B). These data suggest that the mutations in the CDRs, rather than the FW regions restrict the breadth of CAP256.04.

To dissect the role of individual CDRHs, each was individually swapped between the two parental antibodies. CAP256.04^{25H1} neutralized two additional viruses (ZM214 and ZM249) that were resistant to CAP256.04 (Fig 2B). In addition, we observed virus-specific increases in potency for some sensitive viruses (with a 6-18-fold improvement for Du156, Q259, and Du422 and a 250-fold increase in potency for CAP45). In contrast, CAP256.04^{25H2} neutralized the same number of viruses as CAP256.04 (Fig 2B), though again slight virus-specific differences in potency were observed, with CAP45 becoming resistant to CAP256.04^{25H2} while PVO gained sensitivity (Fig 2B). The largest effect of a single CDRH swap was observed for the CDRH3 which differed by six amino acids. CAP256.04^{25H3} neutralized six additional viruses (ZM109, PVO, ZM214, ZM249, Q461 and Q842) (Fig 2B) although with similar potency to CAP256.04 (0.39 μg/mL and 0.17 μg/mL, respectively). This was confirmed in the reverse experiment, where the CAP256.04 CDRH3 was introduced into CAP256.25 (CAP256.25^{04H3}) resulting in reduced breadth (Fig 2B). Overall, these data suggest that the breadth of the CAP256.04 off-track phenotype is modulated by the CDRH3, but potency is attenuated by a combination of all three CDRHs.

Introduction of breadth into CAP256.04 requires a single improbable CDRH3 mutation

As the CAP256.25 CDRH3 conferred additional breadth into CAP256.04, we assessed which residue(s) were responsible for this effect (Fig 2A). Mutating CDRH3 residues that altered the charge (K102N) or aromaticity (F100ddA) of the CDRH3 failed to improve the neutralization of CAP256.04 (S1 Fig). In contrast, the R100rA mutation, which removed a positive charge from the CDRH3, improved the breadth of CAP256.04 from 50% to 94% of this panel, with seven viruses resistant to CAP256.04 becoming sensitive to CAP256.04 R100rA (Fig 2B). Interestingly, this single mutation recapitulated the breadth introduced into CAP256.04 by the entire CAP256.25 CDHR3. The reverse mutant, CAP256.25 A100rR similarly resulted in a

A

Antibody		CDRH1 (26)	CDRH2 (51)	CDRH3 (95 100d 100m 100r 100w)	Length	Charge
bNAb	CAP256.25	QFRFDGYG	ISHDGIKK	DLREDECEEWWSDYYDFGKQLPCAKSRGGLVGIADN	36	-5
off-track	CAP256.04	..S.NR..	..Y..TD.	.....R....-VA..F.K	35	-3

B

Pseudovirus	256.25	256.04^{25H123}	256.04 R100rA	256.04^{25H1} R100rA	256.04^{25H12} R100rA	256.04^{25H2} R100rA	256.04^{25H3}	256.04^{25H1}	256.04^{25H2}	256.25^{04H3}	256.04^{25FR123}	256.04
CAP256.15-wk.SU	0.00001	0.0001	0.001	0.002	0.0002	0.001	0.003	0.001	0.0001	0.001	0.003	0.002
CAP256.6-wk.PI	0.09	1.62	>100	>100	>100	>100	>100	>100	>100	>100	>100	>100
CAP210.E8	0.00001	0.00003	0.01	0.005	0.003	0.004	0.01	0.01	0.004	0.005	0.005	0.01
ZM53 M.PB12.2	0.0001	0.0003	0.004	0.004	0.001	0.002	0.01	0.001	0.001	0.004	0.01	0.004
ZM197.7	0.002	0.002	0.04	0.04	0.04	0.08	0.07	0.19	0.39	8.17	3.80	0.44
Du156.12	0.001	0.002	0.78	0.28	1.74	9.46	1.88	0.77	24.79	50.97	6.38	4.92
Q259.d2.17	0.002	0.005	0.03	0.01	0.04	0.38	0.04	0.04	5.66	14.95	1.13	0.70
CAP45.G3	0.00002	0.0003	0.004	0.002	0.01	0.04	0.002	0.003	>100	>100	0.86	0.77
Du422.01	0.0007	0.03	2.32	0.14	0.38	15.33	5.28	0.52	9.72	8.02	5.40	8.50
ZM109.4	0.003	0.01	16.66	2.04	31.34	>100	29.45	>100	>100	>100	>100	>100
PVO.04	0.08	0.30	35.35	15.48	37.88	50.12	46.51	>100	50.16	>100	>100	>100
ZM214.15	0.003	0.002	3.95	0.31	0.41	4.51	1.88	45.65	>100	>100	>100	>100
ZM249.1	0.01	0.004	0.52	0.10	0.01	0.10	0.24	13.73	>100	>100	>100	>100
AC10.29	0.25	11.47	84.63	38.21	>100	>100	>100	>100	>100	>100	>100	>100
Q461.e2	0.01	0.02	35.28	18.94	>100	>100	94.64	>100	>100	>100	>100	>100
Q842.d12	0.01	0.50	13.09	6.65	1.31	2.34	20.93	>100	>100	>100	>100	>100
MLV	>100	>100	>100	>100	>100	>100	>100	>100	>100	>100	>100	>100
Geo mean IC_{50}	0.002	0.008	0.46	0.18	0.09	0.25	0.44	0.09	0.23	0.37	0.25	0.17
% neutralization	100	100	94	94	81	75	88	63	50	44	50	50

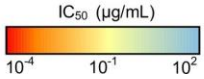

Fig 2. One mutation is required to introduce breadth into CAP256.04 while mutations in CDRH1, CDRH2 and CDRH3 are required for potency. (A) Comparison of the CDR sequences, including the length and charge of the CDRH3 of CAP256.04 (orange) and CAP256.25 (brown). The blue boxes highlights key off-track mutations. (B) Neutralization data using mutants and chimeras (indicated schematically above the table) between CAP256.25 and CAP256.04, with neutralization potency shown by color, as indicated in the key. Neutralization data represents the arithmetic mean titers (IC_{50}, μg/mL) from at least two experiments.

https://doi.org/10.1371/journal.ppat.1008005.g002

substantial loss of breadth (S1 Fig). The combination of R100rA with the CAP256.25 CDRH1 did not confer additional breadth beyond that introduced by R100rA (Fig 2B) and, surprisingly, the addition of the CDRH2 to either CAP256.04 R100rA or CAP256.04^{25H1} R100rA reduced the breadth of these antibodies (Fig 2B).

To model the interactions between V1V2 and CAP256.04 or CAP256.25, we fitted the sequence of CAP256.04 to the crystal structure of CAP256.25 in complex with the CAP256-34 week trimer which shares key contact residues for the CAP256-VRC26 lineage, including N160, R166, D167, K168 and K169 with CAP256.15-wk SU (Fig 3A), and which likely triggered the lineage [22]. The model showed that the N130 glycan projects from the trimer and is

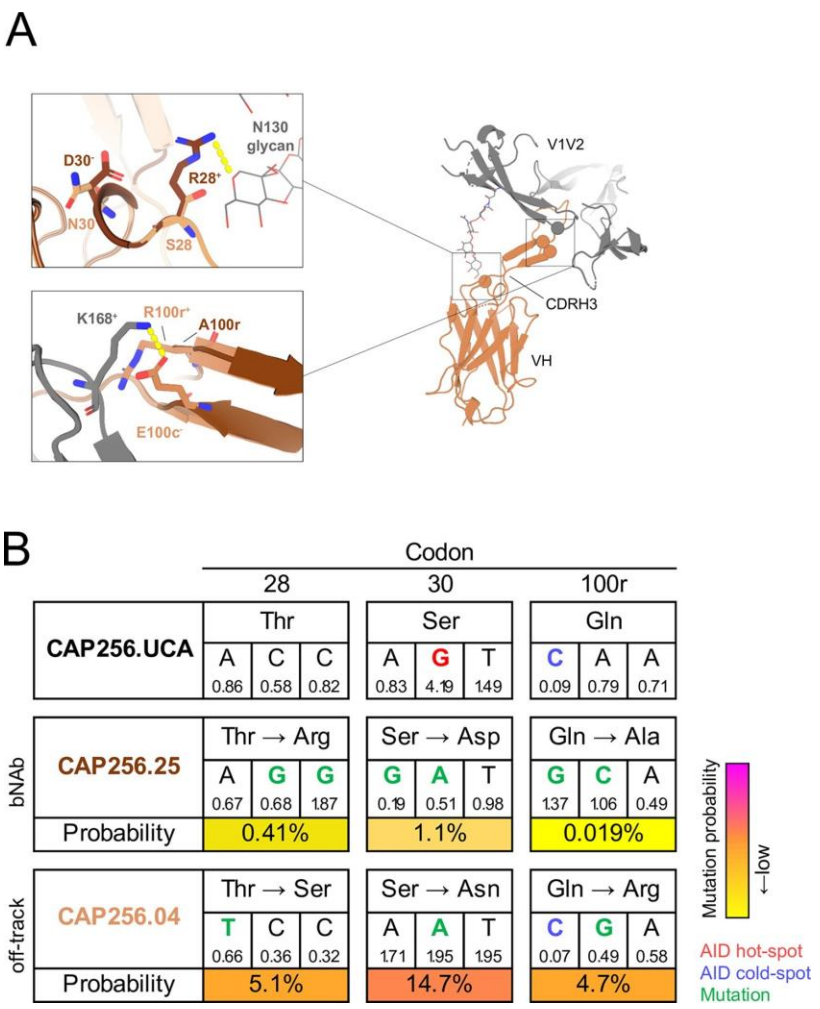

Fig 3. The structural effect and probabilities of the CAP256.04 off-track mutations S28, N30 and R100r. (A) The amino acid sequence of CAP256.04 (orange) was fitted to a model of CAP256.25 (brown) and the V1V2 of trimeric CAP256 34-week Env (grey, [26]) in Swiss-PdbViewer (v4.1.0) and visualized in PyMOL (v2.0.2). The top inset shows the CAP256.25 CDRH1 D30 (brown) residue and a hydrogen bond between CAP256.25 CDRH1 residue R28 (brown), and the glycan at N130. The bottom inset displays CAP256.04 R100r (orange) in proximity to V2 K168. Symbols $^{+}$ and $^{-}$ denote positive and negative charge, respectively. (B) The germline (T28, S30 and Q100r) and mature amino acid sequences (CAP256.25 T28R, S30D and Q100rA, and CAP256.04 T28S, S30N and Q100rR) at codons 28, 30 and 100r are displayed with the nucleotide sequence of each codon. Blue and red text indicates AID cold-and hotspots, respectively. Green text refers to mutations and yellow to pink shading indicates low and high probability mutations, respectively. The mutability scores are shown below each nucleotide.

https://doi.org/10.1371/journal.ppat.1008005.g003

situated proximal to the CDRH1. The CAP256.25 R28 residue was predicted to hydrogen bond with the N130 glycan while CAP256.04 S28 was not predicted to interact with this glycan. Surprisingly, the introduction of S28R to CAP256.04 R100rA and CAP256.04^{25H3} (S1 Fig) decreased the breadth of these antibodies by five and four viruses, respectively, although the

potency remained unchanged. Together with R100rA, the combination of S28R and N30D increased the breadth compared to S28R alone, but two viruses (PVO.04 and AC10.29) remained resistant to neutralization (S1 Fig). The conformation of the CDRH3 is partly supported by the intermolecular interactions between this loop and the CDRH1 and CDRH2 [25,26]. Consequently, the interaction between R28 and the CDRH3 may shift the CDRH1 toward the N130 glycan, which may be countered by the N30 residue (Fig 3A, top panel). Furthermore, the model showed that 100r was positioned in close proximity to the viral residue K168, and that K168 was hydrogen bonded to the CDRH3 residue E100c (Fig 3A, bottom panel). Therefore, due to electrostatic repulsion, R100r likely displaces K168, disrupting the interaction between K168 and E100c. In contrast, CAP256.25 has a small, uncharged Ala at position 100r which would not obstruct the adjacent bond. This suggests that an R100rA mutation may reduce electrostatic repulsion and therefore increase antigen affinity, providing a mechanism for the enhanced breadth associated with this mutation.

To estimate the probability of the occurrence of mutations prior to selection that are associated with the off-track phenotype, we utilized the ARMADiLLO software [34]. We first assessed the probability of the CDRH1 T28 residue (found in the CAP256.UCA) mutating to either 28R (as in CAP256.25) or 28S (in CAP256.04, Fig 2A). We found that the CAP256.25 T28R mutation was improbable (0.41%), requiring two base changes (ACC to AGG), whereas T28S (in CAP256.04) was ten times more probable (5.1%), requiring only one change (ACC to TCC, Fig 3B). Similarly, two base changes were necessary for the improbable (1.1%) mutation S30D (in CAP256.25), whereas S30N (in CAP256.04) was a probable (14.7%) event as it occurred in an AID hot-spot. The combination of T28R and S30D (in CAP256.25), which was necessary for neutralization when transplanted into CAP256.04, was a highly improbable event (0.004%, Fig 3B). Furthermore, the CDRH3 Q100rA mutation, that confers breadth to CAP256.25, was predicted to occur very rarely with a 0.019% probability, requiring two base changes (CAA to GCA), one of which was in an AID cold-spot (Fig 3B). In contrast, we found that Q100rR that results in the off-track phenotype was predicted to occur with a much higher probability of 4.7%, requiring only a single nucleotide change that was not located within an AID cold-spot (Fig 3B). Furthermore, the improbability of the evolution of T28R, N30D and Q100rA was reflected in next-generation sequences of the CAP256 lineage [22,43], where T28R, S30D and Q100rA together accounted for <2% of the sequences. Altogether, this suggests that a single relatively probable mutation in the CDRH3 primarily limits the neutralization breadth of CAP256.04.

The CDRH3 alone modulates neutralization breadth and potency of the off-track antibody CAP256.20

Next, we sought to determine which sites were responsible for the off-track phenotype of CAP256.20 compared to the related bNAb, CAP256.27 (Fig 4A). Of the 6 amino acids that distinguish these CDRH3s, several were charge changes, with an overall CDRH3 charge of -7 and -3 in CAP256.27 and CAP256.20, respectively. First, we transplanted the CDRH3 from CAP256.27 into CAP256.20 (CAP256.20^{27H3}) and tested this chimera for neutralization breadth. In contrast to the CAP256.04/.25 pair, transfer of only the CAP256.27 CDRH3 into CAP256.20 introduced both bNAb-like breadth and potency into the off-track antibody, increasing breadth from 1/16 to 14/16 viruses and potency from 2.92 to 0.05 μg/mL (Fig 4B). In the reverse experiment, replacing the CDRH3 of CAP256.27 with that of CAP256.20 (CAP256.27^{20H3}) almost completely abrogated neutralization (Fig 4B).

To determine which of the six residues within the CDRH3 of 256.20 limited breadth, we focused on three residues which altered the electronegativity of the loop, R100d, H100j and

A

Antibody		CDRH1 (26)	CDRH2 (51)	CDRH3 (95, 100d, 100j, 100n, 100w)	Length	Charge
bNAb	CAP256.27	QFPFSHYG	ITNDGTKK	DQREDECEEWWSDYYDFGKELPCRKFRGLGLAGIFDI	37	-7
off-track	CAP256.20	..A..N..	.....N..	.........R.....H..RV.....Y.......V...	37	-3

B

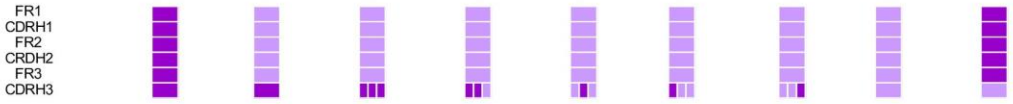

Pseudovirus	256.27	256.20^{27H3}	256.20 R100dW H100jD V100nE	256.20 R100dW H100jD	256.20 H100jD	256.20 R100dW	256.20 V100nE	256.20	256.27^{20H3}
CAP256.15-wk.SU	0.002	0.002	0.001	0.002	0.007	0.06	5.30	>100	>100
CAP256.6-wk.PI	>100	>100	>100	>100	>100	>100	>100	>100	>100
CAP210.E8	0.004	0.006	0.003	0.009	0.20	2.73	>100	>100	>100
CAP45.G3	0.004	0.004	0.006	4.31	>100	>100	>100	>100	>100
ZM53 M.PB12.2	0.001	0.002	0.001	0.001	0.004	0.01	1.01	2.92	2.27
ZM109.4	0.05	0.04	0.05	13.44	>100	>100	>100	>100	>100
ZM197.7	0.007	0.01	0.006	0.02	0.47	5.61	>100	>100	>100
ZM249.1	0.58	0.69	1.65	>100	>100	>100	>100	>100	>100
ZM214.15	0.39	3.07	0.46	3.91	>100	>100	>100	>100	>100
Du156.12	0.005	0.008	0.006	0.63	>100	>100	>100	>100	>100
Du422.01	0.07	0.03	0.05	2.61	>100	>100	>100	>100	>100
Q259.d2.17	0.02	0.05	0.05	4.20	>100	>100	>100	>100	>100
Q461.e2	0.03	0.04	0.004	0.23	>100	>100	>100	>100	>100
Q842.d12	6.60	39.72	10.57	>100	>100	>100	>100	>100	>100
PVO.04	0.54	0.66	0.56	0.89	>100	>100	>100	>100	>100
AC10.29	>100	>100	>100	>100	>100	>100	>100	>100	>100
MLV	>100	>100	>100	>100	>100	>100	>100	>100	>100
Geo mean IC_{50}	0.03	0.05	0.03	0.27	0.04	0.33	2.31	2.92	2.27
% neutralization	88	88	88	75	25	25	13	7	7
CDRH3 charge	-7	-7	-7	-6	-5	-4	-4	-3	-3

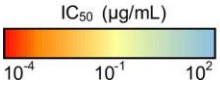

Fig 4. The CDRH3 alone restricts the neutralization breadth and potency of CAP256.20. (A) Comparison of the CDR sequences of CAP256.20 (light purple) and CAP256.27 (purple). The blue box highlights key off-track mutations. (B) Neutralization data using mutants and chimeras (indicated schematically above the table) between CAP256.27 and CAP256.20, with neutralization potency shown by color, as indicated in the key. Neutralization data represents the arithmetic mean titers (IC_{50}, µg/mL) from at least two experiments.

https://doi.org/10.1371/journal.ppat.1008005.g004

V100n (Fig 4A), and mutated these sites alone and in combination. The V100nE mutation, which slightly decreased the charge of the CDRH3 only marginally improved neutralization breadth by one additional virus (the autologous superinfecting virus, CAP256.15-wk SU) (Fig 4B). R100dW also decreased the charge and increased breadth by an additional three viruses (CAP256.15-wk SU, CAP210 and ZM197). Similarly, introduction of an H100jD mutation

conferred neutralization of the same three additional viruses but with greater potency than R100dW (geometric mean potency of 0.04 compared to 0.33 μg/mL, respectively). The combination of R100dW and H100jD increased potency and breadth to a total of 12/16 viruses, while V100nE, R100dW and H100jD together introduced the same bNAb-like broad neutralization and potency as the entire CDRH3 transplant (Fig 4B). In the reverse experiment, mutating positions 100d, 100j and 100n in the CDRH3 of CAP256.27 to match the sequence of CAP256.20 knocked out neutralization against previously sensitive viruses (S2 Fig). Therefore, of the 17 residues that differentiate the HC of CAP256.27 and CAP256.20 only three amino acids, all within the CDRH3, are responsible for limiting the breadth of CAP256.20.

Comparison of the probabilities of the breadth-conferring and restricting mutations between CAP256.27 and the CAP256.UCA showed that the G100nE bNAb mutation was improbable (0.89%), since two base changes were required (Fig 5A). In contrast, the W100dR, D100jH and G100nV mutations that took CAP256.20 off-track are highly probable (10%, 14% and 3%, respectively), as only single base changes were necessary, with the H100j mutation in an AID hot-spot (Fig 5A). The probability of retaining all three mutations that confer breadth (W100d, D100j and G100n) in the absence of selection is 0.33%. Overall, the relatively higher probability of these mutations which restrict breadth highlights the potential ease with which members of bNAb lineages may mature along undesirable pathways.

To explore the basis of these results, we fitted the amino acid sequences of CAP256.20 and CAP256.27 HCs to the crystal structure of CAP256.25 HC in Swiss-PdbViewer (v4.1.0), and then aligned this to a CAP256-34 week trimer structure (Fig 5B, [26]). The YYD motif of CAP256.27 was predicted to hydrogen bond with two K166 residues on two protomers and R166 and K169 on the remaining protomer (Fig 5B, top left). The mutations in CAP256.20 likely disrupt these interactions by placing a positive charge (H100j) proximal to K169 and possibly preventing sulfation of the preceding Tyr [44], which would knock out contacts with K166 (Fig 5B, top right).

Furthermore, the hydrogen bond between E100n, present in CAP256.27, and the N160 glycan was disrupted by the CAP256.20 V100n substitution (Fig 5B, bottom left). In addition, the CAP256.20 R100d mutation, places a positive charge next to K169 resulting in electrostatic repulsion (Fig 5B, bottom right) and possibly preventing the backbone interactions between these residues. Therefore, key interactions between the highly electronegative CDRH3 of CAP256.27 (-7) and the electropositive V2 epitope are abrogated by the more electropositive CDRH3 of CAP256.20 (-3), resulting in the off-track phenotype.

CAP256.20 was dependent on a globally rare Q169 immunotype

We were interested in determining which viral immunotypes (or epitope amino acid variants) drove CAP256.20 away from breadth. The K169 immunotype, which forms part of the CAP256 epitope, is fairly conserved within subtype C viruses (65.9%) (www.hiv.lanl.gov) (Fig 6A) [12]. In contrast, the 169Q immunotype is present in only 6.5% of subtype C viruses (Fig 6A) but dominated the viral population in donor CAP256 across 21 of 28 time points from six to 206 weeks post infection (Fig 6B and S3A Fig). We hypothesized that this globally rare immunotype, which predominated in CAP256, contributed to the evolution of CAP256.20. Introduction of 169Q mutations into eleven heterologous viruses slightly improved the neutralization of four viruses by CAP256.20 (S3B Fig), suggesting a preference of CAP256.20 for 169Q, though other viral determinants clearly contribute to neutralization sensitivity/resistance.

As autologous viruses, rather than heterologous viruses, select mutations during SHM, we determined the sensitivity of autologous viruses containing either a 169Q or 169K

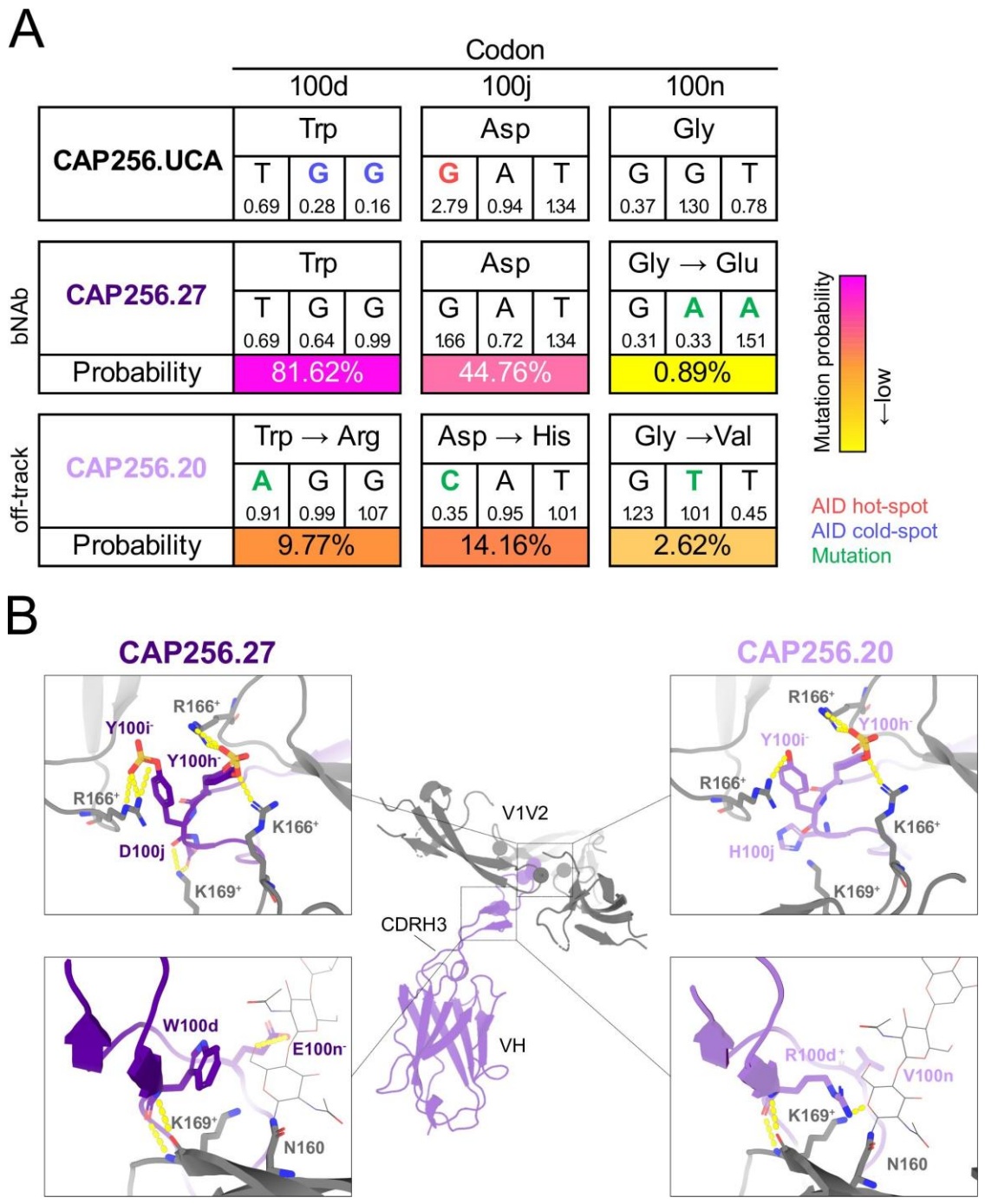
A
Codon
100d
100j
100n
CAP256.UCA
Trp
Asp
Gly
T 0.69
G 0.28
G 0.16
G 2.79
A 0.94
T 1.34
G 0.37
G 1.30
T 0.78
bNAb
CAP256.27
Trp
Asp
Gly → Glu
T 0.69
G 0.64
G 0.99
G 1.66
A 0.72
T 1.34
G 0.31
A 0.33
A 1.51
Probability
81.62%
44.76%
0.89%
off-track
CAP256.20
Trp → Arg
Asp → His
Gly →Val
A 0.91
G 0.99
G 1.07
C 0.35
A 0.95
T 1.01
G 1.23
T 1.01
T 0.45
Probability
9.77%
14.16%
2.62%
Mutation probability
low
AID hot-spot
AID cold-spot
Mutation
B
CAP256.27
CAP256.20
R166+
Y100i-
Y100h-
R166+
K166+
D100j
K169+
V1V2
CDRH3
VH
H100j
W100d
E100n-
K169+
N160
R100d+
V100n
K169+
N160

Fig 5. The probability and structural effect of the CAP256.20 off-track mutations W100dR, D100jH and G100nV. (A) The germline (W100d, D100j and G100n) and mature nucleotide and amino acid sequences (CAP256.27 W100d, D100j and G100nE and CAP256.20 W100dR, D100jH and G100nV) at codons 100d, 100j and 100n are displayed. Blue and red text indicate AID cold- and hot-spots, respectively. Green text refers to mutations, and yellow to pink shading indicates low and high probability mutations, respectively. The mutability scores are below each nucleotide. (B) The sequence of CAP256.20 (light purple) and CAP256.27 (purple) were fitted to a structure of CAP256.25 and trimeric CAP256 34-week Env [26] in Swiss-PdbViewer (v4.1.0) and aligned and visualized in PyMOL (v2.0.2). The top panels shows the interaction between the CDRH3 YYD motif (purple/light purple) and the V2 epitope (grey). The bottom panel displays the CAP256.27 residues W100d and E100n (purple) and CAP256.20 R100d and V100n (light purple) in proximity to K169, $^{+}$ and—denotes positive and negative charge, respectively.

https://doi.org/10.1371/journal.ppat.1008005.g005

immunotype to neutralization by CAP256.20 and CAP256.27. We identified two viruses that naturally contained a 169Q (CAP256.42-wk 5 and CAP256.48-wk 10), and were sensitive to CAP256.20 and CAP256.27^{20H3}. Introduction of Q169K mutations into these viruses knocked out neutralization by these antibodies, and their matched CDRH3 chimeras (Fig 6C). In the reverse experiment, introduction of a 169Q into three autologous viruses (CAP256.34-wk 80, CAP256.59-wk 10b and CAP256.15-wk SU, containing 169K/I and resistant to CAP256.20 and CAP256.27^{20H3}) resulted in increased sensitivity to these antibodies (Fig 6C). In all five

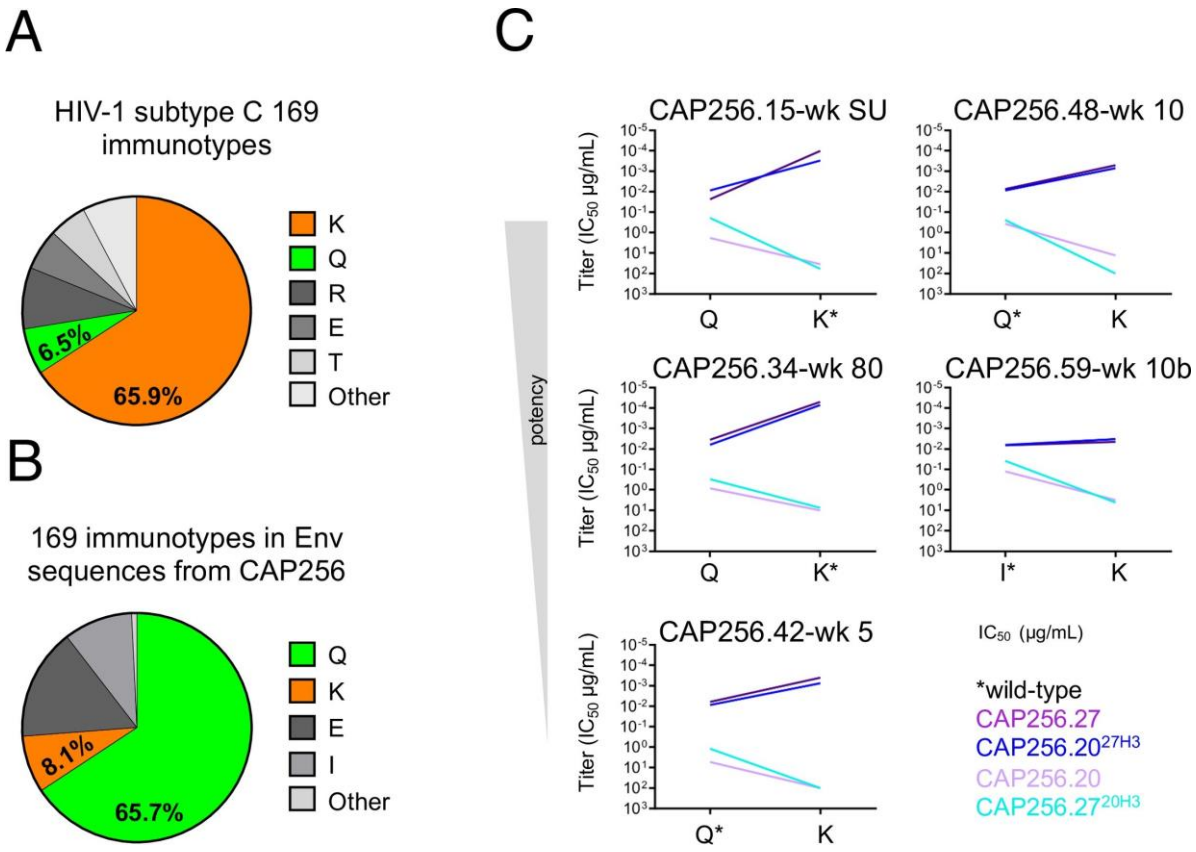

Fig 6. The off-track antibody CAP256.20 neutralizes a globally rare 169Q immunotype that was common in donor CAP256. (A) The K169 (orange) immunotype is common in globally circulating viruses, (B) while 169Q (green) predominates in CAP256 across most time points. (C) Slope graphs displaying the change in neutralization titer (IC_{50}) of CAP256.20 (light purple), CAP256.27 (purple), CAP256.20^{27H3} (blue) and CAP256.27^{20H3} (cyan) against K169 and 169Q autologous viruses.

https://doi.org/10.1371/journal.ppat.1008005.g006

viruses, the 169K immunotype was associated with increased neutralization potency by CAP256.27, CAP256.20^{27H3} and the additional broad CAP256.20 mutants and chimeras (S3C Fig), consistent with previous studies [11,12]. These data indicate a CDRH3-mediated preference of CAP256.20 for the 169Q immunotype, which limited the evolution of breadth in this antibody.

Discussion

A major focus of HIV vaccine design is based on a deep understanding of the development of bNAbs during HIV infection. Studies of HIV/antibody co-evolution have provided a template for the maturation of breadth that is now the basis of B-cell lineage vaccine strategies [12,17–23]. However, much less is known about the maturation of antibodies within bNAb-containing lineages that fail to acquire breadth. We have previously shown that these include both "dead-end" antibodies (that fail to acquire breadth and exhibit low SHM), and "off-track" antibodies that acquire substantial SHM, but little breadth, and are the focus of this study. Here we used previously identified strain-specific "off-track" antibodies that are closely related to broad members of the CAP256-VRC26 bNAb lineage to probe the genetic and viral contributors to their maturation [22]. In two pairs, we identified key breadth-restricting mutations, and defined the probabilities of their occurrence. Furthermore, we show the preferential neutralization of a globally rare immunotype by CAP256.20 impeded the evolution of breadth, providing a mechanism for the development of off-track responses in infection. Together these data provide insights into the challenges associated with driving maturation of antibodies towards breadth, a central question in HIV vaccine design.

Studies of bNAb lineages have highlighted the substantial plasticity in their maturation, enabling the development of breadth through multiple pathways [11,12,21,43]. This suggests that immunization strategies promoting high levels of SHM along diverse pathways may enhance bNAb development. Our data suggests that similarly, the development of off-track antibodies can occur by multiple pathways, and through the acquisition of very few mutations. Indeed, within the CAP256.20/27 pair, only three mutations were sufficient to divert CAP256.20 away from both breadth and potency. Furthermore, the enhanced breadth of CAP256.04 R100rA, which contains a single CDRH3 mutation, in contrast to the six mutations in CAP256.04^{25H3}, suggests substantial mutational "noise". Additionally, we found an increase in breadth when the CAP256.25 CDRH2 or single CDRH1 mutations were introduced into CAP256.04. These data confirm that extensive SHM does not necessarily result in breadth and suggests that many mutations do not impact or negatively affect breadth.

The maturation of bNAbs towards breadth includes a requirement for functionally relevant but improbable mutations [34]. Consistent with previous studies, we find that the key breadth-conferring mutations in the CAP256-VRC26 lineage, such as Q100rA and G100nE, are highly improbable [34] and that mutations that restricted breadth were in many cases relatively probable. Interestingly, the two pairs of CAP256 antibodies provide distinct examples of how the probability of mutations could shape on- versus off-track maturation. In CAP256.20/27, the potential for high probability breadth-limiting mutations (e.g. W100dR, D100jH and G100nV) is evident in pulling the B-cell off-track. In contrast, in the CAP256.04/25 pair, an important improbable mutation associated with breadth, Q100rA, represents a potential bottleneck that CAP256.25 has overcome to achieve breadth, but CAP256.04 has not. The more probable R100r mutation is also present in broader lineage members, suggesting compensatory mechanisms and that multiple pathways to breadth exist. Together these data indicate that, in some instances, the pathway to the off-track phenotype offers less "resistance"

compared to the requirement for highly improbable mutations associated with breadth, and will require careful selection of immunogens to avoid this phenotype [34].

Several studies, including our previous work in the CAP256-VRC26 lineage, have shown how exposure to diverse viral variants contributes to the development of breadth [11,12,22]. This study extends this work to define the mechanisms that select the off-track phenotype within a single lineage. The enrichment of the globally rare 169Q immunotype in CAP256 and the preferential neutralization of this immunotype by CAP256.20, implicates 169Q autologous viral variants in the evolution of this off-track antibody. Early CAP256-VRC26 lineage members (CAP256.01 and CAP256.24) and other off-track antibodies (CAP256.12 and CAP256.13) are unable to neutralize 169Q viruses. However, most lineage members, especially those with breadth, are able to neutralize this immunotype, though to a lesser extent than K169 viruses. This indicates that whereas most lineage members tolerate 169Q, CAP256.20 is uniquely reliant on the globally rare Q169 immunotype, explaining the strain-specificity of this antibody. Structurally, this may be a consequence of the reduced dependence of bNAbs on specific side chain residues within the epitope, compared to an increased dependence of off-track antibodies such as CAP256.20 on such side chains. These data highlight the fact that evolution towards breadth, a desirable outcome from a vaccinology perspective, is distinct from antibody maturation to counter circulating autologous viral variants.

This study provides evidence that affinity maturation to counter globally rare viral immunotypes can drive antibodies within a broad lineage away from breadth. As with the maturation of breadth, off-track antibodies can develop through multiple evolutionary pathways. Furthermore, limited breadth despite high levels of SHM can occur by the introduction of few, but relatively probable, mutations. The inherently stochastic nature of affinity maturation may make avoiding off-track antibodies challenging. Furthermore, additional research is needed to determine if the expansion of 'off-track' B-cell lineages prevents or limits the maturation of bNAbs. However, defining pathways towards and away from breadth will facilitate the selection of immunogens that elicit bNAbs and minimize off-track antibodies. Our data suggests that by selecting sequential immunogens that present globally conserved epitopes, the elicitation of off-track antibodies can be minimized. As immunization strategies improve to allow targeting of specific antibody residues, these data inform the design of immunogens to elicit V2-directed bNAbs.

Materials and methods

Ethics statement

CAP256 is a participant enrolled in the CAPRISA 002 Acute Infection study, established in 2004 in Kwa-Zulu Natal, South Africa. The CAPRISA 002 Acute Infection study was reviewed and approved by the research ethics committees of the University of KwaZulu-Natal (E013/04), the University of Cape Town (025/2004) and the University of the Witwatersrand (MM040202). CAP256, an adult, provided written informed consent. The specificity of her plasma has been described, monoclonal antibodies isolated and autologous Env evolution characterized [11,12,22,45,46].

Overlapping PCR and site-directed mutagenesis

Exchanging the CDRH3s between monoclonal antibodies was achieved with a two-step overlapping PCR. The CDRH3s were amplified with the AccuPrime Pfx DNA Polymerase and reaction mix (Thermo) with primers that were complementary to the recipient antibody. The product was gel extracted (1%, 1x TAE) and purified with the QIAquick Gel Extraction Kit (Qiagen) and used as the mutagenesis primer for the second PCR with the QuikChange

Lightning Multi Site-Directed Mutagenesis Kit (Stratagene). Genes with CDRH1, CDRH2 and CDRH3 exchanges were synthesized (GenScript) and excised with Age1 and Sal1 (Thermo) according to the manufacture's recommendation. Heavy chain fragments were separated in an agarose gel (1% 1x TAE) and ligated (Roche) into the CMVR expression vector as per the manufacturer's protocol. Mutations in both antibody and viral Env genes were introduced by site-directed mutagenesis with the QuikChange Lightening Multi Kit (Stratagene) per the manufacturer's instructions and plasmid sequences were confirmed by Sanger sequencing with the ABI PRISM Big Dye Terminator Cycle Sequencing Ready Reaction kit (Applied Biosystems, Foster City, CA) and resolved on the 3500 genetic analyzer.

Cell lines

The TZM-bl cell-line was obtained from the AIDS Research and Reference Reagent Program and the 293T cell-line was obtained from Dr. George Shaw (University of Pennsylvania, Philadelphia, PA). The cell-lines were cultured at 37˚C (5% CO_2) in Dulbecco's Modified Eagle Medium (DMEM) supplemented with 10% heat-inactivated foetal bovine serum (FBS), 50 μg/mL gentamicin (Sigma) and 25 mM HEPES, at confluency monolayers were disrupted with 0.25% trypsin and 1 mM EDTA (Sigma). The 293F cell-line (Life Technologies) was maintained in serum and antibiotic free FreeStyle 293 Expression media at 37˚C (10% CO_2) in an orbital shaker (130 rpm).

Pseudovirus production

Cloned Envs and pSG3ΔEnv backbone plasmids (NIH AIDS Research and Reference Reagent Program) were co-transfected into 293T cells with 1:3 PEI MAX transfection reagent (Polysciences). Following 48 hours, filtered pseudovirus supernatants were adjusted to 20% FBS and stored at -80˚C.

Antibody expression

Equal quantities of antibody heavy and light chain plasmids were co-transfected into 293F cells using PEI MAX. Monoclonal antibodies were purified from cell-free supernatants after six days using protein A affinity chromatography. Concentration and buffer exchange (1x PBS) was completed with Vivaspin concentrators (Sartorius).

Neutralization assays

Neutralization was measured as previously described by a reduction in luciferase gene expression after single-round infection of TZM-bl cells with Env-pseudotyped viruses [47,48]. Titers were calculated as the reciprocal antibody dilution (IC_{50}) causing 50% reduction of relative light units (RLU).

Models

The crystal structures of CAP256.04 (PDB: 4ORG) was aligned to the crystal structure of CAP256.25 and CAP256-34 week trimer in PyMOL 2.0.2. No structures were available for CAP256.20 and CAP256.27, therefore the amino acid sequences of these antibodies were fitted to the crystal structure of CAP256.25 in Swiss-PdbViewer 4.1.0 and aligned in PyMOL. Protein model representations were created with Swiss-PdbViewer v4.1.0 and PyMOL v2.0.2. Graphs were created in GraphPad Prism 6, sequence alignments were made in BioEdit v7.2.5 and phylogenetic trees were constructed in MEGA v6.06.

Probability of antibody mutations

The Antigen Receptor Mutation Analyzer for Detection of Low Likelihood Occurrences (ARMADiLLO) program estimates the probability of amino acid substitutions prior to antigenic selection [34]. Briefly, 10^4 simulated mature sequences per site of interest are generated with the S5F mutability and substitution models through comparison of the nucleotides sequences of the CAP256.UCA and a given mature lineage member [33]. The probability of particular amino acid substitutions is then estimated by the frequency of the observed site in the set of simulated sequences. Here, a mutation of <2% probability is classified as "improbable" as this reflects a frequency ≀ 2 B-cells per germinal centre harbouring that particular mutation [34]. Probabilities of combinations of mutations are derived from the products of individual probabilities.

Supporting information

S1 Fig. Neutral and deleterious mutations in the CAP256.25/04 pair. Neutralization data using mutants (indicated schematically above the table) between CAP256.25 and CAP256.04, potency indicated as per the key. Arithmetic mean titers (IC_{50}, μg/mL) from at least two experiments are reported.
(TIF)

S2 Fig. Off-track conferring mutations knock out CAP256.27 neutralization. Neutralization data using mutants (indicated schematically above the table) between CAP256.27 and CAP256.20, potency indicated as per the key. Arithmetic mean titers (IC_{50}, μg/mL) from at least two experiments are reported.
(TIF)

S3 Fig. 169Q immunotype predominates in CAP256 and CAP256.20 exhibits weak neutralization of heterologous 169Q viruses. (A) The frequency of the 169Q (green) and 169K (orange) Env immunotypes across 28 time points from six to 206 weeks post infection. # The viruses tested in Fig 3A were isolated at the indicated time points. (B) CAP256.20 neutralization curves of wild-type (orange, 169K/M as indicated,) and 169Q mutant (green) heterologous viruses. (C) An extension of Fig 6B, the neutralization titers of the CAP256.27/20 wild-type and chimeric antibodies (from Fig 4B) were tested against the CAP256.34-wk 80 virus.
(TIF)

Acknowledgments

We thank the clinical staff and participants in the CAPRISA 002 cohort for their commitment to attending the CAPRISA clinics in South Africa. We also thank Bridget Carragher and Clint Potter at the New York Structural Biology Center for assistance with structural determinations.

Author Contributions

Conceptualization: David Sacks, Jinal N. Bhiman, Lynn Morris, Penny L. Moore.

Formal analysis: David Sacks, Kevin Wiehe, Jason Gorman, Penny L. Moore.

Funding acquisition: Peter D. Kwong, Lynn Morris, Penny L. Moore.

Investigation: Jinal N. Bhiman, Kevin Wiehe, Jason Gorman.

Methodology: David Sacks.

Supervision: Lynn Morris, Penny L. Moore.

Visualization: David Sacks.

Writing – original draft: David Sacks, Penny L. Moore.

Writing – review & editing: David Sacks, Jinal N. Bhiman, Kevin Wiehe, Jason Gorman, Peter D. Kwong, Lynn Morris.

References

1. UNAIDS. Fact sheet—Latest statistics on the status of the AIDS epidemic | UNAIDS. 2017.
2. Rerks-Ngarm S, Pitisuttithum P, Nitayaphan S, Kaewkungwal J, Chiu J, Paris R, et al. Vaccination with ALVAC and AIDSVAX to Prevent HIV-1 Infection in Thailand. N Engl J Med. 2009; 361(23):2209–20. https://doi.org/10.1056/NEJMoa0908492 PMID: 19843557
3. Gray ES, Madiga MC, Hermanus T, Moore PL, Wibmer CK, Tumba NL, et al. The Neutralization Breadth of HIV-1 Develops Incrementally over Four Years and Is Associated with CD4+ T Cell Decline and High Viral Load during Acute Infection. J Virol. 2011; 85(10):4828–40. https://doi.org/10.1128/JVI. 00198-11 PMID: 21389135
4. Landais E, Huang X, Havenar-Daughton C, Murrell B, Price MA, Wickramasinghe L, et al. Broadly Neutralizing Antibody Responses in a Large Longitudinal Sub-Saharan HIV Primary Infection Cohort. Trkola A, editor. PLOS Pathog. 2016; 12(1):e1005369. https://doi.org/10.1371/journal.ppat.1005369 PMID: 26766578
5. Rusert P, Kouyos RD, Kadelka C, Ebner H, Schanz M, Huber M, et al. Determinants of HIV-1 broadly neutralizing antibody induction. Nat Med. 2016; 22(11):1260–7. https://doi.org/10.1038/nm.4187 PMID: 27668936
6. Hraber P, Seaman MS, Bailer RT, Mascola JR, Montefiori DC, Korber BT. Prevalence of Broadly Neutralizing Antibody Responses During Chronic HIV-1 Infection. AIDS. 2014; 14(28):163–9.
7. Shingai M, Donau OK, Plishka RJ, Buckler-White A, Mascola JR, Nabel GJ, et al. Passive transfer of modest titers of potent and broadly neutralizing anti-HIV monoclonal antibodies block SHIV infection in macaques. J Exp Med. 2014; 211(10):2061–74. https://doi.org/10.1084/jem.20132494 PMID: 25155019
8. Mascola JR, Stiegler G, VanCott TC, Katinger H, Carpenter CB, Hanson CE, et al. Protection of macaques against vaginal transmission of a pathogenic HIV- 1/SIV chimeric virus by passive infusion of neutralizing antibodies. Nat Med. 2000; 6(2):207–10. https://doi.org/10.1038/72318 PMID: 10655111
9. Wibmer CK, Moore PL, Morris L. HIV broadly neutralizing antibody targets. Curr Opin HIV AIDS. 2015; 10(3):135–43. https://doi.org/10.1097/COH.0000000000000153 PMID: 25760932
10. Pancera M, McLellan JS, Wu X, Zhu J, Changela A, Schmidt SD, et al. Crystal structure of PG16 and chimeric dissection with somatically related PG9: structure-function analysis of two quaternary-specific antibodies that effectively neutralize HIV-1. J Virol. 2010; 84(16):8098–110. https://doi.org/10.1128/JVI. 00966-10 PMID: 20538861
11. Doria-Rose NA, Bhiman JN, Roark RS, Schramm CA, Gorman J, Chuang G-Y, et al. New member of the V1V2-directed CAP256-VRC26 lineage that shows increased breadth and exceptional potency. Sil- vestri G, editor. J Virol. 2016; 90(1):76–91. https://doi.org/10.1128/JVI.01791-15 PMID: 26468542
12. Doria-Rose NA, Schramm CA, Gorman J, Moore PL, Bhiman JN, DeKosky BJ, et al. Developmental pathway for potent V1V2-directed HIV-neutralizing antibodies. Nature. 2014; 508(7498):55–62.
13. Walker LM, Huber M, Doores KJ, Falkowska E, Pejchal R, Julien J-PP, et al. Broad neutralization coverage of HIV by multiple highly potent antibodies. Nature. 2011; 477(7365):466–70. https://doi.org/10.1038/nature10373 PMID: 21849977
14. Huang J, Ofek G, Laub L, Louder MK, Doria-Rose NA, Longo NS, et al. Broad and potent neutralization of HIV-1 by a gp41-specific human antibody. Nature. 2012; 491(7424):406–12. https://doi.org/10.1038/ nature11544 PMID: 23151583
15. Victora GD, Nussenzweig MC. Germinal Centers. Annu Rev Immunol. 2012; 30(1):429–57.
16. Bonsignori M, Liao HX, Gao F, Williams WB, Alam SM, Montefiori DC, et al. Antibody-virus co-evolution in HIV infection: paths for HIV vaccine development. Immunol Rev. 2017; 275(1):145–60. https://doi.org/10.1111/imr.12509 PMID: 28133802
17. Gao F, Bonsignori M, Liao HX, Kumar A, Xia SM, Lu X, et al. Cooperation of B cell lineages in induction of HIV-1-broadly neutralizing antibodies. Cell. 2014; 158(3):481–91. https://doi.org/10.1016/j.cell.2014. 06.022 PMID: 25065977

18. Liao HX, Lynch R, Zhou T, Gao F, Munir Alam S, Boyd SD, et al. Co-evolution of a broadly neutralizing HIV-1 antibody and founder virus. Nature. 2013; 496(7446):469–76. https://doi.org/10.1038/nature12053 PMID: 23552890
19. Bonsignori M, Kreider EF, Fera D, Meyerhoff RR, Bradley T, Wiehe K, et al. Staged induction of HIV-1 glycan-dependent broadly neutralizing antibodies. Sci Transl Med. 2017; 9(381):eaai7514. https://doi. org/10.1126/scitranslmed.aai7514 PMID: 28298420
20. Bonsignori M, Zhou T, Sheng Z, Chen L, Gao F, Joyce MG, et al. Maturation pathway from germline to broad HIV-1 neutralizer of a CD4-mimic antibody. Cell. 2016; 165(2):449–63. https://doi.org/10.1016/j. cell.2016.02.022 PMID: 26949186
21. MacLeod DT, Choi NM, Briney B, Garces F, Ver LS, Landais E, et al. Early antibody lineage diversification and independent limb maturation lead to broad HIV-1 neutralization targeting the Env high-mannose patch. Immunity. 2016; 44(5):1215–26. https://doi.org/10.1016/j.immuni.2016.04.016 PMID: 27192579
22. Bhiman JN, Anthony C, Doria-Rose NA, Karimanzira O, Schramm CA, Khoza T, et al. Viral variants that initiate and drive maturation of V1V2-directed HIV-1 broadly neutralizing antibodies. Nat Med. 2015; 21 (11):1332–6. https://doi.org/10.1038/nm.3963 PMID: 26457756
23. Landais E, Murrell B, Briney B, Murrell S, Rantalainen K, Berndsen ZT, et al. HIV Envelope glycoform heterogeneity and localized diversity govern the initiation and maturation of a V2 apex broadly neutraliz- ing antibody lineage. Immunity. 2017; 47(5):990–1003.e9. https://doi.org/10.1016/j.immuni.2017.11. 002 PMID: 29166592
24. Gorman J, Soto C, Yang MM, Davenport TM, Guttman M, Bailer RT, et al. Structures of HIV-1 Env V1V2 with broadly neutralizing antibodies reveal commonalities that enable vaccine design. Nat Struct Mol Biol. 2016; 23(1):81–90. https://doi.org/10.1038/nsmb.3144 PMID: 26689967
25. Andrabi R, Su CY, Liang CH, Shivatare SS, Briney B, Voss JE, et al. Glycans Function as Anchors for Antibodies and Help Drive HIV Broadly Neutralizing Antibody Development. Immunity. 2017; 47 (3):524–37. https://doi.org/10.1016/j.immuni.2017.08.006 PMID: 28916265
26. Gorman J, Chuang G-Y, Lai Y-T, Shen C-H, Boyington JC, Druz A, et al. Structure of Antibody CAP256-VRC26.25 in Complex with HIV-1 Envelope Reveals a Combined Mode of Trimer-Apex Recognition. Cell Rep. 2019;http://dx.doi.org/10.2139/ssrn.3432644.
27. Scheid JF, Mouquet H, Ueberheide B, Diskin R, Klein F, Oliveira TYK, et al. Sequence and structural convergence. Science. 2011; 333(September):1633–7.
28. Mouquet H, Scharf L, Euler Z, Liu Y, Eden C, Scheid JF, et al. Complex-type N-glycan recognition by potent broadly neutralizing HIV antibodies. Proc Natl Acad Sci. 2012; 109(47):E3268–3277. https://doi. org/10.1073/pnas.1217207109 PMID: 23115339
29. McGuire AT, Glenn JA, Lippy A, Stamatatos L, Doms RW. Diverse recombinant HIV-1 Envs fail to activate B cells expressing the germline B cell receptors of the broadly neutralizing anti-HIV-1 antibodies PG9 and 447-52D. J Virol. 2014; 88(5):2645–57. https://doi.org/10.1128/JVI.03228-13 PMID: 24352455
30. McGuire AT, Hoot S, Dreyer AM, Lippy A, Stuart A, Cohen KW, et al. Engineering HIV envelope protein to activate germline B cell receptors of broadly neutralizing anti-CD4 binding site antibodies. J Exp Med. 2013; 210(4):655–63. https://doi.org/10.1084/jem.20122824 PMID: 23530120
31. Tokuriki N, Tawfik DS. Stability effects of mutations and protein evolvability. Curr Opin Struct Biol. 2009; 19(5):596–604. https://doi.org/10.1016/j.sbi.2009.08.003 PMID: 19765975
32. England P, Nageotte R, Renard M, Page AL, Bedouelle H. Functional characterization of the somatic hypermutation process leading to antibody D1.3, a high affinity antibody directed against lysozyme. J Immunol. 1999; 162(4):2129–36. PMID: 9973487
33. Yaari G, Vander Heiden JA, Uduman M, Gadala-Maria D, Gupta N, Stern JNH, et al. Models of somatic hypermutation targeting and substitution based on synonymous mutations from high-throughput immu- noglobulin sequencing data. Front Immunol. 2013; 4(358).
34. Wiehe K, Bradley T, Meyerhoff RR, Hart C, Williams WB, Easterhoff D, et al. Functional relevance of improbable antibody mutations for HIV broadly neutralizing antibody development. Cell Host Microbe. 2018; 23(6):759–765.e6. https://doi.org/10.1016/j.chom.2018.04.018 PMID: 29861171
35. Sok D, van Gils MJ, Pauthner M, Julien J-P, Saye-Francisco KL, Hsueh J, et al. Recombinant HIV envelope trimer selects for quaternary-dependent antibodies targeting the trimer apex. Proc Natl Acad Sci U S A. 2014; 111(49):17624–9. https://doi.org/10.1073/pnas.1415789111 PMID: 25422458
36. Sok D, Laserson U, Laserson J, Liu Y, Vigneault F, Julien J-P, et al. The effects of somatic hypermutation on neutralization and binding in the PGT121 family of broadly neutralizing HIV antibodies. Trkola A, editor. PLoS Pathog. 2013; 9(11):e1003754. https://doi.org/10.1371/journal.ppat.1003754 PMID: 24278016

37. Wu X, Zhou T, Zhu J, Zhang B, Georgiev I, Wang C, et al. Focused Evolution of HIV-1 Neutralizing Antibodies Revealed by Structures and Deep Sequencing. Science (80-). 2011; 333(6049):1593–602.
38. Tian M, Cheng C, Chen X, Duan H, Cheng HL, Dao M, et al. Induction of HIV neutralizing antibody line- ages in mice with diverse precursor repertoires. Cell. 2016; 166(6):1471–84. https://doi.org/10.1016/j. cell.2016.07.029 PMID: 27610571
39. Escolano A, Steichen JM, Dosenovic P, Kulp DW, Golijanin J, Sok D, et al. Sequential immunization elicits broadly neutralizing anti-HIV-1 antibodies in Ig knockin mice. Cell. 2016; 166(6):1445–1458.e12. https://doi.org/10.1016/j.cell.2016.07.030 PMID: 27610569
40. Bradley T, Fera D, Bhiman J, Eslamizar L, Lu X, Anasti K, et al. Structural constraints of vaccine-induced tier-2 autologous HIV neutralizing antibodies targeting the receptor-binding site. Cell Rep. 2016; 14(1):43–54. https://doi.org/10.1016/j.celrep.2015.12.017 PMID: 26725118
41. Crooks ET, Tong T, Chakrabarti B, Narayan K, Georgiev IS, Menis S, et al. Vaccine-elicited tier 2 HIV-1 neutralizing antibodies bind to quaternary epitopes involving glycan-deficient patches proximal to the CD4 binding site. PLoS Pathog. 2015; 11(5):e1004932. https://doi.org/10.1371/journal.ppat.1004932 PMID: 26023780
42. Steichen JM, Kulp DW, Tokatlian T, Escolano A, Dosenovic P, Stanfield RL, et al. HIV vaccine design to target germline precursors of glycan-dependent broadly neutralizing antibodies. Immunity. 2016; 45 (3):483–96. https://doi.org/10.1016/j.immuni.2016.08.016 PMID: 27617678
43. Johnson EL, Doria-Rose NA, Gorman J, Bhiman JN, Schramm CA, Vu AQ, et al. Sequencing HIV-neutralizing antibody exons and introns reveals detailed aspects of lineage maturation. Nat Commun. 2018; 9(1):4136. https://doi.org/10.1038/s41467-018-06424-6 PMID: 30297708
44. Bundgaard JR, Vuust J, Rehfeld JF. New consensus features for tyrosine O-sulfation determined by mutational analysis. J Biol Chem. 1997; 272(35):21700–05. https://doi.org/10.1074/jbc.272.35.21700 PMID: 9268297
45. Moore PL, Gray ES, Sheward D, Madiga M, Ranchobe N, Lai Z, et al. Potent and broad neutralization of HIV-1 subtype C by plasma antibodies targeting a quaternary epitope including residues in the V2 loop. J Virol. 2011; 85(7):3128–41. https://doi.org/10.1128/JVI.02658-10 PMID: 21270156
46. Moore PL, Sheward D, Nonyane M, Ranchobe N, Hermanus T, Gray ES, et al. Multiple pathways of escape from HIV broadly cross-neutralizing V2-dependent antibodies. J Virol. 2013; 87(9):4882–94. https://doi.org/10.1128/JVI.03424-12 PMID: 23408621
47. Wei X, Decker JM, Wang S, Hui H, Kappes JC, Wu X, et al. Antibody neutralization and escape by HIV-1. Nature. 2003; 422(6929):307–12. https://doi.org/10.1038/nature01470 PMID: 12646921
48. Montefiori DC. Evaluating Neutralizing Antibodies Against HIV, SIV, and SHIV in Luciferase Reporter Gene Assays. In: Current Protocols in Immunology. Hoboken, NJ, USA: John Wiley & Sons, Inc.; 2005. p. 12.11.1–12.11.17.

Supplemental figure 1

Pseudovirus	256.25	256.25 A100rR	256.04 R100rA	256.04^{25H1} R100rA	256.04 S28R N30D R100rA	256.04 S28R R100rA	256.04^{25H3} S28R	256.04	256.04 F100ddA	256.04 K102N	256.04 F100ddA K102N
CAP256.15-wk.SU	0.0001	0.0001	0.001	0.002	0.001	0.031	0.008	0.002	<0.02	<0.02	0.002
CAP256.6-wk.PI	4.120	>100	>100	>100	>100	>100	>100	>100	>100	>100	>100
CAP210.E8	0.0001	0.0001	0.01	0.005	0.006	0.143	0.088	0.009	<0.02	<0.02	0.006
ZM53 M.PB12.2	0.0001	0.0001	0.004	0.004	0.004	0.128	0.066	0.004	<0.02	<0.02	0.005
ZM197.7	0.002	0.006	0.04	0.04	0.14	2.36	1.32	0.44	1.73	3.06	1.77
DU156.12	0.001	0.02	0.78	0.28	0.41	0.08	0.06	4.92	7.08	10.68	6.91
Q259.d2.17	0.002	0.01	0.03	0.01	0.03	0.66	2.30	0.70	0.40	1.16	0.44
CAP45.G3	0.0002	0.0005	0.004	0.002	0.006	0.07	0.25	0.77	0.79	7.97	0.65
DU422.01	0.05	0.02	2.32	0.14	1.27	29.44	40.33	8.50	15.26	24.81	10.90
ZM109.4	0.003	>100	16.66	2.04	15.10	>100	>100	>100	>100	>100	>100
PVO.04	0.08	1.15	35.35	15.48	>100	>100	>100	>100	>100	>100	>100
ZM214.15	0.003	>100	3.95	0.31	1.01	2.126	5.762	>100	>100	>100	>100
ZM249.1	0.005	>100	0.52	0.10	0.30	0.821	2.622	>100	>100	>100	>100
AC10.29	0.25	>100	84.63	38.21	>100	>100	>100	>100	>100	>100	>100
Q461.e2	0.03	0.72	35.28	18.94	47.64	>100	>100	>100	>100	>100	>100
Q842.d12	0.010	2.86	13.09	6.65	47.57	>100	>100	>100	>100	>100	>100
MLV	>100	>100	>100	>100	>100	>100	>100	>100	>100	>100	>100

Mean IC_{50}	0.005	0.009	0.46	0.18	0.21	0.44	0.51	0.17	nd	nd	0.20
% breadth	100	69	94	94	81	63	63	50	50	50	50

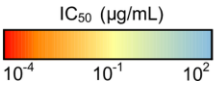

Supplemental figure 2

Pseudovirus	256.27	256.20	256.27 W100dR	256.27 D100jH	256.27 E100nV	256.27 W100dR D100jH E100nV
CAP256.15-wk.SU	0.002	>100	0.002	0.001	0.0002	>100
CAP256.6-wk.PI	>100	>100	>100	>100	>100	>100
CAP210.E8	0.004	>100	0.005	0.05	0.004	>100
CAP45.G3	0.004	>100	>100	>100	0.09	>100
ZM53 M.PB12.2	0.001	2.92	0.002	0.001	0.001	18.80
ZM109.4	0.05	>100	>100	>100	0.83	>100
ZM197.7	0.007	>100	0.08	0.67	0.02	>100
ZM249.1	0.58	>100	>100	>100	0.25	>100
ZM214.15	0.39	>100	>100	>100	23.26	>100
Du156.12	0.005	>100	>100	>100	0.003	>100
Du422.01	0.07	>100	>100	>100	0.50	>100
Q259.d2.17	0.02	>100	>100	>100	0.45	>100
Q461.e2	0.03	>100	>100	>100	0.06	>100
Q842.d12	6.60	>100	>100	>100	15.68	>100
PVO.04	0.54	>100	63.83	94.54	0.70	>100
AC10.29	>100	>100	>100	>100	>100	>100
MLV	>100	>100	>100	>100	>100	>100
Mean IC_{50}	0.03	2.92	0.04	0.08	0.09	18.80
% neutralization	88	7	31	31	88	7
CDRH3 charge	-7	-3	-6	-5	-6	-3

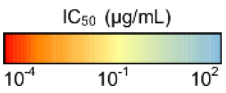

Supplemental figure 3

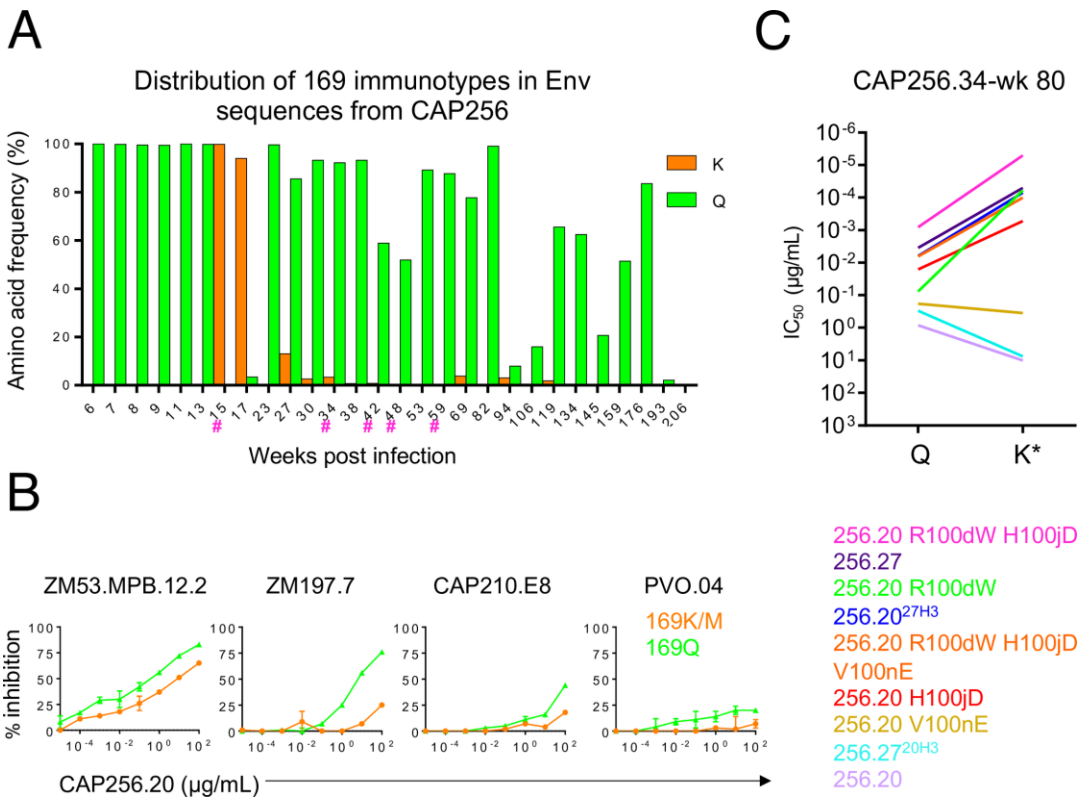

7.6 Appendix F: Publication support letter

NATIONAL INSTITUTE FOR COMMUNICABLE DISEASES
Division of the National Health Laboratory Service

Centre for HIV and Sexually Transmitted Infections
1 Modderfontein Road, Sandringham, 2031
Email: davids@nicd.ac.za
Tel: 011 386 6362

To whom it may concern

Student's contribution to published article

I, David Sacks, declare that I contributed adequately towards the research findings published in the article stated below, which is included in my thesis:

Sacks D, Bhiman JN, Wiehe K, Gorman J, Kwong PD, Morris L, Moore PL. Somatic hypermutation to counter a globally rare viral immunotype drove off-track antibodies in the CAP256-VRC26 HIV-1 V2-directed bNAb lineage. PLoS Pathog. 2019;15(9):e1008005.

All co-authors have agreed to this paper being included as part of this PhD thesis.

Name of candidate: David Sacks
Telephone: 072 389 8551 Email: davids@nicd.ac.za

Signature: _____ Date: 26 February 2020

Name of Supervisor 1: Prof Penny L Moore
Telephone: 011 386 6331 Email: pennym@nicd.ac.za

Signature: _____ Date: 26 February 2020

Name of Supervisor 2: Prof Lynn Morris
Telephone: 011 386 6362 Email: lynnm@nicd.ac.za

Signature: _____ Date: 26 February 2020

7.7 Appendix G: Supervisors letter

NATIONAL INSTITUTE FOR COMMUNICABLE DISEASES
Division of the National Health Laboratory Service

Centre for HIV and Sexually Transmitted Infections
1 Modderfontein Road, Sandringham, 2031
Email: pennym@nicd.ac.za
Tel: 011 386 6331

26 February 2020

To whom it may concern

Letter of Support: David Sacks - PhD thesis

I am writing to confirm that the thesis submitted by David Sacks satisfies the requirements for a PhD. David is the first author of a paper published in PLOS Pathogens (1) and a second manuscript is in preparation for the Journal of Virology, where David will again be first author (2). All co-authors have agreed to these papers/manuscripts being included as part of David's PhD thesis.

(1) Sacks D, Bhiman JN, Wiehe K, Gorman J, Kwong PD, Morris L, Moore PL. Somatic hypermutation to counter a globally rare viral immunotype drove off-track antibodies in the CAP256-VRC26 HIV-1 V2-directed bNAb lineage. PLOS Pathog. 2019;15(9):e1008005.
(2) Sacks D, Wiehe K, Morris L, Moore PL. Complementary roles of heavy and light chain somatic hypermutation in conferring breadth and potency to the CAP256-VRC26 bNAb lineage. J Virol. *Manuscript in preparation*.

Yours Sincerely,

Prof. Penny Moore (Supervisor)
Reader: University of the Witwatersrand
DST/NRF South African Research Chair of Virus-Host Dynamics
Acting Head: HIV Virology Section, Centre for HIV and STIs, National Institute for Communicable Diseases, Division of the NHLS
Honorary Senior Scientist: Centre for the AIDS Programme of Research in South Africa (CAPRISA), University of KwaZulu-Natal
Adjunct Member: Institute of Infectious Disease and Molecular Medicine, University of Cape Town

7.8 Appendix H: Turn-it-in report

Turnitin Originality Report

Processed on: 20-Feb-2020 10:44 AM SAST
ID: 1260737332
Word Count: 35614
Submitted: 1

0502955k:for_turnitin.pdf By David Sacks

Similarity Index	Similarity by Source	
13%	Internet Sources:	9%
	Publications:	8%
	Student Papers:	8%

1 1% match ()
https://www.ncbi.nlm.nih.gov/pubmed/31479499

2 1% match (publications)
David Sacks, Jinal N. Bhiman, Kevin Wiehe, Jason Gorman, Peter D. Kwong, Lynn Morris, Penny L. Moore. "Somatic hypermutation to counter a globally rare viral immunotype drove off-track antibodies in the CAP256-VRC26 HIV-1 V2-directed bNAb lineage", PLOS Pathogens, 2019

3 < 1% match (student papers from 11-Apr-2016)
Submitted to University of Witwatersrand

4 < 1% match ()
http://hdl.handle.net

5 < 1% match (Internet from 23-Jun-2018)
https://d-nb.info/1059237768/34

6 < 1% match (publications)
Simone I. Richardson, Carol Crowther, Nonhlanhla N. Mkhize, Lynn Morris. "Measuring the ability of HIV-specific antibodies to mediate trogocytosis", Journal of Immunological Methods, 2018

7 < 1% match (Internet from 11-Mar-2019)
http://www.ici2013.org

8 < 1% match (student papers from 12-Nov-2013)
Submitted to University of Birmingham

9 < 1% match (Internet from 21-Apr-2015)
http://edoc.rki.de

10 < 1% match (Internet from 02-Sep-2019)
https://journals.plos.org/plospathogens/article?id=10.1371%2Fjournal.ppat.1006987

All remaining sources are <1% similar

David Sacks

Prof Penny L. Moore

26 February 2020

Date

26 February 2020

Date

7.9 Appendix I: PCR primers

Appendix table 1. Sanger sequencing primer sequences.

Vector	Primer	Sequence
CMVR	1012F	GCTGACAGACTAACAGACTG
	1012R	GCAAACAACAGATGGCTGGC
	CMVR F	CTAGTTAACGGTGGAGGGCAGTGT
	CMVR R	CACCCCCCAGAATAGAATGACACC
pcDNA 3.1	A589R	CAGAGTGGGGTTAACTTTACAC
	EnvB	AGAAAGAGCAGAAGACAGTGGCAATGA
	E175	TTTAGCATGTGATGCACAAAATAG
	EnvAdir	CACCGGCTTAGGCATCTCCTATAGCAGGAAGAA

Appendix table 2. Primer sequences for off-track antibody restriction-free cloning and site-directed mutagenesis.

Assay	Primer	Sequence
Restriction-free cloning	256.27^{20H3} F	CTGCGAGCTGAGGACACGGCACTATATTTCTGT
	256.27^{20H3} R	GAGACGATGACCATTGTCCCGTGGCCCCA
	256.20^{27H3} F	CTGCGAGTTGAGGACACGGCGCGATATTTCTGT
	256.20^{27H3} R	GAAGAGACGATGACCATTGTTCCGTGGCCCCA
	256.04^{25H3} F	CTGCGAGCTGAGGACACGGCTCTGTATTACTGT
	256.04^{25H3} R	TGAAGAGACGATGACCATTGTCCCTTGGCCCCA
	256.25^{04H3} F	TGCGACCTGAGGACACGGCTCTCTACTACTGT
	256.25^{04H3} R	AAGAGACGGTGACCATTGTCCCTTGGCCCCA
Site-directed mutagenesis	256.04^{25H1} S28R F	GTGCAGCCTCTCAATTCAGGTTTAATAGATATGGCATGCAC
	256.04^{25H1} S28R N30D F	GCAGCCTCTCAATTCAGGTTTGATAGATATGGCATGCACTGGGTC
	256.04^{25H1} S28R N30D R31G F	GCCTCTCAATTCAGGTTTGATGGATATGGCATGCACTGGGTCCG
	256.04^{25H2} T157C F	TGGAGTGGGTGGCAGCTATATCACATGATGGAACTGATAAATACCAC
	256.04^{25H2} T157C C167T F	GGGTGGCAGCTATATCACATGATGGAATTGATAAATACCACGCTGATAAAGTGT
	256.04^{25H2} T157C C167T G169A F	TGGCAGCTATATCACATGATGGAATTAATAAATACCACGCTGATAAAGTGTGGGG
	256.04^{25H2} T157C C167T G169A T171A F	TGGCAGCTATATCACATGATGGAATTAAAAAATACCACGCTGATAAAGTGTGGGG
	256.04 R100rA F	GGAAACAACTCCCTTGCGCAAAGTCACGGGGCG
	256.04 F100ddA F	GGGCGTGGCTGGAATTGCTGATAAGTGGGGCC
	256.04 K102N F	CGTGGCTGGAATTTTTGATAACTGGGGCCAAGGGACAATGG
	256.04 F100ddA K102N F	GGCTGGAATTGCTGATAACTGGGGCCAAGGGACAATGG
	256.25 A100rR F	GAAACAACTCCCTTGCCGAAAGTCACGCGGCGG
	256.20 R100dW F	GACGAATGTGAAGAGTGGTGGTCAGATTATTATCATTTTGGGAGAG
	256.20 H100jD F	GAAGAGAGGTGGTCAGATTATTATGATTTTGGGAGAGTTCTCCCTTG
	256.20 V100nE F	GATTATTATCATTTTGGGAGAGAACTCCCTTGCCGAAAGTACCG
	256.20 R100dW H100jD F	GAAGAGTGGTGGTCAGATTATTATGATTTTGGGAGAGTTCTCCCTTG
	256.20 R100dW H100jD V100nE F	GATTATTATGATTTTGGGAGAGAACTCCCTTGCCGAAAGTACCG
	256.27 W100dR F	CAGCGAGAAGACGAATGTGAAGAGAGGTGGTCGGATTATTATGATTTTG
	256.27 D100jH F	GGTGGTCGGATTATTATCATTTTGGGAAAGAACTCCCTTGCCG
	256.27 E100nV F	CGGATTATTATGATTTTGGGAAAGTTCTCCCTTGCCGAAAATTCCGGG
	256.27 D100jH E100nV F	CGGATTATTATCATTTTGGGAAAGTTCTCCCTTGCCGAAAATTCCGGG

Appendix table 3. Primer sequences for *env* site-directed mutagenesis.

Site-directed mutagenesis	DU422 K169Q F	CAATACAACCACAGAATTAAGAGATAAGCAACAGAAAGTGTATGCACTTTTTTATAAACC
	ZM197 K169Q F	CAATATAACCACAGAAGTAAGAGATAGGCAGACAAAACAAAGGGCACTTTTTTATAAAC
	CAP210 K169Q F	CAATGCAACCACAGAACTAAGAGATAAGCAAAAGAAGGAGTATGCACTTTTTTATAG
	CAP45 K169Q F	CAATATAACCACAGAGCTAAGAGATAAGCAACAGAAAGCGTATGCACTTTTTTATAG
	DU156 K169Q F	CAATACAACCACAGAACTAAGAGATAAGCAACAGAAAGTGTATGCACTTTTTTATAG
	ZM109 K169Q F	CAATATAACCACAGATGTAAAAGATAGACAACAGAAGGTGAATGCAACTTTTTATG
	ZM233 K169Q F	CAATATGACCACAGAACTAAGAGATAAGCAACGGAAAGTGAATGTACTTTTTTATAAAC
	ZM249 K169Q F	CAATATAACTACAGAGCTAAGAGATAAGCAACAGAAAGTGTATGCACTTTTTTATAAAC
	Q259 K169Q F	CAATATAACCACAGAACTAAGGGATAAGCAACAGAAAGTACATTCACTTTTTTAC
	Q461 K169Q F	CAATATAACCACAGAACTAAGAGATAAGCAACAGAAAGTCTATTCACTGTTTTATAAAC
	Q842 R169Q F	CAATATGACCACAGAACTAAGGGATAAGCAACAGAAAGTATATTCACTTTTTTATAAAC
	ZM214 N169Q F	CAAGGTAAACTCAGAACTAAGAGATAAACAAAGGAGAGAACATGCATTGTTTTATAAAC
	PVO M169Q F	CAATGTCACCACAGACATAAGAGATAGACAGCAGAAAGTATATGCGCTTTTTTATAG
	ZM53 K169Q F	CAATGCAACCACAGAACTAAGAGATAAGCAAAAGCAAGTGTATGCACTTTTTTATAAAC
	59-wk 10b I169Q F	CAATGCGACCACAGAAGTAAGAGATAAGCAAAAGAAAGAATATGCACTCTTTTATAG
	256.3.14.10 Q169K F	CAATACAACCACAGAGGTAAGAGATAAGAAAAAGAAAGAATATGCACTCTTTTATAG
	34-wk 80 K169Q F	CAATGCGACCACAGAATTAAGAGATAAGCAAAGGAGAGAATATGCACTCTTTTATAG
	6-wk PI Q169K F	CAATACAATCACAGAGGTAAGAGATAAGAAAAAGAAAGAATATGCACTCTTTTATAG
	3.14.10 Q169K F	CAATACAACCACAGAGGTAAGAGATAAGAAAAAGAAAGAATATGCACTCTTTTATAG
	42-wk 5 Q169K F	CGACCACAGAATTAAGAGATAAGAAAAAGAAAGAATATGCACTCTTTTATAG
	15-wk SU K169Q F	CGACCACAGAATTAAGAGATAAGCAAAAGAAAGAATATGCACTCTTTTATAG

Appendix table 4. Primer sequences for the CAP256.UCA restriction-free cloning and site-directed mutagenesis.

Assay	Primer	Sequence
Site-directed mutagenesis	UCA G100qC F	CGATTGGTTACCCTTGCCAAGACCCACGGGGC
	UCA N100aC F	GATCTGGGAGAAAGCGAATGTGAAGAGTGGGCGACG
	256.UCA^{25L2} F	CAAACTCCTCATCTATGAAACTGACAAGCGACCCTCAGGGATTCC
	256.UCA^{25H2} F	CCAGGCAAGGGGCTGGAGTGGGTGGCAGTTATATCACATGATGGAATTAAAAAATACTATGC AGACTCCGTGAAGGGCCGATTCACC
	256.UCA^{25H2} R	GGTGAATCGGCCCTTCACGGAGTCTGCATAGTATTTTTTAATTCCATCATGTGATATAACTGC CACCCACTCCAGCCCCTTGCCTGG
Restriction-free cloning	256.25^{UCAH3} F	CTGAGGACACGGCTCTCTACTACTGTGCGAAAG
	256.25^{UCAH3} R	GAGACGGTGACCATTGTCCCTTGGCCCCAG
	256.UCA^{25H3} R	GAGACGGTGACCATTGTCCCTTGGCCCC
	256.UCA^{25H3} F	GAGGACACGGCTGTGTACTACTGTGCGAAAGA

Appendix table 5. Primer sequences for the IgG4 CMVR$_{HC}$ vector modification and cloning.

Assay	Primer	Sequence
Restriction-site PCR	5' AgeI VH 3	CTGCAACCGGTGTACATTCTGAGGTGCAGCTGGTGGAG
	3' SalI JH 3	TGCGAAGTCGACGCTGAAGAGACGGTGACCATTG
	5' AgeI VL 1	CTGCTACCGGTTCCTGGGCCCAGTCTGTGCTGACKCAG
	3' XhoI CL	CTCCTCACTCGAGGGYGGGAACAGAGTG
IgG4 CMVR$_{HC}$ Site-directed mutagenesis	IgG remove Age F	CTTCCCCGAACCCGTGACGGTGTCGTGG
	G4aI SalI GTCG	GTCATCGTCTCAGCGTCGACCAAGGGCCCATC
	G4aI SalI CG	GGTCATCGTCTCAGCTACGACCAAGGGCCCATCG

8. References

1. Centers for Disease Control. Kaposi's sarcoma and Pneumocystis pneumonia among homosexual men-New York City and California. MMWR Morb Mortal Wkly Rep. 1981;30(25):305–8.
2. Rozenbaum W, Coulaud JP, Saimot AG, Klatzmann D, Mayaud C, Carette MF. Multiple opportunistic infection in a male homosexual in France. Lancet. 1982;1(8271):572–3.
3. Vilaseca J, Arnau JM, Bacardi R, Mieras C, Serrano A, Navarro C. Kaposi's sarcoma and toxoplasma gondii brain abscess in a Spanish homosexual. Lancet. 1982;1(8271):572.
4. Masur H, Michelis MA, Greene JB, Onorato I, Vande Stouwe RA, Holzman RS, et al. An Outbreak of Community-Acquired Pneumocystis carinii Pneumonia: Initial Manifestation of Cellular Immune Dysfunction. N Engl J Med. 1981;305(24):1431–8.
5. Gallo RC, Salahuddin SZ, Popovic M, Shearer GM, Kaplan M, Haynes BF, et al. Frequent detection and isolation of cytopathic retroviruses (HTLV-III) from patients with AIDS and at risk for AIDS. Science. 1984;224(4648):500–3.
6. Barré-Sinoussi F, Chermann JC, Rey F, Nugeyre MT, Chamaret S, Gruest J, et al. Isolation of a T-lymphotropic retrovirus from a patient at risk for acquired immune deficiency syndrome (AIDS). Science. 1983;220(4599):868–71.
7. Curran JW, Jaffe HW, Hardy AM, Morgan WM, Selik RM, Dondero TJ. Epidemiology of HIV infection and AIDS in the United States. Science. 1988;239(4840):610–6.
8. UNAIDS. Fact sheet - Latest global and regional statistics on the status of the AIDS epidemic. UNAIDS Fact Sheet 2017. 2017.
9. Samji H, Cescon A, Hogg RS, Modur SP, Althoff KN, Buchacz K, et al. Closing the Gap: Increases in Life Expectancy among Treated HIV-Positive Individuals in the United States and Canada. Okulicz JF, editor. PLoS One. 2013;8(12):e81355.
10. Hammer SM, Squires KE, Hughes MD, Grimes JM, Demeter LM, Currier JS, et al. A controlled trial of two nucleoside analogues plus indinavir in persons with human immunodeficiency virus infection and CD4 cell counts of 200 per cubic millimeter or less. N Engl J Med. 1997;337(11):725–33.
11. Mitsuya H, Weinhold KJ, Furman PA, St Clair MH, Lehrman SN, Gallo RC, et al. 3'-Azido-3'-deoxythymidine (BW A509U): An antiviral agent that inhibits the infectivity and cytopathic effect of human T-lymphotropic virus type III/lymphadenopathy-associated virus in vitro. Proc Natl Acad Sci USA. 1985;82(20):7096–100.
12. Weller SC, Davis-Beaty K. Condom effectiveness in reducing heterosexual HIV transmission. Cochrane Database Syst Rev. 2002;(1):CD003255.
13. Johnson WD, O'Leary A, Flores SA. Per-partner condom effectiveness against HIV for men who have sex with men. AIDS. 2018;32(11):1499–505.
14. Fonner VA, Dalglish SL, Kennedy CE, Baggaley R, O'Reilly KR, Koechlin FM, et al. Effectiveness and safety of oral HIV preexposure prophylaxis for all populations. AIDS. 2016;30(12):1973–1983.
15. Grant RM, Lama JR, Anderson PL, McMahan V, Liu AY, Vargas L, et al. Preexposure chemoprophylaxis for HIV prevention in men who have sex with men. N Engl J Med. 2010;363(27):2587–99.
16. Baeten JM, Donnell D, Ndase P, Mugo NR, Campbell JD, Wangisi J, et al. Antiretroviral Prophylaxis for HIV Prevention in Heterosexual Men and Women. N Engl J Med. 2012;367(5):399–410.

17. Abdool Karim Q, Abdool Karim SS, Frohlich JA, Grobler AC, Baxter C, Mansoor LE, et al. Effectiveness and Safety of Tenofovir Gel, an Antiretroviral Microbicide, for the Prevention of HIV Infection in Women. Science. 2010;329(5996):1168–74.

18. Baeten JM, Palanee-Phillips T, Brown ER, Schwartz K, Soto-Torres LE, Govender V, et al. Use of a Vaginal Ring Containing Dapivirine for HIV-1 Prevention in Women. N Engl J Med. 2016;375(22):2121–32.

19. Rodger AJ, Cambiano V, Bruun T, Vernazza P, Collins S, van Lunzen J, et al. Sexual Activity Without Condoms and Risk of HIV Transmission in Serodifferent Couples When the HIV-Positive Partner Is Using Suppressive Antiretroviral Therapy. JAMA. 2016;316(2):171–81.

20. Mandelbrot L, Tubiana R, Le Chenadec J, Dollfus C, Faye A, Pannier E, et al. No Perinatal HIV-1 Transmission From Women With Effective Antiretroviral Therapy Starting Before Conception. Clin Infect Dis. 2015;61(11):1715–25.

21. Klatt NR, Silvestri G, Hirsch V. Nonpathogenic Simian Immunodeficiency Virus Infections. Cold Spring Harb Perspect Med. 2012;2(1):a007153–a007153.

22. Faria NR, Rambaut A, Suchard MA, Baele G, Bedford T, Ward MJ, et al. The early spread and epidemic ignition of HIV-1 in human populations. Science. 2014;346(6205):56–61.

23. Hahn BH, Shaw GM, De Cock KM, Sharp PM. AIDS as a zoonosis: Scientific and public health implications. Science. 2000;287(5453):607–14.

24. Worobey M, Gemmel M, Teuwen DE, Haselkorn T, Kunstman K, Bunce M, et al. Direct evidence of extensive diversity of HIV-1 in Kinshasa by 1960. Nature. 2008;455(7213):661–4.

25. HIV Circulating Recombinant Forms (CRFs) [Internet]. 2019 [cited 2019 Dec]. Available from: https://www.hiv.lanl.gov/content/sequence/HIV/CRFs/CRFs.html

26. Hemelaar J, Elangovan R, Yun J, Dickson-Tetteh L, Fleminger I, Kirtley S, et al. Global and regional molecular epidemiology of HIV-1, 1990-2015: a systematic review, global survey, and trend analysis. Lancet Infect Dis. 2019;19(2):143–55.

27. Magiorkinis G, Angelis K, Mamais I, Katzourakis A, Hatzakis A, Albert J, et al. The global spread of HIV-1 subtype B epidemic. Infect Genet Evol. 2016;46:169–79.

28. Takehisa J, Kraus MH, Ayouba A, Bailes E, Van Heuverswyn F, Decker JM, et al. Origin and biology of simian immunodeficiency virus in wild-living western gorillas. J Virol. 2009;83(4):1635–48.

29. Julian Villabona-Arenas C, Domyeum J, Mouacha F, Butel C, Delaporte E, Peeters M, et al. HIV-1 group O infection in Cameroon from 2006 to 2013: Prevalence, genetic diversity, evolution and public health challenges. Infect Genet Evol. 2015;36:210–6.

30. Rodgers MA, Vallari AS, Harris B, Yamaguchi J, Holzmayer V, Forberg K, et al. Identification of rare HIV-1 Group N, HBV AE, and HTLV-3 strains in rural South Cameroon. Virology. 2017;504:141–51.

31. Campbell-Yesufu OT, Gandhi RT. Update on human immunodeficiency virus (HIV)-2 infection. Clin Infect Dis. 2011;52(6):780–7.

32. Lemey P, Pybus OG, Bin W, Saksena NK, Salemi M, Vandamme AM. Tracing the origin and history of the HIV-2 epidemic. Proc Natl Acad Sci USA. 2003;100(11):6588–92.

33. Goff SP. Retroviridae: The Retroviruses and Their Replication. In: Knipe DM, Howley PM, editors. Fields Virology. 6th ed. Philadelphia: Wolters Kluwer Health; 2013. p. 1424–73.

34. Foley B, Apetrei C, Mizrachi I, Rambaut A, Korber B, Leitner T, et al., editors. HIV Sequence Compendium 2018. Los Alamos, New Mexico: Los Alamos National Laboratory, Theoretical Biology and Biophysics; 2018.

35. Karn J, Stoltzfus CM. Transcriptional and posttranscriptional regulation of HIV-1 gene expression. Cold Spring Harb Perspect Med. 2012;2(2):a006916.

36. Ganser-Pornillos BK, Yeager M, Sundquist WI. The structural biology of HIV assembly. Curr Opin Struct Biol. 2008;18(2):203–17.

37. Ganser-Pornillos BK, Cheng A, Yeager M. Structure of Full-Length HIV-1 CA: A Model for the Mature Capsid Lattice. Cell. 2007;131(1):70–9.

38. Lesbats P, Engelman AN, Cherepanov P. Retroviral DNA Integration. Chem Rev. 2016;116(20):12730–57.

39. Sundquist WI, Kräusslich HG. HIV-1 assembly, budding, and maturation. Cold Spring Harb Perspect Med. 2012;2(7):a006924.

40. Ward AB, Wilson IA. The HIV-1 envelope glycoprotein structure: nailing down a moving target. Immunol Rev. 2017;275(1):21–32.

41. Faust TB, Binning JM, Gross JD, Frankel AD. Making Sense of Multifunctional Proteins: Human Immunodeficiency Virus Type 1 Accessory and Regulatory Proteins and Connections to Transcription. Annu Rev Virol. 2017;4(1):241–60.

42. Korber B, Gaschen B, Yusim K, Thakallapally R, Kesmir C, Detours V. Evolutionary and immunological implications of contemporary HIV-1 variation. Br Med Bull. 2001;58:19–42.

43. Zanini F, Puller V, Brodin J, Albert J, Neher RA. In vivo mutation rates and the landscape of fitness costs of HIV-1. Virus Evol. 2017;3(1):vex003.

44. Mansky LM, Temin HM. Lower in vivo mutation rate of human immunodeficiency virus type 1 than that predicted from the fidelity of purified reverse transcriptase. J Virol. 1995;69(8):5087–94.

45. Cromer D, Grimm AJ, Schlub TE, Mak J, Davenport MP. Estimating the in-vivo HIV template switching and recombination rate. AIDS. 2016;30(2):185–92.

46. Piatak M, Saag MS, Yang LC, Clark SJ, Kappes JC, Luk KC, et al. High levels of HIV-1 in plasma during all stages of infection determined by competitive PCR. Science. 1993;259(5102):1749–54.

47. Perelson AS, Neumann AU, Markowitz M, Leonard JM, Ho DD. HIV-1 Dynamics in Vivo: Virion Clearance Rate, Infected Cell Life-Span, and Viral Generation Time. Science. 1996;271(5255):1582–6.

48. Perelson AS, Nelson PW. Mathematical Analysis of HIV-I: Dynamics in Vivo. SIAM Rev. 1999;41(1):3–44.

49. Spira S, Wainberg MA, Loemba H, Turner D, Brenner BG. Impact of clade diversity on HIV-1 virulence, antiretroviral drug sensitivity and drug resistance. J Antimicrob Chemother. 2003;51(2):229–40.

50. Wilen CB, Tilton JC, Doms RW. HIV: Cell binding and entry. Cold Spring Harb Perspect Med. 2012;2(8).

51. Lee B, Sharron M, Montaner LJ, Weissman D, Doms RW. Quantification of CD4, CCR5, and CXCR4 levels on lymphocyte subsets, dendritic cells, and differentially conditioned monocyte-derived macrophages. Proc Natl Acad Sci USA. 1999;96(9):5215–20.

52. Campbell EM, Hope TJ. HIV-1 capsid: The multifaceted key player in HIV-1 infection. Nat Rev Microbiol. 2015;13(8):471–483.

53. Malim MH, Bieniasz PD. HIV restriction factors and mechanisms of evasion. Cold Spring Harb Perspect Med. 2012;2(5):a006940.

54. Levin JG, Mitra M, Mascarenhas A, Musier-Forsyth K. Role of HIV-1 nucleocapsid protein in HIV-1 reverse transcription. RNA Biol. 2010;7(6):754–74.

55. Van Lint C, Bouchat S, Marcello A. HIV-1 transcription and latency: An update.

Retrovirology. 2013;10(67).

56. Daugherty MD, Liu B, Frankel AD. Structural basis for cooperative RNA binding and export complex assembly by HIV Rev. Nat Struct Mol Biol. 2010;17(11):1337–42.

57. Carlson LA, Briggs JAG, Glass B, Riches JD, Simon MN, Johnson MC, et al. Three-Dimensional Analysis of Budding Sites and Released Virus Suggests a Revised Model for HIV-1 Morphogenesis. Cell Host Microbe. 2008;4(6):592–9.

58. Guo J, Wu T, Anderson J, Kane BF, Johnson DG, Gorelick RJ, et al. Zinc Finger Structures in the Human Immunodeficiency Virus Type 1 Nucleocapsid Protein Facilitate Efficient Minus- and Plus-Strand Transfer. J Virol. 2000;74(19):8980–8.

59. Zhu P, Liu J, Bess J, Chertova E, Lifson JD, Grisé H, et al. Distribution and three-dimensional structure of AIDS virus envelope spikes. Nature. 2006;441(7095):847–52.

60. Buzon V, Natrajan G, Schibli D, Campelo F, Kozlov MM, Weissenhorn W. Crystal structure of HIV-1 gp41 including both fusion peptide and membrane proximal external regions. PLoS Pathog. 2010;6(5):e1000880.

61. Pettit SC, Everitt LE, Choudhury S, Dunn BM, Kaplan AH. Initial Cleavage of the Human Immunodeficiency Virus Type 1 GagPol Precursor by Its Activated Protease Occurs by an Intramolecular Mechanism. J Virol. 2004;78(16):8477–85.

62. Klasse PJ, Depetris RS, Pejchal R, Julien J-P, Khayat R, Lee JH, et al. Influences on Trimerization and Aggregation of Soluble, Cleaved HIV-1 SOSIP Envelope Glycoprotein. J Virol. 2013;87(17):9873–9885.

63. Lyumkis D, Julien J, Val N De, Cupo A, Potter CS, Klasse P, et al. Cryo-EM structure of a fully glycosylated soluble cleaved HIV-1 envelope trimer. Science. 2013;342(6165):1484–90.

64. Kwong PD, Wyatt R, Robinson J, Sweet RW, Sodroski J, Hendrickson WA. Structure of an HIV gp120 envelope glycoprotein in complex with the CD4 receptor and a neutralizing human antibody. Nature. 1998;393(6686):648–59.

65. Wyatt R, Kwong PD, Desjardins E, Sweet RW, Robinson J, Hendrickson WA, et al. The antigenic structure of the HIV gp120 envelope glycoprotein. Nature. 1998;393(6686):705–11.

66. Munro JB, Gorman J, Ma X, Zhou Z, Arthos J, Burton DR, et al. Conformational dynamics of single HIV-1 envelope trimers on the surface of native virions. Science. 2014;346(6210):759–63.

67. Herschhorn A, Gu C, Moraca F, Ma X, Farrell M, Smith AB, et al. The β20-β21 of gp120 is a regulatory switch for HIV-1 Env conformational transitions. Nat Commun. 2017;8(1049).

68. Sok D, Pauthner M, Briney B, Lee JH, Saye-Francisco KL, Hsueh J, et al. A Prominent Site of Antibody Vulnerability on HIV Envelope Incorporates a Motif Associated with CCR5 Binding and Its Camouflaging Glycans. Immunity. 2016;45(1):31–45.

69. Moore J, McKeating J, Weiss R, Sattentau Q. Dissociation of gp120 from HIV-1 virions induced by soluble CD4. Science. 1990;250(4984):1139–42.

70. Gallo SA, Finnegan CM, Viard M, Raviv Y, Dimitrov A, Rawat SS, et al. The HIV Env-mediated fusion reaction. Biochim Biophys Acta - Biomembr. 2003;1614(1):36–50.

71. Seabright GE, Doores KJ, Burton DR, Crispin M. Protein and Glycan Mimicry in HIV Vaccine Design. J Mol Biol. 2019;431(12):2223–47.

72. Doores KJ, Bonomelli C, Harvey DJ, Vasiljevic S, Dwek RA, Burton DR, et al. Envelope glycans of immunodeficiency virions are almost entirely oligomannose antigens. Proc Natl Acad Sci. 2010;107(31):13800–5.

73. Behrens A-J, Vasiljevic S, Pritchard LK, Harvey DJ, Andev RS, Krumm SA, et al. Composition and Antigenic Effects of Individual Glycan Sites of a Trimeric HIV-1

Envelope Glycoprotein. Cell Rep. 2016;14(11):2695–706.

74. Patel P, Borkowf CB, Brooks JT, Lasry A, Lansky A, Mermin J. Estimating per-act HIV transmission risk. AIDS. 2014;28(10):1509–19.

75. de Witte L, Nabatov A, Pion M, Fluitsma D, De Jong MA, De Gruijl T, et al. Langerin is a natural barrier to HIV-1 transmission by Langerhans cells. Nat Med. 2007;13(3):367–71.

76. Stremlau M, Owens CM, Perron MJ, Kiessling M, Autissier P, Sodroski J. The cytoplasmic body component TRIM5α restricts HIV-1 infection in Old World monkeys. Nature. 2004;427(6977):848–53.

77. Lahouassa H, Daddacha W, Hofmann H, Ayinde D, Logue EC, Dragin L, et al. SAMHD1 restricts the replication of human immunodeficiency virus type 1 by depleting the intracellular pool of deoxynucleoside triphosphates. Nat Immunol. 2012;13(3):223–8.

78. Ryoo J, Choi J, Oh C, Kim S, Seo M, Kim S-Y, et al. The ribonuclease activity of SAMHD1 is required for HIV-1 restriction. Nat Med. 2014;20(8):936–41.

79. Goujon C, Moncorgé O, Bauby H, Doyle T, Ward CC, Schaller T, et al. Human MX2 is an interferon-induced post-entry inhibitor of HIV-1 infection. Nature. 2013;502(7472):559–62.

80. Neil SJD, Zang T, Bieniasz PD. Tetherin inhibits retrovirus release and is antagonized by HIV-1 Vpu. Nature. 2008;451(7177):425–30.

81. Sheehy AM, Gaddis NC, Choi JD, Malim MH. Isolation of a human gene that inhibits HIV-1 infection and is suppressed by the viral Vif protein. Nature. 2002;418(6898):646–50.

82. Shattock RJ, Moore JP. Inhibiting sexual transmission of HIV-1 infection. Nat Rev Microbiol. 2003;1:25–34.

83. Felts RL, Narayan K, Estes JD, Shi D, Trubey CM, Fu J, et al. 3D visualization of HIV transfer at the virological synapse between dendritic cells and T cells. Proc Natl Acad Sci. 2010;107(30):13336–41.

84. Keele BF, Giorgi EE, Salazar-Gonzalez JF, Decker JM, Pham KT, Salazar MG, et al. Identification and characterization of transmitted and early founder virus envelopes in primary HIV-1 infection. Proc Natl Acad Sci. 2008;105(21):7552–7.

85. Derdeyn CA, Hunter E. Viral characteristics of transmitted HIV. Curr Opin HIV AIDS. 2008;3(1):16–21.

86. Murray JM, Kelleher AD, Cooper DA. Timing of the Components of the HIV Life Cycle in Productively Infected CD4+ T Cells in a Population of HIV-Infected Individuals. J Virol. 2011;85(20):10798–805.

87. Chen HY, Di Mascio M, Perelson AS, Ho DD, Zhang L. Determination of virus burst size in vivo using a single-cycle SIV in rhesus macaques. Proc Natl Acad Sci USA. 2007;104(48):19079–84.

88. Cohen MS, Shaw GM, McMichael AJ, Haynes BF. Acute HIV-1 infection. N Engl J Med. 2011;364(20):1943–54.

89. Brenchley JM, Price DA, Schacker TW, Asher TE, Silvestri G, Rao S, et al. Microbial translocation is a cause of systemic immune activation in chronic HIV infection. Nat Med. 2006;12(12):1365–71.

90. Streeck H, Jolin JS, Qi Y, Yassine-Diab B, Johnson RC, Kwon DS, et al. Human Immunodeficiency Virus Type 1-Specific CD8+ T-Cell Responses during Primary Infection Are Major Determinants of the Viral Set Point and Loss of CD4+ T Cells. J Virol. 2009;83(15):7641–8.

91. Goonetilleke N, Liu MKP, Salazar-Gonzalez JF, Ferrari G, Giorgi E, Ganusov V V., et al. The first T cell response to transmitted/founder virus contributes to the control of acute

viremia in HIV-1 infection. J Exp Med. 2009;206(6):1253–72.

92. Maartens G, Celum C, Lewin SR. HIV infection: Epidemiology, pathogenesis, treatment, and prevention. Lancet. 2014;384(9939):258–71.

93. Kiepiela P, Ngumbela K, Thobakgale C, Ramduth D, Honeyborne I, Moodley E, et al. CD8+ T-cell responses to different HIV proteins have discordant associations with viral load. Nat Med. 2007;13(1):46–53.

94. Goulder PJR, Walker BD. HIV and HLA Class I: An Evolving Relationship. Immunity. 2012;37(3):426–40.

95. Carrington M, Nelson GW, Martin MP, Kissner T, Vlahov D, Goedert JJ, et al. HLA and HIV-1: heterozygote advantage and B*35-Cw*04 disadvantage. Science. 1999;283(5408):1748–52.

96. Badley AD, Pilon AA, Landay A, Lynch DH. Mechanisms of HIV-associated lymphocyte apoptosis. Blood. 2000;96(9):2951–64.

97. Moir S, Chun T-W, Fauci AS. Pathogenic Mechanisms of HIV Disease. Annu Rev Pathol Mech Dis. 2011;6:223–48.

98. Murphy K, Weaver C. Janeway's Immunobiology. 9th ed. New York: Garland Science; 2017.

99. Klasse PJ. Neutralization of Virus Infectivity by Antibodies: Old Problems in New Perspectives. Adv Biol. 2014;1–24.

100. Schroeder HWJ, Cavacini L. Structure and Function of Immunoglobulins. J Allergy Clin Immunol. 2011;6:595–603.

101. Sela-Culang I, Kunik V, Ofran Y. The structural basis of antibody-antigen recognition. Front Immunol. 2013;4(302).

102. Lefranc MP. IMGT, the international imMunoGeneTics information System. Cold Spring Harb Protoc. 2011;6:595–603.

103. Schatz DG, Ji Y. Recombination centres and the orchestration of V(D)J recombination. Nat Rev Immunol. 2011;11(4):251–63.

104. Gellert M. V(D)J Recombination: RAG Proteins, Repair Factors, and Regulation. Annu Rev Biochem. 2002;71(1):101–32.

105. Bassing CH, Swat W, Alt FW. The mechanism and regulation of chromosomal V(D)J recombination. Cell. 2002;109:S45-55.

106. Li Z, Woo CJ, Iglesias-Ussel MD, Ronai D, Scharff MD. The generation of antibody diversity through somatic hypermutation and class switch recombination. Genes Dev. 2004;18(1):1–11.

107. Gallerano D, Ndlovu P, Makupe I, Focke-Tejkl M, Fauland K, Wollmann E, et al. Comparison of the specificities of IgG, IgG-subclass, IgA and IgM reactivities in African and European HIV-infected individuals with an HIV-1 clade C proteome-based array. PLoS One. 2015;10(2):e0117204.

108. Abbas A, Lichtman AH, Pillai S. Cellular and Molecular Immunology. 9th ed. Merritt J, editor. Philadelphia: Elsevier; 2017.

109. Ackerman ME, Nimmerjahn F, editors. Antibody Fc: Linking Adaptive and Innate Immunity. 1st ed. Academic Press; 2014.

110. Fagarasan S, Honjo T. Intestinal IgA synthesis: Regulation of front-line body defences. Nat Rev Immunol. 2003;3(1):63–72.

111. Grönwall C, Vas J, Silverman GJ. Protective roles of natural IgM antibodies. Front Immunol. 2012;3(66).

112. Burton OT, Oettgen HC. Beyond immediate hypersensitivity: Evolving roles for IgE antibodies in immune homeostasis and allergic diseases. Immunol Rev.

2011;242(1):128–43.

113. Chen K, Cerutti A. The function and regulation of immunoglobulin D. Curr Opin Immunol. 2011;23(3):345–52.

114. Vidarsson G, Dekkers G, Rispens T. IgG subclasses and allotypes: From structure to effector functions. Front Immunol. 2014;5(520).

115. Aalberse RC, Stapel SO, Schuurman J, Rispens T. Immunoglobulin G4: An odd antibody. Clin Exp Allergy. 2009;39(4):469–77.

116. Aalberse RC, Schuurman J. IgG4 breaking the rules. Immunology. 2002;105(1):9–19.

117. Aalberse RC, van der Gaag R, van Leeuwen J. Serologic aspects of IgG4 antibodies. I. Prolonged immunization results in an IgG4-restricted response. J Immunol. 1983;130(2):722–6.

118. Hardy RR, Hayakawa K. B cell development pathways. Annu Rev Immunol. 2001;19:595–621.

119. Melchers F. Checkpoints that control B cell development. J Clin Invest. 2015;125(6):2203–10.

120. Kranich J, Krautler NJ. How follicular dendritic cells shape the B-cell antigenome. Front Immunol. 2016;7(225).

121. Crotty S. T Follicular Helper Cell Biology: A Decade of Discovery and Diseases. Immunity. 2019;50(5):1132–48.

122. Louie DAP, Liao S. Lymp node subcapsular sinus macrophages as the frontline of lymphatic immune defense. Front Immunol. 2019;10(347).

123. Victora GD, Nussenzweig MC. Germinal Centers. Annu Rev Immunol. 2012;30(1):429–57.

124. De Silva NS, Klein U. Dynamics of B cells in germinal centres. Nat Rev Immunol. 2015;15(3):137–48.

125. Di Noia JM, Neuberger MS. Molecular Mechanisms of Antibody Somatic Hypermutation. Annu Rev Biochem. 2007;76:1–22.

126. Yoshida T, Mei H, Dörner T, Hiepe F, Radbruch A, Fillatreau S, et al. Memory B and memory plasma cells. Immunol Rev. 2010;237(1):117–39.

127. Cowell LG, Kepler TB, Litwin S, Claflin JL. The nucleotide-replacement spectrum under somatic hypermutation exhibits microsequence dependence that is strand-symmetric and distinct from that under germline mutation. J Immunol. 2000;164(4):1971–6.

128. Yaari G, Vander Heiden JA, Uduman M, Gadala-Maria D, Gupta N, Stern JNH, et al. Models of somatic hypermutation targeting and substitution based on synonymous mutations from high-throughput immunoglobulin sequencing data. Front Immunol. 2013;4(358).

129. Peled JU, Kuang FL, Iglesias-Ussel MD, Roa S, Kalis SL, Goodman MF, et al. The Biochemistry of Somatic Hypermutation. Annu Rev Immunol. 2008;26:481–511.

130. Krokan HE, Bjoras M. Base Excision Repair. Cold Spring Harb Perspect Biol. 2013;5(4):a012583–a012583.

131. Honjo T, Kinoshita K, Muramatsu M. Molecular Mechanism of Class Switch Recombination: Linkage with Somatic Hypermutation. Annu Rev Immunol. 2002;20(1):165–96.

132. Yu L, Guan Y. Immunologic basis for long HCDR3s in broadly neutralizing antibodies against HIV-1. Front Immunol. 2014;5:28–32.

133. Wu X, Zhang Z, Schramm CA, Joyce MG, Do Kwon Y, Zhou T, et al. Maturation and diversity of the VRC01-antibody lineage over 15 years of chronic HIV-1 infection. Cell. 2015;161(3):470–85.

134. Bruhns P, Jönsson F. Mouse and human FcR effector functions. Vol. 268, Immunological Reviews. Blackwell Publishing Ltd; 2015. p. 25–51.

135. Weber SS, Oxenius A. Antibody-Dependent Cellular Phagocytosis and Its Impact on Pathogen Control. In: Ackerman ME, Nimmerjahn F, editors. Antibody Fc: Linking Adaptive and Innate Immunity. 1st ed. Academic Press; 2014. p. 29–47.

136. Roman VRG, Murray JC, Weiner LM. Antibody-Dependent Cellular Cytotoxicity (ADCC). In: Ackerman ME, Nimmerjahn F, editors. Antibody Fc: Linking Adaptive and Innate Immunity. 1st ed. Academic Press; 2014. p. 1–27.

137. Richardson SI, Crowther C, Mkhize NN, Morris L. Measuring the ability of HIV-specific antibodies to mediate trogocytosis. J Immunol Methods. 2018;463:71–83.

138. Lindorfer MA, Köhl J, Taylor RP. Interactions Between the Complement System and Fcγ Receptors. In: Ackerman ME, Nimmerjahn F, editors. Antibody Fc: Linking Adaptive and Innate Immunity. 1st ed. Academic Press; 2014. p. 49–74.

139. Smyth MJ, Cretney E, Kelly JM, Westwood JA, Street SEA, Yagita H, et al. Activation of NK cell cytotoxicity. Mol Immunol. 2005;42(4):501–10.

140. Liu J, Wang Y, Xiong E, Hong R, Lu Q, Ohno H, et al. Role of the IgM Fc Receptor in Immunity and Tolerance. Front Immunol. 2019;10(529).

141. Ackerman ME, Dugast A-S, McAndrew EG, Tsoukas S, Licht AF, Irvine DJ, et al. Enhanced Phagocytic Activity of HIV-Specific Antibodies Correlates with Natural Production of Immunoglobulins with Skewed Affinity for Fc R2a and Fc R2b. J Virol. 2013;87(10):5468–76.

142. Tay MZ, Liu P, Williams LD, McRaven MD, Sawant S, Gurley TC, et al. Antibody-Mediated Internalization of Infectious HIV-1 Virions Differs among Antibody Isotypes and Subclasses. Douek DC, editor. PLOS Pathog. 2016;12(8):e1005817.

143. Forthal DN, Landucci G, Bream J, Jacobson LP, Phan TB, Montoya B. FcγRIIa Genotype Predicts Progression of HIV Infection. J Immunol. 2007;179(11):7916–23.

144. Lassaunière R, Musekiwa A, Gray GE, Kuhn L, Tiemessen CT. Perinatal HIV-1 transmission: Fc gamma receptor variability associates with maternal infectiousness and infant susceptibility. Retrovirology. 2016;13(1):40.

145. Wren LH, Chung AW, Isitman G, Kelleher AD, Parsons MS, Amin J, et al. Specific antibody-dependent cellular cytotoxicity responses associated with slow progression of HIV infection. Immunology. 2013;138(2):116–23.

146. Chung AW, Navis M, Isitman G, Wren L, Silvers J, Amin J, et al. Activation of NK cells by ADCC antibodies and HIV disease progression. J Acquir Immune Defic Syndr. 2011;58(2):127–31.

147. Tomaras GD, Haynes BF. HIV-1-specific antibody responses during acute and chronic HIV-1 infection. Curr Opin HIV AIDS. 2009;4(5):373–9.

148. Binley JM, Lybarger EA, Crooks ET, Seaman MS, Gray E, Davis KL, et al. Profiling the Specificity of Neutralizing Antibodies in a Large Panel of Plasmas from Patients Chronically Infected with Human Immunodeficiency Virus Type 1 Subtypes B and C. J Virol. 2008;82(23):11651–68.

149. Abbas A, Vasilescu A, Do H, Hendel H, Maachi M, Goutalier FX, et al. Analysis of IGG and IGG4 in HIV-1 seropositive patients and correlation with biological and genetic markers. Biomed Pharmacother. 2005;59(1–2):38–46.

150. Tomaras GD, Yates NL, Liu P, Qin LL, Fouda GG, Chavez LL, et al. Initial B-cell responses to transmitted human immunodeficiency virus type 1: virion-binding immunoglobulin M (IgM) and IgG antibodies followed by plasma anti-gp41 antibodies with ineffective control of initial viremia. J Virol. 2008;82(24):12449–63.

151. Liu P, Overman RG, Yates NL, Alam SM, Vandergrift N, Chen Y, et al. Dynamic antibody specificities and virion concentrations in circulating immune complexes in acute to

chronic HIV-1 infection. J Virol. 2011;85(21):11196–207.

152. Landais E, Huang X, Havenar-Daughton C, Murrell B, Price MA, Wickramasinghe L, et al. Broadly Neutralizing Antibody Responses in a Large Longitudinal Sub-Saharan HIV Primary Infection Cohort. Trkola A, editor. PLoS Pathog. 2016;12(1):e1005369.

153. Gray ES, Madiga MC, Hermanus T, Moore PL, Wibmer CK, Tumba NL, et al. The Neutralization Breadth of HIV-1 Develops Incrementally over Four Years and Is Associated with CD4+ T Cell Decline and High Viral Load during Acute Infection. J Virol. 2011;85(10):4828–40.

154. Doria-Rose NA, Klein RM, Daniels MG, O'Dell S, Nason M, Lapedes A, et al. Breadth of Human Immunodeficiency Virus-Specific Neutralizing Activity in Sera: Clustering Analysis and Association with Clinical Variables. J Virol. 2010;84(3):1631–6.

155. Piantadosi A, Panteleeff D, Blish CA, Baeten JM, Jaoko W, McClelland RS, et al. Breadth of Neutralizing Antibody Response to Human Immunodeficiency Virus Type 1 Is Affected by Factors Early in Infection but Does Not Influence Disease Progression. J Virol. 2009;83(19):10269–74.

156. Euler Z, van Gils MJ, Bunnik EM, Phung P, Schweighardt B, Wrin T, et al. Cross-Reactive Neutralizing Humoral Immunity Does Not Protect from HIV Type 1 Disease Progression. J Infect Dis. 2010;201(7):1045–53.

157. Gray ES, Moore PL, Choge IA, Decker JM, Bibollet-Ruche F, Li H, et al. Neutralizing Antibody Responses in Acute Human Immunodeficiency Virus Type 1 Subtype C Infection. J Virol. 2007;81(12):6187–96.

158. Derdeyn CA, Moore PL, Morris L. Development of broadly neutralizing antibodies from autologous neutralizing antibody responses in HIV infection. Curr Opin HIV AIDS. 2014;9(3):210–6.

159. Hraber P, Seaman MS, Bailer RT, Mascola JR, Montefiori DC, Korber BT. Prevalence of Broadly Neutralizing Antibody Responses During Chronic HIV-1 Infection. AIDS. 2014;14(28):163–9.

160. Landais E, Moore PL. Development of broadly neutralizing antibodies in HIV-1 infected elite neutralizers. Retrovirology. 2018;15(61).

161. Walker LM, Huber M, Doores KJ, Falkowska E, Pejchal R, Julien J-PP, et al. Broad neutralization coverage of HIV by multiple highly potent antibodies. Nature. 2011;477(7365):466–70.

162. Moore PL. The Neutralizing Antibody Response to the HIV-1 Env Protein. Curr HIV Res. 2017;16(1):21–8.

163. Richardson SI, Chung AW, Natarajan H, Mabvakure B, Mkhize NN, Garrett N, et al. HIV-specific Fc effector function early in infection predicts the development of broadly neutralizing antibodies. Douek DC, editor. PLOS Pathog. 2018;14(4):e1006987.

164. Burton DR, Hangartner L. Broadly Neutralizing Antibodies to HIV and Their Role in Vaccine Design. Annu Rev Immunol. 2016;34(1):635–59.

165. Buchacher A, Predl R, Strutzenberger K, Steinfellner W, Trkola A, Purtscher M, et al. Generation of Human Monoclonal Antibodies against HIV-1 Proteins; Electrofusion and Epstein-Barr Virus Transformation for Peripheral Blood Lymphocyte Immortalization. AIDS Res Hum Retroviruses. 1994;10(4):359–69.

166. Burton DR, Pyati J, Koduri R, Sharp SJ, Thornton GB, Parren PW, et al. Efficient neutralization of primary isolates of HIV-1 by a recombinant human monoclonal antibody. Science. 1994;266(5187):1024–7.

167. Wibmer CK, Moore PL, Morris L. HIV broadly neutralizing antibody targets. Curr Opin HIV AIDS. 2015;10(3):135–43.

168. McCoy LE. The expanding array of HIV broadly neutralizing antibodies. Retrovirology. 2018;15(70).

169. Cerutti N, Loredo-Varela JL, Caillat C, Weissenhorn W. Antigp41 membrane proximal external region antibodies and the art of using the membrane for neutralization. Curr Opin HIV AIDS. 2017;12(3):250–6.

170. Molinos-Albert LM, Clotet B, Blanco J, Carrillo J. Immunologic Insights on the Membrane Proximal External Region: A Major Human Immunodeficiency Virus Type-1 Vaccine Target. Front Immunol. 2017;8:1154.

171. Williams LD, Ofek G, Schätzle S, McDaniel JR, Lu X, Nicely NI, et al. Potent and broad HIV-neutralizing antibodies in memory B cells and plasma. Sci Immunol. 2017;2(7):eaal2200.

172. Huang J, Ofek G, Laub L, Louder MK, Doria-Rose NA, Longo NS, et al. Broad and potent neutralization of HIV-1 by a gp41-specific human antibody. Nature. 2012;491(7424):406–12.

173. Nelson JD, Brunel FM, Jensen R, Crooks ET, Cardoso RMF, Wang M, et al. An Affinity-Enhanced Neutralizing Antibody against the Membrane-Proximal External Region of Human Immunodeficiency Virus Type 1 gp41 Recognizes an Epitope between Those of 2F5 and 4E10. J Virol. 2007;81(8):4033–43.

174. Song L, Sun ZYJ, Coleman KE, Zwick MB, Gach JS, Wang JH, et al. Broadly neutralizing anti-HIV-1 antibodies disrupt a hinge-related function of gp41 at the membrane interface. Proc Natl Acad Sci USA. 2009;106(22):9057–62.

175. Rujas E, Caaveiro JMM, Partida-Hanon A, Gulzar N, Morante K, Apellániz B, et al. Structural basis for broad neutralization of HIV-1 through the molecular recognition of 10E8 helical epitope at the membrane interface. Sci Rep. 2016;6(1):38177.

176. Cardoso RMF, Zwick MB, Stanfield RL, Kunert R, Binley JM, Katinger H, et al. Broadly Neutralizing Anti-HIV Antibody 4E10 Recognizes a Helical Conformation of a Highly Conserved Fusion-Associated Motif in gp41. Immunity. 2005;22(2):163–73.

177. Falkowska E, Le KM, Ramos A, Doores KJ, Lee JH, Blattner C, et al. Broadly Neutralizing HIV Antibodies Define a Glycan-Dependent Epitope on the Prefusion Conformation of gp41 on Cleaved Envelope Trimers. Immunity. 2014;40(5):657–68.

178. Scharf L, Scheid JF, Lee JH, West AP, Chen C, Gao H, et al. Antibody 8ANC195 reveals a site of broad vulnerability on the HIV-1 envelope spike. Cell Rep. 2014;7(3):785–95.

179. Huang J, Kang BH, Pancera M, Lee JH, Tong T, Feng Y, et al. Broad and potent HIV-1 neutralization by a human antibody that binds the gp41–gp120 interface. Nature. 2014;515(7525):138–42.

180. Scharf L, Wang H, Gao H, Chen S, McDowall AW, Bjorkman PJ. Broadly Neutralizing Antibody 8ANC195 Recognizes Closed and Open States of HIV-1 Env. Cell. 2015;162(6):1379–90.

181. Lee JH, Leaman DP, Kim AS, Torrents De La Penã A, Sliepen K, Yasmeen A, et al. Antibodies to a conformational epitope on gp41 neutralize HIV-1 by destabilizing the Env spike. Nat Commun. 2015;6(1):8167.

182. Kong R, Xu K, Zhou T, Acharya P, Lemmin T, Liu K, et al. Fusion peptide of HIV-1 as a site of vulnerability to neutralizing antibody. Science. 2016;352(6287):828–33.

183. van Gils MJ, van den Kerkhof TLGM, Ozorowski G, Cottrell CA, Sok D, Pauthner M, et al. An HIV-1 antibody from an elite neutralizer implicates the fusion peptide as a site of vulnerability. Nat Microbiol. 2017;2(2):16199.

184. Yuan M, Cottrell CA, Ozorowski G, van Gils MJ, Kumar S, Wu NC, et al. Conformational Plasticity in the HIV-1 Fusion Peptide Facilitates Recognition by Broadly Neutralizing Antibodies. Cell Host Microbe. 2019;25(6):873-883.e5.

185. Blattner C, Lee JH, Sliepen K, Derking R, Falkowska E, de la Peña AT, et al. Structural Delineation of a Quaternary, Cleavage-Dependent Epitope at the gp41-gp120 Interface on Intact HIV-1 Env Trimers. Immunity. 2014;40(5):669–80.

186. Daniels CN, Saunders KO. Antibody responses to the HIV-1 envelope high mannose patch. In: Advances in Immunology. Academic Press Inc.; 2019. p. 11–73.

187. Bonsignori M, Kreider EF, Fera D, Meyerhoff RR, Bradley T, Wiehe K, et al. Staged induction of HIV-1 glycan-dependent broadly neutralizing antibodies. Sci Transl Med. 2017;9(381):eaai7514.

188. Freund NT, Wang H, Scharf L, Nogueira L, Horwitz JA, Bar-On Y, et al. Coexistence of potent HIV-1 broadly neutralizing antibodies and antibody-sensitive viruses in a viremic controller. Sci Transl Med. 2017;9(373):eaal2144.

189. MacLeod DT, Choi NM, Briney B, Garces F, Ver LS, Landais E, et al. Early antibody lineage diversification and independent limb maturation lead to broad HIV-1 neutralization targeting the Env high-mannose patch. Immunity. 2016;44(5):1215–26.

190. Zhou T, Zheng A, Baxa U, Chuang GY, Georgiev IS, Kong R, et al. A Neutralizing Antibody Recognizing Primarily N-Linked Glycan Targets the Silent Face of the HIV Envelope. Immunity. 2018;48(3):500-513.e6.

191. Schoofs T, Barnes CO, Suh-Toma N, Golijanin J, Schommers P, Gruell H, et al. Broad and Potent Neutralizing Antibodies Recognize the Silent Face of the HIV Envelope. Immunity. 2019;50(6):1513-1529.e9.

192. Zhou T, Lynch RM, Chen L, Acharya P, Wu X, Doria-Rose NA, et al. Structural repertoire of HIV-1-neutralizing antibodies targeting the CD4 supersite in 14 donors. Cell. 2015;161:1280–92.

193. Scheid JF, Mouquet H, Ueberheide B, Diskin R, Klein F, Oliveira TYK, et al. Sequence and Structural Convergence of Broad and Potent HIV Antibodies That Mimic CD4 Binding. Science. 2011;333(6049):1633–7.

194. Zhou T, Zhu J, Wu X, Moquin S, Zhang B, Acharya P, et al. Multidonor analysis reveals structural elements, genetic determinants, and maturation pathway for HIV-1 neutralization by VRC01-class antibodies. Immunity. 2013;39:245–58.

195. Balla-Jhagjhoorsingh SS, Corti D, Heyndrickx L, Willems E, Vereecken K, Davis D, et al. The N276 Glycosylation Site Is Required for HIV-1 Neutralization by the CD4 Binding Site Specific HJ16 Monoclonal Antibody. PLoS One. 2013;8(7):e68863.

196. Umotoy J, Bagaya BS, Joyce C, Schiffner T, Menis S, Saye-Francisco KL, et al. Rapid and Focused Maturation of a VRC01-Class HIV Broadly Neutralizing Antibody Lineage Involves Both Binding and Accommodation of the N276-Glycan. Immunity. 2019;51(1):141-154.e6.

197. Liao HX, Lynch R, Zhou T, Gao F, Munir Alam S, Boyd SD, et al. Co-evolution of a broadly neutralizing HIV-1 antibody and founder virus. Nature. 2013;496(7446):469–76.

198. Montero M, van Houten NE, Wang X, Scott JK. The Membrane-Proximal External Region of the Human Immunodeficiency Virus Type 1 Envelope: Dominant Site of Antibody Neutralization and Target for Vaccine Design. Microbiol Mol Biol Rev. 2008;72(1):54–84.

199. Walker LM, Phogat SK, Chan-Hui PY, Wagner D, Phung P, Goss JL, et al. Broad and potent neutralizing antibodies from an african donor reveal a new HIV-1 vaccine target. Science. 2009;326(5950):285–9.

200. Bonsignori M, Hwang K-K, Chen X, Tsao C-Y, Morris L, Gray E, et al. Analysis of a Clonal Lineage of HIV-1 Envelope V2/V3 Conformational Epitope-Specific Broadly Neutralizing Antibodies and Their Inferred Unmutated Common Ancestors. J Virol. 2011;85(19):9998–10009.

201. Sok D, van Gils MJ, Pauthner M, Julien J-P, Saye-Francisco KL, Hsueh J, et al. Recombinant HIV envelope trimer selects for quaternary-dependent antibodies targeting the trimer apex. Proc Natl Acad Sci USA. 2014;111(49):17624–9.

202. Cale EM, Gorman J, Radakovich NA, Crooks ET, Osawa K, Tong T, et al. Virus-like

Particles Identify an HIV V1V2 Apex-Binding Neutralizing Antibody that Lacks a Protruding Loop. Immunity. 2017;46(5):777–791.e10.

203. Landais E, Murrell B, Briney B, Murrell S, Rantalainen K, Berndsen ZT, et al. HIV Envelope glycoform heterogeneity and localized diversity govern the initiation and maturation of a V2 apex broadly neutralizing antibody lineage. Immunity. 2017;47(5):990–1003.e9.

204. Doria-Rose NA, Bhiman JN, Roark RS, Schramm CA, Gorman J, Chuang G-Y, et al. New member of the V1V2-directed CAP256-VRC26 lineage that shows increased breadth and exceptional potency. Silvestri G, editor. J Virol. 2016;90(1):76–91.

205. Doria-Rose NA, Schramm CA, Gorman J, Moore PL, Bhiman JN, DeKosky BJ, et al. Developmental pathway for potent V1V2-directed HIV-neutralizing antibodies. Nature. 2014;508(7498):55–62.

206. Gorman J, Chuang G-Y, Lai Y-T, Shen C-H, Boyington JC, Druz A, et al. Structure of Antibody CAP256-VRC26.25 in Complex with HIV-1 Envelope Reveals a Combined Mode of Trimer-Apex Recognition. Cell Rep. 2019;

207. Gorman J, Soto C, Yang MM, Davenport TM, Guttman M, Bailer RT, et al. Structures of HIV-1 Env V1V2 with broadly neutralizing antibodies reveal commonalities that enable vaccine design. Nat Struct Mol Biol. 2016;23(1):81–90.

208. Mclellan JS, Pancera M. Structure of HIV-1 gp120 V1/V2 domain with broadly neutralizing antibody PG9. Nature. 2012;480(7377):336–43.

209. Pejchal R, Walker LM, Stanfield RL, Phogat SK, Koff WC, Poignard P, et al. Structure and function of broadly reactive antibody PG16 reveal an H3 subdomain that mediates potent neutralization of HIV-1. Proc Natl Acad Sci USA. 2010;107(25):11483–8.

210. Lee JH, Andrabi R, Su CY, Yasmeen A, Julien JP, Kong L, et al. A Broadly Neutralizing Antibody Targets the Dynamic HIV Envelope Trimer Apex via a Long, Rigidified, and Anionic β-Hairpin Structure. Immunity. 2017;46(4):690–702.

211. Lee JH, De Val N, Lyumkis D, Ward AB. Model building and refinement of a natively glycosylated HIV-1 Env protein by high-resolution cryoelectron microscopy. Structure. 2015;23(10):1943–51.

212. Escolano A, Dosenovic P, Nussenzweig MC. Progress toward active or passive HIV-1 vaccination. J Exp Med. 2017;214(1):3–16.

213. Haynes BF, Shaw GM, Korber B, Kelsoe G, Sodroski J, Hahn BH, et al. HIV-Host Interactions: Implications for Vaccine Design. Cell Host Microbe. 2016;19(3):292–303.

214. Mascola JR, Haynes BF. HIV-1 Neutralizing Antibodies: Understanding Nature's Pathways. Immunol Rev. 2013;254(1):225–44.

215. Rappuoli R, Bottomley MJ, D'Oro U, Finco O, De Gregorio E. Reverse vaccinology 2.0: Human immunology instructs vaccine antigen design. J Exp Med. 2016;213(4):469–81.

216. Moore PL, Gorman J, Doria-Rose NA, Morris L. Ontogeny-based immunogens for the induction of V2-directed HIV broadly neutralizing antibodies. Immunol Rev. 2017;275(1):217–29.

217. Kwong PD, Mascola JR. HIV-1 Vaccines Based on Antibody Identification, B Cell Ontogeny, and Epitope Structure. Immunity. 2018;48(5):855–71.

218. Burton DR. What are the most powerful immunogen design vaccine strategies?: Reverse vaccinology 2.0 shows great promise. Cold Spring Harb Perspect Biol. 2017;9(11):a030262.

219. Victora GD, Mouquet H. What are the primary limitations in B-cell affinity maturation, and how much affinity maturation can we drive with vaccination?: Lessons from the antibody response to HIV-1. Cold Spring Harb Perspect Biol. 2018;10(5).

220. Gao F, Bonsignori M, Liao HX, Kumar A, Xia SM, Lu X, et al. Cooperation of B cell

lineages in induction of HIV-1-broadly neutralizing antibodies. Cell. 2014;158(3):481–91.

221. Simonich CA, Williams KL, Verkerke HP, Williams JA, Nduati R, Lee KK, et al. HIV-1 Neutralizing Antibodies with Limited Hypermutation from an Infant. Cell. 2016;166(1):77–87.

222. Simonich CA, Doepker L, Ralph D, Williams JA, Dhar A, Yaffe Z, et al. Kappa chain maturation helps drive rapid development of an infant HIV-1 broadly neutralizing antibody lineage. Nat Commun. 2019;10(1).

223. Bhiman JN, Anthony C, Doria-Rose NA, Karimanzira O, Schramm CA, Khoza T, et al. Viral variants that initiate and drive maturation of V1V2-directed HIV-1 broadly neutralizing antibodies. Nat Med. 2015;21(11):1332–6.

224. Hoot S, McGuire AT, Cohen KW, Strong RK, Hangartner L, Klein F, et al. Recombinant HIV Envelope Proteins Fail to Engage Germline Versions of Anti-CD4bs bNAbs. PLoS Pathog. 2013;9(1):e1003106.

225. McGuire AT, Glenn JA, Lippy A, Stamatatos L, Doms RW. Diverse recombinant HIV-1 Envs fail to activate B cells expressing the germline B cell receptors of the broadly neutralizing anti-HIV-1 antibodies PG9 and 447-52D. J Virol. 2014;88(5):2645–57.

226. Ota T, Doyle-Cooper C, Cooper AB, Huber M, Falkowska E, Doores KJ, et al. Anti-HIV B Cell Lines as Candidate Vaccine Biosensors. J Immunol. 2012;189(10):4816–24.

227. McGuire AT, Hoot S, Dreyer AM, Lippy A, Stuart A, Cohen KW, et al. Engineering HIV envelope protein to activate germline B cell receptors of broadly neutralizing anti-CD4 binding site antibodies. J Exp Med. 2013;210(4):655–63.

228. Klein F, Diskin R, Scheid JF, Gaebler C, Mouquet H, Georgiev IS, et al. Somatic mutations of the immunoglobulin framework are generally required for broad and potent HIV-1 neutralization. Cell. 2013;153(1):126–38.

229. Bonsignori M, Zhou T, Sheng Z, Chen L, Gao F, Joyce MG, et al. Maturation pathway from germline to broad HIV-1 neutralizer of a CD4-mimic antibody. Cell. 2016;165(2):449–63.

230. Georgiev IS, Rudicell RS, Saunders KO, Shi W, Kirys T, McKee K, et al. Antibodies VRC01 and 10E8 Neutralize HIV-1 with High Breadth and Potency Even with Ig-Framework Regions Substantially Reverted to Germline. J Immunol. 2014;192(3):1100–6.

231. Liao HX, Bonsignori M, Alam SM, McLellan JS, Tomaras GD, Moody MA, et al. Vaccine Induction of Antibodies against a Structurally Heterogeneous Site of Immune Pressure within HIV-1 Envelope Protein Variable Regions 1 and 2. Immunity. 2013;38(1):176–86.

232. Pancera M, McLellan JS, Wu X, Zhu J, Changela A, Schmidt SD, et al. Crystal structure of PG16 and chimeric dissection with somatically related PG9: structure-function analysis of two quaternary-specific antibodies that effectively neutralize HIV-1. J Virol. 2010;84(16):8098–110.

233. Steichen JM, Kulp DW, Tokatlian T, Escolano A, Dosenovic P, Stanfield RL, et al. HIV vaccine design to target germline precursors of glycan-dependent broadly neutralizing antibodies. Immunity. 2016;45(3):483–96.

234. Mouquet H, Scharf L, Euler Z, Liu Y, Eden C, Scheid JF, et al. Complex-type N-glycan recognition by potent broadly neutralizing HIV antibodies. Proc Natl Acad Sci. 2012;109(47):E3268-3277.

235. Scharf L, West AP, Sievers SA, Chen C, Jiang S, Gao H, et al. Structural basis for germline antibody recognition of HIV-1 immunogens. Elife. 2016;5:e13783.

236. Sliepen K, Medina-Ramírez M, Yasmeen A, Moore JP, Klasse PJ, Sanders RW. Binding of inferred germline precursors of broadly neutralizing HIV-1 antibodies to native-like envelope trimers. Virology. 2015;486:116–20.

237. Ma B-J, Alam SM, Go EP, Lu X, Desaire H, Tomaras GD, et al. Envelope

Deglycosylation Enhances Antigenicity of HIV-1 gp41 Epitopes for Both Broad Neutralizing Antibodies and Their Unmutated Ancestor Antibodies. Trkola A, editor. PLoS Pathog. 2011;7(9):e1002200.

238. Morris L, Chen X, Alam M, Tomaras G, Zhang R, Marshall DJ, et al. Isolation of a Human Anti-HIV gp41 Membrane Proximal Region Neutralizing Antibody by Antigen-Specific Single B Cell Sorting. Nixon DF, editor. PLoS One. 2011;6(9):e23532.

239. Andrabi R, Voss JE, Liang CH, Briney B, McCoy LE, Wu CY, et al. Identification of Common Features in Prototype Broadly Neutralizing Antibodies to HIV Envelope V2 Apex to Facilitate Vaccine Design. Immunity. 2015;43(5):959–73.

240. Alam SM, Dennison SM, Aussedat B, Vohra Y, Park PK, Fernández-Tejada A, et al. Recognition of synthetic glycopeptides by HIV-1 broadly neutralizing antibodies and their unmutated ancestors. Proc Natl Acad Sci USA. 2013;110(45):18214–9.

241. Jardine J, Julien J-P, Menis S, Ota T, Kalyuzhniy O, McGuire A, et al. Rational HIV immunogen design to target specific germline B cell receptors. Science. 2013;340(6133):711–6.

242. Sok D, Laserson U, Laserson J, Liu Y, Vigneault F, Julien J-P, et al. The effects of somatic hypermutation on neutralization and binding in the PGT121 family of broadly neutralizing HIV antibodies. Trkola A, editor. PLoS Pathog. 2013;9(11):e1003754.

243. Huber M, Le KM, Doores KJ, Fulton Z, Stanfield RL, Wilson IA, et al. Very Few Substitutions in a Germ Line Antibody Are Required To Initiate Significant Domain Exchange. J Virol. 2010;84(20):10700–7.

244. Wu X, Zhou T, Zhu J, Zhang B, Georgiev I, Wang C, et al. Focused Evolution of HIV-1 Neutralizing Antibodies Revealed by Structures and Deep Sequencing. Science. 2011;333(6049):1593–602.

245. Sajadi MM, Dashti A, Rikhtegaran Tehrani Z, Tolbert WD, Seaman MS, Ouyang X, et al. Identification of Near-Pan-neutralizing Antibodies against HIV-1 by Deconvolution of Plasma Humoral Responses. Cell. 2018;173(7):1783-1795.e14.

246. Kong L, Ju B, Chen Y, He L, Ren L, Liu J, et al. Key gp120 Glycans Pose Roadblocks to the Rapid Development of VRC01-Class Antibodies in an HIV-1-Infected Chinese Donor. Immunity. 2016;44(4):939–50.

247. Soto C, Ofek G, Joyce MG, Zhang B, McKee K, Longo NS, et al. Developmental pathway of the MPER-Directed HIV-1-Neutralizing antibody 10E8. PLoS One. 2016;11(6):e0157409.

248. Mabvakure BM, Scheepers C, Garrett N, Abdool Karim S, Williamson C, Morris L, et al. Positive Selection at Key Residues in the HIV Envelope Distinguishes Broad and Strain-Specific Plasma Neutralizing Antibodies. J Virol. 2019;93(6):e01685-18.

249. Henderson R, Watts BE, Ergin HN, Anasti K, Parks R, Xia SM, et al. Selection of immunoglobulin elbow region mutations impacts interdomain conformational flexibility in HIV-1 broadly neutralizing antibodies. Nat Commun. 2019;10(654).

250. Scheepers C, Shrestha RK, Lambson BE, Jackson KJL, Wright IA, Naicker D, et al. Ability To Develop Broadly Neutralizing HIV-1 Antibodies Is Not Restricted by the Germline Ig Gene Repertoire. J Immunol. 2015;194(9):4371–8.

251. Gorny MK, Sampson J, Li H, Jiang X, Totrov M, Wang XH, et al. Human anti-V3 HIV-1 monoclonal antibodies encoded by the VH5-51/VL lambda genes define a conserved antigenic structure. PLoS One. 2011;6(12):e27780.

252. Ovchinnikov V, Louveau JE, Barton JP, Karplus M, Chakraborty AK. Role of framework mutations and antibody flexibility in the evolution of broadly neutralizing antibodies. Elife. 2018;7:e33038.

253. Kumar S, Panda H, Makhdoomi MA, Mishra N, Safdari HA, Chawla H, et al. An HIV-1 Broadly Neutralizing Antibody from a Clade C-Infected Pediatric Elite Neutralizer

Potently Neutralizes the Contemporaneous and Autologous Evolving Viruses. Silvestri G, editor. J Virol. 2018;93(4):e01495-18.

254. Moody MA, Yates NL, Amos JD, Drinker MS, Eudailey JA, Gurley TC, et al. HIV-1 gp120 Vaccine Induces Affinity Maturation in both New and Persistent Antibody Clonal Lineages. J Virol. 2012;86(14):7496–507.

255. Scherer EM, Smith RA, Simonich CA, Niyonzima N, Carter JJ, Galloway DA. Characteristics of Memory B Cells Elicited by a Highly Efficacious HPV Vaccine in Subjects with No Pre-existing Immunity. PLoS Pathog. 2014;10(10):e1004461.

256. Jardine JG, Sok D, Julien J-P, Briney B, Sarkar A, Liang C-H, et al. Minimally Mutated HIV-1 Broadly Neutralizing Antibodies to Guide Reductionist Vaccine Design. Trkola A, editor. PLOS Pathog. 2016;12(8):e1005815.

257. Roider J, Maehara T, Ngoepe A, Ramsuran D, Muenchhoff M, Adland E, et al. High-Frequency, Functional HIV-Specific T-Follicular Helper and Regulatory Cells Are Present Within Germinal Centers in Children but Not Adults. Front Immunol. 2018;9:1975.

258. Jeger-Madiot R, Heredia M, Graff-Dubois S. Germinal centers B-cell reaction and T follicular helper cells in response to HIV-1 infection. Curr Opin HIV AIDS. 2019;14(4):246–52.

259. Havenar-Daughton C, Lee JH, Crotty S. Tfh cells and HIV bnAbs, an immunodominance model of the HIV neutralizing antibody generation problem. Immunol Rev. 2017;275(1):49–61.

260. Goo L, Chohan V, Nduati R, Overbaugh J. Early development of broadly neutralizing antibodies in HIV-1–infected infants. Nat Med. 2014;20(6):655–8.

261. Ditse Z, Muenchhoff M, Adland E, Jooste P, Goulder P, Moore PL, et al. HIV-1 Subtype C-Infected Children with Exceptional Neutralization Breadth Exhibit Polyclonal Responses Targeting Known Epitopes. J Virol. 2018;92(17):e00878-18.

262. Roush SW, Murphy T V., Basket MM, Iskander JK, Moran JS, Seward JF, et al. Historical comparisons of morbidity and mortality for vaccine-preventable diseases in the United States. J Am Med Assoc. 2007;298(18):2155–63.

263. Van Panhuis WG, Grefenstette J, Jung SY, Chok NS, Cross A, Eng H, et al. Contagious diseases in the United States from 1888 to the present. N Engl J Med. 2013;369(22):2152–8.

264. Stern AM, Markel H. The history of vaccines and immunization: Familiar patterns, new challenges. Health Aff. 2005;24(3):611–21.

265. Plotkin SA. Correlates of protection induced by vaccination. Clin Vaccine Immunol. 2010;17(7):1055–65.

266. Plotkin SA. Correlates of Vaccine-Induced Immunity. Clin Infect Dis. 2008;47(3):401–9.

267. Plotkin SA. History of vaccination. Proc Natl Acad Sci USA. 2014;111(34):12283–7.

268. Rappuoli R. Glycoconjugate vaccines: Principles and mechanisms. Sci Transl Med. 2018;10(456):eaat4615.

269. Del Giudice G, Rappuoli R, Didierlaurent AM. Correlates of adjuvanticity: A review on adjuvants in licensed vaccines. Semin Immunol. 2018;39:14–21.

270. Amanna IJ, Carlson NE, Slifka MK. Duration of humoral immunity to common viral and vaccine antigens. N Engl J Med. 2007;357(19):1903–15.

271. Robinson HL, Amara RR. T cell vaccines for microbial infections. Nat Med. 2005;11(4S):S25.

272. Keller MA, Stiehm ER. Passive immunity in prevention and treatment of infectious diseases. Clin Microbiol Rev. 2000;13(4):602–14.

273. Connor EM. Palivizumab, a humanized respiratory syncytial virus monoclonal antibody, reduces hospitalization from respiratory syncytial virus infection in high-risk infants. the IMpact-RSV study group. Radiology. 1999;210(1):295–6.

274. Saphire EO, Schendel SL, Fusco ML, Gangavarapu K, Gunn BM, Wec AZ, et al. Systematic Analysis of Monoclonal Antibodies against Ebola Virus GP Defines Features that Contribute to Protection. Cell. 2018;174(4):938-952.e13.

275. Gilchuk P, Kuzmina N, Ilinykh PA, Huang K, Gunn BM, Bryan A, et al. Multifunctional Pan-ebolavirus Antibody Recognizes a Site of Broad Vulnerability on the Ebolavirus Glycoprotein. Immunity. 2018;49(2):363-374.e10.

276. IAVI Trials Database - IAVI - International AIDS Vaccine Initiative [Internet]. [cited 2019 Oct]. Available from: https://www.iavi.org/trials-database/

277. Seaman MS, Janes H, Hawkins N, Grandpre LE, Devoy C, Giri A, et al. Tiered Categorization of a Diverse Panel of HIV-1 Env Pseudoviruses for Assessment of Neutralizing Antibodies. J Virol. 2010;84(3):1439–52.

278. Flynn NM, Forthal DN, Harro CD, Judson FN, Mayer KH, Para MF, et al. Placebo-Controlled Phase 3 Trial of a Recombinant Glycoprotein 120 Vaccine to Prevent HIV-1 Infection. J Infect Dis. 2005;191(5):654–65.

279. Pitisuttithum P, Gilbert P, Gurwith M, Heyward W, Martin M, van Griensven F, et al. Randomized, Double-Blind, Placebo-Controlled Efficacy Trial of a Bivalent Recombinant Glycoprotein 120 HIV-1 Vaccine among Injection Drug Users in Bangkok, Thailand. J Infect Dis. 2006;194(12):1661–71.

280. Balasubramanian P, Williams C, Shapiro MB, Sinangil F, Higgins K, Nádas A, et al. Functional Antibody Response Against V1V2 and V3 of HIV gp120 in the VAX003 and VAX004 Vaccine Trials. Sci Rep. 2018;8(1):542.

281. Chung AW, Ghebremichael M, Robinson H, Brown E, Choi I, Lane S, et al. Polyfunctional Fc-effector profiles mediated by IgG subclass selection distinguish RV144 and VAX003 vaccines. Sci Transl Med. 2014;6(228):228ra38.

282. Buchbinder SP, Mehrotra D V, Duerr A, Fitzgerald DW, Mogg R, Li D, et al. Efficacy assessment of a cell-mediated immunity HIV-1 vaccine (the Step Study): a double-blind, randomised, placebo-controlled, test-of-concept trial. Lancet. 2008;372(9653):1881–93.

283. Gray GE, Allen M, Moodie Z, Churchyard G, Bekker L-G, Nchabeleng M, et al. Safety and efficacy of the HVTN 503/Phambili study of a clade-B-based HIV-1 vaccine in South Africa: a double-blind, randomised, placebo-controlled test-of-concept phase 2b study. Lancet Infect Dis. 2011;11(7):507–15.

284. Rolland M, Tovanabutra S, deCamp AC, Frahm N, Gilbert PB, Sanders-Buell E, et al. Genetic impact of vaccination on breakthrough HIV-1 sequences from the STEP trial. Nat Med. 2011;17(3):366–71.

285. Janes H, Friedrich DP, Krambrink A, Smith RJ, Kallas EG, Horton H, et al. Vaccine-induced gag-specific T cells are associated with reduced viremia after HIV-1 infection. J Infect Dis. 2013;208(8):1231–9.

286. Hammer SM, Sobieszczyk ME, Janes H, Karuna ST, Mulligan MJ, Grove D, et al. Efficacy trial of a DNA/rAd5 HIV-1 preventive vaccine. N Engl J Med. 2013;369(22):2083–92.

287. Clements-Mann ML, Weinhold K, Matthews TJ, Graham BS, Gorse GJ, Keefer MC, et al. Immune Responses to Human Immunodeficiency Virus (HIV) Type 1 Induced by Canarypox Expressing HIV-1 $_{Mn}$ gp120, HIV-1 $_{SF2}$ Recombinant gp120, or Both Vaccines in Seronegative Adults. J Infect Dis. 1998;177(5):1230–46.

288. Nitayaphan S, Pitisuttithum P, Karnasuta C, Eamsila C, de Souza M, Morgan P, et al. Safety and Immunogenicity of an HIV Subtype B and E Prime-Boost Vaccine Combination in HIV-Negative Thai Adults. J Infect Dis. 2004;190(4):702–6.

289. Belshe RB, Stevens C, Gorse GJ, Buchbinder S, Weinhold K, Sheppard H, et al. Safety and Immunogenicity of a Canarypox-Vectored Human Immunodeficiency Virus Type 1 Vaccine with or without gp120: A Phase 2 Study in Higher- and Lower-Risk Volunteers. J Infect Dis. 2001;183(9):1343–52.

290. Rerks-Ngarm S, Pitisuttithum P, Nitayaphan S, Kaewkungwal J, Chiu J, Paris R, et al. Vaccination with ALVAC and AIDSVAX to Prevent HIV-1 Infection in Thailand. N Engl J Med. 2009;361(23):2209–20.

291. Haynes BF, Gilbert PB, McElrath MJ, Zolla-Pazner S, Tomaras GD, Alam SM, et al. Immune-correlates analysis of an HIV-1 vaccine efficacy trial. N Engl J Med. 2012;366(14):1275–86.

292. ClinicalTrials.gov. Pivotal Phase 2b/3 ALVAC/Bivalent gp120/MF59 HIV Vaccine Prevention Safety and Efficacy Study in South Africa [Internet]. 2016 [cited 2020 Feb]. Available from: https://clinicaltrials.gov/ct2/show/record/NCT02968849

293. National Institute of Allergy and Infectious Diseases. Experimental HIV Vaccine Regimen Ineffective in Preventing HIV [Internet]. 2020 [cited 2020 Feb]. Available from: https://www.niaid.nih.gov/news-events/experimental-hiv-vaccine-regimen-ineffective-preventing-hiv

294. Bradley T, Fera D, Bhiman J, Eslamizar L, Lu X, Anasti K, et al. Structural constraints of vaccine-induced tier-2 autologous HIV neutralizing antibodies targeting the receptor-binding site. Cell Rep. 2016;14(1):43–54.

295. Hessell AJ, Malherbe DC, Pissani F, McBurney S, Krebs SJ, Gomes M, et al. Achieving Potent Autologous Neutralizing Antibody Responses against Tier 2 HIV-1 Viruses by Strategic Selection of Envelope Immunogens. J Immunol. 2016;196(7):3064–78.

296. Malherbe DC, Doria-Rose NA, Misher L, Beckett T, Puryear WB, Schuman JT, et al. Sequential Immunization with a Subtype B HIV-1 Envelope Quasispecies Partially Mimics the In Vivo Development of Neutralizing Antibodies. J Virol. 2011;85(11):5262–74.

297. Hessell AJ, McBurney S, Pandey S, Sutton W, Liu L, Li L, et al. Induction of neutralizing antibodies in rhesus macaques using V3 mimotope peptides. Vaccine. 2016;34(24):2713–21.

298. Earl PL, Broder CC, Long D, Lee SA, Peterson J, Chakrabarti S, et al. Native oligomeric human immunodeficiency virus type 1 envelope glycoprotein elicits diverse monoclonal antibody reactivities. J Virol. 1994;68(5):3015–26.

299. Shu W, Ji H, Lu M. Trimerization specificity in HIV-1 gp41: Analysis with a GCN4 leucine zipper model. Biochemistry. 1999;38(17):5378–85.

300. Julien JP, Cupo A, Sok D, Stanfield RL, Lyumkis D, Deller MC, et al. Crystal structure of a soluble cleaved HIV-1 envelope trimer. Science. 2013;342(6165):1477–83.

301. Lee JH, Ozorowski G, Ward AB. Cryo-EM structure of a native, fully glycosylated, cleaved HIV-1 envelope trimer. Science. 2016;351(6277):1043–8.

302. Harris A, Borgnia MJ, Shi D, Bartesaghi A, He H, Pejchal R, et al. Trimeric HIV-1 glycoprotein gp140 immunogens and native HIV-1 envelope glycoproteins display the same closed and open quaternary molecular architectures. Proc Natl Acad Sci USA. 2011;108(28):11440–11445.

303. Sharma SK, de Val N, Bale S, Guenaga J, Tran K, Feng Y, et al. Cleavage-Independent HIV-1 Env Trimers Engineered as Soluble Native Spike Mimetics for Vaccine Design. Cell Rep. 2015;11(4):539–50.

304. Guenaga J, Dubrovskaya V, de Val N, Sharma SK, Carrette B, Ward AB, et al. Structure-Guided Redesign Increases the Propensity of HIV Env To Generate Highly Stable Soluble Trimers. J Virol. 2016;90(6):2806–17.

305. Binley JM, Sanders RW, Clas B, Schuelke N, Master A, Guo Y, et al. A Recombinant

Human Immunodeficiency Virus Type 1 Envelope Glycoprotein Complex Stabilized by an Intermolecular Disulfide Bond between the gp120 and gp41 Subunits Is an Antigenic Mimic of the Trimeric Virion-Associated Structure. J Virol. 2000;74(2):627–43.

306. Sanders RW, Vesanen M, Schuelke N, Master A, Schiffner L, Kalyanaraman R, et al. Stabilization of the Soluble, Cleaved, Trimeric Form of the Envelope Glycoprotein Complex of Human Immunodeficiency Virus Type 1. J Virol. 2002;76(17):8875–89.

307. Torrents de la Peña A, Sanders RW. Stabilizing HIV-1 envelope glycoprotein trimers to induce neutralizing antibodies. Retrovirology. 2018;15(1).

308. Rutten L, Lai YT, Blokland S, Truan D, Bisschop IJM, Strokappe NM, et al. A Universal Approach to Optimize the Folding and Stability of Prefusion-Closed HIV-1 Envelope Trimers. Cell Rep. 2018;23(2):584–95.

309. Do Kwon Y, Pancera M, Acharya P, Georgiev IS, Crooks ET, Gorman J, et al. Crystal structure, conformational fixation and entry-related interactions of mature ligand-free HIV-1 Env. Nat Struct Mol Biol. 2015;22(7):522–31.

310. Sanders RW, Derking R, Cupo A, Julien JP, Yasmeen A, de Val N, et al. A Next-Generation Cleaved, Soluble HIV-1 Env Trimer, BG505 SOSIP.664 gp140, Expresses Multiple Epitopes for Broadly Neutralizing but Not Non-Neutralizing Antibodies. PLoS Pathog. 2013;9(9):e1003618.

311. Julien JP, Lee JH, Ozorowski G, Hua Y, De La Peña AT, De Taeye SW, et al. Design and structure of two HIV-1 clade c SOSIP.664 trimers that increase the arsenal of native-like env immunogens. Proc Natl Acad Sci USA. 2015;112(38):11947–11952.

312. Pugach P, Ozorowski G, Cupo A, Ringe R, Yasmeen A, de Val N, et al. A Native-Like SOSIP.664 Trimer Based on an HIV-1 Subtype B env Gene. J Virol. 2015;89(6):3380-95.

313. De Taeye SW, Ozorowski G, Torrents De La Peña A, Guttman M, Julien JP, Van Den Kerkhof TL, et al. Immunogenicity of Stabilized HIV-1 Envelope Trimers with Reduced Exposure of Non-neutralizing Epitopes. Cell. 2015;163(7):1702–15.

314. He L, Kumar S, Allen JD, Huang D, Lin X, Mann CJ, et al. HIV-1 vaccine design through minimizing envelope metastability. Sci Adv. 2018;4(11):eaau6769.

315. Feng Y, Tran K, Bale S, Kumar S, Guenaga J, Wilson R, et al. Thermostability of Well-Ordered HIV Spikes Correlates with the Elicitation of Autologous Tier 2 Neutralizing Antibodies. PLoS Pathog. 2016;12(8):e1005767.

316. Lei L, Yang YR, Tran K, Wang Y, Chiang C-I, Ozorowski G, et al. The HIV-1 Envelope Glycoprotein C3/V4 Region Defines a Prevalent Neutralization Epitope following Immunization. Cell Rep. 2019;27(2):586-598.e6.

317. Cheng C, Pancera M, Bossert A, Schmidt SD, Chen RE, Chen X, et al. Immunogenicity of a Prefusion HIV-1 Envelope Trimer in Complex with a Quaternary-Structure-Specific Antibody. Kirchhoff F, editor. J Virol. 2016;90(6):2740–55.

318. Crooks ET, Tong T, Chakrabarti B, Narayan K, Georgiev IS, Menis S, et al. Vaccine-elicited tier 2 HIV-1 neutralizing antibodies bind to quaternary epitopes involving glycan-deficient patches proximal to the CD4 binding site. PLoS Pathog. 2015;11(5):e1004932.

319. Dubrovskaya V, Tran K, Ozorowski G, Guenaga J, Wilson R, Bale S, et al. Vaccination with Glycan-Modified HIV NFL Envelope Trimer-Liposomes Elicits Broadly Neutralizing Antibodies to Multiple Sites of Vulnerability. Immunity. 2019;51(5):915-929.e7.

320. Sanders RW, Van Gils MJ, Derking R, Sok D, Ketas TJ, Burger JA, et al. HIV-1 neutralizing antibodies induced by native-like envelope trimers. Science. 2015;349(6244):aac4223-1-aac4223-10.

321. McCoy LE, van Gils MJ, Ozorowski G, Messmer T, Briney B, Voss JE, et al. Holes in the Glycan Shield of the Native HIV Envelope Are a Target of Trimer-Elicited Neutralizing Antibodies. Cell Rep. 2016;16(9):2327–38.

322. Ringe RP, Ozorowski G, Rantalainen K, Struwe WB, Matthews K, Torres JL, et al. Reducing V3 Antigenicity and Immunogenicity on Soluble, Native-Like HIV-1 Env SOSIP Trimers. J Virol. 2017;91(15):e00677-17.

323. Klasse PJ, LaBranche CC, Ketas TJ, Ozorowski G, Cupo A, Pugach P, et al. Sequential and Simultaneous Immunization of Rabbits with HIV-1 Envelope Glycoprotein SOSIP.664 Trimers from Clades A, B and C. PLoS Pathog. 2016;12(9):e1005864.

324. Klasse PJ, Ketas TJ, Cottrell CA, Ozorowski G, Debnath G, Camara D, et al. Epitopes for neutralizing antibodies induced by HIV-1 envelope glycoprotein BG505 SOSIP trimers in rabbits and macaques. Desrosiers RC, editor. PLOS Pathog. 2018;14(2):e1006913.

325. Voss JE, Andrabi R, McCoy LE, de Val N, Fuller RP, Messmer T, et al. Elicitation of Neutralizing Antibodies Targeting the V2 Apex of the HIV Envelope Trimer in a Wild-Type Animal Model. Cell Rep. 2017;21(1):222–35.

326. Kulp DW, Steichen JM, Pauthner M, Hu X, Schiffner T, Liguori A, et al. Structure-based design of native-like HIV-1 envelope trimers to silence non-neutralizing epitopes and eliminate CD4 binding. Nat Commun. 2017;8(1):1655.

327. Dubrovskaya V, Guenaga J, de Val N, Wilson R, Feng Y, Movsesyan A, et al. Targeted N-glycan deletion at the receptor-binding site retains HIV Env NFL trimer integrity and accelerates the elicited antibody response. Trkola A, editor. PLOS Pathog. 2017;13(9):e1006614.

328. Zhou T, Doria-Rose NA, Cheng C, Stewart-Jones GBE, Chuang G-Y, Chambers M, et al. Quantification of the Impact of the HIV-1-Glycan Shield on Antibody Elicitation. Cell Rep. 2017;19(4):719–32.

329. Cheng C, Xu K, Kong R, Chuang G-Y, Corrigan AR, Geng H, et al. Consistent elicitation of cross-clade HIV-neutralizing responses achieved in guinea pigs after fusion peptide priming by repetitive envelope trimer boosting. Ansari AA, editor. PLoS One. 2019;14(4):e0215163.

330. Saunders KO, Verkoczy LK, Jiang C, Zhang J, Parks R, Chen H, et al. Vaccine Induction of Heterologous Tier 2 HIV-1 Neutralizing Antibodies in Animal Models. Cell Rep. 2017;21(13):3681–90.

331. Pauthner M, Havenar-Daughton C, Sok D, Nkolola JP, Bastidas R, Boopathy A V, et al. Elicitation of Robust Tier 2 Neutralizing Antibody Responses in Nonhuman Primates by HIV Envelope Trimer Immunization Using Optimized Approaches. Immunity. 2017;46(6):1073-1088.e6.

332. Duan H, Chen X, Boyington JC, Cheng C, Zhang Y, Jafari AJ, et al. Glycan Masking Focuses Immune Responses to the HIV-1 CD4-Binding Site and Enhances Elicitation of VRC01-Class Precursor Antibodies. Immunity. 2018;49(2):301-311.e5.

333. Jardine JG, Kulp DW, Havenar-Daughton C, Sarkar A, Briney B, Sok D, et al. HIV-1 broadly neutralizing antibody precursor B cells revealed by germline-targeting immunogen. Science. 2016;351(6280):1458–63.

334. Medina-Ramírez M, Garces F, Escolano A, Skog P, Taeye SW de, Moral-Sanchez I Del, et al. Design and crystal structure of a native-like HIV-1 envelope trimer that engages multiple broadly neutralizing antibody precursors in vivo. J Exp Med. 2017;214(9):2573–90.

335. Briney B, Sok D, Jardine JG, Kulp DW, Skog P, Menis S, et al. Tailored Immunogens Direct Affinity Maturation toward HIV Neutralizing Antibodies. Cell. 2016;166(6):1459–70.

336. Escolano A, Steichen JM, Dosenovic P, Kulp DW, Golijanin J, Sok D, et al. Sequential Immunization Elicits Broadly Neutralizing Anti-HIV-1 Antibodies in Ig Knockin Mice. Cell. 2016;166(6):1445-1458.e12.

337. Escolano A, Gristick HB, Abernathy ME, Merkenschlager J, Gautam R, Oliveira TY, et

al. Immunization expands B cells specific to HIV-1 V3 glycan in mice and macaques. Nature. 2019;570(7762):468–73.

338. Havenar-Daughton C, Sarkar A, Kulp DW, Toy L, Hu X, Deresa I, et al. The human naive B cell repertoire contains distinct subclasses for a germline-targeting HIV-1 vaccine immunogen. Sci Transl Med. 2018;10(448):eaat0381.

339. Steichen JM, Lin Y-C, Havenar-Daughton C, Pecetta S, Ozorowski G, Willis JR, et al. A generalized HIV vaccine design strategy for priming of broadly neutralizing antibody responses. Science. 2019;eaax4380.

340. Saunders KO, Wiehe K, Tian M, Acharya P, Bradley T, Munir Alam S, et al. Targeted selection of HIV-specific antibody mutations by engineering B cell maturation. Science. 2019;366(6470):eaay7199.

341. Parren PW, Marx PA, Hessell AJ, Luckay A, Harouse J, Cheng-Mayer C, et al. Antibody protects macaques against vaginal challenge with a pathogenic R5 simian/human immunodeficiency virus at serum levels giving complete neutralization in vitro. J Virol. 2001;75(17):8340–7.

342. Moldt B, Rakasz EG, Schultz N, Chan-Hui P-Y, Swiderek K, Weisgrau KL, et al. Highly potent HIV-specific antibody neutralization in vitro translates into effective protection against mucosal SHIV challenge in vivo. Proc Natl Acad Sci. 2012;109(46):18921–5.

343. Julg B, Liu P-T, Wagh K, Fischer WM, Abbink P, Mercado NB, et al. Protection against a mixed SHIV challenge by a broadly neutralizing antibody cocktail. Sci Transl Med. 2017;9(408):eaao4235.

344. Julg B, Tartaglia LJ, Keele BF, Wagh K, Pegu A, Sok D, et al. Broadly neutralizing antibodies targeting the HIV-1 envelope V2 apex confer protection against a clade C SHIV challenge. Sci Transl Med. 2017;9(406):eaal1321.

345. Gautam R, Nishimura Y, Pegu A, Nason MC, Klein F, Gazumyan A, et al. A single injection of anti-HIV-1 antibodies protects against repeated SHIV challenges. Nature. 2016;533(7601):105–9.

346. Lu CL, Murakowski DK, Bournazos S, Schoofs T, Sarkar D, Halper-Stromberg A, et al. Enhanced clearance of HIV-1-infected cells by broadly neutralizing antibodies against HIV-1 in vivo. Science. 2016;352(6288):1001–4.

347. Halper-Stromberg A, Lu CL, Klein F, Horwitz JA, Bournazos S, Nogueira L, et al. Broadly neutralizing antibodies and viral inducers decrease rebound from HIV-1 latent reservoirs in humanized mice. Cell. 2014;158(5):989–99.

348. Bournazos S, Klein F, Pietzsch J, Seaman MS, Nussenzweig MC, Ravetch J V. Broadly neutralizing anti-HIV-1 antibodies require Fc effector functions for in vivo activity. Cell. 2014;158(6):1243–53.

349. Hessell AJ, Hangartner L, Hunter M, Havenith CEG, Beurskens FJ, Bakker JM, et al. Fc receptor but not complement binding is important in antibody protection against HIV. Nature. 2007;449(7158):101–4.

350. Hessell AJ, Rakasz EG, Poignard P, Hangartner L, Landucci G, Forthal DN, et al. Broadly neutralizing human anti-HIV antibody 2G12 is effective in protection against mucosal SHIV challenge even at low serum neutralizing titers. PLoS Pathog. 2009;5(5):e1000433.

351. Morris L, Mkhize NN. Prospects for passive immunity to prevent HIV infection. PLoS Med. 2017;14(11):e1002436.

352. Pegu A, Yang Z, Boyington JC, Wu L, Ko S-Y, Schmidt SD, et al. Neutralizing antibodies to HIV-1 envelope protect more effectively in vivo than those to the CD4 receptor. Sci Transl Med. 2014;6(243):243ra88.

353. Xu L, Pegu A, Rao E, Doria-Rose N, Beninga J, McKee K, et al. Trispecific broadly neutralizing HIV antibodies mediate potent SHIV protection in macaques. Science.

2017;358(6359):85–90.

354. Ko SY, Pegu A, Rudicell RS, Yang ZY, Joyce MG, Chen X, et al. Enhanced neonatal Fc receptor function improves protection against primate SHIV infection. Nature. 2014;514(7524):642–645.

355. Zalevsky J, Chamberlain AK, Horton HM, Karki S, Leung IWL, Sproule TJ, et al. Enhanced antibody half-life improves in vivo activity. Nat Biotechnol. 2010;28(2):157–9.

356. Caskey M. Broadly neutralizing antibodies for the treatment and prevention of HIV infection. Curr Opin HIV AIDS. 2020;15(1):49–55.

357. Bar KJ, Sneller MC, Harrison LJ, Justement JS, Overton ET, Petrone ME, et al. Effect of HIV Antibody VRC01 on Viral Rebound after Treatment Interruption. N Engl J Med. 2016;375(21):2037–50.

358. Mendoza P, Gruell H, Nogueira L, Pai JA, Butler AL, Millard K, et al. Combination therapy with anti-HIV-1 antibodies maintains viral suppression. Nature. 2018;561(7724):479–84.

359. van Loggerenberg F, Mlisana K, Williamson C, Auld SC, Morris L, Gray CM, et al. Establishing a Cohort at High Risk of HIV Infection in South Africa: Challenges and Experiences of the CAPRISA 002 Acute Infection Study. Ugarte-Gil CA, editor. PLoS One. 2008;3(4):e1954.

360. Moore PL, Gray ES, Sheward D, Madiga M, Ranchobe N, Lai Z, et al. Potent and broad neutralization of HIV-1 subtype C by plasma antibodies targeting a quaternary epitope including residues in the V2 loop. J Virol. 2011;85(7):3128–41.

361. Andrabi R, Su CY, Liang CH, Shivatare SS, Briney B, Voss JE, et al. Glycans Function as Anchors for Antibodies and Help Drive HIV Broadly Neutralizing Antibody Development. Immunity. 2017;47(3):524–37.

362. Crooks ET, Grimley SL, Cully M, Osawa K, Dekkers G, Saunders K, et al. Glycoengineering HIV-1 Env creates 'supercharged' and 'hybrid' glycans to increase neutralizing antibody potency, breadth and saturation. PLoS Pathog. 2018;14(5):e1007024.

363. Richardson SI, Lambson BE, Crowley AR, Bashirova A, Scheepers C, Garrett N, et al. IgG3 enhances neutralization potency and Fc effector function of an HIV V2-specific broadly neutralizing antibody. Doores KJ, editor. PLOS Pathog. 2019;15(12):e1008064.

364. Mahomed S, Garrett N, Capparelli E, Baxter C, Zuma NY, Gengiah T, et al. Assessing the safety and pharmacokinetics of the monoclonal antibodies, VRC07-523LS and PGT121 in HIV negative women in South Africa: Study protocol for the CAPRISA 012A randomised controlled phase I trial. BMJ Open. 2019;9(7):e030283.

365. Moore PL, Sheward D, Nonyane M, Ranchobe N, Hermanus T, Gray ES, et al. Multiple pathways of escape from HIV broadly cross-neutralizing V2-dependent antibodies. J Virol. 2013;87(9):4882–94.

366. Barouch DH, Yang Z-Y, Kong W-P, Korioth-Schmitz B, Sumida SM, Truitt DM, et al. A Human T-Cell Leukemia Virus Type 1 Regulatory Element Enhances the Immunogenicity of Human Immunodeficiency Virus Type 1 DNA Vaccines in Mice and Nonhuman Primates. J Virol. 2005;79(14):8828–34.

367. Lefranc MP. Nomenclature of the Human Immunoglobulin Heavy (IGH) Genes. Exp Clin Immunogenet. 2001;18(2):100–16.

368. Wei X, Decker JM, Liu H, Zhang Z, Arani RB, Kilby JM, et al. Emergence of resistant human immunodeficiency virus type 1 in patients receiving fusion inhibitor (T-20) monotherapy. Antimicrob Agents Chemother. 2002;46(6):1896–905.

369. Sarzotti-Kelsoe M, Bailer RT, Turk E, Lin CL, Bilska M, Greene KM, et al. Optimization and validation of the TZM-bl assay for standardized assessments of neutralizing antibodies against HIV-1. J Immunol Methods. 2014;409:131–46.

370. Platt EJ, Wehrly K, Kuhmann SE, Chesebro B, Kabat D. Effects of CCR5 and CD4 Cell Surface Concentrations on Infections by Macrophagetropic Isolates of Human Immunodeficiency Virus Type 1. J Virol. 1998;72(4):2855–2864.

371. Reed LJ, Muench H. A simple method of estimating fifty per cent endpoints. Am J Epidemiol. 1938;27(3):493–7.

372. Guex N, Peitsch MC. SWISS-MODEL and the Swiss-PdbViewer: an environment for comparative protein modeling. Electrophoresis. 1997;18(15):2714–23.

373. Kumar S, Stecher G, Li M, Knyaz C, Tamura K. MEGA X: Molecular Evolutionary Genetics Analysis across Computing Platforms. Mol Biol Evol. 2018;35(6):1547–9.

374. Rusert P, Kouyos RD, Kadelka C, Ebner H, Schanz M, Huber M, et al. Determinants of HIV-1 broadly neutralizing antibody induction. Nat Med. 2016;22(11):1260–7.

375. Shingai M, Donau OK, Plishka RJ, Buckler-White A, Mascola JR, Nabel GJ, et al. Passive transfer of modest titers of potent and broadly neutralizing anti-HIV monoclonal antibodies block SHIV infection in macaques. J Exp Med. 2014;211(10):2061–74.

376. Mascola JR, Stiegler G, VanCott TC, Katinger H, Carpenter CB, Hanson CE, et al. Protection of macaques against vaginal transmission of a pathogenic HIV- 1/SIV chimeric virus by passive infusion of neutralizing antibodies. Nat Med. 2000;6(2):207–10.

377. Bonsignori M, Liao HX, Gao F, Williams WB, Alam SM, Montefiori DC, et al. Antibody-virus co-evolution in HIV infection: paths for HIV vaccine development. Immunol Rev. 2017;275(1):145–60.

378. Tokuriki N, Tawfik DS. Stability effects of mutations and protein evolvability. Curr Opin Struct Biol. 2009;19(5):596–604.

379. England P, Nageotte R, Renard M, Page AL, Bedouelle H. Functional characterization of the somatic hypermutation process leading to antibody D1.3, a high affinity antibody directed against lysozyme. J Immunol. 1999;162(4):2129–36.

380. Wiehe K, Bradley T, Meyerhoff RR, Hart C, Williams WB, Easterhoff D, et al. Functional relevance of improbable antibody mutations for HIV broadly neutralizing antibody development. Cell Host Microbe. 2018;23(6):759–765.e6.

381. Tian M, Cheng C, Chen X, Duan H, Cheng HL, Dao M, et al. Induction of HIV neutralizing antibody lineages in mice with diverse precursor repertoires. Cell. 2016;166(6):1471–84.

382. Johnson EL, Doria-Rose NA, Gorman J, Bhiman JN, Schramm CA, Vu AQ, et al. Sequencing HIV-neutralizing antibody exons and introns reveals detailed aspects of lineage maturation. Nat Commun. 2018;9(1):4136.

383. Bundgaard JR, Vuust J, Rehfeld JF. New consensus features for tyrosine O-sulfation determined by mutational analysis. J Biol Chem. 1997;272(35):21700–05.

384. Schramm CA, Douek DC. Beyond hot spots: Biases in antibody somatic hypermutation and implications for vaccine design. Front Immunol. 2018;9(1876).

385. Chuang GY, Zhou J, Acharya P, Rawi R, Shen CH, Sheng Z, et al. Structural Survey of Broadly Neutralizing Antibodies Targeting the HIV-1 Env Trimer Delineates Epitope Categories and Characteristics of Recognition. Structure. 2019;27(1):196–206.e6.

386. Hwang JK, Wang C, Du Z, Meyers RM, Kepler TB, Neuberg D, et al. Sequence intrinsic somatic mutation mechanisms contribute to affinity maturation of VRC01-class HIV-1 broadly neutralizing antibodies. Proc Natl Acad Sci USA. 2017;114(32):8614–9.

387. McCoy LE, Falkowska E, Doores KJ, Le K, Sok D, van Gils MJ, et al. Incomplete Neutralization and Deviation from Sigmoidal Neutralization Curves for HIV Broadly Neutralizing Monoclonal Antibodies. Trkola A, editor. PLOS Pathog. 2015;11(8):e1005110.

388. McGuire AT, Dreyer AM, Carbonetti S, Lippy A, Glenn J, Scheid JF, et al. Antigen

modification regulates competition of broad and narrow neutralizing HIV antibodies. Science. 2014;346(6215):1380–3.

389. De Pascalis R, Iwahashi M, Tamura M, Padlan EA, Gonzales NR, Santos AD, et al. Grafting of "Abbreviated" Complementarity-Determining Regions Containing Specificity-Determining Residues Essential for Ligand Contact to Engineer a Less Immunogenic Humanized Monoclonal Antibody. J Immunol. 2002;169(6):3076–84.

390. Sliepen K, Sanders RW. HIV-1 envelope glycoprotein immunogens to induce broadly neutralizing antibodies. Expert Rev Vaccines. 2016;15(3):349–65.

391. Alter G, Barouch D. Immune Correlate-Guided HIV Vaccine Design. Cell Host Microbe. 2018;24(1):25–33.

392. Giudicelli V, Chaume D, Lefranc M-P. IMGT/V-QUEST, an integrated software program for immunoglobulin and T cell receptor V-J and V-D-J rearrangement analysis. Nucleic Acids Res. 2004;32(Web Server issue):W435-40.

393. Boesch AW, Osei-Owusu NY, Crowley AR, Chu TH, Chan YN, Weiner JA, et al. Biophysical and functional characterization of rhesus macaque IgG subclasses. Front Immunol. 2016;7(589).

394. Pollara J, Hart L, Brewer F, Pickeral J, Packard BZ, Hoxie JA, et al. High-throughput quantitative analysis of HIV-1 and SIV-specific ADCC-mediating antibody responses. Cytom Part A. 2011;79 A(8):603–12.

395. Ackerman ME, Mikhailova A, Brown EP, Dowell KG, Walker BD, Bailey-Kellogg C, et al. Polyfunctional HIV-Specific Antibody Responses Are Associated with Spontaneous HIV Control. Douek DC, editor. PLOS Pathog. 2016;12(1):e1005315.

396. Ackerman ME, Moldt B, Wyatt RT, Dugast AS, McAndrew E, Tsoukas S, et al. A robust, high-throughput assay to determine the phagocytic activity of clinical antibody samples. J Immunol Methods. 2011;366(1–2):8–19.

397. Wu T Te, Johnson G, Kabat EA. Length distribution of CDRH3 in antibodies. Proteins Struct Funct Genet. 1993;16(1):1–7.

398. Briney BS, Willis JR, Hicar MD, Thomas JW, Crowe JE. Frequency and genetic characterization of V(DD)J recombinants in the human peripheral blood antibody repertoire. Immunology. 2012;137(1):56–64.

399. Motea EA, Berdis AJ. Terminal deoxynucleotidyl transferase: The story of a misguided DNA polymerase. Biochim Biophys Acta - Proteins Proteomics. 2010;1804(5):1151–66.

400. Thai T-H, Kearney JF. Distinct and Opposite Activities of Human Terminal Deoxynucleotidyltransferase Splice Variants. J Immunol. 2004;173(6):4009–19.